Improving Fe/Zn concentration in Indica rice by a novel combination of a sucrose transporter and nicotianamine synthase overexpression

By

Thanh Hai Tran

Thesis
Submitted to Flinders University
for the degree of

Doctor of Philosophy

The College of Science and Engineering
August 2021

Improving Fe/Zn concentration in Indica rice by a novel combination of a sucrose transporter and nicotianamine synthase overexpression

Thanh Hai Tran

A thesis submitted for the degree of Doctor of Philosophy

at

The College of Science and Engineering

Flinders University

South Australia

August 2021

CONTENTS

Page

LIST OF FIGURES

Page

LIST OF TABLES

Page

SUMMARY

Although rice supplies over half of the global food requirement, its relatively low micronutrient content presents as a "hidden" malnutrition amongst many people, mainly in developing countries. Biofortification of crops is a way to address this malnutrition-inducing micronutrient deficiency, and rice is an excellent candidate for this approach. However, in cereals like rice, there is often a negative correlation between micronutrient content and yield, making the combination of these two important traits a great challenge for breeders.

Sucrose, produced by plants through photosynthesis, is an important nutrient, which does not only impact yield, but is also involved in a source-sink communication network. A balance between nutrient utilisation in the sink tissues, and nutrient synthesis in source tissues is tightly coordinated; thus, any enhancement of sucrose demand in the sink could stimulate its translocation from the source. Targeted overexpression of sucrose transporters provides a promising method to enhance the uptake capacity and partitioning of sucrose, resulting in increased sink strength. Such a strategy was first reported in wheat by Weichert *et al.* (2010), where the endosperm-specified overexpression of the barley sucrose transporter (*HvSUT1*) led to an increase in seed storage protein synthesis. Of great interest was that higher micronutrient levels were also found in the grain of these transgenic plants (Saalbach *et al.* 2014). A similar strategy used in the Japonica rice cultivar, Nipponbare, found similar results (Huynh 2015), although the formation of insoluble Fe/Zn complexes with phytate resulted in their limited translocation, especially Fe, into the inner endosperm.

Nicotianamine (NA) and 2'-deoxymugineic acid (DMA) are two natural chelators of metal cations, including Fe and Zn. In rice, NA is synthesized by the enzyme, nicotianamine synthase (NAS), which is a product of three *OsNAS* genes (*OsNAS1*, *2* and *3*). Therefore, what is hypothesised here, is that a novel combination of endosperm specific expression of *HvSUT1*

and *OsNAS2* will drive more sucrose and micronutrient loading into the grain, and the availability of an alternative chelator in NA, will increase the translocation of Fe/Zn complexes into the inner endosperm.

To test this hypothesis, research was conducted in three main steps. First, along with single gene constructs of *HvSUT1* and *OsNAS2*, a novel combination of *HvSUT1* and the rice nicotianamine synthase gene (*OsNAS2*) was introduced into Indica rice (cv. IR64) by *Agrobacterium*-mediated transformation. Two promoters, *Glb-1* and *GluA2* cloned from Nipponbare rice, were used to drive the endosperm specific expression of *HvSUT1* and *OsNAS2*, respectively. Multiple homozygous one- or two-insert transgenic lines were identified by quantitative real-time PCR. Also, a *GluA2::uidA* fusion construct was made and transformed into IR64 to confirm the tissue specific expression of the *Glu2A* promoter.

Second, immature grains from T2 plants were used in immunoblot analyses to test tissue specific and temporal expression of the transgenes during grain filling. OsNAS2 was expressed in the rice grain at the highest level 5 days after anthesis (DAA), and then decreased until 15 DAA. HvSUT1 was expressed from 5 DAA to 15 DAA and reached its highest level of expression at approximately 10 DAA. An unexpected vigorous growth phenotype was found in transgenic IR64 rice overexpressing *HvSUT1*, with or without *OsNAS2*, during the vegetative growth phase, but as yet no definitive results have been found for the resulting yield in these transgenic plants. Such a phenotype was not reported by Huynh (2015) in *HvSUT1* transgenic Nipponbare rice.

Finally, Inductively Coupled Plasma Mass Spectrometry (ICP-MS) was used to measure micronutrient concentrations in the grains of the transgenic rice. Fe increased by approximately 100 % and around 30% for Zn, Cu and Mn in the polished grain overexpressing a combination of *HvSUT1* and *OsNAS2*. Histochemical analysis of Fe distribution using Perls/DAB/$CoCl_2$

staining, and Zn distribution using DTZ staining, revealed striking differences in the distribution and intensity in both dorsal and ventral sides of *HvSUT1+OsNAS2* transgenic grain, not visible in the grains of the non-transgenic and the single construct transgenic lines. Furthermore, based on the molar ratios of phytate to Fe and Zn, micronutrient bioavailability may be improved in these transgenic seed.

In general, these data indicate a positive correlation between HvSUT1 protein levels and the uptake of micronutrients during grain filling in IR64 transgenic rice. The combination of *HvSUT1* and *OsNAS2* expression showed remarkable changes in Fe accumulation and distribution in the grain that may exist in a form more available for uptake in the human gut. A vigorous growth phenotype of the transgenic rice overexpressing *HvSUT1* was an unexpected outcome of this study and is worthy of further investigation. These results are reported in the context of the literature and some speculative hypotheses are raised to stimulate and foster further experimentation.

Key words: Fe/Zn biofortification, barley sucrose transporter, nicotianamine synthase, rice

DECLARATION

I certify that this thesis:

1. does not incorporate without acknowledgment any material previously submitted for a degree or diploma in any university; and

2. to the best of my knowledge and belief, does not contain any material previously published or written by another person except where due reference is made in the text.

Thanh Hai Tran

ACKNOWLEDGMENT

I would like to express my thanks and gratitude to my three supervisors, who have made a great contribution into my thesis in a variety of ways. First and foremost, I would like to thank Assoc. prof. Peter Anderson for his wonderful supervision and assistance in the entire progress of my PhD research completion. During my research time, he continuously supported suggestions and recommendations to overcome many difficulties in my experiments. He also listened to my ideas and explanations and then provided many helpful advises to improve the outcome of my experiments.

I would like to acknowledge the help of Assoc. prof. Colin Jenkins and Prof. James Stangoulis, my two other supervisors. Colin offered his great advice and knowledge in multiple aspects of my PhD research. Also, James and his lab members, Lachlan Palmer, Lyndon Palmer, Georgia Guild, Emma DeCourcy-Ireland and Carolyn Smith supported my nutrient analyses very much. I am really grateful for their time and expertise to my experiments and analyses.

I would like to thank all current and former members of the plant research lab in Biological Sciences at Flinders University; Carly Schramm, Dr. Yuri Shavrukov, Dr. Crystal Sweetman, Dr. My-my Huynh, Prof. Kathleen Soole, Prof. David Day, Lauren Philp-Dutton, Nick Booth, Barry Rainbird, and Troy Miller who shared their experiences and comments to improve the results of my experiments in the lab meetings.

I have also to thank the Flinders University Research Scholarship (FURS) and Australian Government Research Training Program Scholarship to fund to do my PhD research at Flinders University, and an International conference travel grant and College of Science and Engineering-HRD international conference travel grant support for attending the XXVIII Plant and Animal genome conference in USA in 11-16/01/2020.

I would like to thank very much, Dr. Julien Pierre Bonneu and Dr. Alex Johnson (The University of Melbourne), for kindly providing the cDNA of *OsNAS2*, Ms. Melissa Pickering (University of Adelaide) for her generous advice on rice transformation, and Ms. Pat Vilimas (Flinders University) for providing a training.

Last but not least important, I have to thank my family for their encouragement, and a big, special thanks goes to Dut and my son, Dinh, who have shared this wonderful journey by their love and support.

ABBREVIATIONS

2,4-D:	2, 4-dichlorophenoxyacetic acid
BAP:	6-benzylaminopurine
BLAST:	Basic Logical Alignment Tool
bp:	Base pairs
cds:	Coding sequence
CTAB:	Cety trimethyl ammonium bromide
DAB:	3,3'-diaminobenzidine
DAA:	Day after anthesis
DAG:	Day after germination
DTZ:	Dithizone
DMSO:	Dimethyl sulphoxide
dNTPs:	Deoxyribonucleotide triphosphates
DTT:	1, 4-dithiothreitol
EAR:	estimated average requirement
EDTA:	Ethylenediaminetetraacetic acid
EFSA:	European Food Safety Authority
E.coli:	*Escherichia coli*
GUS:	β-glucoronidase
NCBI:	National Centre for Biotechnology Information
HvSUT1:	Barley (*Hordeum vulgare*) sucrose transporter 1
ICP-MS:	Inductively coupled plasma mass spectrometry.
IE(s):	Immature embryo(s)
ISAAA:	International Service for the Acquisition of Agri-biotech Applications
OsNAS2:	Rice (*Oryza sativa*) Nicotianamine synthase 2
LB:	Luria-Bertani
TSS:	Transformation & Storage Solution
Nos:	Nopaline synthase
PCR:	Polymerase chain reaction
PC2:	Physical Containment Level 2

qPCR:	Quantitative real-time polymerase chain reaction
SBE4:	Starch branching enzyme 4
SDS:	Sodium dodecyl sulphate
Tris:	Tris(hydroxymethyl)aminomethane
*uid*A:	Reporter gene encoding β-glucuronidase
µF:	microfarad
X-gal:	5-bromo-4-chloro-3-indolyl-β-D-galactopyranoside
WT:	Wild type

List of publication

Thanh Hai Tran, My-my Huynh, Carly Schramm, Georgia E. Guild, James C. R. Stangoulis, Colin L.D. Jenkins and Peter A. Anderson. Fe/Zn Re-distribution in Japonica and Indica Rice by Barley Sucrose Transporter Overexpression. Poster session presented at: The Plant and Animal Genome XXVII Conference (PAG), 2020 January 11-15; San Diego.

CHAPTER 1. LITERATURE REVIEW

1.1. Introduction

Micronutrient malnutrition (hidden hunger) is an urgent global health problem found in undeveloped, developing, and even developed countries. Its effects are on all age groups, but especially women of reproductive age and young children, who tend to be at greatest risk of suffering the adverse influence of micronutrient deficiency. Over two billion people in the world are affected by iron (Fe) and zinc (Zn) deficiencies (WHO & FAO 2006). As Fe plays a vital role in basic function of the human body and is a co-factor for multiple enzymes and other proteins involved in physiological processes, particularly in brain, muscle and red blood cells, symptoms of its deficiency are diverse and debilitating. The most significant health consequences include anaemia, impaired physical and cognitive development, poor pregnancy outcomes, higher risk of illness in children, lower work productivity in adults, and increased susceptibility to infectious diseases (Ciccolini *et al.* 2017; WHO & FAO 2006). According to WHO and FAO (2006), it is estimated that Fe deficiency is responsible for approximately 0.8 million deaths each year (accounting for 1.5% of total deaths in the world).

Zn, another essential micronutrient for humans, is involved in the regulation of RNA and DNA synthesis whilst also a co-factor for many enzymes critical to cellular growth and differentiation (Mayer *et al.* 2008). Zn deficiency results in impaired growth, immune dysfunction, increased morbidity and mortality rate, adverse pregnancy outcomes, and abnormal cognitive development. Zn deficiency can be a direct cause of childhood death. The issue of Zn deficiency became more urgent, when 17.3% of the world's population were found to suffer from inadequate Zn intake (Wessells & Brown 2012).

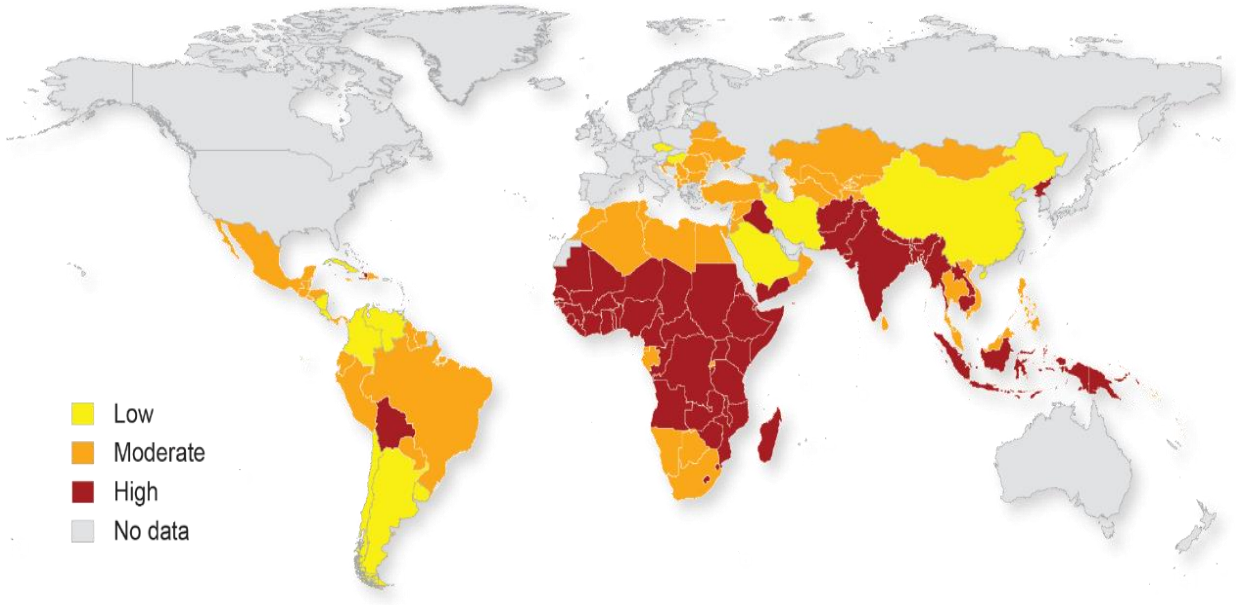

Figure 1.1. The map presenting worldwide distribution of Fe, Zn, and vitamin A deficiencies in children under 5 years old. The classification of anaemia prevalence, Zn (, and vitamin A are weighted to give the final 3-point scale of low (yellow), moderate (orange) and high (red), adapted from HarvestPlus 2012, 'Biofortification: Improving Nutrition through Agriculture', AIARD Annual Conference, Washington, DC (HarvestPlus 2012; USAID 2019).

Micronutrient deficiency not only affects human health and well-being, it also causes a heavy burden on families, communities, and countries. Micronutrient deficiency is one of the most major concerns for global food and nutritional security due to its potential to have long-term consequences. It is therefore imperative to develop an effective and sustainable solution to combat the deficiencies in Fe and Zn in much of the world's population.

As mentioned, Fe and Zn deficiencies are indiscriminate, but tend to be more prevalent in developing countries where many people consume large amounts of a single stable crop for their daily diets. If this staple is very low in Fe and Zn content and access to diverse diets with nutritious food such as fruits, vegetables and foods from animal sources are unaffordable, then deficiency is

unavoidable. In comparison with dietary diversification and supplementation with Fe and Zn fortified foods, biofortification to develop new cultivars with enriched levels of Fe and Zn via traditional breeding or biotechnology is an economically sustainable way to combat Fe and Zn deficiencies in developing countries. Biofortification is well documented to be a feasible and cost-effective solution for delivering essential micronutrients to a large population in resource-poor countries around the globe (Bouis *et al.* 2011b; Bouis & Saltzman 2017). Which crops are chosen for Fe and Zn biofortification is therefore of critical consideration if large and sustainable improvements in Fe and Zn nutrition worldwide are to be realized?

Among cereal crops, rice (*Oryza sativa* L.) is a staple food for more than half of the world's population and provides approximately 20% of dietary calories for the global population (GRiSP 2013). Unfortunately, the rice grain, especially after polishing, contains very little micronutrient content (particularly Fe and Zn) because most of the micronutrients, especially Fe are distributed in the outer layers of the rice grain where Fe and Zn form insoluble complexes with phytate and then are removed by milling. The milled rice grain (white rice) contains only 2 mg/kg of Fe and 16 mg/kg of Zn, compared with 6-24 mg/kg and 14-58 mg/kg in the unpolished grain (brown rice) (White & Broadley 2009). Thus, overdependence on rice provides levels of Fe and Zn below the minimum daily requirement for humans, that lead to symptoms of deficiency.

For rice, Indica varieties are a particularly important group because they represent roughly 70% of total rice production and more than 70% of rice trade worldwide (Mahesh *et al.* 2016; Zhang *et al.* 2016). Indica rice is mostly grown and consumed in tropical and subtropical regions where many people are significantly vulnerable to Fe and Zn malnutrition. Given its importance as a major crop and its low levels of Fe and Zn, Indica rice is an excellent candidate for

biofortification, and any improvements would have lasting and significant benefits to global food security and human health.

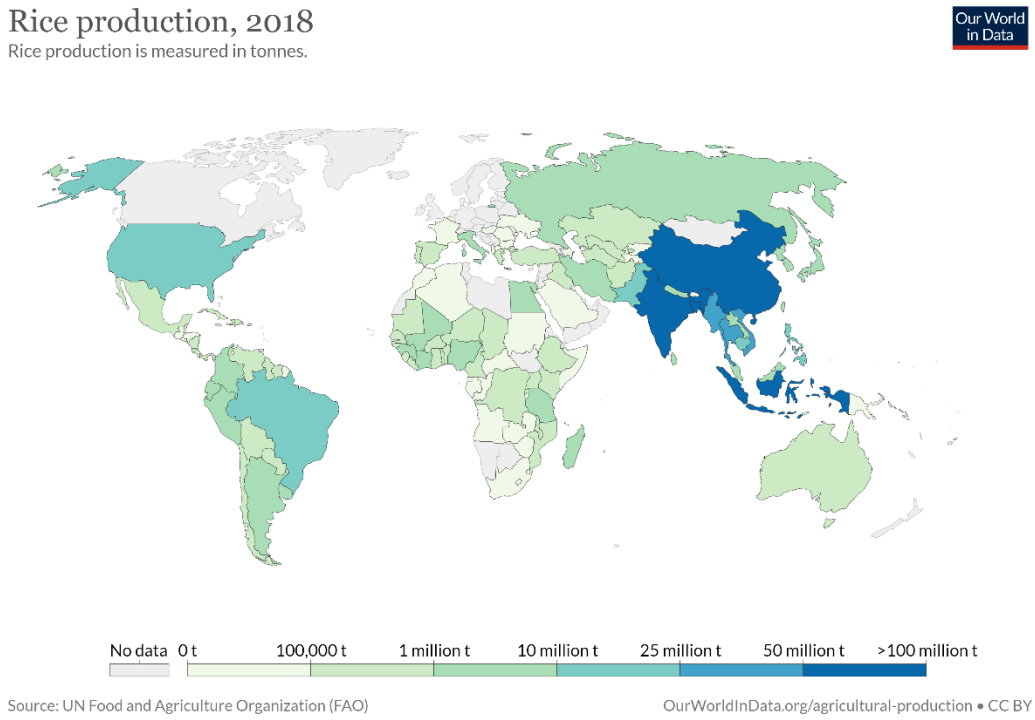

Figure 1.2. The map representing the global rice production in tones. The figure was adapted from 'Agricultural Production' by Ritchie and Roser (2020)

Fertilizer application, conventional breeding, and biotechnology have been used for Fe and Zn enrichment in rice grains, reviewed by Sperotto *et al.* (2012); Palmgren *et al.* (2008); and Nakandalage *et al.* (2016). Mineral fertilization has, however, caused much controversy due to its unsustainable effectiveness, high cost and environmental damage (Rengel *et al.* 1999). Some successes in breeding for Fe-enriched rice cultivars via traditional and molecular genetic approaches were attained, such as IR68144 with Fe concentration of 20.4 mg/kg and 16 mg/kg in unpolished and polished grains, respectively (Welch *et al.* 2000). However, the gene pool for Fe and Zn improvement from rice wild relatives is very limited. To obtain farmers' willingness to

grow new varieties, breeding for micronutrient enriched crops combined with traits of high yield should be considered. This combination of traits is difficult to achieve as many rice breeding programs that have concentrated on yield and given the negative correlation with micronutrient content, this has led to the selection of low micronutrient content in grains. It is very difficult to find a good explanation for why there is such a negative relationship between yield and nutritional quality (Liang *et al.* 2014; Uauy *et al.* 2006). This research question may become even more topical given that many important crops grown under conditions of elevated CO_2 show lower nutrient content in their grain (Loladze 2002; Myers *et al.* 2014). Rice is a typical example of this phenomenon with significant reductions in protein (10.3%), Fe (8%), and Zn (5.1%) in the grain of plants grown in CO_2 concentration approximately 50% higher than the current atmospheric conditions (Zhu *et al.* 2018). This observation will only exacerbate the problem of global micronutrient malnutrition (Beach *et al.* 2019; Smith & Myers 2018).

Most nutrients, including sugars, amino acids, minerals, and micronutrients are translocated through a common phloem pathway from source supply to recipient sink (such as grains). Although the overall pattern of translocation in the phloem can be as simple as source-to-sink translocation, the specific pathway for different solutes is often very complex. Not all nutrients are equally transported into all sinks in a plant, and it depends on the stages of plant development and how a sink and source communicate. Thus, certain sinks are preferentially supplied with nutrients at different stages of growth. For instance, grains would be the predominant sink for nutrient translocation at the reproductive stage where the sink strength is more likely to be stronger to mobilise the nutrient flow toward itself, rather than other parts of the plants such as the shoots or roots. How a plant can sense and regulate nutrient flow into the appropriate sink

organs at the appropriate time is an intriguing question. It is not surprising that sucrose serves as one of the chemical signals involved in source-sink communication (Yu *et al.* 2015).

For sucrose translocation, the phloem pathway is a critical means of communication between source and sink, acting to coordinate the rate of loading and unloading of sucrose at source leaves and sink ends of the phloem pathway, respectively. This establishes a difference in hydrostatic pressure to drive the nutrition flow from source to sink (Patrick & Offler 2001; Patrick *et al.* 2015). At different stages of plant development, the rate of sucrose translocation between competing sinks is positively determined by the hydrostatic pressure difference of each sink. The translocation rate of sucrose to the seed sink is regulated by the sink's capacity to accumulate/metabolise/store sucrose (sink strength). Manipulation of the sink strength via over-expressing sucrose transporters (SUTs) could enhance the translocation rate of sucrose into the sink. Consequently, a range of sucrose metabolic processes in the sink are triggered for rapid utilisation and storage of sucrose (increasing sink activity), and perhaps other nutrients as well. Because sucrose (along with potassium) is the major osmotic species of phloem sap, a further consequence of increasing sucrose uptake could be to change the translocation rate of other minor osmotic species (micronutrients). Attainment of higher yield in the edible part of crop plants are primary goals that are, in part, dependent on carbohydrate uptake and partitioning. Thus, improving sink strength via overexpressing SUTs could be a relevant and novel strategy for better yield and nutrition in the grain, often the edible portions of a crop plant.

In the last several decades, many biochemical and molecular advances in our knowledge of cell-to-cell and long-distance translocation of macronutrients (like sugar and amino acids) and micronutrients (like Fe and Zn) in plants have been made. These advances provide a better picture of nutrient translocation in the phloem and together provide important alternative opportunities to

modify acquisition and translocation pathways to improve yield and nutritional quality in crop plants. Altering the expression of critical components involved in the translocation of nutrients is a basic premise to uncouple the inverse correlation between yield traits and nutritional quality in an edible part of a plant like rice. Although an increasing number of studies have been reported to achieve these outcomes, not all have been successful under all circumstances, particularly in the field trials. In many cases, the difference between laboratory-based studies and field trials remains unclear. What is clear is that a greater understanding of the physiological and biochemical processes of macro- and micro-nutrients translocation and signalling is required if novel avenues for improving yield and nutritional quality are to be realised. Therefore, the first objective of this review is to briefly summarise current understanding and knowledge of sugar (sucrose) transport and signalling. Secondly, an updated understanding of key components and molecular mechanisms for Fe/Zn translocation from source to sink at the cereal grain filling period. Thirdly, to provide a picture of the dynamic process of mineral translocation into the grain. In addition, the review will venture into genetic engineering approaches for improving micronutrients partitioning to the grain, all the while focussing attention on rice. Finally, a framework for the aims and hypotheses of this thesis and the context for this research will be presented.

1.2. A mass flow model for remobilisation of assimilated solutes from source to sink tissues

The assimilated solutes that are translocated to the phloem are remobilized via the phloem from the source supply (such as leaves and roots), to the sinks (such as roots, tubers, developing fruits/seeds and immature leaves). In the sinks, metabolism or storage of translocated assimilates takes place. Phloem tissue in angiosperms consists of sieve elements (SEs), companion cells (CCs) and phloem parenchyma cells (PP) (Patrick & Offler 1995; Van Bel 2003). Adjacent SEs are interconnected via sieve pores at their terminal ends. Regarding their morphology, SEs and CCs

undergo two opposite pathways of differentiation. Although both cells originate from a similar mother cell, mature SEs retain a minimal cellular organisation, losing most of the organelles found in living cells such as the nucleus, tonoplast and ribosomes, while mature CCs remain alive having a normal suite of organelles (Van Bel 2003). However, functional as well as physical association of CC and SE is crucial because CCs are considered as a main supply of essential compounds for the growth of SEs via the many plasmodesmata on the membranes of adjoining cells. Their close relationship is referred to as the sieve element/companion cell complex (SE/CC complex) (Aoki *et al.* 2012).

The model of pressure-driven mass flow explains the mechanism of transport in angiosperms through the phloem continuum. This model, first presented by Ernst Münch in 1930 (cited in Taiz and Zeiger (2010)), has been accepted widely by many researchers. The model argues that remobilization of solutes is controlled by three overlapping functional regions in the phloem system. First, solutes are released from the source to collect into the small veins of leaves (collection phloem/ phloem loading). Second, these solutes are transported in the sieve tube continuum by transport phloem to the sink where, third; the solutes move from the phloem into surrounding cells of sink tissues for metabolism or storage (phloem unloading) (Van Bel 2003). Among the three regions, the transport phloem accounts for the largest proportion of the phloem system in a plant (Van Bel 2003). For transport phloem, the pressure-driven flow model elegantly explains the passive mechanism of solutes transport. At phloem loading in the source, as consequence of solutes collection into SEs, the concentration of solute increases, then generating a gradual decrease in water potential in the SE. As the water potential is lower in the SE tube than in the adjacent xylem system, water from the xylem moves into the phloem generating an increasing turgor pressure. In contrast, a decrease in solutes concentration in SEs at the sink due

to unloading phloem leads to low turgor pressure in these SEs at sink. The difference of hydrostatic pressure in SEs between sink and source propels the bulk flow of solutes from the sinks to the source. During long-distance transport of solute in the SE network, the flow of solutes passes through the sieve plates along the SE system. The role of the sieve plate is not fully understood but may act as a valve to maintain the gradient of solute concentrations formed along the transport phloem that is separated by these sieve plates. The resistance of sieve plates may not only produce, but also maintain, the gradient of solute concentration in the transport phloem assisting the correct partitioning of solutes.

1.3. Long-distance transport of sucrose

In early research on the mobilisation of solutes in phloem loading and unloading, both passive and active mechanisms - symplasmic and apoplasmic loadings were identified. Apoplasmic and symplasmic movements are used in different combinations in different species. However, recently an additional mechanism called symplasmic polymer trapping has been recognised in some other species (De Schepper *et al.* 2013). The three mechanisms of solute translocation in phloem loading, phloem transport and phloem unloading are discussed in the next sections.

1.3.1. Mechanisms of solute transport in phloem loading

Symplasmic phloem loading is also known as passive symplasmic diffusion. In species that use symplasmic loading, the assimilated solutes such as ions, sugar, hormones, and amino acids in mesophyll cells are passively loaded into the phloem by bulk flow. This (flow model) strategy was recognised by Turgeon et al (2010). In this process, the concentration of solutes is highest in photosynthetic cells, gradually decreasing to the lowest point at the phloem. In addition, the study of the leaf anatomy showed the regular presence of plasmodesmata at CC/SE complex interface

(Braun *et al.* 2014). Through these plasmodesmata, solutes continue their diffusion route to the lowest concentration in the phloem. This process is passive, requiring no energy to transport the solutes. The driving force for transport is generated from the difference in solute concentration between photosynthetic cells and the SEs.

The second mechanism is polymer trapping which is utilised to translocate mainly the raffinose-family oligosaccharides (RFOs) such as raffinose, stachyose and verbascose as well as sucrose, and is found in some species of Cucurbitaceae and Lamiaceae (Aoki *et al.* 2012). Here the plasmodesmata are abundant at the companion cell/ phloem parenchyma cell (CC/PP) complex interface of phloem tissue. Low molecular weight sugars, including sucrose that are synthesized in the mesophyll cells diffuse into intermediate cells (ICs) which are a special kind of CCs. In the cytoplasm of the ICs, larger carbohydrates, such as RFO oligosaccharides, are synthesized from these lower molecular weight sugar molecules, and transported into SE through plasmodesmata which connects between the SEs and the ICs. The size exclusion limits of plasmodesmata interconnecting IC/SE allow RFO transit but the size exclusion limits of plasmodesmata interconnecting MC/IC are smaller only allowing sucrose transit while preventing back diffusion of the larger RFO molecules (Zhang & Turgeon 2018).

The third mechanism is called apoplasmic loading and is used by some species of Apiaceae and Rosaceae to load sugar alcohols such as sorbitol and mannitol. In this form of transport, phloem cells have few plasmodesmata at the CC/PP interface (Braun *et al.* 2014). Thus, solutes are not transported by the symplasmic route from MC to SE. In apoplasmic species, solutes are symplasmically moved from the site of synthesis into bundle sheath cell (BSC) via PP; however, in order to load solutes into the SE, the process of apoplasmic phloem loading is required. Here, the export of solutes into the apoplasm occurs via specific proteins such as *Sugar Will Eventually*

be Exported Transporters (SWEETs) (Chen *et al.* 2012) which are probably located on the plasma membrane of phloem parenchyma cells. Afterwards, the solutes are imported again at the CC/SE complexes via membrane proteins prior to phloem transport. These membrane proteins are sucrose transporters, for example, SUT1, studied in the research presented here (Hirose *et al.* 1997). The mechanism of apoplasmic flow requires energy in the form of ATP to move the solutes from a low concentration to a high concentration, via changes in electrochemical potential. Apoplasmic loading species are able to attain a very high concentration of sucrose in SE cells (>1M) (Berthier *et al.* 2009). Anatomical analysis shows that CCs in species that use the apoplasmic route have many specific features such as numerous cell wall invaginations to increase the plasma membrane surface and few PD at the interface. To date, the mechanisms described above are the three main routes in long-distance transport in plant (Julius *et al.* 2017). Each plant species utilize one or a combination of these loading mechanisms (Braun *et al.* 2014). Hence, for the purposes of manipulating this system for biofortification purpose, it is important to determine the predominant mechanism of phloem loading in the plant species under study.

1.3.2. Source of imported sugar into sink grain

The autotrophic, photosynthetic fixation of carbon dioxide into sugar takes place in the mesophyll cells (MC) of the leaf. Subsequently, the sugar is transported into BSC and PP via plasmodesmata (PD). The PD pores are in the cell wall of MC to symplasmically connect the cytoplasm of adjacent cells such as BSC and PP, prior to transport of sugar into the leaf veins for phloem loading. In most herbaceous crop species, sucrose is considered as the sole transported sugar in the phloem (Zhang & Turgeon 2018). In the developing seed, the sucrose photosynthesized in proximal leaves is the principal source supply for metabolism and storage in the seed, while sucrose from photosynthesis in the reproductive structure is very limited (Zamski

& Schaffer 1996). In rice, leaf sheaths (especially the second leaf sheath below the flag leaf) and the flag leaf sheath serve as major sources of sugar, which is remobilised and transported into grains during grain filling (Hirose *et al.* 1999). For cereal crops, the remobilization of stored sucrose plays a decisive role in final grain weight.

1.3.3. Phloem loading of sucrose in rice

Most graminaceous plants use the active apoplasmic mechanism to transport sucrose from mesophyll cell (MC) to the phloem (Figure 1.3A) (Aoki *et al.* 2012)**.** Because rice is one of the most important staple crops in the world, the mechanism of phloem loading in rice has received considerable attention from its anatomy and physiology to its molecular biology and these features will be summarised below.

Many anatomical studies, although useful, have not provided a clear explanation of the predominant mechanism of phloem loading in rice. Kaneko *et al.* (1980) (cited by Braun *et al.* (2014)) used transmission electron microscopy to suggest the symplasmic route of sucrose remobilization into the phloem. However, four years later, the method used on rice leaf sheaths showed that the CC/SE complex is located near the apoplasmic space and that sucrose is likely transported via the apoplasmic route before it is moved into the transport phloem (Chonan *et al.* 1984). Later, Botha and Evert (1988) (cited by Braun *et al.* (2014)) suggested that sucrose synthesized from MC was loaded into the vein via the symplasmic route due to the presence of PD. Collectively, these data suggest that symplasmic loading is occurring in rice, but most likely is a minor contributor, compared to apoplasmic loading. In general, apoplasmic loading species have fewer PD at the CC/SE interface (De Schepper *et al.* 2013), however, it is difficult to determine the predominant phloem loading mechanism by anatomy alone and, thus other physiological and molecular analyses are needed.

The focus of physiological research into phloem loading has been on determining the difference in sucrose concentration between photosynthetic cells and the phloem. The procedure of aphid stylectomy has greatly assisted in this knowledge by obtaining pure phloem sap for accurate measurement of sucrose concentration**.** Hayashi and Chino (1990) reported that sucrose is the sole sugar in the phloem sap of rice, ranging from 205mM to 754mM. However, the sucrose concentration in MC were not reported in this study making it difficult to speculate about the mechanism of phloem loading in rice basing on physiology.

In apoplasmic phloem loading species, efflux and influx transporters of sucrose in the membrane of the CC/SE interface play an extremely important role in sucrose translocation in phloem tissue. Hence, when the *OsSUT1* cDNA from rice leaves is successfully cloned by Hirose *et al.* (1997), high expression of *OsSUT1* in leaf sheath cells was found and this expression was affected by the development of sink tissues (Hirose *et al.* 1997). This points to the apoplasmic route in phloem loading of sucrose mediated by sucrose transporters on the plasma membrane.

In order to further examine the involvement of the apoplasmic mechanism in phloem loading in rice, the anatomical distribution of *SUT* expression was needed. *OsSUT1* expression is localized in the leaf blade and leaf sheath of rice but was identified to have higher expression in the leaf sheath than on leaf blade (Hirose *et al.* 1997). In situ hybridization of the SUT1 mRNA showed expression in the CCs of the phloem in the leaf sheath (Matsukura *et al.* 2000). In a similar study by Scofield *et al.* (2007), the presence of the OsSUT1 protein was observed in SEs, CC and peripheral cells of the phloem of the flag leaf blade and the flag leaf sheath. Based on localization of mRNA, the product of the *OsSUT1* gene is suggested to function in transport of sucrose.

To gain a clearer understanding of the role of OsSUT1 in rice, two independent studies used reverse genetics to generate transgenic rice with an antisense version of *OsSUT1* under

control of the *CaMV35S* promoter. The data showed a decrease in OsSUT1 content, but this was unlikely to cause the effects on carbohydrate accumulation and photosynthetic capacity in the rice flag leaf (Ishimaru *et al.* 2001; Scofield *et al.* 2002), but led to damaged grain yield and germination (Scofield *et al.* 2002). This might be due to inadequate expression of antisense *OsSUT1* for repression of *OsSUT1* in leaf (Braun *et al.* 2014; Scofield *et al.* 2002), or other *SUT* genes compensating for the loss of *OsSUT1*. In fact, along with *OsSUT1*, four additional *SUT* genes in the rice genome were identified, namely *OsSUT2*, *OsSUT3*, *OsSUT4* and *OsSUT5* (Aoki *et al.* 2003).

Another explanation might be that the transport of sucrose in rice from photosynthetic cells to the phloem is preferentially carried out through the symplasm, whereas the apoplasmic route acts to a lesser extent. This explanation is consistent with previously published analysis in phloem tissue (Ishimaru *et al.* 2004; Scofield *et al.* 2007). In these studies, it is suggested that sucrose is transported from MC to phloem via the symplasmic pathway and the preferential role of OsSUT1 is in retrieval of leaked sucrose from the apoplasm (Eom *et al.* 2012; Ishimaru *et al.* 2004; Scofield *et al.* 2007). However, a report of Wang *et al.* (2015a), who generated transgenic rice over-expressing the *Arabidopsis* sucrose transporter (*AtSUC2*) in the companion cells of the phloem as a crucial step to enhance the sucrose translocation from the leaves to the phloem suggested an apoplasmic pathway for sucrose loading to the phloem. Another reports of Wang *et al.* (2021) also highlighted a vital role of apoplasmic phloem loading in the export of sucrose from rice leaves. Taking all these data together, it seems likely that the mechanism of phloem loading from leaf blade to the phloem in rice seems to be a combination of the symplasmic and apoplasmic pathway (Figure 1.3A).

1.3.4. Transport phloem

Phloem loading of sucrose is finished in minor veins of the leaf, followed by the collection of solutes into veins through a vein network (Figure 1.3B). The solutes are continuously transported through sieve tubes with arrays of sieve plates along the phloem pathway. This process is named as transport phloem (Van Bel & Hafke 2005). During the process of transport phloem, appreciable amounts of translocating solutes leak into the apoplasmic space along the sieve tubes, yet is subsequently reloaded into the proximal sieve tube via sucrose/H+ symporters located along the pathway (Aoki *et al.* 2012; De Schepper *et al.* 2013; Thorpe *et al.* 2005). This process is called the leakage-retrieval mechanism of the transport phloem and has been demonstrated in several studies using ^{14}C-labelled sucrose (De Schepper *et al.* 2013; Thorpe *et al.* 2005). A suggestion is that the role of the leakage-retrieval mechanism might be to maintain the turgor pressure along the transport phloem (Van Bel 2003; Van Bel & Hafke 2005). It is believed that the apoplasmic corridors along sieve tubes might be narrow enough to reduce turgor pressure arising at the sieve plates (De Schepper *et al.* 2013; Van Bel 2003). The leakage of solutes might play a role in storage of excess assimilates in parenchyma cells in order to regulate the turgor pressure caused by the increasing translocation from source to sink.

The SE/CC complex in transport phloem under normal conditions is symplasmically isolated from surrounding cells and only a few plasmodesmata are observed between SE/CC complex and PP (Van Bel 2003). Therefore, the solutes leak from sieve tubes into the apoplasmic space along the phloem via passive diffusion (De Schepper *et al.* 2013; Thorpe *et al.* 2005). In contrast, in order to reload the leaked solutes, an active process known as retrieval mechanism is performed via plasma membrane proteins in the SE/CC complex. This process requires energy to recover the leaked solutes from the low concentration in the apoplasm to a high concentration in

the sieve tube (De Schepper *et al.* 2013; Thorpe *et al.* 2005). A sucrose transporter is responsible for transport of sucrose into the sieve tube. The localization of SUTs in the SE/CC complex along the transport phloem has been reported in a number of plant species. For wheat and rice, TaSUT1 and OsSUT1 have been positioned in the SE/CC complex respectively (Aoki *et al.* 2003; Aoki *et al.* 2004). In particular, the role of OsSUT1 is suggested in the retrieval of leaked sucrose in phloem loading of rice leaves (Scofield *et al.* 2007).

1.3.5. Phloem unloading and post-phloem transport in sink.

Following phloem transport via sieve tubes, the solutes are transported into non-photosynthetic tissue (sink) such as developing grains, young leaves, roots, and reproductive tissue. While the pathway of phloem loading in rice is unclear and controversial, the understanding of sucrose transport into the rice grain is far clearer than for some other higher plants. In all angiosperm species, the filial tissue and maternal tissue of the grain is separated by an apoplasmic space (Aoki *et al.* 2012; Oparka & Gates 1981b). Consequently, the apoplasmic route is formed and no plasmodesmata are present to connect between these tissues after fertilization (Patrick & Offler 1995).

During development of the rice grain, the solutes are transported into the vascular bundle terminal of the phloem pathway. Due to the symplasmic discontinuity between maternal and filial tissues, the solutes are first unloaded from the nucellus cell layer of maternal tissue into the apoplasmic space. The solutes then move into the filial tissue through the aleurone/subaleurone layer surrounding the endosperm of grain (Aoki *et al.* 2012; Oparka & Gates 1981b; Patrick & Offler 1995). This process is known as phloem unloading (Figure 1.3C) and takes place in the pericarp vein on the top of the grain via the apoplasmic pathway (Furbank *et al.* 2001). The analysis of cellular development in the grain, reported by Furbank *et al.* (2001), reinforce that the maternal

tissues is separated from filial tissues by the apoplasm. In the vascular bundle region, the pigment strand is underlaid by nucellus projections (Oparka & Gates 1981a). The nucellus extends laterally from the inner cells of the nucellus projection region, to a single layer of cells with increasing distance from the vascular bundle region and encloses the filial tissue. A cuticle is formed at the pericarp/nucellus boundary. The nucellus/nucellus projection consist of many small, densely cytoplasmic cells which are adjacent to the multiple aleurone/subaleurone of filial tissue. A symplasmic route exists between the SE/CC complex and nucellus, while the symplasmic discontinuity between nucellus and aleurone cells is observed (Furbank *et al.* 2001; Oparka & Gates 1981b). The aleurone cells and endosperm of filial tissue are connected via the symplasm, but based on anatomical analysis, an apoplasmic mechanism is proposed in the transport of solutes between maternal and filial tissue, for instance of sucrose translocation. Effluxers such as the SWEET 11 and/or SWEET15 proteins (Chen *et al.* 2012; Ma *et al.* 2017; Yang *et al.* 2018) on maternal cells and an influxer (for example OsSUT1) on filial cells are suggested to facilitate this transport.

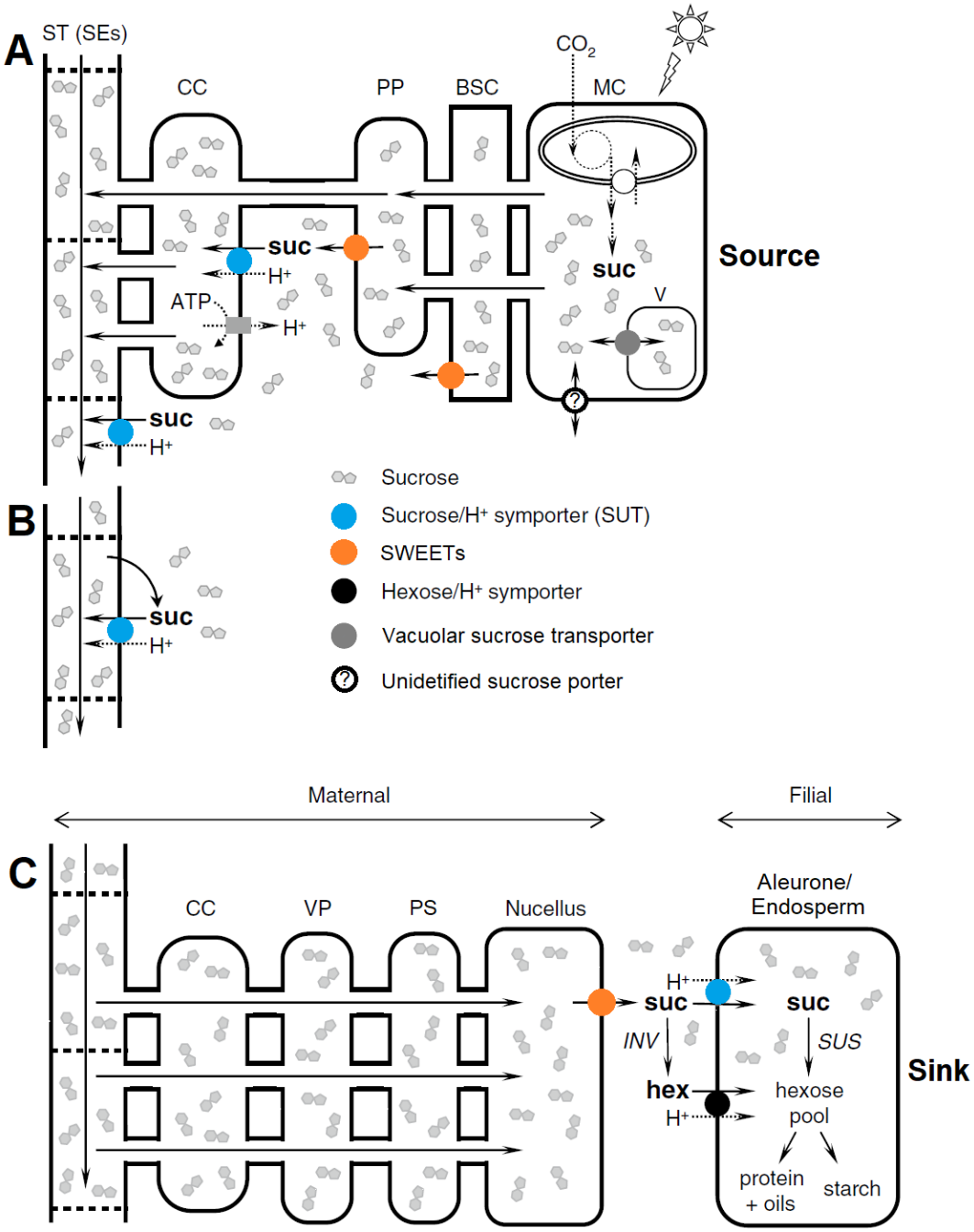

Figure 1.3. Long-distance transport of sucrose from source leave to sink grain. The model was updated from Aoki *et al.* (2012). **(A)** Phloem loading: Sucrose move symplasmically from the cytosol of mesophyll cell, where sucrose is produced by photosynthesis, to the bundle sheath cell (BSC) and the phloem parenchyma (PP) through plasmodesmata. For temporal storage, sucrose is transported into the vacuoles (V) of mesophyll cell, then exported into the cytosol before further

translocation via vacuolar sucrose transporter, OsSUT2 (Eom *et al.* 2011) (grey open circle). Sucrose moves continuously the sieve element/companion cell (SE/CC) complex via a combination of the symplasmic and apoplasmic pathway in rice, sucrose is translocated into the SE/CC complex via apoplasmic route by SWEETs (orange open circle) and SUT1 (blue open circle) transporter which localise to the SE or the CC**; (B)** Transport phloem: Sucrose is translocated to sink tissues through the sieve tube (ST) continuum. OsSUT1 is present in the phloem and plays a role in retrieving sucrose leaked out of the phloem tubes; **(C)** Phloem unloading/post-phloem (example for rice): First, sucrose from the phloem tubes moves out of the phloem tubes to maternal tissues (the CC, the vascular parenchyma (VP), the pigment strand (PS), and nucellus cells) via symplasmic routes. Second, sucrose is exported to the apoplasmic space via OsSWEET11 or/and OsSWEET15, and then imported into filial tissues (aleurone/endosperm cells) via OsSUT1, or via hexose/H^+ symporter following cleavage by cell wall invertases (INV).

1.3.6. Predicted structural models of sucrose transporter.

Hundreds of sucrose transporters (SUT) from many plant species have been reported and their sequences can be found in public databases. Based on phylogenetic analysis of the amino acid sequences of these protein, three (Aoki *et al.* 2012; Lalonde *et al.* 2004), four groups (Sauer 2007), or five groups (Kühn & Grof 2010) have been described. In general, SUTs from dicot species are classified in one group, which are functionally characterised as sucrose transporters, such as AtSUC5 from *Arabidopsis* (Nühse *et al.* 2004), JrSUT1 of walnut (*Juglans regia* L.) (Decourteix *et al.* 2006), NtSUT3 from tobacco (Lemoine *et al.* 1999) and VfSUT1 from fava bean (*Vicia faba* L.) (Weber *et al.* 1997). Another group encompasses monocot SUT sequences responsible for sucrose translocation, including ZmSUT1, OsSUT1, ShSUT1 and HvSUT1 from maize, rice, sugarcane, and barley, respectively (Aoki *et al.* 1999; Hirose *et al.* 1997; Reinders *et*

al. 2006; Weschke *et al.* 2000). Group 3 (often added into the monocot's SUT group) were named SUT2/SUT3 group. Group 4 encompasses SUT4 sequences (named SUT4 group). Both these groups contain SUTs from monocot and dicot species. Group 5 including SUT5/SUT6 sequences was classified to be monocot-specific clade (for example ZmSUT5 (ACF85284) and ZmSUT6 (ACF85673)) (Kühn & Grof 2010). Alignment analysis of identical amino acid is not easy to predict their physiological functions.

Structural investigations of the sucrose transporter have been carried out on only dicot plant species, including spinach, *Arabidopsis* and *Plantago major* (Riesmeier *et al.* 1992; Sauer & Stolz 1994; Stolz *et al.* 1999). These three independent analyses of sucrose transporters have confirmed a structural model of 12 transmembrane helices with C-terminal and N-terminal projections on the cytoplasmic side of the plasma membrane (Figure 1.4). All recent reviews have agreed with this structural model and that transport of sucrose is carrier-mediated by probably 1:1 sucrose/H+ co-transport dependent on ATPase activity (Wang *et al.* 1995). In the review of Sauer (2007), the structural model of SUTs from group 1 and 2 were proposed to fit the same model so all SUTs may share a similar 3D model.

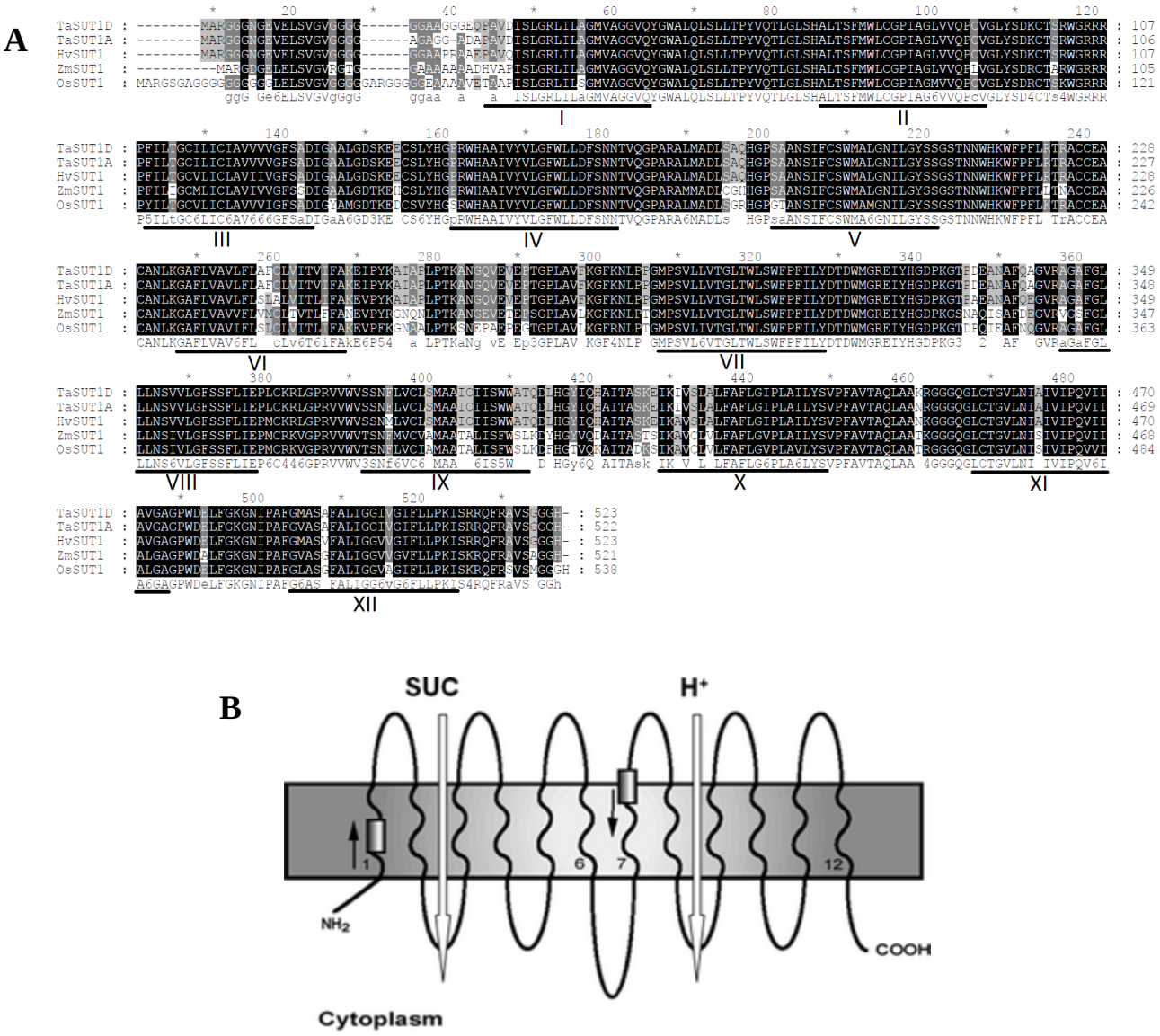

Figure 1.4. Alignment of amino acid sequence of HvSUT1, OsSUT1, ZmSUT1, TaSUT1A, and TaSUT1D was performed by GeneDoc. A. High level of conservation between residues in rice and maize, barley and wheat showed similarity of 84%, 82%, and 81%, respectively. The three shade levels represent degrees of conservation from 100, 80 and 60%. Twelve predicted transmembrane helices in the OsSUT1 protein (Hirose *et al.* 1997) are underlined and numbered in Latin numerals. Accession numbers of HvSUT1, OsSUT1, ZmSUT1, TaSUT1A, and TaSUT1D are Q9M422, Q9LKH3, Q9SXM0, AAM13408, and AAM13410, respectively. **B**. Predicted

structural model of plant sucrose transporter with the twelve transmembrane helices, and both C and N termini on intercellular side (Aoki *et al.* 2012).

1.3.7. Role of sucrose/proton symporter in phloem unloading.

In general, the post-phloem transport of sucrose in monocots has still received only limited attention. However, a proposed pathway of sucrose uptake into the endosperm of cereal grains is considered to be similar to that of dicotyledonous seeds (Aoki *et al.* 2012). The apoplasmic pathway requires an efflux transporter on the nucellus cell membrane to export sucrose into the apoplasm and an influxer on the aleurone cell membrane to import sucrose into the endosperm of the grain.

In 1995, a general model for the pathway of sucrose transport in the developing grain of cereal species was reported by Patrick and Offler (1995). An influxer on the plasma membrane of filial tissue cells was thought to be responsible for sucrose uptake and to be energy-dependent (Patrick & Offler 1995). Fortunately, cDNA encoding OsSUT1 which is considered to be responsible for sucrose transport was cloned (Hirose *et al.* 1997). *OsSUT1* expression was shown to be at its highest in the aleurone/subaleurone layer of filial tissue during grain filling and OsSUT1 was proposed to localize on the aleurone layers of the rice endosperm tissue (Furbank *et al.* 2001). Interestingly, Furbank et al. (2001) also showed by using radioactively labelled sucrose in the presence and absence of para-Chloromercuribenzenesulfonic acid (pCMBS), a potent inhibitor of sucrose transporter activity, the rate of sucrose uptake into the grain is modified during the filling stage. All these data support the role of sucrose uptake by OsSUT1 into the rice endosperm of developing grain.

In order to test the hypothesis that OsSUT1 is responsible for sucrose uptake in the grain, two independent analyses using antisense repression of *OsSUT1* gene expression under the

regulation of *35S* promoter were carried out, and the results were very similar (Ishimaru *et al.* 2001; Scofield *et al.* 2002). The plants expressing *35S::antisense OsSUT1* had reduced ability to fill grains resulting in a significantly lower final grain weight. Damage was also evident in the grain phenotype (Ishimaru *et al.* 2001; Scofield *et al.* 2002). These studies support the hypothesis that OsSUT1 plays a critical role of sucrose uptake capacity of grain.

Along with *OsSUT1*, the rice genome contains four additional sucrose transporter genes. Among them, *OsSUT3*, *4* and *5* were considered to be involved in supply to growing tissues and temporary storage tissues (Aoki *et al.* 2003). Unlike the other four *SUT* genes, *OsSUT2* expression was found to be equivalent in all tissues that were analysed. Therefore, the specific role of *OsSUT2* remains difficult to assess. Subsequently, transgenic rice expressing a construct of the *OsSUT2 promoter::GUS* gene was generated to observe its expression pattern. The result showed that *OsSUT2* was strongly expressed in the MC of rice leaves (Eom *et al.* 2011). A further analysis on transgenic rice with a T-DNA insertion containing *OsSUT2*, under the control of a constitutive over-expression promoter, showed an increase in soluble sugar concentration and a reduction in sugar export from leaves. The authors suggested that *OsSUT2* serves as a vacuolar sucrose transporter and plays a possible role to export sucrose from the vacuole to the cytosol of MC, prior to phloem loading (Eom *et al.* 2011). Of all the *OsSUT* genes, *OsSUT1* is the likely candidate to transport sucrose across the aleurone/subaleurone membrane from the apoplasm to the endosperm of filial tissue during grain filling.

The second cDNA of a monocot sucrose transporter to be cloned was the maize *ZmSUT1* (Aoki *et al.* 1999). Unlike other cereal crops, *ZmSUT1* does not seems to be preferentially involved in sucrose uptake into endosperm tissue during grain filling, due to its expression in a variety of tissues of the whole plant, especially in mature leaves. Similar results were seen by Slewinski *et*

al. (2009). Thus, *ZmSUT1* probably plays an important role in phloem loading in maize leaves, although there are no definitive reports that confirms or refutes the role of *ZmSUT1* in the sucrose uptake during filling grain (Baker *et al.* 2016).

In the barley genome, there are two members of the *SUT* gene family, namely *HvSUT1* and *HvSUT2* (Weschke *et al.* 2000) which were cloned from barley caryopses tissue. Although both of them have sucrose uptake activity under heterologous expression in yeast cells, and their expression was observed in maternal and filial tissues of the caryopses, *HvSUT1* was suggested to preferentially function in sucrose import into the endosperm during grain filling (Weschke *et al.* 2000). This is verified by the following four pieces of evidence:

(1) *HvSUT1* expression is preferentially detected on the nucellus projection and endospermic layers where the sucrose uptake into grain takes place, while *HvSUT2* expression was detectable in all tissue of the source and the sink (Weschke *et al.* 2000). (2) An alignment of the primary sequence of all *SUT* genes from 38 species revealed that *HvSUT1* had a close similarity with *OsSUT1* from rice and *TaSUT1* from wheat, while *HvSUT2* belonged to a different clade of the phylogeny tree (Aoki *et al.* 2012; Weschke *et al.* 2000). (3) A positive correlation exists between *HvSUT1* expression and sucrose level in barley caryopses (Weschke *et al.* 2000). (4) With *HvSUT1* over-expression in transgenic rice and wheat under the regulation of endosperm specific promoters, an enhancement in sucrose concentration in transgenic grains was reported, compared to their non-transgenic controls (Huynh 2015; Saalbach *et al.* 2014; Weichert *et al.* 2010; Weschke *et al.* 2003). Therefore, *HvSUT1* is strongly implicated to play an important role in sucrose import to the endosperm during grain development, while *HvSUT2* was considered as a housekeeping gene (Saalbach *et al.* 2014; Weschke *et al.* 2000) and/or acts as a vacuolar sucrose transporter (Endler *et al.* 2006).

1.3.8. Role of SWEET transporters in sucrose translocation.

In the general model for sucrose transport in monocotyledonous plants, an effluxer of sucrose in the maternal cell layer membrane is required to export sucrose into the apoplasm (Van Bel 2003). The understanding of which transporter protein facilitates sucrose export remained unclear for many years. Because the translocation of sucrose into the endosperm is discontinuous, exported into the apoplasm is considered a prerequisite to import by SUT1. Chen *et al.* (2012) filled the gap of knowledge in long-distance transport when they reported the SWEET proteins that are involved in sucrose export into the apoplasm prior to its uptake by SUT1 in the apoplasmic pathway.

In *Arabidopsis thaliana*, a screening for sucrose efflux capacity of approximately 50 genes encoding membrane proteins was carried out in a human cell line which lacked the activity of sucrose transport. As a result, AtSWEET10-15 could transport sucrose across the membrane, especially AtSWEET11 and 12, which were considered to be promising candidates in sucrose efflux. This was due to their high expression in parenchyma cells proximal to the CC/SE complex of leaves and their co-expression with genes involved in phloem loading in leaves (Chen *et al.* 2012). Mutant plants with T-DNA interruption of both *AtSWEET11* and *AtSWEET12* showed an adverse impact on their growth (Chen *et al.* 2012). However, the separate mutant plants with T-DNA insertion of *AtSWEET11* or *ATSWEET12* had no different phenotype to wild type plants. According to Braun (2012), neither *AtSWEET11* or *AtSWEET12* can be partially compensated by *AtSWEET13*.

For rice, Chen *et al.* (2012) also reported the sucrose export capacity of *OsSWEET11* and *OsSWEET14* in human cell lines expressing these genes. The authors also suggested that both these genes play a crucial role in sucrose export in leaves. However, the role of *OsSWEET* genes in the

sucrose transport during grain filling is still unclear as all experiments so far have focused on leaf tissue. Furthermore, the species using the apoplasmic mechanism in phloem loading can easily explain the role of SWEET protein in phloem loading in leaves. However, in species such as rice that may use the symplasmic pathway to load sucrose, their role seems not so crucial in sucrose export in leaves. Interestingly, *Xa13* (known as *SWEET11*), a rice gene giving susceptibility to *Xanthomonasoryzae* pv. oryzae, was up-regulated by pathogen infection because its expression is considered to be essential for bacterium growth (Yuan *et al.* 2009). A possible explanation is that microbes might stimulate the *SWEET11* expression to efflux more sucrose in to the apoplasm as a source of their nutrition (Chen 2014). This observation provides additional support for the role of SWEET11 in sucrose export into the endosperm during filling grain. Although little scientific evidence is reported, it is possible that *OsSWEET* genes are involved in phloem unloading of sucrose. Many studies on *SWEET11,* such as its cloning and localisation on the caryopses, and transgenic and mutation analyses, need to be carried out in order to verify the role of *SWEET* in sucrose export into the apoplasm during grain filling. Recently, two studies of Ma *et al.* (2017) and Yang *et al.* (2018) reinforced the role of OsSWEET11 or/and OsSWEET15 in sucrose efflux from the nucellus cells into the rice endosperm during the grain-filling stage via analyses of knockout mutant of these genes.

1.4. Source-sink regulation via sink strength and its effect on yield and nutritional quality

Regulation between sink and source is essential to determine a pattern of nutrient allocation through the plant (Figure 1.5). During the reproductive stage in rice, photoassimilates and other nutrients from the source supply are predominantly imported into the grains, rather than the shoots or roots. This source-sink regulation is driven by sink strength, defined as the competitive ability of a sink organ to import photoassimates and other nutrients (Braun *et al.* 2014; Yu *et al.* 2015).

Therefore, the sink strength is also key to drive the nutrient stream to the sink. An enhancement of a given sink, like the grain, could result in beneficial impacts, for instance grain yield micronutrient (Braun *et al.* 2014; Yu *et al.* 2015), and other nutrients like protein and micronutrient (Huynh 2015; Saalbach *et al.* 2014; Stomph *et al.* 2011; Weichert *et al.* 2010). Beside sink size, sink activity is one of the crucial parameters to enhance the sink strength through physiological capabilities (capacity of nutrient import or biosynthesis of macromolecules and storage capacity) (Bihmidine *et al.* 2013; Smith *et al.* 2018). Various strategies to increase the sink strength via sucrose manipulation have been demonstrated, including overexpression of invertase (INV), an enzyme for sucrose hydrolysis, sucrose synthase (Sus) for sucrose degradation, ADP-glucose pyrophosphorylase (AGPase), an importance enzyme in starch biosynthesis, trehalose-6-phosphate synthase (TPS) for regulation of carbohydrate metabolism, sucrose exporter (SWEET) and importer (SUT1). Amongst these, elevated expression of a sucrose transporter (*SUT1*) in the developing grains has been demonstrated to increase the sink strength through an increase in sucrose uptake. As sucrose reaches the sink cells, it initiates a wide range of metabolic processes and biosynthesis for grain growth and development, and then the transition into storage and maturation modes in the sink. Therefore, sucrose is likely to be a signal for sink-source regulation in nutrient allocation (Braun *et al.* 2014; Roitsch 1999; Yu *et al.* 2015). Enhancing sucrose uptake could positively stimulate all these processes, leading to an increase in nutrient demand for the grain sink, and other nutrients. A more detailed discussion of this can be found in Chapter 5. In general, increasing the grain sink strength is promising to improve grain yield and nutritional quality, for instance micronutrients.

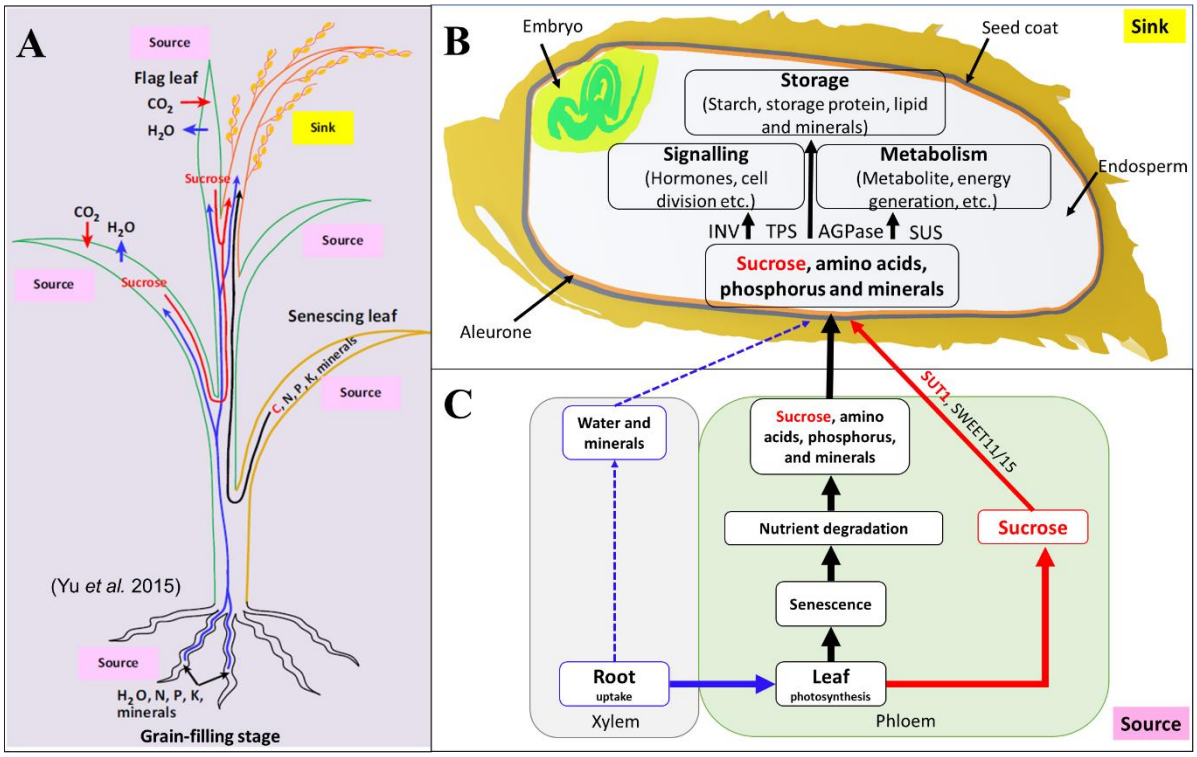

Figure 1.5. Model of assimilate translocation and sink-source communication at the grain-filling stage in rice. (A). A road map of sucrose and other nutrients translocation from different sources to the grain at grain-filling stage (Yu *et al.* 2015); (C). During the rice grain-filling stage, sucrose is translocated from mature leaves (particularly the flag leaf - main source) via photosynthesis to developing grains (sink). Other nutrients such as nitrogen (N), phosphorus (P), Potassium (K) and minerals in senescing leaves are also remobilized into the developing grains via phloem and xylem pathways. (B). The grain is the dominant sink at the grain-filling stage. Along with others nutrient, once sucrose reaches the sink cells, it triggers carbohydrate metabolism, signalling and then transition into the storage phase. These processes together determine sink strength. The red arrows present the path of direct sucrose transport from leaves via photosynthesis, black lines indicate the path of sucrose and other nutrients remobilisation from senescing leaves, blue dash lines indicate the path of water and minerals into developing grains

via the xylem, and a blue thick line indicates most of the water and minerals imported into developing seeds is delivered through the phloem. Invertase (INV), sucrose synthase (SuSy), ADP-glucose pyrophosphorylase (AGPase), trehalose-6-phosphate synthase (TPS), sucrose exporter (SWEET) and SUT1: sucrose importer.

1.5. Pathway of micronutrient translocation into rice grains.

1.5.1. Source of mineral importing to developing grains.

In contrast with sugar, micronutrients, especially Fe and Zn, are obtained from an external supply. These transition elements are imported from the soil solution to the phloem, and they are then accumulated in filial tissue of cereals (Person et al 1998). Fe plays a key role in photosynthesis during vegetative and reproductive stage. Deficiency of Fe can lead to the failure of chlorophyll function in photosynthesis, resulting in the development of chlorosis in young leaves (Bashir *et al.* 2010).

Although Fe is an abundant mineral in the soil, its phytoavailability is extremely low under neutral, basic or aerobic conditions. This is because Fe tends to be oxidised to an insoluble Fe^{3+} in iron oxide (Fe_2O_3). In the soil solution, the equilibrium constant of Fe^{3+} is approximately 10^{-17}M which is inadequate for the minimum requirement of Fe in plants (10^{-9} – 10^{-4}M) (Bashir *et al.* 2013b; Guerinot 2010). Three sophisticated strategies have evolved to absorb this essential amount of Fe from the soil for plant growth. For strategy 1, found in all plants except graminaceous species, plants lower soil pH by excretion of protons in order to increase Fe^{3+} availability in the rhizosphere. The acidification is carried out by a H^+ pump ATPase on the root cell membrane (Santi & Schmidt 2009). Once the rhizosphere is acidified, the insoluble Fe^{3+} is reduced to soluble Fe^{2+} via reduction by Ferric Reductase Oxidase. An example of this process is carried out by the *AtFRO2* gene in

Arabidopsis (Robinson *et al.* 1999). Finally, reduced Fe^{2+} is transported into root cells by a transmembrane Fe-transporter 1 (IRT1) (Eide *et al.* 1996).

While the strategy 1 species are based on reduction, strategy 2 plants excrete small molecules of phytosiderophore (PS), also called the mugineic acid (MA) family, into the rhizosphere via a Fe-regulated transporter, encoded from one member of the family TOM1/OsZIFL4. The MA molecules have a high affinity for Fe^{3+} and can combine to form a soluble Fe^{3+}-complex (such as Fe^{3+}-MA). The Fe^{3+}-complex is then transported into the root cell through a transmembrane transporter known as the yellow stripe-like (YSL)/Yellow Stripe 1 (YS1) family. For strategy 3, known as a combined strategy, the uptake of Fe is performed by both reduction and chelation-based processes. This third strategy is that found in rice (Ishimaru *et al.* 2006; Walker & Connolly 2008). The combined strategy may be employed to absorb the Fe and Zn cations via different transporter proteins.

For the Fe uptake, rice plants excrete a specific phytosiderophore- deoxymugineic acid (DMA) (Römheld & Marschner 1990) through a vesicle-mediated process (Mizuno *et al.* 2003; Nozoye *et al.* 2014a; Nozoye *et al.* 2014b). This is carried out by a Transporter Of Mugineic acids 1 (*TOM1),* or a new member of the zinc-induced facilitator-like (ZIFL) family (Nozoye *et al.* 2011; Ricachenevsky *et al.* 2011). DMA chelates soluble Fe^{3+} in the soil to form Fe^{3+}- DMA. This complex is then transported into the root epidermis via OsYSL15 (Inoue *et al.* 2009; Lee *et al.* 2009a; Palmer & Guerinot 2009). Compared to other grasses, rice release less DMA (Mori *et al.* 1991). Interestingly, in addition to the above mechanism, the rice root can also take up available Fe^{2+} in the soil. In spite of the absence of H^+ excretion and reduction by Fe^{3+} reductases in the plasma membrane, the uptake of available Fe^{2+} in rice can take place via two Fe^{2+} transporters, namely OsIRT1 and OsIRT2 (Walker & Connolly 2008). In general, the uptake Fe^{2+} and Fe^{3+}-PS

can occur in rice plants and depends on their availabilities in the soil. Due to similar chemical property of Fe and Zn, divalent cations, a strategy of Zn uptake from the soil to the roots is hypothesised to be similar.

Many Zn complexes are present in the soil and Zn solubility and availability for uptake into plants rely on many factors. Under low availability of Zn in the soil, rice plants can employ a model of the Zn uptake via two different molecular mechanisms. First is PS secretion to form Zn-PS, and second is the absorption of Zn^{2+} via the OsZIP family of proteins (Suzuki *et al.* 2008b; Welch & Shuman 1995). Interestingly, this model is similar role in Fe transport model and many components of these mechanisms could share a similar role in Fe transport, such as transporter-like protein ZIP gene family, YSL transporter gene family and PS (NA/DMA). *TOM1* and the genes of DMA biosynthesis are involved in the PS secretion to form the Zn-PS complex. This complex is transported into root cells via the YSL transporters (Bashir *et al.* 2012; Ishimaru *et al.* 2011). However, the mechanism of Zn^{2+} transport via the OsZIP proteins is more likely to be the dominant mechanism for Zn uptake through roots (Suzuki *et al.* 2008b). The OsZIP protein family in rice, namely OsIRT1, OsZIP1, OsZIP3, OsZIP4, OsZIP5, OsZIP8 and OsZIP9 have been examined for their role in transporting Zn^{2+} in roots (Huang *et al.* 2020; Ishimaru *et al.* 2007; Ishimaru *et al.* 2006; Lee & An 2009; Ramesh *et al.* 2003; Sato *et al.* 2011; Yang *et al.* 2009). Amongst these OsZIP family proteins, OsZIP1, OsZIP3 and OsZIP8 seem to be the best candidate proteins for Zn uptake from the soil because they are expressed in the root under Zn deficiency and can complement Zn-uptake deficient yeast mutants (Ramesh *et al.* 2003; Yang *et al.* 2009). Although OsITR1 overexpression led to increased Zn content in roots, it has less affinity for Zn, compared to Fe (Ishimaru *et al.* 2006; Lee & An 2009).

1.5.2. A possible pathway of Fe and Zn transport from roots to grains via xylem is poorly characterised.

After Fe and Zn uptake, they are transported symplasmically through a variety of root cells, and then loaded in the xylem (Palmgren *et al.* 2008). During the symplasmic translocation of Fe and Zn cations in the cytosol of root cells, low molecular weight chelators or organic acids (citrate or malate) bind to the Fe and Zn cations to form their soluble complexes. However, it is unclear what kind of chelators bind to metals in the roots of rice, possibly citrate as suggested by Durrett *et al.* (2007). These authors also suggest that Fe is loaded into the xylem of *Arabidopsis* plants as a ferric-citrate complex via AtFRD3. In rice, OsFRDL1, belongs to the same family of multidrug and toxic compound extrusion (MATE) transporters with AtFRD3, suggested to play a crucial role for loading Fe into the rice xylem as the Ferric-citrate complex (Inoue *et al.* 2004; Yokosho *et al.* 2009). Thus, citrate could serve as a chelator of Fe and probably Zn in the root pericycle cells with loading into the xylem done by OsFRDL1 (Palmgren *et al.* 2008). Another report of Huang *et al.* (2020) suggested that OsZIP9 localized at the root exodermis and endodermis plays a vital role in root Zn uptake.

How then are other complex forms, like Fe-DMA/NA and Zn-NA/DMA, absorbed by the YSL transporters and uploaded into the xylem? Are they loaded into the rice xylem by other transporter proteins, or converted to Fe- and Zn-citrate complexes before loading into the xylem by OsFRDL1? In *Arabidopsis*, two other proteins, AtHMA2 and AtHMA4 (HEAVY MENTAL TRANSPORTING ATPASES 2 and 4), are suggested to pump Zn into the surrounding cells of the root xylem (Hussain *et al.* 2004). The HMA protein family has been described in cereal plants (Palmgren *et al.* 2008). In rice, Takahashi *et al.* (2012a) reported nine homologs of *OsHMA* genes, *OsHMA2* belongs to the same phylogenetic subgroup with *AtHMA2* and *AtHMA4*. The expression

of *OsHMA2* was mainly observed in the rice roots and a strong loss-of-function mutation in *OsHMA2* caused Zn levels to decrease in the mutant rice leaves. Thus, OsHMA2 is likely to play a role in Zn loading into the rice xylem (Takahashi *et al.* 2012b; Yamaji *et al.* 2013). In general , Fe-citrate and Zn-citrate seem to be the more dominant complex forms for Fe and Zn transport in the xylem of rice (Abadía *et al.* 2002).

In cereals the xylem is discontinuous at the base of each single seed. Therefore, it is proposed that Fe and Zn are transferred from the xylem to the phloem before being transported into grains. However, rice is an exception. There is a xylem continuity at the base of the rice grain (Krishnan & Dayanandan 2003; Stomph *et al.* 2011; Stomph *et al.* 2009). Therefore, Fe and Zn could potentially be directly transported in the root to the grain via the xylem and translocated from the phloem as well (Sperotto 2013; Stomph *et al.* 2011; Stomph *et al.* 2009). However, the possible transport of Fe and Zn from roots to grains via the xylem is poorly characterised and should be investigated more thoroughly.

1.5.3. Fe and Zn translocation in phloem loading

While the mechanism of Fe and Zn loading into developing grains through the xylem is still unclear, Fe and Zn translocation from roots into young leaves and grains mainly occur through the phloem network (Sperotto *et al.* 2012; Tsukamoto *et al.* 2009). The Fe and Zn translocations begin with Fe and Zn unloading from the xylem, where its complexes are actively taken up by surrounding cells and then symplasmically transported into the phloem until they reach their destination in the leaves or grains. Due to differences in pH between the xylem and phloem, Fe and Zn would likely change their ligands from citrate into others like NA and DMA. So, what are the transmembrane proteins involved in their transport prior to unloading into surrounding cells?

1.5.3.1. Fe and Zn homeostasis

In the alkaline environment of the phloem sap, Fe^{2+} and Fe^{3+} ions would precipitate and be toxic to the plant (Grusak 1994; von Wirén *et al.* 1999). Thus, chelation of Fe is essential in phloem transport, and this may apply to Zn as well. For plants, the mugineic acid family of phytosiderophores (MAs) and nicotianamine (NA) are ubiquitous chelators of Fe^{3+}, Fe^{2+} and Zn^{2+}, and thus are considered as prime candidates for Fe and Zn mobilisation in phloem transport. The role of chelators is to bind Fe or Zn ions to form a stable complex at the alkaline pH of the phloem sap (von Wirén *et al.* 1999). The biosynthesis pathway of MAs has been well documented (Figure 1.6). MAs are synthesised from L-methionine where three L-methionine molecules are combined to form NA through NAS (nicotianamine synthetase) catalysis (Mori and Nishizawa, 1987; Shojima *et al*., 1990). In graminaceous species, nicotianamine aminotransferase (NAAT) subsequently catalyses the transfer of an amino group of NA to produce the keto form of NA. The resultant form is reduced to deoxymuginic acid (DMA) and other MAs by deoxymugineic acid synthase (DMAS). Both DMA and NA are suggested to be involved in Fe and Zn homeostasis in the rice phloem. For DMA, it plays a vital role in acquisition of soil Fe, and in internal Fe homeostasis in the phloem. To mobilise Fe^{3+} in long-distance transport, DMA forms a Fe^{3+}-DMA complex. Under Fe-sufficient conditions, DMA is detected in both rice leaves and roots, but the expression of *DMAS1* has only been detected in the rice roots, but not in the rice leaves (Bashir *et al.* 2006), and DMA is probably translocated from the root in a complex with Fe. In rice experiencing Fe deficiency, the concentration of DMA increases in shoots (Bashir *et al.* 2006). Furthermore, the biosynthesis of DMA is also regulated by *NAS* and *NAAT1* genes (Inoue *et al.* 2008). Using the *GUS* reporter gene, the same patterns of NASs, NAAT1 and DMAS1 expression was observed in the phloem companion cells in rice (Bashir *et al.* 2006; Inoue *et al.* 2008). These

results support the hypothesis that DMA is involved in Fe homeostasis and Fe translocation in rice. Although the analysis of a transgenic plant overexpressing the *DMAS1* gene has not been carried out, a knock-down mutant of *OsDMAS1* was investigated to highlight the important role of *OsDMAS1* in Fe homeostasis in the rice plant (Bashir *et al.* 2017).

Before an analysis of phloem sap was possible, it was very difficult to predict the chemical forms of Fe and Zn complexes in the phloem sap. Thus, several opposing predictions emerged. Based on calculations of stability constants of Fe complexed with either NA or DMA, von Wirén *et al.* (1999) predicted that NA can chelate both Fe^{2+} and Fe^{3+} in cytosolic conditions, and that Fe^{2+}-NA is more dominant than Fe^{3+}-DMA in the phloem. Reichman and Parker (2002), using similar calculations, suggested that Fe^{3+}-DMA is more abundant. Fortunately, a metabolic analysis of the rice phloem sap by Nishiyama *et al.* (2012) reported that DMA is the predominant chelator of Fe^{3+} in the rice phloem sap, and a small fraction of Fe^{2+}-NA and Fe^{3+}-citrate forms also could exist.

Similarly, NA is also proposed to be the major low molecular weight chelating compound for Zn translocation via phloem in rice (Nishiyama *et al.* 2012). DMA has not been suggested to be a chelating form of Zn in the rice phloem, although Zn-DMA was detected in wheat root sap and exudates of plants grown in Fe and Zn deficient conditions (Suzuki *et al.* 2008b; Xuan *et al.* 2006). To respond to Zn or/ and Fe deficiency, the plant DMA synthesis could be upregulated to production of MAs, including DMA. In high concentrations of DMA, Zn might have more chance to chelate with DMA providing assistance to Zn-NA in conditions of Zn deficiency.

In general, Fe and Zn can be transported as Fe^{3+}- DMA, Fe^{2+}- NA, Fe^{3+}-citrate, Zn-NA, Zn-citrate in the rice phloem and xylem, following uptake via membrane proteins like the YSL family and ZIPs which will described in the following section.

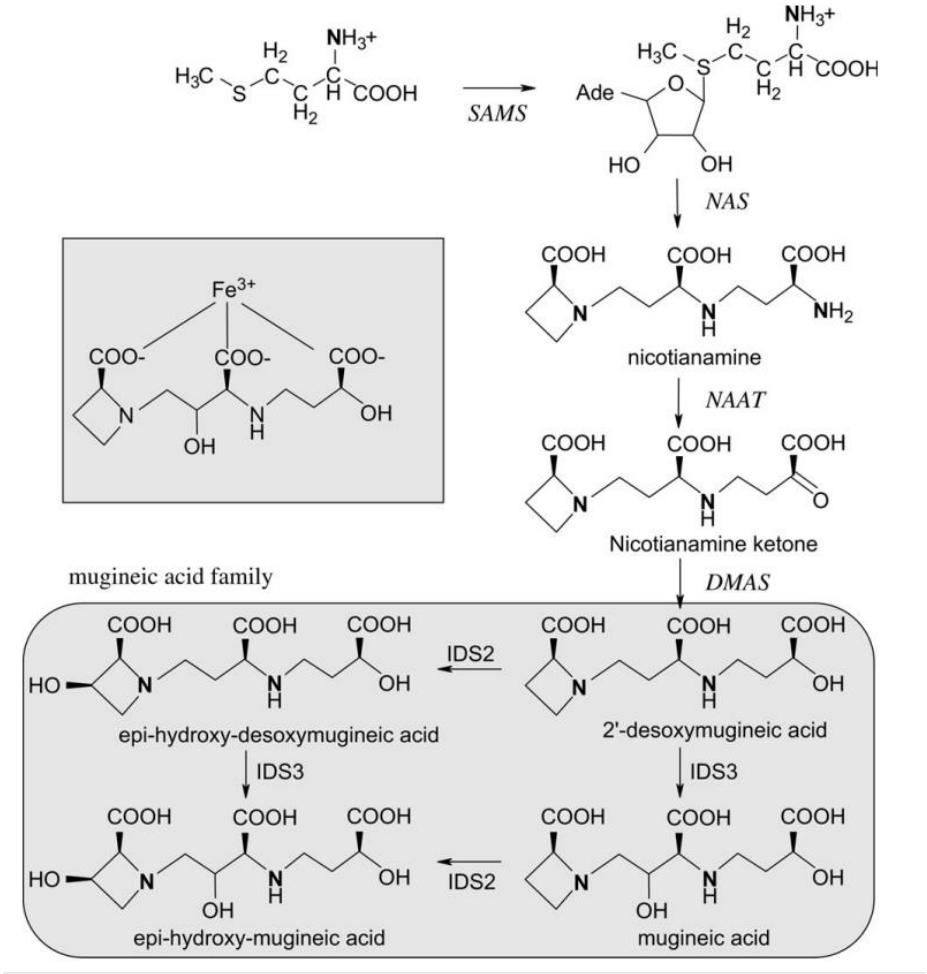

Figure 1.6. Pathway of biosynthesis of nicotianamine catalyzed by nicotinamine synthase (NAS) and DMA catalyzed by deoxymugineic acid synthase (DMAS) from methionine. This was modified from Kobayashi *et al.* (2005) and apart from Sharma and Dietz (2006).

1.5.3.2. Nicotianamine synthase (NAS) and nicotianamine (NA) in rice grains.

NA is a non-protein amino acid and is synthesised by 3 genes in rice that are regulated differentially by Fe (Inoue *et al.* 2003), namely *OsNAS1*, *OsNAS2* and *OsNAS3*. A similar expression pattern and very close location of *OsNAS1* and *OsNAS2* on rice chromosome 3 is reported (Inoue *et al.* 2003). Under Fe-sufficient conditions, *OsNAS1* and *OsNAS2* expression were only detected in root pericycle and companion cells. Much higher expression is induced in all

tissues in roots and in vascular bundles in leaves of in rice grown in Fe-deficient conditions. In contrast with *OsNAS1* and *OsNAS2*, *OsNAS3* is more likely to be expressed in leaves of Fe-sufficient rice. In rice plants suffering from Fe deficiency, *OsNAS3* was only slightly upregulated in root cells and suppressed in leaves (Inoue *et al.* 2003). The different pattern of expression of *OsNAS3* compared with *OsNAS1* and *2* suggests it plays a unique role in Fe regulation in rice. In the study of Aung *et al.* (2019), *OsNAS3* was suggested to play a role in Fe detoxification under Fe excess condition.

During rice germination under Fe-deficient and Fe-limited conditions, only *OsNAS1* and *OsNAS3* are upregulated in the endosperm of rice grains, while *OsNAAT* and *OsDMAS*, that are responsible for DMA production, are not expressed in this region. These results imply that NA plays a crucial role in Fe homeostasis for long-distance transport, in addition to its role as a precursor of DMA biosynthesis (Nozoye *et al.* 2007). Based on a Rice Expression Profile Database (RiceXPro) *OsNAS2* expression was not detected during the rice endosperm development under normal growth condition (Wang *et al.* 2010).

In an attempt to increase Fe accumulation in the rice grain, three independent, transgenic lines overexpressing a single *NAS* gene driven by the *35S* promoter were generated (Johnson *et al.* 2011). All transgenic rice plants showed an increase in NA concentration and Fe concentration in rice grains. Of particular interest, the *OsNAS2* line increased Fe up to 4.2 fold, compared to WT (Johnson *et al.* 2011). A positive correlation between NA concentration and Fe concentration supported, more confidently, the hypothesis that NA is probably responsible for transport of Fe into the grain (Nozoye *et al.* 2007). Also, this report showed more Fe and Zn in transgenic lines is distributed in the aleurone, subaleurone and outer layers of endosperm of the grain. Transgenic grain overexpressing the *OsNAS2* gene was analysed for the distribution of nutrients in grains by

two highly sensitive techniques, Synchrotron X-ray fluorescence microscopy (XFM) and high-resolution secondary ion mass spectrometry (NanoSIMS). The report confirmed that most Fe was co-localised with phytic acid in the aleurone, while Fe was probably co-localised with NA or DMA chelator in subaleurone and outer-layer endosperm of grain (Kyriacou *et al.* 2014).

Although *OsNAS2* is a great candidate for increasing Fe and Zn content, little attention has been paid to its product, the NAS2 protein. To date, there is only one report of NAS2 protein location and structure in the rice roots (Nozoye *et al.* 2014a). In this study, the authors suggested the OsNAS2 protein is localised to vesicles derived from the rough endoplasmic reticulum (rER). Because the vesicle membrane is not able to fuse with the root cell membrane directly, NA and/or DMA is speculated to biosynthesise in the vesicles before they may be exported into the cytoplasm through specific transporters, the identity of which remains unknown. Two transmembrane helices at the N- and C-termini on the outside of the vesicle are predicted based on the amino acid sequence (Figure 1.7). Moreover, the tyrosine (YXXϕ) and di-leucine (LL) motifs, both found at the N-terminus (Figure 1.8) were found to be vital for the proper function of the OsNAS2 protein (Nozoye *et al.* 2014a). There is no knowledge about the role of NAS2 in the rice endosperm, although it might similar to that in the rice root cells.

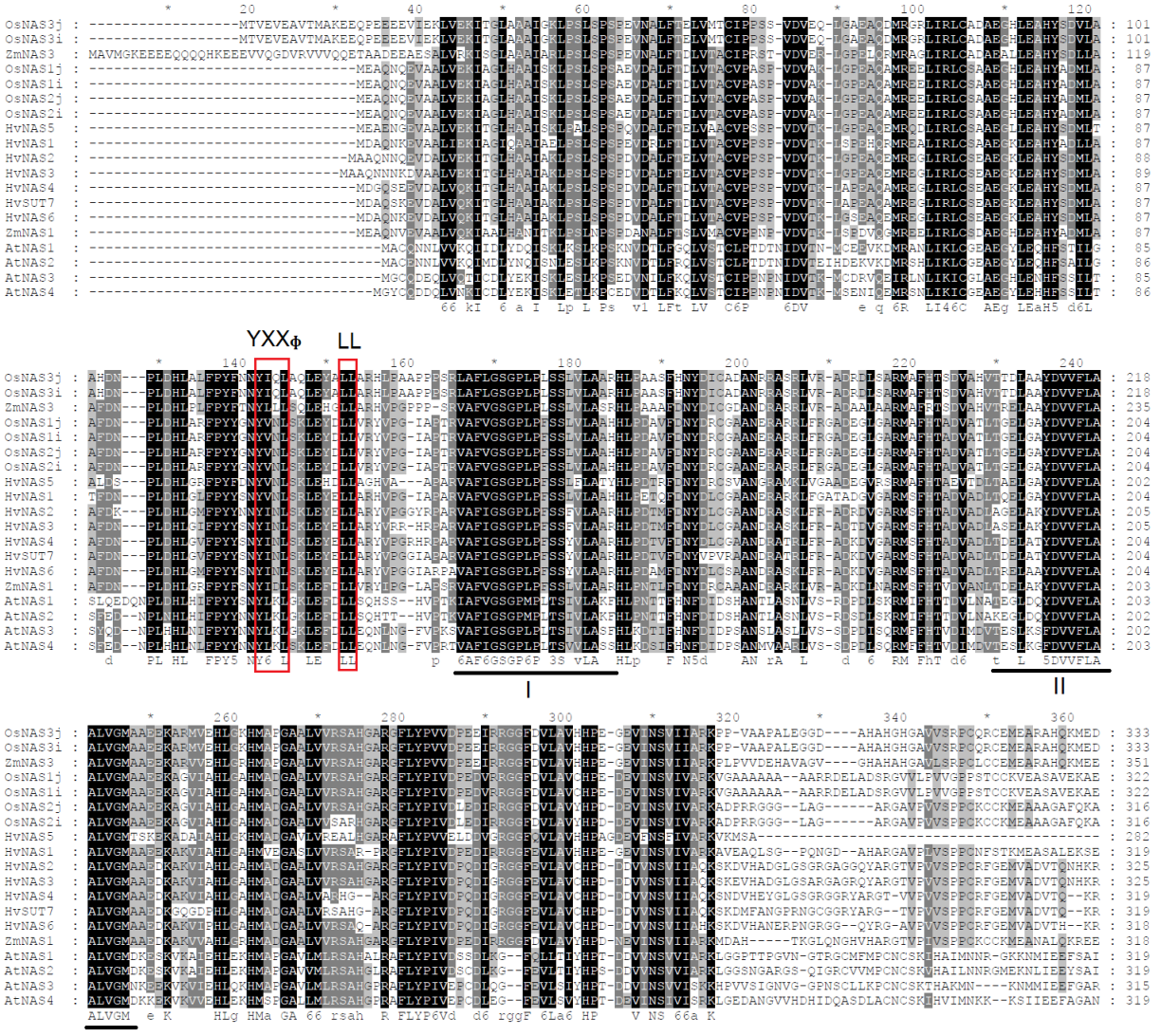

Figure 1.7. Alignment of amino acid sequence of nicotianamine synthase proteins from Indica rice, Japonica rice, barley, maize, and *Arabidopsis*, was performed by GeneDoc. The three shade levels represent conservation degrees 100, 80 and 60%. Based on the sequence of OsNAS2, two transmembrane helices with the N-terminus and the C-terminus on the outside of the vesicle were predicted by the TMpred program (https://embnet.vital-it.ch/software/TMPRED_form.html), numbered in Latin. YXX motif and LL motif were in two red boxes.

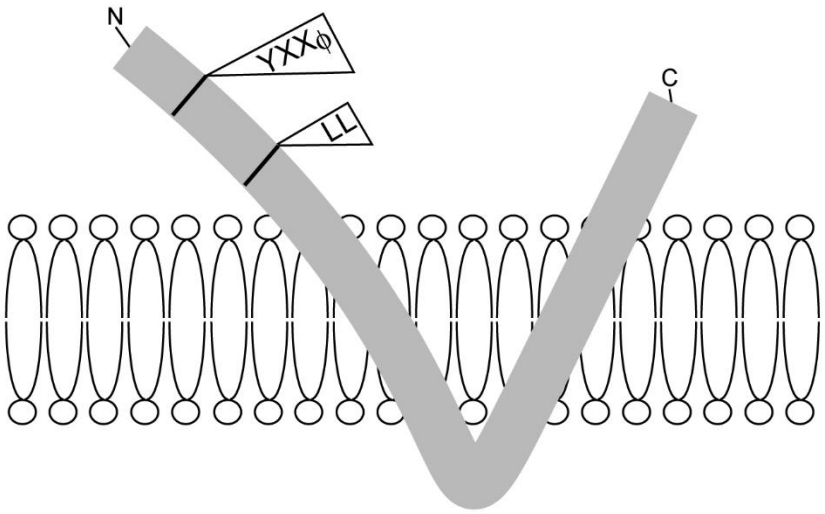

Figure 1.8. A structural model of NAS2 proteins and location on vesicles. The model, proposed by Nozoye *et al.* (2014a), contains the tyrosine (YXXϕ) motif and the di-leucine (LL) motif, both of which are vital for the proper function of the OsNAS2 protein.

1.5.3.3. Transporters of Fe and Zn complexes

Transport of Fe is a complicated process which requires an array of proteins. Among these, the YSL family consisting of well-characterised transmembrane transporters has been shown to function as a proton-coupled symporter of a Fe-chelator complex in phloem loading (Schaaf *et al.* 2004). To date, there are 18 paralogs of YSL family genes found in the rice genome (Koike *et al.* 2004), all potentially playing a role in Fe transport in a particular place of the rice plant. In phloem transport, OsYSL2, OsYSL15, OsYSL16, and OsYSL18 are suggested to function in Fe transport in vegetative tissue and reproductive organs in rice. Based on a phylogenetic analysis of the YSL transporter family, OsYSL2, OsYSL15 and OsYSL16 were classified into the same subgroup, whereas OsYSL18 was in a different subgroup (Yordem *et al.* 2011). OsYSL2 is suggested to transport Fe-NA (Koike *et al.* 2004), whereas OsYSL15, OsYSL16 and OsYSL18 are transporters for Fe-DMA.

OsYSL2 is likely to be involved in translocation of Fe^{2+}-NA in the rice phloem because the expression of *OsYSL2* is detected in the phloem under Fe-sufficient conditions (Ishimaru *et al.* 2010; Koike *et al.* 2004). A positive correlation between *OsYSL2* expression in the flag leaf and Fe concentration in the grain, was reported by Sperotto *et al.* (2010). This role of OsYSL2 is supported by an analysis of a knockdown mutant of *OsYSL2* in rice. The result showed Fe accumulation was in the roots, while Fe concentration in the shoot and grain decreased. The opposite was obtained in overexpression of *OsYSL2* under the control of the *OsSUT1* promoter, leading to a 4.4-fold increase in Fe level of polished grain (Ishimaru *et al.* 2010). This is strong evidence to confirm the function of OsYSL2 in Fe phloem loading.

In addition to a dominant transporter of Fe^{3+}-DMA in the rhizosphere, OsYSL15 is also considered to function in Fe^{3+}-DMA transport in phloem loading. Under Fe sufficiency, the expression of *OsYSL15* is detected in the phloem and during flowering and grain filling (Inoue *et al.* 2009). Collectively, these data strongly suggest OsYSL15 involvement in the transport of Fe^{3+}-DMA into phloem as well. Similarly, OsYSL16 is also suggested to play a crucial role in Fe^{3+}-DMA transport in rice (Kakei *et al.* 2012). This is supported by the growth of a mutant yeast defective in Fe uptake but expressing *OsYSL16*, on medium supplied with Fe^{3+}-DMA, but not for Fe^{2+}. Furthermore, the expression of OsYSL16 is detected in the vascular bundle of young leaves (Kakei *et al.* 2012). Another transporter of the Fe^{3+}-DMA complex in phloem tissue is OsYSL18, which is suggested to play an important role in translocation of Fe into grains in rice (Aoyama *et al.* 2009).

Due to the presence of Zn-NA complexes in the phloem sap (Nishiyama *et al.* 2012), the YSL proteins could also be involved in the transport of Zn into the phloem. However, there is little evidence to suggest this. Unlike the YSL proteins, several members of Zinc-regulated transporter

and Iron-regulated like transporter (ZIP) gene family are well characterized to transport Zn in the phloem (Bashir *et al.* 2012). The ZIP family transporter gene, OsZIP3, is also involved for the unloading Zn from the rice xylem to the phloem (Sasakietal., 2015), and OsZIP4, OsZIP5 and OsZIP8 were suggested to be Zn transporters responsible for Zn translocation from the roots to the shoots (Bashir *et al.* 2012; Ishimaru *et al.* 2007; Yang *et al.* 2009).

In summary, Fe and Zn bound in their complexes (NA, DMA, citrate) are translocated to the shoots and developing tissues. Depending on tissue demand at different physiological stages, Fe and Zn can be allocated to the leaves and stems during vegetative growth and then translocated to the developing grains during grain-filling. The many isoforms of the YSL and ZIP transporters indicate the intricate developmental and anatomical steps that Fe and Zn must undergo in a plant and how a plant must respond it its environmental conditions to maintain nutrient homeostasis. For breeding biofortified rice, much attention should be paid to understanding the translocation of Fe and Zn into the rice grains, including Fe and Zn source for storage, mechanisms of translocation, and distribution in the rice grains.

1.5.3.4. Translocation of Fe and Zn into the grains

The sources of Fe and Zn for remobilisation into developing seeds differs between species, but is most probably a combination of stems, leaves and roots (Stomph *et al.* 2011; Stomph *et al.* 2009). For example, 65-75% of remobilised Fe into the wheat grain originates from the shoot (Garnett & Graham 2005), compared with only 4% in rice (Marr *et al.* 1995). For Zn, more than 50% in the rice grain originated from that taken up during vegetative growth (at seedling and tillering), and remobilised later when leaves senesce (Wu *et al.* 2010). This means that the translocation of Fe and Zn from the old leaves make a great contribution to grain Fe and Zn in rice.

A smaller contribution could be the result of the root-to-grain translocation via both the phloem and xylem during the reproductive stage.

The Fe and Zn loaded into the rice grain derives either from (1) remobilization of stored Fe and Zn in leaves as they senesce via the phloem, or (2) as a result of direct loading from the soil via the xylem (Figure 1.9). Although the direct root-to-grain translocation through the xylem is not fully investigated, both mechanisms require a step of micronutrient unloading (Fe and Zn) from the phloem or xylem to the endosperm of the grains. Because the filial and maternal tissues of the grain are isolated by the apoplasmic space, membrane transporters on the filial and the maternal tissues are essential to efflux and influx the complexes of Fe and Zn into the endosperm of the grain, followed by transport into the embryos. Therefore, the unloading and loading of Fe and Zn into the endosperm are likely to be major bottlenecks. Unfortunately, very little is known about this step of grain filling. More knowledge of chelated forms of Fe and Zn and their specific transporters is crucial for their Fe and Zn biofortification in crop plants like rice.

Recently, a few proteins which function in Zn and Fe unloading into the endosperm have been identified. *OsYSL2* expression is detected in the endosperm and embryo of the rice ovary at 5 DAA. OsYSL2 was firstly suggested Koike *et al.* (2004) as a critical transporter for the Fe-NA complex into the rice endosperm. The role of OsYSL2 in the transport of Fe into the rice endosperm was reinforced by Ishimaru *et al.* (2010). In this study, the authors found an opposite effect between the RNAi-induced OsYSL1-knockdown line, and the OsYSL2-overexpressed line, with a significantly lower Fe concentration in the grains of the RNAi lines and a higher concentration in the overexpressing line, compared to the non-transgenic line. Bashir *et al.* (2013a), based on the data extracted from RiceXPro, suggested OsYSL16 seems to be good candidate for increasing Fe transport into the grains, however, there has not been any analysis of

over-expression or RNAi lines yet reported in the literature. As mentioned above, if OsYSL2 and OsYSL16 are involved the Fe transport in the seed, NA and DMA would be crucial chelators for Fe and Zn. Expression of genes involved in NA and DMA synthesis, including OsNAS1 and OsNAS3, OsNAAT1 and OsDMAS1, showed an increase in the developing ovary at 1 to 7 DAA (Bashir *et al.* 2012). For Zn transport, OsZIP4 and OsZIP8 seem particularly important for Zn transport to grains (Bashir *et al.* 2012; Yang *et al.* 2009).

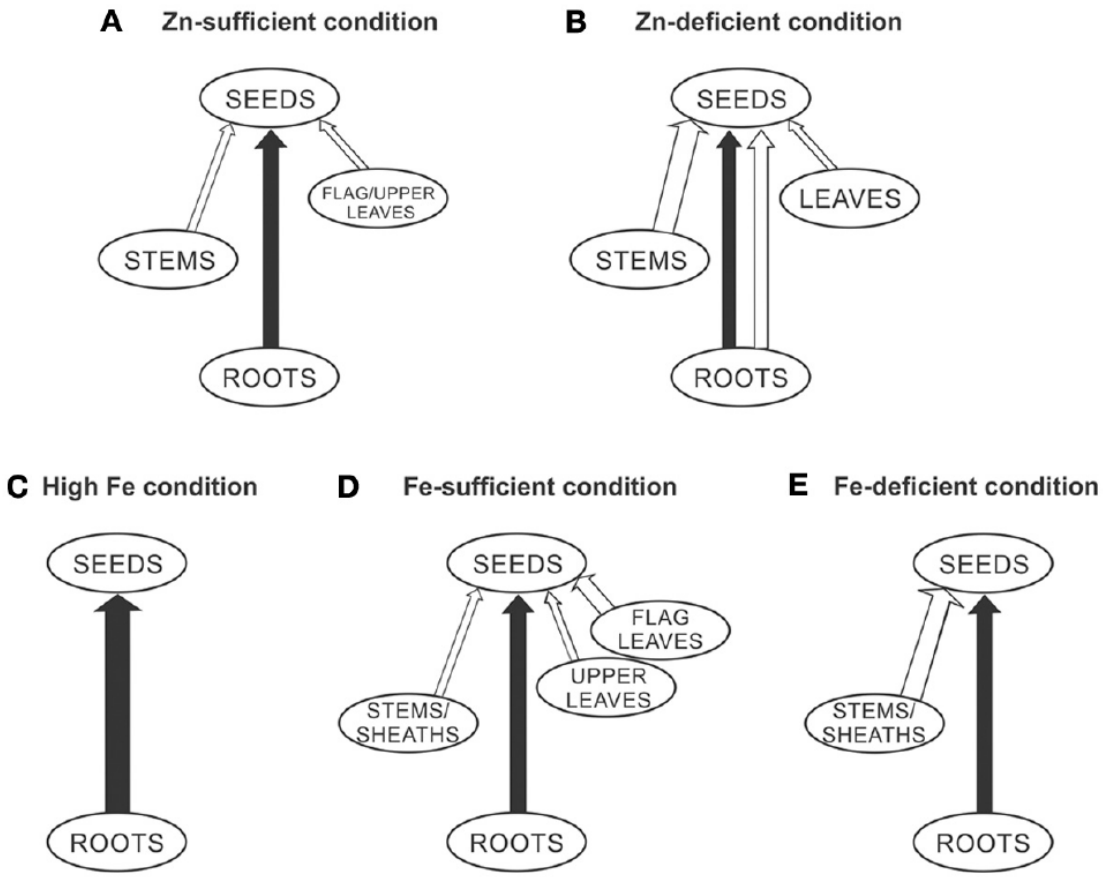

Figure 1.9. A model of Zn and Fe sources allocating into the rice grains under different Fe and Zn supplies via both the xylem and phloem. This model is proposed by Sperotto (2013). A. Zn-sufficient condition; B. Zn-deficient condition; C. High Fe condition; D. Fe-sufficient condition; E. Fe-deficient condition. Arrows indicate continued root uptake, through the xylem

(black arrows) and through the phloem (mineral remobilization, white arrows). The thicknesses of the arrows represent greater or less active processes.

1.5.4. Distribution and storage of minerals in rice grains

The mineral-bound complexes firstly reach the aleurone layer and then move into the inner part of the endosperm via the symplasmic pathway before they finally reach into the embryos. Depending on the mobilization of mineral complexes, the deposition of minerals in different cereal grains is different. Advances of imaging techniques allows localization of the minerals in the rice grain (Díaz-Benito *et al.* 2018; Huynh 2015; Johnson *et al.* 2011; Kyriacou *et al.* 2014; Trijatmiko *et al.* 2016), and mineral changes during grain development (Iwai *et al.* 2012; Sakai *et al.* 2015). The results of these studies highlight that Fe and Zn were most abundant in the aleurone layers and the scutellum of the embryo, and lowest in the endosperm.

During rice grain development, most of the Fe and Zn immediately bind with phytic acid to form phytate which is found localized in the aleurone layer (Iwai *et al.* 2012; Sakai *et al.* 2015). Very little Fe moves into the inner endosperm of the developing grains, whereas a greater proportion of Zn was observed to move into the inner endosperm (Iwai *et al.* 2012). The different patterns of mineral movement could be due to differently complexed forms of the minerals. For instance, most of the Fe and Zn exist as insoluble phytate complexes, which are unable to continuously mobilise. However, a very small fraction of the Fe forms soluble complexes with other chelators like NA, DMA and proteins, which are able to move deeper into the endosperm (Iwai *et al.* 2012; Kyriacou *et al.* 2014). This presents a great challenge for genetic engineering and breeding of Fe and Zn biofortified cereals, particularly in rice, because the Fe and Zn in the aleurone layer is removed during polishing, and their co-localisation with phytate leads to very low bioavailability of Fe and Zn (Fredlund *et al.* 2006; Hallberg *et al.* 1989). Bioavailability is

defined as the amount of minerals released for digestion in the intestine of mammals. Hence, the goal of the Fe and Zn biofortification should focus not only on increasing Fe and Zn contents in the endosperm, but also to improve their bioavailability. Unfortunately, there is no clear understanding of the molecular mechanisms of mineral transport in the endosperm cells, including in what complex of minerals occur, whether there is an exchange of ligands, and whether there are other mineral-stored forms different from that of phytate.

1.6. Genetic modification approaches for Fe and Zn biofortification in rice

Despite global concerns about genetic engineering, novel approaches for Fe/Zn biofortification have been explored over the last 15 years (reviewed by Sperotto *et al.* (2012) and Bashir *et al.* (2013a)). There have been many notable successes in increasing Fe and Zn content in the rice grain, but the most important aim of Fe and Zn biofortification in rice is to increase their concentrations and bioavailability in the endosperm. Many single-gene strategies have failed to achieve both these aims. It is noticeable that several approaches of multiple transgenes have succeeded in Fe and Zn enrichment, and improvement of their bioavailability in white rice (Trijatmiko *et al.* 2016; Wu *et al.* 2019). All approaches to date of Fe /Zn biofortification in rice are summarised in Table 1.1 and Table 1.2. However, negative yield and growth traits were reported in several approaches, and they should be considered seriously in future attempts at rice Fe/Zn biofortification.

Table 1.1. Genetically engineered approaches to Fe/Zn improvement in rice.

Gene	Promoter	Cultivar	Growth condition	Grain	Fe		Zn		Yield /growth change	Reference
					Concentration (μg/g)	Fold change	Concentration (μg/g)	Fold change		
SoyferH1	*OsGluB1*	Japonica cv. Kitaake	Greenhouse	Unpolished	13.3-38.1	3			No data	Goto *et al.* (1999)
				Polished						
SoyferH	*OsGluB1*	Japonica cv Taipei 309	Greenhouse	Unpolished	22.07	2.2			No data	Lucca *et al.* (2002)
				Polished						
SoyferH1	*OsGlb1*	Japonica cv. Kitaake	Greenhouse	Unpolished	15	1.5			No data	Qu *et al.* (2005)
				Polished						
SoyferH	*OsGluB1*	Indica cv. IR68144	Greenhouse	Unpolished	37	3.7			Similar	Vasconcelos *et al.* (2003)
				Polished			55.5	1.65		
OsFer2	*OsGluA2*	Indica cv. Swarna	Greenhouse	Unpolished	15.9	1.2			Similar	Paul *et al.* (2012)
				Polished			30.75	1.37		
HvNAS1	*OsActin1 & 35S*	Japonica cv. Tsukinohikari	Greenhouse	Unpolished	42	1.4	45	1.28	No data	Masuda *et al.* (2009)
				Polished	9	2.25	28	1.4		
OsNAS1	*OsUbi-1*	Japonica cv. Xiushiu 110	Greenhouse	Unpolished	~27	2	~120	5	Growth penalty	Zheng *et al.* (2010)
				Polished						
OsNAS1	*OsGluB1*	Japonica cv. Xiushiu 110	Greenhouse	Unpolished	18.68	1.5	36.99	1.6	Similar	
				Polished	5	1	29.07	1.3		
OsNAS3-D1		Japonica cv. Dongjin	Greenhouse	Unpolished	32	2.9	44	2.2	No data	Lee *et al.* (2009b)
				Polished	12	2.6	33	2.2		
OsNAS 1	*35S*	Japonica cv. Nipponbare	Greenhouse	Unpolished	47	2	63	1.5	No data	Johnson *et al.* (2011)
				Polished	9.7	2	48	1.4		
OsNAS 2	*35S*	Japonica cv. Nipponbare	Greenhouse	Unpolished	64	2.9	91	2.1		
				Polished	19	4.2	76	2.2		
OsNAS 3	*35S*	Japonica cv. Nipponbare	Greenhouse	Unpolished	51	2.3	65	1.5		
				Polished	9.9	2.2	49	1.4		
OsYSL2	*OsSUT1*	Japonica cv. Tsukinohikari	Greenhouse	Unpolished					No data	Ishimaru *et al.* (2010)
				Polished	7.6	4				
HvIDS3	*35S*	Japonica cv. Tsukinohikari	Paddy field	Unpolished					Similar	Masuda *et al.* (2008)
				Polished	1.5	1.4	14	1.35		
HvIDS3	*35S*		Paddy field	Unpolished					Similar	

		Japonica cv. Tsukinohikari		Polished	7.3	1.25	15.3	1.36		Suzuki *et al.* (2008a)
OsIRT1	*Ubiquitin*	Japonica cv. Dongjin	Field test	Unpolished	12	1.1	22	1.1	Penalty	Lee and An (2009)
				Polished						
MxIRT1	*35S*	Japonica		Unpolished	30.5	2.5	45	2.6	No data	Tan *et al.* (2015)
				Polished						
OsYSL15	*Actin1*	Japonica cv. Dongjin	Paddy field	Unpolished	14	1.1	23	1.0?	Similar, but low tillering and height	Lee *et al.* (2009a)
				Polished						
HvYS1	*Ubi-1*			Unpolished	25	1.7			No data	Banakar *et al.* (2017)
				Polished	9	2.25				
OsIRO2	*35S*	Japonica cv. Tsukinohikari	Greenhouse	Unpolished	16	2.6	14	1.4	Similar	Ogo *et al.* (2011)
				Polished						
OsTOM1	*35S*	Japonica cv. Tsukinohikari	Greenhouse	Unpolished	18	1.1	45	1.6	No data	Nozoye *et al.* (2011)
				Polished						

Note: Endosperm-specific promoters (*OsGlb1*: rice 26 kDa α-globulin, *OsGluB1:* rice glutelin B-1, *OsGluA2:* rice glutelin A2*); constitutive promoters (35S:* the 35S promoter of cauliflower mosaic virus, *Ubi-1:* Ubiquitin, *Actin1).*

Table 1.2. Combined approaches to Fe/Zn improvement in rice.

Gene	Promoter	Cultivar	Growth condition	Grain	Fe		Zn		Yield /growth change	Reference
					Concentration (μg/g)	Fold change	Concentration (μg/g)	Fold change		
AtNAS1,	*35S*	Japonica cv. Taipei 309	Greenhouse	Unpolished	15	1.5	40	1.3	No penalty	Wirth *et al.* (2009)
Pvfer	*OsGlb1*			Polished	6.9	6.3	30	1.4		
Afphytase	*OsGlb1*									
SoyferH2	*OsGluB1*	Japonica cv. Tsukinohikari	Field trial	Unpolished					No penalty	Masuda *et al.* (2012)
SoyferH2	*OsGlb1*			Polished	4.0	4.4				
HvNAS1	*OsActin1*									
OsYSL2	*OsSUT1*									
OsYSL2	*OsGlb1*									
SoyferH2	*OsGluB1*	Tropical Japonica	Greenhouse	Unpolished	26-30.4	1.15-1.37	46.6-51.9	1.12-1.24	No data	Aung *et al.* (2013)
SoyferH2	*OsGlb1*									

HvNAS1 ***OsYSL2*** ***OsYSL2***	*OsActin1* *OsGluB1* *OsGlb1*	cv. Paw San Yin		Polished	3.96-5.02	3.0-3.4	36.1-39.2	1.2-1.3		
SoyferH2 ***SoyferH2*** ***HvNAS1*** ***HvNAAT-A*** ***HvNAAT-B*** ***IDS3***	*OsGluB1* *OsGlb1*	Japonica cv. Tsukinohikari	Normal soil in greenhouse	Unpolished					No data	Masuda *et al.* (2013b)
				Polished		4				
OsNAS2 ***SoyferH1***	*35S* *OsGluA2*	Indica cv. IR64	Field test	Unpolished					No penalty, but lower	Trijatmiko *et al.* (2016)
				Polished	14-15		45.7	2.5		
AtIRT1 ***AtNAS1*** ***PvFer***	*AtIRT1* *35S* *OsGlb1*	Japonica cv. Nipponbare	Greenhouse	Unpolished					Similar	Boonyaves *et al.* (2017)
				Polished	10.46	3.8	33.17	1.8		
AtNAS1 ***PvFer*** ***AtFRD3***	*p35S* *pGlb* *pUbi*	Japonica cv. Nipponbare	Greenhouse	Unpolished	26.74	5.4	64.73	2.4	Similar, but lower height	Wu *et al.* (2018)
				Polished	11.08	1.5	40.09	2.4		
PvFer ***AtFRD3***	*pGlb* *pUbi*	Japonica cv. Nipponbare	Greenhouse	Unpolished	~ 22	1.2	36.19	1.4		
				Polished	~ 11	5.4	28.03	1.7		
AtNRAMP3 ***AtNAS1*** ***PvFER***	*pOsOle18* *pCaMV35S* *pOsGlb-1*	Japonica cv. Nipponbare	Greenhouse	Unpolished	29.75	1.6	63.04	2.1	Similar, but lower height	Wu *et al.* (2019)
				Polished	12.77	6	45.60	2.3		
AtNRAMP3 ***AtNAS1*** ***PvFER***	*pOsOle18* *pCaMV35S* *pOsGlb-1*	Indica cv IR64	Greenhouse	Unpolished	21.38	1.6	48.18	1.4	Similar	
				Polished	13.65	5	48	2.5		

Note: Endosperm-specific promoters (*OsGlb1*: rice 26 kDa α-globulin, *OsGluB1:* rice glutelin B-1, *OsGluA2:* rice glutelin A2, *OsOle18:* rice 18-kDa oleosin gene*); constitutive promoters (35S:* the 35S promoter of cauliflower mosaic virus, *Ubi-1:* Ubiquitin, *Actin1).*

1.7. The aims of the project

A combination of high yield and nutrient-enriched traits in cereal grains is a great challenge for breeders and seems to be particularly difficult given the negative correlation between the two traits. It means that breeding a crop to contain more nutrients, like Fe and Zn, often results in a lower yield and vice versa. A clear understanding of the cause of this phenomenon would be very beneficial for crop breeders and particularly given the negative impacts of elevated CO_2 on grain nutrient content, especially Fe and Zn (Myers *et al.* 2014; Zhu *et al.* 2018). At the seed filling stage, assimilates such as sucrose, amino acids, macronutrients, and micronutrients are available to remobilise into the same predominant sink (i.e. the developing grain) through the same phloem route. Sucrose is an important nutrient component, which does not only impact grain yield, but also is involved in source-sink communication via an integrated signalling network. Sucrose serves as a signal to trigger carbon metabolism for grain development, seed maturation and transition into the storage phase, through changes in gene expression, hormones, and metabolites. A balance between nutrient utilisation in the grain sink and supply in source tissues is tightly coordinated; thus, any enhancement of sucrose demand in the sink could stimulate the sucrose translocation from the source. Sucrose plays a key role to determine the direction of nutrient flow and metabolic pathways controlling the seed maturation and storage. Gene overexpression of sucrose transporters (enhancing sink strength) is a promising avenue for enhancing uptake capacity and partitioning.

The barley sucrose transporter gene (*HvSUT1*), when ectopically overexpressed in winter wheat cv. Certo, regulated by the barley Hordein B1 promoter (endosperm- specific promoter), positively stimulated sucrose uptake capacity in transgenic wheat grains (Weichert et al., 2010). This resulted in elevated sucrose uptake into the grains with cascading effects on the grain metabolism, particularly increased accumulation of grain storage proteins and hormonal signals

(for example cytokinin) for growth and cell proliferation. Consequently, the *HvSUT1*-overexpressing wheat grains showed an increase in the storage protein synthesis and total protein content as well. Under glasshouse conditions, in which nutrient availability was limited, positive impacts on protein yield and grain yield were unclear. Thus, further analysis of the T3 to T5 generations of the *HvSUT1*-overexpressing wheat, grown under field-like conditions was done by Saalbach *et al.* (2014). Here, the transgenic wheat line had a significant increase in grain yield (by 28%) and higher protein yield. Moreover, an additional benefit of higher Fe and Zn concentration (20-40%) in the wheat grains was seen. It is likely because of an increased sink strength and higher grain storage protein probably resulted in a positive correlation with micronutrient contents (Stomph *et al.* 2011; Stomph *et al.* 2009). Based on these studies, Huynh (2015) tested a similar hypothesis of *HvSUT1* overexpression in Japonica rice (cv. Nipponbare). In this case, overexpression of *HvSUT1* was controlled by the rice endosperm-specific promoter Globulin 1 (*Glb-1*). Huynh (2015) reported increased sucrose uptake in the rice grains expressing *HvSUT1* and more Fe and Zn mobilised to the inner endosperm.

In general, overexpression of sucrose transporter to enhance sink strength is a promising strategy for improving Fe and Zn in crops, including rice. However, the strategy will be more successful if Fe and Zn concentration could get closer to the estimated average requirement (EAR) and with improved bioavailability, as well as unchanged or even higher grain yield. However, no beneficial effect on the grain yield was seen by Huynh (2015), when the transgenic rice plants were grown under green-house conditions where the nutrient supply availability is low. Furthermore, elemental maps generated by LA-ICP-MS, showed the signals of Fe and Zn in the transgenic grains were much more abundant in the outer layers of the endosperm, compared to non-transgenic grains. A significantly higher phytate concentration was also seen in the transgenic

rice grains (Huynh 2015). A possibility is that the higher phytate caused the Fe and Zn to be locked in the aleurone layer, limiting its mobilisation into the starchy endosperm. Therefore, the presence of other chelators to compete with phytate in the outer layer of the endosperm could be a strategy to improve the Fe and Zn relocations into the starchy endosperm.

In rice, NA/DMA play key roles in metal homeostasis as ubiquitous metal chelators (Fe^{+2}, Fe^{+3} and Zn^{+2}) to form soluble complexes. NA is synthesised by 3 genes that are regulated differentially by Fe and Zn (Inoue *et al.* 2003), namely *OsNAS1*, *OsNAS2* and *OsNAS3*. Among these genes, *OsNAS2* is likely to be the best candidate to generate NA under control of constitutive promoter (Johnson *et al.* 2011). Moreover, NA have been reported to be a novel enhancer of Fe/Zn bioavailability. Lee et al. (2012) suggest that an increase in mineral bioavailability in rice grains can be achieved by increasing *NAS* expression or *NAS* gene's product (probably NA level). This implies that NA may improve Fe/Zn bioavailability in rice grain. Three independent studies of Zheng et al. (2010), Eagling et al. (2014), and Beasley *et al.* (2019b) confirmed that NA was a more effective enhancer of Fe uptake in human Caco-2 cells. This supports the idea that Fe and Zn -NA complexes will enhance mineral bioavailability in rice.

In this study, we hypothesised that the strategy of increasing grain sink strength via sucrose transporter overexpression could be more effective for Fe/Zn translocation into the rice endosperm if in combination with *OsNAS2* overexpression in the endosperm cells. This might reduce co-localization of Fe/Zn with phytate and minimize losses by milling. To test the hypothesis, this project has three major objectives. Chapter 2 described the aim to generate three populations of homozygous transgenic rice based on three constructs: (1) containing the barley sucrose transporter (*HvSUT1*) under control of the rice globulin endosperm specific promoter (*Glb-1*), (2) containing the chelator synthesis gene, nicotianamine synthase 2 (*OsNAS2*) driven by a rice

glutelin A2 promoter (*GluA2*), and (3) containing both gene constructs. The promoter *GluA2* controls gene expression in the aleurone cells at 5-7 DAA when the cells in the central region of the endosperm are alive to uptake nutrients (Wu *et al.* 2016b). The three constructs were transformed into the widely popular Indica cultivar, IR64, using the *Agrobacterium*-mediated method. Homozygous lines with single or two inserts from the three constructs were confirmed using quantitative real-time PCR.

Research presented in Chapter 3 aimed to test successful expression of *HvSUT1* and *OsNAS2* under the control of rice endosperm-specific promoters in immature grains from the homozygous lines. Immunoblotting analysis was done to examine the protein expression levels during grain development in homozygous lines. Two antibodies, anti-OsNAS2 and anti-HvSUT1 were used to detect HvSUT1 and OsNAS2 proteins, to demonstrate the temporal pattern of HvSUT1 and OsNAS2 protein occurrence during grain development. In addition, growth and yield parameters of the homozygous plants were analysed.

Research presented in Chapter 4 aimed to determine the effects of the transgene expression on micronutrient concentration, distribution, and bioavailability in polished and unpolished grains compared to non-transgenic control grains. ICP-MS was employed to analyse Fe and Zn levels and Perls/DAB/$CoCl_2$ and DTZ staining were used to demonstrate Fe and Zn distribution in the rice grains, respectively.

CHAPTER 2: DEVELOPMENT OF HOMOZYGOUS TRANSGENIC RICE LINES WITH SINGLE T-DNA INSERTS

2.1. Introduction

To achieve the nutritional target of 13 mg/kg of Fe and 28mg/kg of Zn biofortification in polished rice to reach 30% of the dietary estimated average requirement (EAR) (Bouis *et al.* 2011a), two major bottlenecks for Fe and Zn entrances into the grain endosperm should be considered: (1) the presence of high amount of phytic acid in the aleurone layer, and (2) alternative soluble forms of Fe and Zn complexes in the developing endosperm tissue to facilitate Fe/Zn movement into the inner endosperm. With this in mind, Fe biofortification is more challenging than Zn. It is not easy for Fe to move beyond the outer layer of rice grains, because of the presence of phytate that forms insoluble complexes with Fe. Consequently, most Fe is locked in the outer layer of grains and then removed by the milling processing to produce commercial white rice. The insoluble property of phytate-metal complexes is made more challenging because the phytate is an inhibitor for Fe and Zn uptake in the human gut. Unfortunately, rice germplasm has a very limited gene pool for increasing Fe and Zn concentrations and their bioavailability in the rice endosperm. Consequently, numerous conventional breeding efforts for developing Fe and Zn enriched rice have not reached the 30% EAR in polished grains.

Genetic engineering approaches for Fe/Zn biofortification have been explored in rice for more than 15 years (reviewed by Sperotto *et al.* (2012); Bashir *et al.* (2013a)) and offer a great opportunity to increase the Fe and Zn content in the inner endosperm. To do this, an efficient and productive platform of rice transformation has a decisive role to play in genomic study and generation of transgenic rice. Despite recent developments in gene editing and biolistic gene delivery, the most common method to transform a plant is using *Agrobacterium tumefaciens* to

elucidate gene functions and to add, subtract or modify compounds within the plant for applied biotechnology applications, or to gain fundamental knowledge of plant molecular biology. The first part requires a binary vector that is designed to deliver a T-DNA into plant cells. In common binary vectors, a T-DNA region and a vector backbone are the two main components (Komari *et al.* 2006).

The T-DNA region, containing one or/and multiple genes, according to the objective of research project, is transferred into the infected rice cells, then it is stably integrated into the genome (Watson *et al.* 2016). Another crucial element on the T-DNA region is a selectable marker gene cassette, which needs to be expressed in transgenic callus. This callus can allow survival on selection medium, and regeneration of new plantlets. Hygromycin phosphotransferase (*aph4*, *hph* or *hpt*), phosphomannose-isomerase (*pmi*), neomycin phosphotransferase (*npt*II), and phosphoinothricin acetyl transferase (*bar*) genes are employed as selectable markers for cereal transformation (Datta & Datta 2006; Hiei & Komari 2008). Among these, the *hpt* gene is one of the best marker genes in rice transformation and was used as a selectable marker in this study (Datta & Datta 2006; Hiei & Komari 2008). The *hpt* gene, originating from *E. coli*, confers plant resistance to the antibiotic hygromycin B (Rao *et al.* 1983). There is no evidence that the HPH (APH4) protein is toxic, allergenic, or harmful to people or/and animals, and the environment (EFSA 2004; Lu *et al.* 2007; OGTR 2017). Many transformation events, which have used the *hpt* gene as selectable marker, have been approved for commercial trade in many countries, such as USA and Australia (ISAAA 2020).

On the vector backbone containing the antibiotic-resistance gene, replication functions and mobilization functions, comprise the binary vector system which has been developed for this

purpose (Hellens *et al.* 2000; Hoekema *et al.* 1983). These allow propagation in *E. coli* and *Agrobacterium tumefaciens* prior to transfer into plant cells (Bevan 1984).

Rice transformation mediated by *A. tumefaciens* is more preferable than polyethylene glycol (PEG) or particle bombardment because of the relatively low cost, low copy number of T-DNA insertion events, transfer capability for large segments of T-DNA, and stable integration. It is not surprising that more than 80% of transgenic rice studies reported in the literature have used *A. tumefaciens* as a common technique for producing the transgenic plants (Hiei & Komari 2008). It is remarkable that many of these studies have been reported on Japonica rice, but very few on Indica rice. This is most likely due to the very low efficiency of transformation in Indica rice transgenesis. Many efforts have been made to increase the frequency of transformation events in Indica rice as it accounts for over 70% of rice production worldwide (Mahesh *et al.* 2016; Tie *et al.* 2012; Zhang *et al.* 2016).

More than two decades ago, the first protocol for rice transformation mediated by *Agrobacterium* was reported to be successful for Japonica subspecies (Hiei *et al.* 1994). Multiple types of tissues, such as shoot apex, root, scutellum, immature embryo, root callus, scutellum callus and suspension cells were screened as potential starting materials for *Agrobacterium*-mediated transformation in rice. Interestingly, many transformants were obtained from scutellum-derived calli, but very few from immature embryos. This may explain why many later reports focused on optimising a protocol of transformation from mature embryos. Thus, the protocol for *Agrobacterium*-mediated transformation in Indica rice, such as IR64, first adopted mature embryo-derived callus tissues. Very low efficiency was, however, reported. Because IR64 is known to be a recalcitrant cultivar for *Agrobacterium*-mediated transformation and tissue culture, much effort has been invested to improve the efficiency of transformation in Indica rice (Sahoo *et al.* 2011;

Sahoo & Tuteja 2012; Tie *et al.* 2012). There are many variable factors, including genotype, vigour of callus/tissue culture, strains of *Agrobacterium*, age and type of tissue being inoculated, expression construct, selection marker genes, and selective agents. Surprisingly, very few papers have reported a successful protocol using mature embryos as starting material for *Agrobacterium*-mediated transformation in Indica rice. Two comprehensive investigations, by Hiei *et al.* (2006) and Hiei and Komari (2008), reported immature embryo as a starting material for producing transgenic Indica rice by *Agrobacterium*-mediated transformation with higher efficiency. There were two limitations; first, availability of explant materials for transformation throughout the year, especially in temperate zones; and second, the time-consuming and tedious nature of the process (Sahoo *et al.* 2011; Sahoo & Tuteja 2012). However, the consensus view is that *Agrobacterium*-mediated transformation of immature embryos of Indica rice yields the highest transformation efficiency (Hervé & Kayano 2006; Sahoo *et al.* 2011; Sahoo & Tuteja 2012). This was confirmed by a comprehensive study of Hiei and Komari (2008) in which both mature embryo- derived and immature embryo-derived calli from 13 Japonica and 11 Indica rice varieties were used as starting materials for *Agrobacterium*-transformation. For IR64, no transgenic plants were generated by the mature embryo-derived callus protocol and a low number of transgenic plants (from 3-13 plants/callus) were obtained from the immature embryo protocol (Hiei & Komari 2008).

Development of homozygous transgenic lines is a fundamental requirement in most of the downstream applications and studies of genetic transformation. In genetic modification, multiple T-DNAs are often integrated into a host genome using particle bombardment making downstream analysis very complicated, and hence *Agrobacterium*-mediated transformation is a preferred method. The successful transformation process produces a first generation (T0) of hemizygous plants (where the transgene is inserted without an allelic counterpart), which might contain one,

two or multiple copies of the transgene in the host genome at the same or different locations. After self-pollination, the transgene segregates according to Mendelian principles. This means that the population in the subsequent generation (T1) have some homozygous, hemizygous and null plants. To ensure stable heritance of the transgene cassette, only homozygous plants should be used for further analysis and application. This derivation is a time-consuming and laborious process for rice. An efficient and rapid technique for determining the gene copy number, and screening for homozygous plants in the T1 generation, is a very crucial step for fast-tracking selection and breeding of transgenic plants, especially rice.

For *Arabidopsis thaliana* with a short life cycle (< 1 month), selection of homozygous lines can be achieved via marker selection with a selectable marker resistance, but it is required to be repeated over several generations. This becomes more time consuming for crops like rice, barley, wheat, and maize, because these crops have a long-life cycle (4-5 months) and require space and resources for growing to generate subsequent generations. Consequently, endpoint PCR for target gene quantification, and Southern blot analysis are utilised in selection and development of homozygous plants.

To date, Southern blot and quantitative real-time PCR (qPCR) are the two most common methods for quantifying number of inserts or transgenes in transgenic plants. Southern blot analysis (Southern 1975) is a powerful and reliable method to determine the insert number of transgenes in the host genome, but required large amount of genomic DNA and is a time-consuming and expensive procedure. In addition to Southern blot analysis, qPCR is a rapid technique to determine copy number and zygosity of transgenes in the host genome (Bubner & Baldwin 2004; Bubner *et al.* 2004; German *et al.* 2003). The qPCR is based on the detection of fluorescence generated during the amplification process. The fluorescence can be produced by an

intercalating dye that fluoresces as it binds to double-stranded DNA. Alternatively, a probe containing both a fluorescence and a quencher (Taqman) targeted to internal region of transgene. During the extension step in the qPCR assay, DNA polymerase will remove the probe, breaking down and releasing the fluorescence from the quencher. The result of the reaction is expressed as a Ct value. The comparative Ct ($2^{-\Delta\Delta Ct}$) method was used for determining copy number of transgenes (Bubner & Baldwin 2004), the details of which will be described in Section 2.2.7. Many analyses on copy number or/and zygosity of transgenes have employed the qPCR technique in several species such as maize (Ingham *et al.* 2001; Schmidt & Parrott 2001; Shou *et al.* 2004; Song *et al.* 2002), tomato (German *et al.* 2003; Mason *et al.* 2002), tobacco (Bubner *et al.* 2004), wheat (Gadaleta *et al.* 2011; Li *et al.* 2004) and rice (Yang *et al.* 2005). Most studies showed a robust effectiveness of copy number determination, but effective outcomes for zygosity was unclear, except for the studies of Ingham *et al.* (2001). Afterward, two reports of Mieog *et al.* (2013) and Wang *et al.* (2015b) showed that qPCR could be used to screen for homozygous transgenic cereal crops. However, these protocols have not been well adapted and practiced for multiple gene stacking and all constructs.

Most of the reported studies focused on overexpressing one or many genes directly involved in Fe/Zn uptake, transport, and storage within the rice plant (see Table 1.1 and Table1.2 in Chapter 1). In this study, a different strategy to develop Fe and Zn-enriched rice is presented by overexpressing *HvSUT1*. Based on the results reported by Weschke *et al.* (2000), Saalbach *et al.* (2014), and Huynh (2015), it was shown that *HvSUT1* is a potential candidate gene for further research in Fe and Zn biofortification. The preliminary data presented by (Huynh 2015) showed that although more Fe and Zn mobilized to the endosperm, higher phytate concentrations still presented a major barrier to their mobilization into the inner endosperm. In this study, the strategy

of *HvSUT1*-mediated Fe and Zn biofortification is expanded to include *OsNAS2* overexpression, with both the transgenes under the regulation of two endosperm-specific promoters to facilitate Fe/Zn mobilization. To test the strategy, many homozygous transgenic Indica rice plants containing four different gene cassettes would be required. Therefore, high-throughput rice transformation and fast-tracking of homozygous transgenic rice in the T1 generation is the major objective in this chapter. Here, along with the single gene construct of *HvSUT1* described by Huynh (2015), two gene constructs of *OsNAS2* built for this study with, or without *HvSUT1* were introduced into Indica rice (cv. IR64). Two endosperm specific promoters, *Glb-1* and *GluA2* cloned from Nipponbare rice (Furtado *et al.* 2008; Hwang *et al.* 2002; Qu & Takaiwa 2004; Qu *et al.* 2008), were used to drive the expression of *HvSUT1* and *OsNAS2*, respectively. Another *GluA2:uidA* fusion construct was also made and transformed into IR64 to verify the tissue specific expression of the *Glu2A* promoter. The combination of *OsNAS2* and *HvSUT1* is a novel strategy for Fe/Zn biofortification. With a transformation efficiency of nearly 45%, the improved protocol for *Agrobacterium*-mediated transformation using immature embryos was used to produce four populations of multiple transgenic rice lines. An accurate and reliable qPCR technique optimised and reported by Schramm (2015) and Tran (2015), was applied to the three different transgenic lines containing the three gene constructs of *OsNAS2* or/and *HvSUT1* to develop many homozygous, independent lines with low transgene copy number in the T1 generation.

2.2. Methods

2.2.1. Preparation of binary vectors for rice transformation

2.2.1.1. Amplification of the *GluA2* promoter from rice genomic DNA and ligation into vector pIPKb001

Genomic DNA (gDNA) was extracted from rice leaves by using an Isolate II plant DNA kit (Bioline) according to the manufacturer's instruction. Oligonucleotides of primer SpeIGluA2F and HindIIIGluA2R were used to amplify an 839 bp *GluA2* promoter (accession number: EU264103) from rice cv. Nipponbare genomic rice. *Spe*I and *Hind*III restriction sites were introduced into the amplified fragment of the *GluA2* promoter at its 5' and 3'ends, respectively for subsequent digestion and ligation into the multiple cloning sites of pIPKb001. The PCR cycling protocol was performed with Phusion Taq polymerase (NEB) (Appendix A, Table 6.5). The 839bp PCR product was visualized on a 1% agarose gel, then the DNA fragment excised from the gel and further purified using the Wizard® SV gel and PCR clean up kit (Promega). The PCR product was checked again by electrophoresis on a 1% agarose gel.

Two parallel double digests of pIPKb001 and the PCR product of the *GluA2* promoter with *Spe*I-HF and *Hind*III-HF (New England BioLabs) in 50 µl reaction at 37^0C for 1 hour were done, consisting of 1X CutSmart® Buffer, 10 units of each restriction enzyme and 1 µg of DNA. The digest of the *GluA2* PCR product was heat-inactivated at 80^0C for 20 minutes and further purified by gel purification using the Wizard® SV Gel and PCR Clean-Up System. To the digest of pIPKb001, a treatment with thermosensitive shrimp alkaline phosphate (TSAP) (Promega), to prevent self-ligation (Promega), was performed at 37^0C for 15 minutes, followed by a heat-activation at 80^0C for 20 minutes. A 20-µl ligation reaction between the digested *GluA2* promoter fragment and pIPKb001 with an insert: vector ratio of 1:3 was carried out at 16^0C overnight by T4 ligase (NEB). The ligation reaction was heat-inactivated at 65^0C for 10 minutes before proceeding to transformation into the *ccdb*-resistant *E.coli* strain DB3.1, by heat-shocking at 42^0C for 45 seconds. Transformed *E. coli* cells carrying the recombinant vector were selected on LB plates containing 25 µg/ml spectinomycin and 17 µg/ml chloramphenicol at 37^0C. One colony growing

on the selective medium was tested by colony PCR and analytical restriction digest of plasmid DNA with *EcoR*V for verifying integration of the *GluA2* promoter into pIPKb001. The integrated vector (pIPKb001:*GluA2*) was confirmed by sequence analysis done at the Australian Genome Research Facility (AGRF).

2.2.1.2. Amplification of *OsNAS2* gene for Gateway cloning

The pCR8::*OsNAS2* plasmid carrying the *OsNAS2* coding sequence was kindly provided by A/Prof. Alex Johnson and Dr. Julien Pierre Bonneu (The University of Melbourne, Australia). A ~ 1000-bp fragment of the *OsNAS2* coding sequence was amplified by the oligonucleotides *att*B1-OsNAS2F and *att*B2-OsNAS2R to introduce the *att*B sites for the Gateway cloning. The PCR product of the *OsNAS2* encoding region was purified using the Wizard® SV Gel and PCR Clean-Up System before conducting BP recombination reactions to clone into the pDOR221 vector. About 150 ng (50 fmol) of donor vector (pDOR221) and 34ng (50fmol) of the OsNAS2 PCR product were combined in a 10 µl BP reaction with 2 µl of BP Clonase™ enzyme mix (Invitrogen) at room temperature for an hour. The BP reaction was treated with 1 µl of 2 µg/µl Proteinase K solution at 37^0C for 10 minutes before transformation. The 10 µl BP reaction was transformed into 50 µl of competent *E.coli* strain DH5α by heat-shock, then selected on LB plates containing 100 µg/ml Kanamycin at 37^0C. A colony growing on the selective plate was inoculated into LB broth containing 100 µg/ml of Kanamycin for plasmid DNA isolation using the Wizard® Plus SV minipreps DNA purification system (Promega). The recombinant vector (pENTR221:*OsNAS2*) containing the *OsNAS2* encoding region was also verified by sequencing.

Two parallel 10-µl LR recombination reactions between entry vector pENTR221:*OsNAS2* or pENTR221:*gus* and the destination vector pIPKb001::*GluA2* were conducted using 2 µl of LR Clonase II enzyme mix and then incubated at room temperature overnight. The LR reactions were

treated with 1 µl of 2 µg/µl Proteinase K solution at 37^0C for 10 minutes, before transforming into 50 µl of DH5α competent cells by heat-shock. A positive colony growing on selective LB plate containing 100 µg/ml of Spectinomycin was verified for integration of *GluA2: OsNAS2* (SC2) and *GluA2:uidA* (GUS) by analytical digestion test with *Xho*I and *Eco*RV, respectively.

2.2.1.3. Generation of double gene cassette construct (DC) containing *GluA2:OsNAS2* and *Glb-1:HvSUT1*

The oligonucleotides *Spe*I-GluA2F and *Spe*I-NosTR were used to amplify the whole of the *GluA2:OsNAS2* gene cassette. A ~2000bp PCR product was generated with, of the *GluA2:OsNAS2* construct with introduced *Spe*I sites at the 5' and 3' ends. Two separate single *Spe*I digests of pIPKb001 containing *Glb-1:HvSUT1* (from Huynh (2015)) and the PCR product of *GluA2:OsNAS2* construct were conducted in 20-µl reactions, and incubated at 37^0C for 1 hour. For the digest of pIPKb001 containing *Glb-1:HvSUT1*, a further treatment with thermosensitive shrimp alkaline phosphatase (TSAP) was carried out at 37^0C for 15 minutes. These digests were further purified using the Wizard® SV Gel and PCR Clean-Up System before ligation as described before. A 10 µl-reaction of the ligation was transformed into 50 µl of DH5α competent cells by the heat shock method. Transformed cells were selected on LB plate with 100 µg/ml Spectinomycin at 37^0C. A positive colony was inoculated for plasmid DNA isolation and verified by analytical digestion with *Sac*I and *Eco*RV to test for integration and the expected orientation. This colony was further tested by sequence analysis. This gene construct was designed as *GluA2:OsNAS2-Glb-1:HvSUT1* construct (or DC for double construct).

2.2.1.4. *In-silico* analysis of *cis* elements of promoter sequences.

Nucleotide sequences (~1 kbp upstream of transcription start site) of the two cloned promoters *GluA2* (this study) and *Glb-1* (Huynh 2015) and three reference promoter sequences,

namely rice glutelin A2 (*refGluA2*- Accession no: EU264103) published by Qu *et al.* (2008), glutelin B1 (*GluB1*) published by (Wu *et al.* 2000), and 896bp-*α*-Globulin (*RefGlb*) published by Hwang *et al.* (2002) and Nakase *et al.* (1996) were used for scanning of cis-elements by PLACE (https://www.dna.affrc.go.jp/PLACE/?action=newplace).

2.2.2. Preparation of *Agrobacterium* for transformation.

2.2.2.1. *Agrobacterium* strains and construct used for transformation

Three binary vectors containing three different constructs, namely *Glb-1:HvSUT1* (SC1), *GluA2:OsNAS2* (SC2) and *GluA2:OsNAS2-Glb-1:HvSUT1* (DC) constructs, were separately transferred into *Agrobacterium* cell by electroporation. A mixture of about 200ng of each binary vector and 40 µl of *Agrobacterium* competent cell strain AGL1 was transferred into a chilled electroporation cuvette on ice-bath for 2 minutes. The gene pulser (Bio-Rad, USA) apparatus was set with voltage to 2.5 kV, the capacitance at 25 µF and a resistance of 200Ω. A pulse for ~5.00 milliseconds was delivered and 1 ml of SOC media immediately added into the cuvette. Cells were transferred to a 1.5 ml Eppendorf tube and incubated at 28^0C with shaking ~ 100rpm for 2 hours for cell recovery. Transformed *Agrobacterium* cells were selected on LB plate containing 20 µg/ml of Rifampicin and 25 µg/ml of Spectinomycin for 2 days at 28^0C. A positive colony growing on selective LB media was inoculated into LB broth containing 20 µg/ml of Rifampicin and 25 µg/ml of Spectinomycin and incubated for 2 days at 28^0C for plasmid isolation and then an analytical digestion test. For virulence gene induction a single AGL1 colony harbouring the correct destination plasmid was inoculated into 10 ml of LB broth with Rifampicin (20 µg/ml) and Spectinomycin (25 µg/ml) and incubated with shaking at 28ºC. A 500 µl-aliquot of AGL1 harbouring the correct destination plasmid was stored at -80^0C for rice callus or immature embryo infection.

2.2.2.2. Preparation of *A. tumefaciens* inoculum.

A 500-µl aliquot of frozen AGL1 cells harbouring the correct transformation plasmid was placed in an ice bath for thawing for 5 minutes. A 200 µl aliquot of AGL1 cells was streaked out on a LB plate containing 20 µg/ml Rifampicin and 25 µg/ml Spectinomycin and incubated at 28^0C for 2 or 3 days. The AGL1 cells of single colony were collected by a loop and suspended in 10 ml of A200 medium with 10 µl of freshly made 20 mg/ml Acetosyringone (100 µM final concentration). The *Agrobacterium* were completely suspended by gently inverting several times. To use for immature embryo transformation, the suspension of the AGL1 cells was adjusted to 3 x 10^9 colony-forming units (CFU) per ml (OD 0.3 at 600 nm). Then the suspension was incubated at room temperature for 1 hour in a shaker before infecting the immature embryos.

2.2.2.3. Preparation of plant materials for transformation

Mature seeds of rice IR64 were sown in soil in 6-cell pots in a greenhouse. After 2 weeks, the seedlings were transplanted into soil in 3-L pots in a greenhouse with a temperature setting of 28^0C/25^0C (day/night) and setting of 14:10 h photoperiod. High purity (MilliQ) water with pH from 5.2 to 5.8 was used for daily watering.

2.2.2.4. Immature embryo transformation

Agrobacterium- mediated transformation of immature embryo in rice IR64 (*Oryza sativa* L.) was carried out based on the protocol published by Slamet-Loedin *et al.* (2014) with several modifications (Figure 2.1). Roughly 50 immature seeds harvested from one third the top of multiple rice panicles at 8-12 days after anthesis (DAA) were dehulled to remove the glumes, lemma and palea of the immature seeds, and then collected into 50-ml Falcon tube. The immature seeds were rinsed in 70% ethanol for 10 seconds and then in 25 ml of 50% commercial bleach solution with a drop of Tween 20 for 5 minutes in a shaker. All subsequent steps were carried out

under a laminar flow cabinet. The sterilised seeds were transferred into another sterile 50ml Falcon tube and then rinsed in sterile MilliQ water 6 times. Immature embryos were isolated by forceps and transferred onto A201 medium. The scutellum side of the immature embryos facing up, had a 5 µl drop of *Agrobacterium* suspension placed on it and then incubated for 15 minutes to allow the *Agrobacterium* suspension to infiltrate the medium. Before the immature embryos were placed to fresh A201 medium plates in the dark at 25^0C for 7 days, they were rolled on the surface of the plate around the *Agrobacterium* inoculum to eliminate overgrowth of *Agrobacterium* during cocultivation period. After the cocultivation step, the immature embryos were removed from their elongated shoots with a scalpel. The immature embryos were quickly dried by gently pressing on a sterile filter papers several times, before they were transferred onto A202 medium containing 100 mg/L of timentin after which they were large enough to be cut into four pieces on a sterile filter paper. All pieces of the immature embryos were incubated onto A203 medium containing 100 mg/L timentin and 30mg/L hygromycin B under continuous light at 30^0C for a first selection of 10 days, after which they were passed through two more rounds of selection on A203 medium containing 100 mg/L timentin and 30mg/L hygromycin, under continuous light at 30^0C for 20 days. After three selection rounds, some calli were vigorously growing on the A203 selection medium. These embryogenic calli were transferred to A204 medium containing 100mg/L timentin and 50mg/L hygromycin for pre-regeneration, then incubated under continuously light at 30^0C for 10 days. After which some proliferating calli with green spots were transferred to regeneration medium (A205) for 14 days for shooting. Nine well-regenerated plantlets (shoots) were transferred into a single Magenta vessel containing MS30 medium with 30mg/L hygromycin and 100mg/L timentin for root induction. This rooting step was for 14 days under continuous light condition at 30^0C. Other small shoots were transferred onto fresh the A205 medium to grow into well-

regenerated plantlets before transferring into MS30 medium for root induction. Well-developed transgenic plants were transferred to pots containing Jefferies® soil mix wetted by MilliQ water (pH 5.6-5.8) at 14 hours light :10 hours dark with a temperature setting of 28/26^{0}C (day/night).

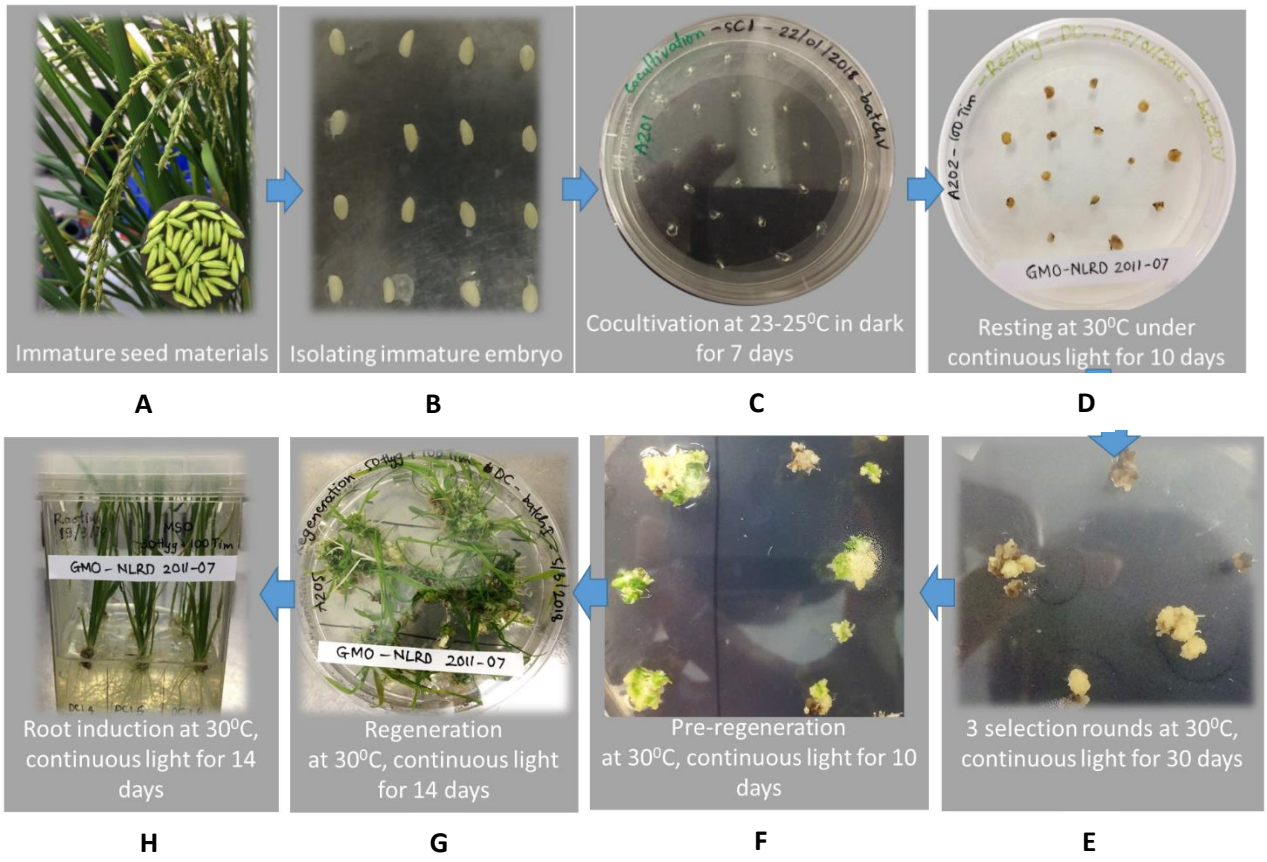

Figure 2.1. A high efficiency protocol for IR64 transformation using immature embryo. A. Immature seed materials, B. Isolation of immature embryos; C. Embryos co-cultivated with *Agrobacterium* strain AGL1 harboring the appropriate plasmid; D. Immature embryos under resting medium for recovery; E. Calli under selection medium; F. Pre-regeneration step for hygromycin-resistant calli; G. Regeneration for hygromycin-resistant shoot; H. Root induction step.

2.2.4. Rice growth condition

Mature rice seeds of transgenic lines were sterilised by rinsing with 70% ethanol for 30 seconds, then in 50% commercial bleach with a drop of Tween-20. The seeds were rinsed in the

bleach solution for 20 min with gentle shaking. The sterilised seeds were rinsed five times with MilliQ water. The seeds were germinated in MilliQ water-prewet Whatman paper and then incubated at 29^0C for 36 h under dark condition, and then incubated under photoperiod of 14h/10h for day/night for 7 days after germination. Seedlings were transplanted into Jefferies® soil in a growth chamber under photoperiod conditions of 14h day/10h night for a further 7 days. Seedlings were then transplanted into a 5L pot in Jefferies® soil in the greenhouse and the temperature was maintained from 25-29^0C and the photoperiod conditions were 14h day/10h night with supplementary lighting.

2.2.5. End-point PCR for confirming transgene integration

Rice genomic DNA (gDNA) used for end-point PCR and qPCR was isolated from leaves using an Isolate II plant DNA kit (Bioline). Young leaf tissue (~100mg) was ground in liquid nitrogen to a fine powder using pre-chilled mortar and pestle. Following binding and washing of the Bioline resin, the gDNA was eluted twice in 50 µl elution buffer (5mM Tris-HCl, pH 8.5) to achieve the highest yield possible of DNA. The quantity of gDNA was estimated using a spectrophotometer (Nanodrop 2000, Thermo Scientific).

Genomic DNA extracted from leaves of transgenic lines (T0, T1 or T2) was used to detect transgene integration and segregation in the genome. A 25µl- PCR consisted of 1X GoTaq® Green Reaction Buffer (Promega), 2mM $MgCl_2$, 0.4mM dNTPs, 0.4 µM for each primer (Appendix A) and 2 µl of 4.26 ng/µl DNA template. The PCR cycling protocol was as follows; initial denaturation for 10 minutes at 95^0C, followed by 30 cycles of 95^0C for 30 seconds, 64^0C for 30 seconds and 72^0C for 30 seconds, and 72^0C for 10 minutes. PCR products were visualized on a 1% agarose gel.

2.2.6. Standard curve establishment

Efficient, reproducible, and dynamic range qPCR was determined by making a standard curve using serial 10-fold dilutions of the target gene (10^5, 10^4, 10^3, 10^2 and 10^1 copies/µl). The absolute quantification of copy number of target sequence per haploid genome was calculated based on the mass of genomic DNA, or plasmid DNA, and UV absorption at 260nm as the formula below.

$$m = n \times (1.096 \times 10^{-21} \text{ g/bp})$$

where m is mass (g) of genomic DNA or plasmid and n is rice genome size of 389 Mb (International Rice Genome Sequencing Project 2005).

The standard curve of the Ct value against the log of the starting template DNA amount at each dilution was generated. Each dilution had three replicates. The amplification efficiencies of the primer pairs for the reference gene and the transgene were compared with each other. The primer pairs for the reference gene and the transgene were chosen to be similar and nearly 100% and within 5% of each other. Based on the standard deviation of five dilutions in the standard curve, a dynamic concentration of DNA template should have the lowest standard deviation in five dilutions and then used in zygosity analysis.

2.2.7. qPCR assay for zygosity identification

Reactions were done using the CFX96TM Real-time PCR detection system (BioRAD). A 20µl reaction consisted of 10 µl (1X) KiCqStart SYBR Green qPCR ReadyMix (Sigma, Cat#KCQS00), 300nM for each primer and 5 µl of gDNA template (0.426 ng/µl ~10^4 copies/µl). A standard 2-step protocol was as follows: 1 cycle for DNA denaturation at 95^0C for 10 minutes, followed by 40 cycles of 95^0C for 15 seconds and 60^0C for 30 seconds and a melting curve was

generated in 0.5^0C increments starting at 60^0C. Reactions of a reference gene (*SBE4*) and the transgenes were run in triplicate.

As the amplification efficiency of reference gene and transgenes were similar and nearly 100% and within 5% of each other, the zygosity of transgenic plants was determined by the $2^{-\Delta\Delta Ct}$ (Livak) method. The difference, ΔCt, between the Ct value for transgene and for reference gene for the test plant was calculated, then normalized to the ΔCt for a calibrator plant to obtain copy number calculation (ΔΔCt). Then the resulting ΔΔCt value was incorporated to determine zygosity of the test plant. The $2^{-\Delta\Delta Ct}$ (Livak) method was calculated using steps below:

First, the Ct value of transgene (*HvSUT1*) was normalized to that of the reference gene, starch-branching enzyme 4 (*SBE4*) for both test plants and calibrator:

$$\Delta Ct(test) = Ct(target, test) – Ct(ref, test)$$

$$\Delta Ct(calibrator) = Ct(target, calibrator) – Ct(ref, calibrator)$$

Second, ΔCt of test plant was normalised to that of the calibrator to obtain ΔΔCt:

$$\Delta\Delta Ct = \Delta Ct(test) – \Delta Ct(calibrator)$$

Finally, the 2-fold difference was then simply 2 to the power of -ΔΔCt: $2^{-\Delta\Delta Ct}$

Therefore, if the calibrator is hemizygous, that is a single-insert plant, the $2^{-\Delta\Delta Ct}$ of a homozygous single-insert plant will be twice that of the calibrator.

2.3. Results

2.3.1. Designing vectors for rice transformation

2.3.1.1. Preparation and verification of *Glb-1:HvSUT1* (SC1)

To examine if a novel combination of *OsNAS2* and *HvSUT1* overexpression in the rice grain can improve Fe/Zn contents and bioavailability in the endosperm, three T-DNA constructs carrying *HvSUT1* or/and *OsNAS2* were prepared. A single gene cassette of *HvSUT1* under the control of the rice 26kDa-Globulin 1 promoter for endosperm-specific expression, designated from now on as SC1, was cloned into binary vector pIPKb001 by Huynh (2015) (Figure 2.2). The identity of this binary vector was verified by plasmid DNA extraction and *Eco*RI digestion. A single band of the digested SC1 was visualised on 1% agarose gel, compared to two bands of digested empty pIPKb001 as expected (Figure 2.2B). There were two *Eco*RI sites in the hygromycin-resistant and chloramphenicol resistant genes. The recombinant plasmid had a single site for restriction enzyme *Eco*RI, when the *HvSUT1* gene without *Eco*RI site was replaced into the chloramphenicol resistant gene. This plasmid DNA was sequenced for verification. A 982-bp region of the 26kDa Globulin 1 promoter (*Glb-1*) and the 1930-bp region of the *HvSUT1* cds were confirmed by DNA sequencing.

The sequence of the *Glb-1* promoter was aligned with the reference (AY427575). An additional adenine (A) was found in the SC1 plasmid obtained from Huynh (2015). No difference between the *HvSUT1* sequence was found, compared to the sequencing data obtained from Huynh (2015). A BLAST analysis (Appendix A-Figure 6.1) of the 1930-bp *HvSUT1* sequence aligned against the barley's data collection (taxid:4512) in the NCBI database showed four sequences of *HvSUT1* cds with more than 99.8% of identity, including AM055812.1 (2044 bp) published by

Sivitz *et al.* (2005), AJ272309.1 (2044 in length) published by Weschke *et al.* (2000), AK371431.1 (2155 bp) and AK367120.1 (2155 bp) published by Matsumoto *et al.* (2011). No difference in the sequence of *HvSUT1* was observed in cds region.

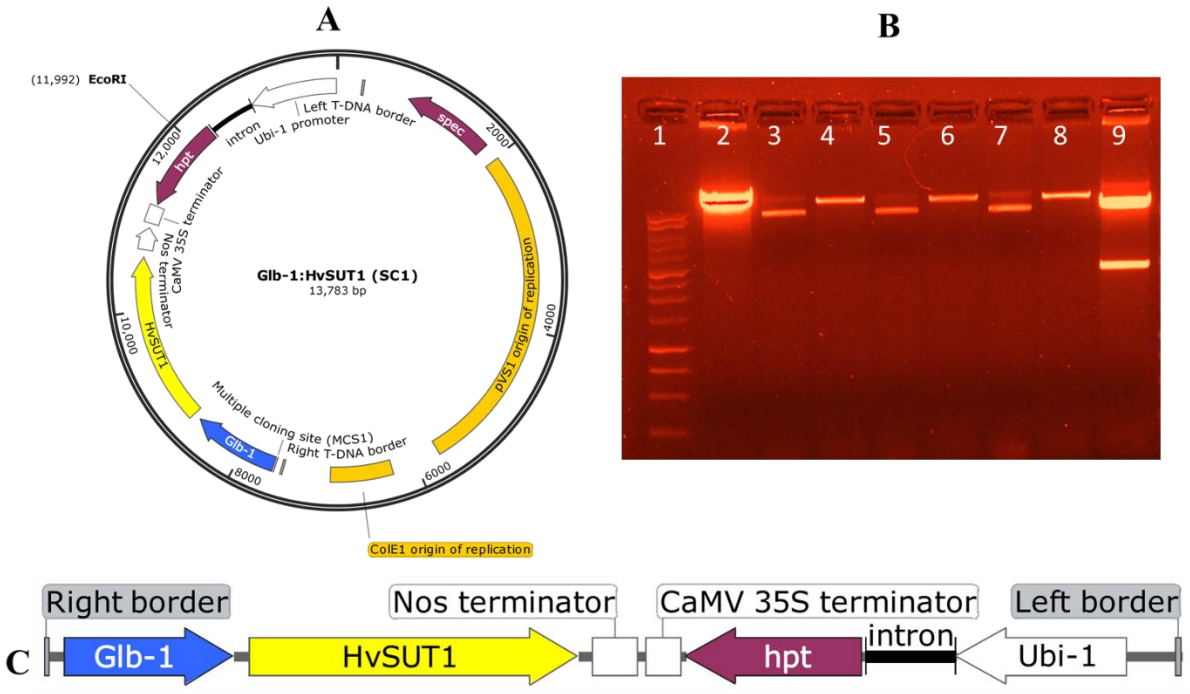

Figure 2.2. Verification of SC1 construct containing *Glb-1: HvSUT1*. **A**. The representative scheme of plasmid pIPKb001 containing *Glb-1: HvSUT1* (13.783Kb). T-DNA and the backbone of a binary expression vector has a single *Eco*RI restriction enzyme site. **B**. Digests with *Eco*RI to confirm identity of cloned destination plasmids. Lane 1: marker; Lane 2: positive control - the digested recombinant plasmid containing *Glb-1:HvSUT1* from *E. coli*; Lane 3, 5, and 7: undigested plasmids from *Agrobacterium* colony 1, 2 and 3; Lane 4, 6, and 8: digested plasmids from *Agrobacterium* colony 1, 2 and 3; Lane 9: negative control- digested empty plasmid pIPKb001. **C**. T-DNA region with *HvSUT1* gene under control of endosperm-specific promoter *Glb1* and hygromycin (*hpt*) gene under control of *Ubi-1* promoter.

2.3.1.2. Cloning and sequencing of rice *GluA2* promoter

For the single gene cassette of the *OsNAS2* under the control of the rice Glutenin A2 *(GluA2)* promoter designated as SC2, a single band of roughly 900bp was amplified from rice (Nipponbare) genomic DNA with *GluA2* promoter specific primers. The length of the PCR product (839 bp) was as expected and purified for cloning. At lower annealing temperature of 65^0C, multiple bands of 700 bp – 1000bp were observed and not appropriate for cloning (Appendix A-Figure 6.2). The putative *GluA2* promoter PCR product was digested with *Spe*I and *Hind*III and then cloned into the multiple cloning site of pIPKb001. The pIPKb001 clone containing the putative promoter *GluA2* (pIPKb001:p*GluA2*) was verified for integration and correct orientation by colony PCR, analytical restriction digestion and DNA sequencing.

A putative colony carrying the pIPKb001:*pGluA2* was determined via colony PCR with *GluA2* promoter specific primers and digestion of purified plasmid DNA by digestion with *Eco*RV (see Appendix A-Figure 6.2). A PCR product of roughly 850 bp was visualized on 1% agarose gel. The plasmid from that colony was confirmed for the integration of *GluA2* promoter into pIPKb001 by single digestion with *Eco*RV. The plasmid from the putative colony carrying the pIPKb001:p*GluA2* was cut to form two bands (>10,000 bp and 900 bp), whereas a single band of more than 10kb was visualised in the empty plasmid of pIPKb001 (original pIPKb001 and re-ligated pIPKb001). The results of the digestions were very similar with the expected results basing on analysis of restriction enzyme sites via NEB cutter V2.0 (BioLabs) (http://nc2.neb.com/NEBcutter2/). This indicated the successful integration of *GluA2* promoter into pIPKb001 vector. A further verification of the sequence and correct orientation of the cloned *GluA2* promoter was carried out by DNA sequencing at the AGRF. The fragment of the *GluA2* promoter was between the position of the *Spe*I and *Hin*dIII sites and its orientation was correct.

The sequence of the *GluA2* promoter was aligned with the reference (EU264103.1) (Appendix A-Figure 6.3) and there were three changes in single nucleotide on *GluA2* promoter's sequence, including 2 positions of cytosine (C) replaced by adenine (A) and missing one adenine (A). It is impossible to know if these changes are derived from genetic drift in the rice plants used in DNA extraction in this study and those used to generate the sequence on NBCI, or they are the result of changes during PCR and cloning. An analysis of *cis*-elements for endosperm -specific expression on two cloned promoters in rice is presented in the next section.

2.3.1.3. *In silico* analysis of *cis* elements for endosperm-specific expression in two cloned *GluA2 and Glb-1* promoters

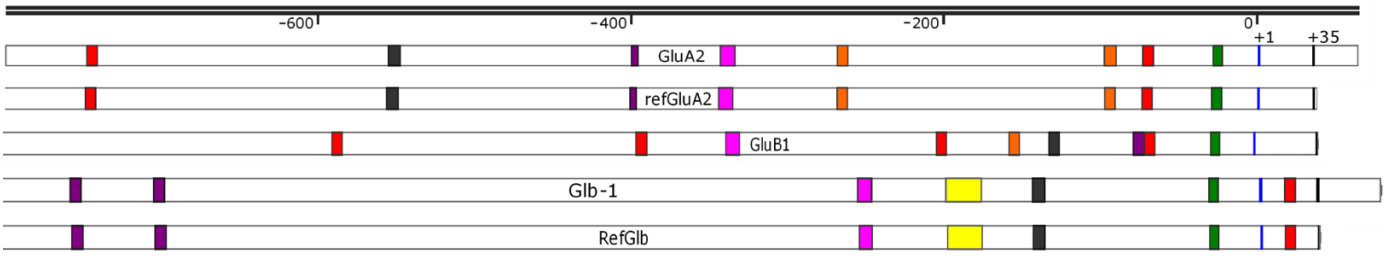

Figure 2.3. Location of *cis*-elements in the nucleotide sequence of the cloned glutelin A2 promoter (*GluA2*), the reference promoter of glutelin A2, (*refGluA2*), the cloned 26kDa globulin-1 promoter (*Glb-1*), 896-bp α-globulin (*RefGlb*), and glutelin B1 (*GluB1*) promoters. *GluA2* and *Glb-1* promoters were cloned in this study and used to screen for the *cis*-elements by PLACE. *GluB1* (Wu *et al.* 2000), *refGluA2* and *RefGlb* (Hwang *et al.* 2002; Nakase *et al.* 1996) are three references for *GluA2* and *Glb-1*, respectively. Purple rectangle: ACGT motif, Pink rectangle: GCAA motif; Yellow rectangle: A+T rich region; **Black** rectangle: Prolamin box; Green rectangle: TATA box; Red rectangle: AACA motif; Orange rectangle: GCN4; Blue line: the transcription start site (+1). **Black** line: the site at +35 from the transcription start site.

The *GluA2* and *Glb-1* promoters were expected to drive endosperm specific expression in rice. To ensure a strong and tissue-specific transcription activity of the transgenes, the sequences of the cloned *GluA2* and *Glb-1* promoters were analysed for the presence of functional *cis*-elements by the PLACE (https://www.dna.affrc.go.jp/PLACE/?action=newplace). The functional *cis*-elements that could be involved in controlling the rice endosperm-specific expression were investigated and compared between the cloned sequence and three reference sequences of *refGluA2* (accession no: EU264103) (Qu *et al.* 2008), *GluB1* (Wu *et al.* 2000) and *RefGlb* (Hwang *et al.* 2002; Nakase *et al.* 1996), which have been well-analysed (Figure 2.3). Five essential motifs for the rice endosperm specific expression, namely the GCN4 (TGAGTCA) motif, AACA (AACAAAC) motif, ACGT motif, GCAA motif (GCAAAATGA in glutelin), and prolamin-box (TGCAAAG) motifs were present in the sequences of the *GluA2, refGluA2* and *GluB1* promoters. The components of five of the *cis* elements in the *GluA2* promoter were the same as that in the *refGluA2*. The *GluA2* and *GluB1* promoters had a single copy of the ACGT motif, the GCAA motif and the prolamin box, while the GCN4 and the AACA motifs had two and one copies in the *GluA2* promoter, respectively and one and three copies in the *GluB1* promoter.

The *cis*-elements of the cloned *Glb-1* promoter were the same as the reference sequence of the *RefGlb* promoter. There were two copies of the ACGT motif and a single copy of the GCAA motif (CACAAAAG in globulin), A+T rich region, and Prolamin box. However, the cloned *Glb-1* and *RefGlb* promoters contained a copy of the AACA motif located at 15bp downstream of the transcription start site. No copy of GCN4 motifs was found in the *Glb-1* and *RefGlb* promoters, whereas the *GluA2* and *GluB1* promoters did not contain A+T rich region. All the promoters had a TATA box located at ~ 25 bp upstream of the transcription start site. On the basis of this analysis

it was assumed that the amplified and cloned promoters would function properly. In addition, the results of Huynh (2015) confirm the activity of the *Glb-1* promoter in Japonica rice.

In order to predict the activity of the Japonica *OsGluA2* and *OsGlb-1* promoters in transgenic Indica rice, the Indica and Japonica promoters were compared (Figure 2.4). Fourteen nucleotide differences in the region of the *Glb-1* promoter between Indica and Japonica rice were present, compared with 4 polymorphisms in the region of the *GluA2* promoter. In addition, the sequences of the cloned *GluA2* and *Glb-1* promoters had 1-3 nucleotide differences with the Japonica promoters. Both the cloned *GluA2* and *Glb-1* promoters contained all conserved *cis* regulatory elements essential for their endosperm-specific expression, therefore, their correct function between these different rice sub-species was predicted.

In order to verify the tissue specificity of the *GluA2* promoter, a *GluA2:uidA* fusion was made and transformed into Indica rice cv. IR64. Previous research of Huynh (2015) has performed a similar analysis of the *Glb-1* promoter in transgenic Japonica rice cultivar Nipponbare. The author demonstrated that the *Glb-1* promoter drove GUS expression specific in rice endosperm. A further analysis on the *GluA2* promoter would also be conducted in Chapter 3.

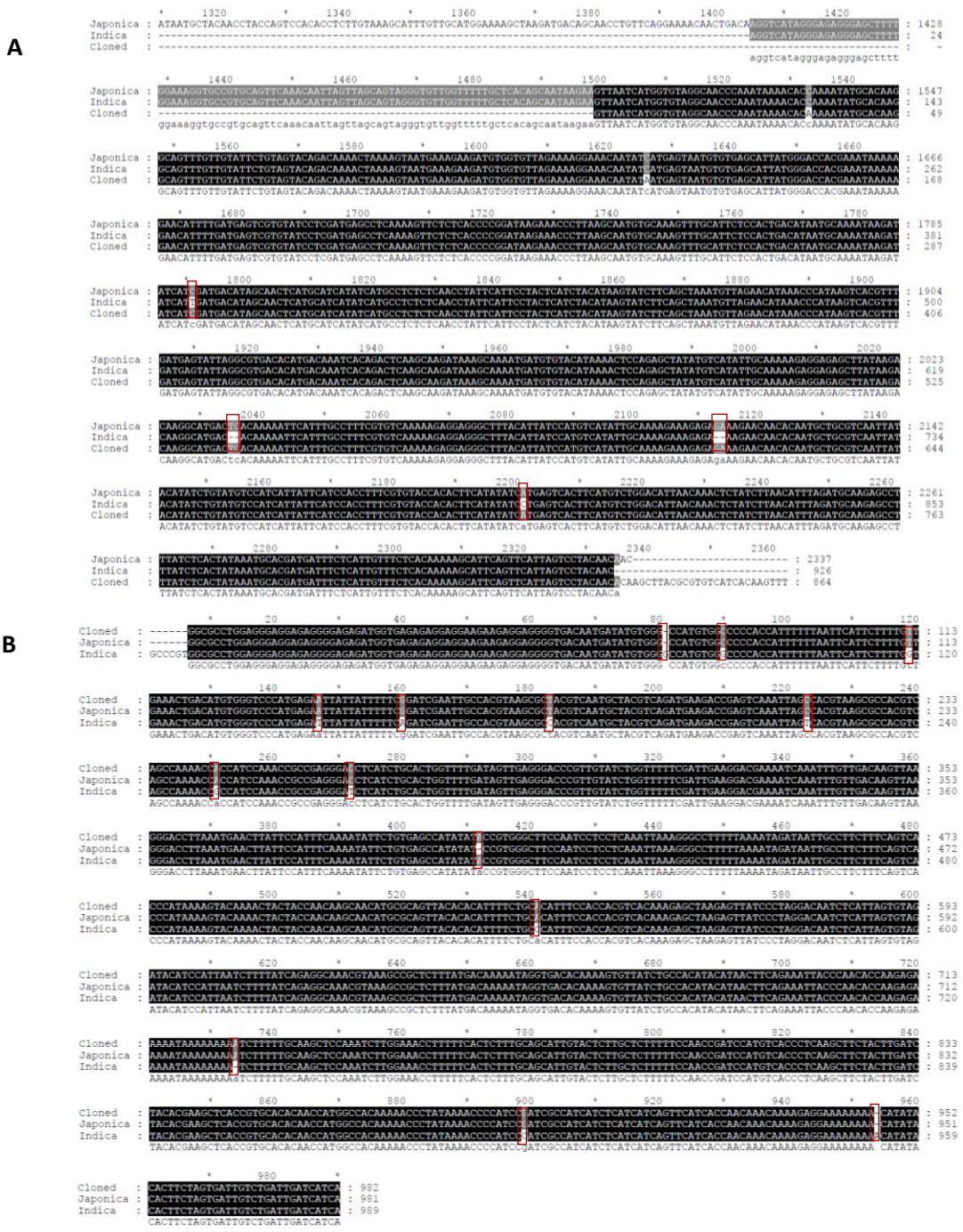

Figure 2.4. Variations of the promoter regions of glutelin A2 and globulin genes between Indica and Japonica rice. A: Alignment of nucleotide acid sequences of the *GluA2* promoter from Indica and Japonica rice. B. Alignment of nucleotide acid sequences of the *Glb-1* promoter from Indica and Japonica rice. Red box presents nucleotide acid variations.

2.3.1.4. Construction of binary vectors carrying *GluA2:OsNAS2* (SC2) and *GluA2:uidA* (GUS)

The single gene cassette of the *OsNAS2* under the control of the *GluA2* promoter was designated as SC2. A fragment of *OsNAS2* (981bp) with *att*B recombination sites was amplified from pCR8/GW-*OsNAS2*. The *att*B-PCR product of *OsNAS2* was used in a BP recombination reaction with a donor (pDONR221^{TM}) vector to create an entry vector containing the *OsNAS2* encoding region (pENTRY221:*OsNAS2*), 3528 bp in length. The entry vector was transformed and replicated in the *E. coli* strain DH5α. Many colonies were derived from a single BP recombination reaction. Plasmid DNA extracted from nine colonies and one empty pDONR221 were analysed by digestion with *Apa*I (Appendix A-Figure 6.4).

The putative plasmid from a single colony containing the pENTRY221:*OsNAS2* vector was then used in a LR recombination reaction with the pIPKb001:*GluA2* destination vector. Six colonies with recombinant destination vectors (pIPKb001:*GluA2:OsNAS2)* were obtained after transformation the LR reaction mix into *E.coli* strain DH5α. All colonies screened by colony PCR and analysed by restriction digestion with *Xho*I showed an expected pattern by gel electrophoresis (Figure 2.5B). The pIPKb001:*GluA2:OsNAS2* construct (12627 bp) was sequenced across of region of the *GluA2* promoter and the *OsNAS2* cds (Figure 2.5). The DNA sequence was free of errors, compared with the previous sequencing results. For the sequence of the *OsNAS2* region, there was a SNP (C replaced for T) at 321-bp downstream from the start codon (ATG). This change was recognised by the Johnson's lab of the University of Melbourne and was ignored as it did not change the amino acid at this codon. Upstream of *OsNAS2* was the *GluA2* promoter the downstream was the Nopaline Synthase (*Nos*) terminator, both identical in sequence to the previous results.

Another LR recombination reaction run in parallel with that described above was done between the pIPKb001:*GluA2* destination vector and the pENTRY221:*uidA* entry vector to make the *GluA2:uidA* gene construct. Plasmid DNA from four recombinant destination clones and the empty pIPKb001:*GluA2* destination vector and the pIPK001 backbone were analysed by *Eco*RV digestion. The result of analytical restriction enzyme digestion of these DNAs with *Eco*RV was as expected, with four band of 231 bp, 877bp, 1182 bp, and 11196 bp found in the pIPKb001:*GluA2:uidA* plasmid (Figure 2.6).

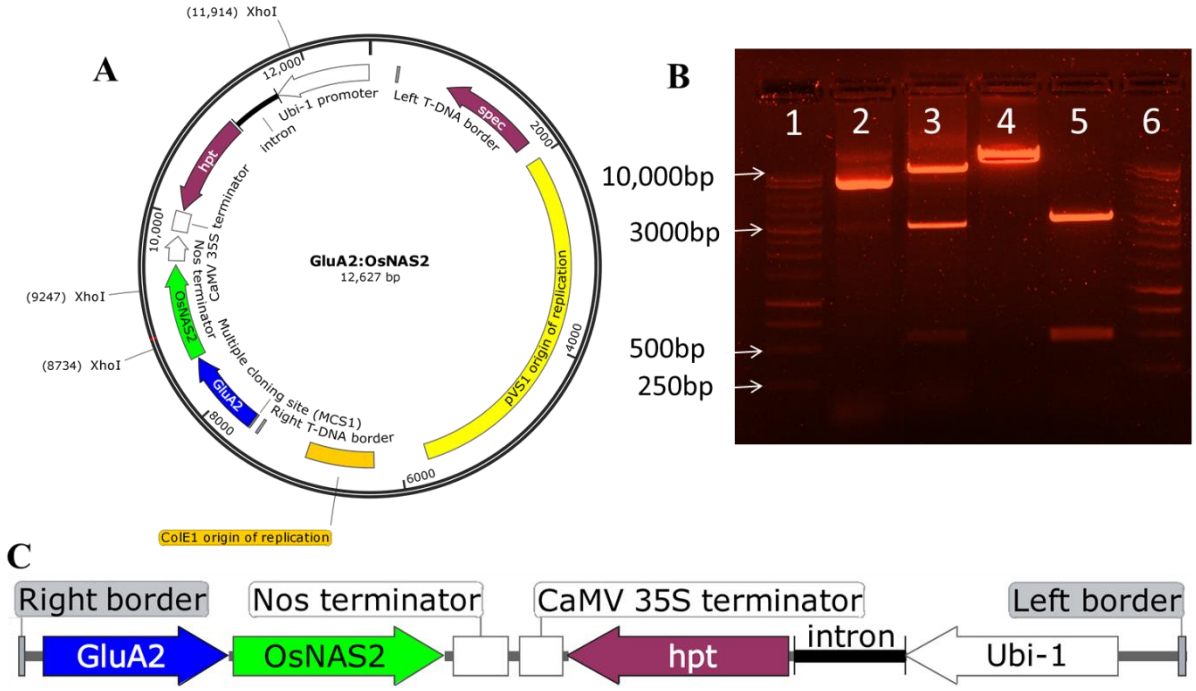

Figure 2.5. Digests to confirm identity of cloned destination plasmids used in rice transformation. A. The representative scheme of plasmid pIPKb001 containing *GluA2: OsNAS2* (12.627 Kbp). T-DNA and the backbone of a binary expression vector has three *Xho*I restriction enzyme sites. **B**. Digests with *Xho*I to confirm identity of cloned destination plasmids. Lane 1: marker; Lane 2: undigested the recombinant plasmid containing *GluA2:OsNAS2* from *E. coli*; Lane 3, digested the recombinant plasmid containing *GluA2:OsNAS2* from *E. coli,* there were three

bands (513 bp, 2667 bp, and 9447 bp); Lane 4: digested the pIPKb001:p*GluA2* destination vector with single *Xho*I digestion site; Lane 5: two bands (513 bp and 3015 bp) for the pENTRY221:*OsNAS2* vector with two *Xho*I digestion sites. **C**. T-DNA region with *OsNAS2* gene under control of the endosperm-specific promoter *GluA2* and hygromycin (*hpt*) gene under control of the *Ubi-1* promoter.

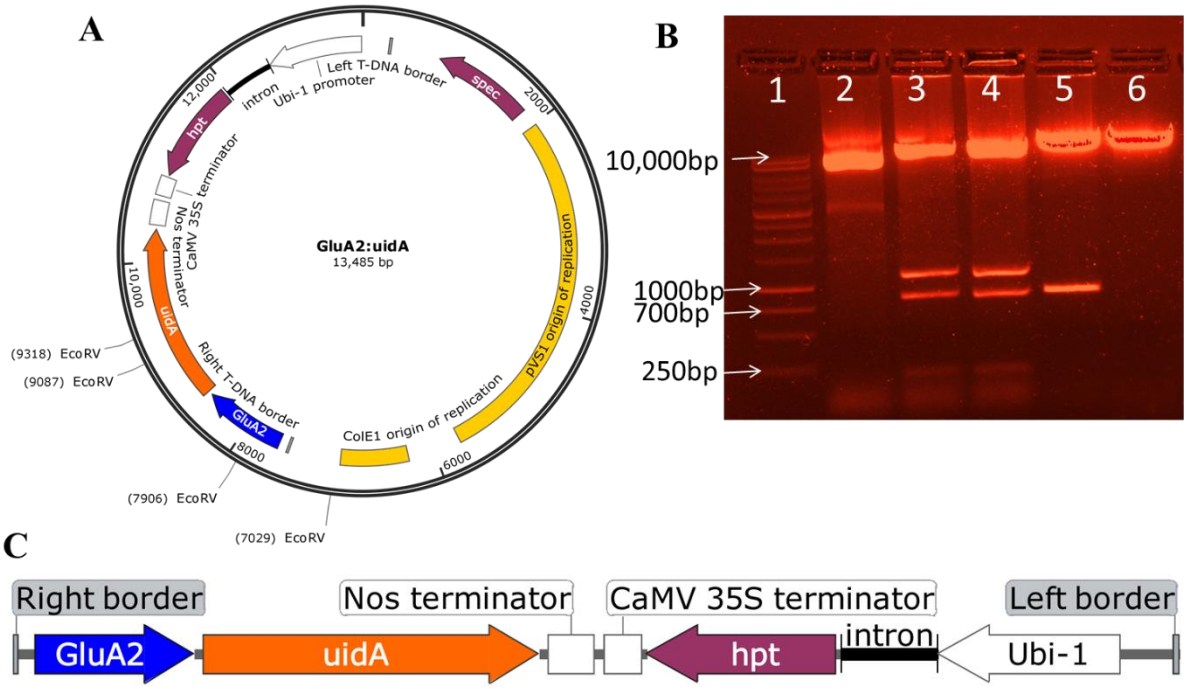

Figure 2.6. Digests to confirm identity of cloned destination plasmid used in rice transformation. A. The representative scheme of plasmid pIPKb001 containing *GluA2: uidA* (13.485 Kb). T-DNA and the backbone of a binary expression vector with four *Eco*RV restriction enzyme sites. **B**. Digests with *Eco*RV to confirm identity of cloned destination plasmids. Lane 1: marker; Lane 2: undigested the recombinant plasmid containing *GluA2:uidA* from *E. coli*; Lane 3 and 4, digested the recombinant plasmid containing *GluA2:uidA* from *E. coli*, there were four bands (231 bp, 877bp, 1182 bp and 11196 bp); Lane 5: digested pIPKb001:p*GluA2* destination vector with two *Eco*RV digestion sites ; Lane 6: digested the empty vector of pIPKb001 with single

*Eco*RV digestion site. **C**. T-DNA region with *uidA* reporter gene under control of the endosperm-specific promoter *GluA2* and hygromycin (*hpt*) gene under control of the *Ubi-1* promoter.

2.3.1.5. Preparation, verification and transformation of binary vector carrying *GluA2:OsNAS2 – Glb-1:HvSUT1* (DC1) into *Agrobacterium tumefaciens*.

A 2180bp-PCR product of the whole *GluA2*:*OsNAS2*:*NosT* gene cassette with flanking *Spe*I sites was amplified from the SC2 construct. The PCR product was cloned into the SC1 construct containing *Glb-1:HvSUT1* by single restriction enzyme (*Spe*I) and transformed into DH5α cells. Eight of the ten colonies that were screened by colony PCR showed positive results. Further analytical digestions of plasmid DNA extractions from 6 colonies with *Sac*I were carried out to verify the successful combination of the two cassettes (the *GluA2:OsNAS2:NosT* and *Glb-1:HvSUT1:NosT*) to form a double construct designated as DC1. Two bands of 877 bp and 15059 bp were observed in the digests of the plasmid from colony 1 and 10, whereas the digests of colony 3, 6, 7, and 8 showed two band of 2462 bp and 13474 bp. Two different patterns of bands on the gel showed two different orientations of the cassette *GluA2:OsNAS2:NosT* (Figure 2.7). The forward orientation, which was seen in the plasmid from colony 1 and 10 (Figure 2.7D) was used for rice transformation. The reverse orientation was found in colony 3,6,7, and 8 (Figure 2.7E).

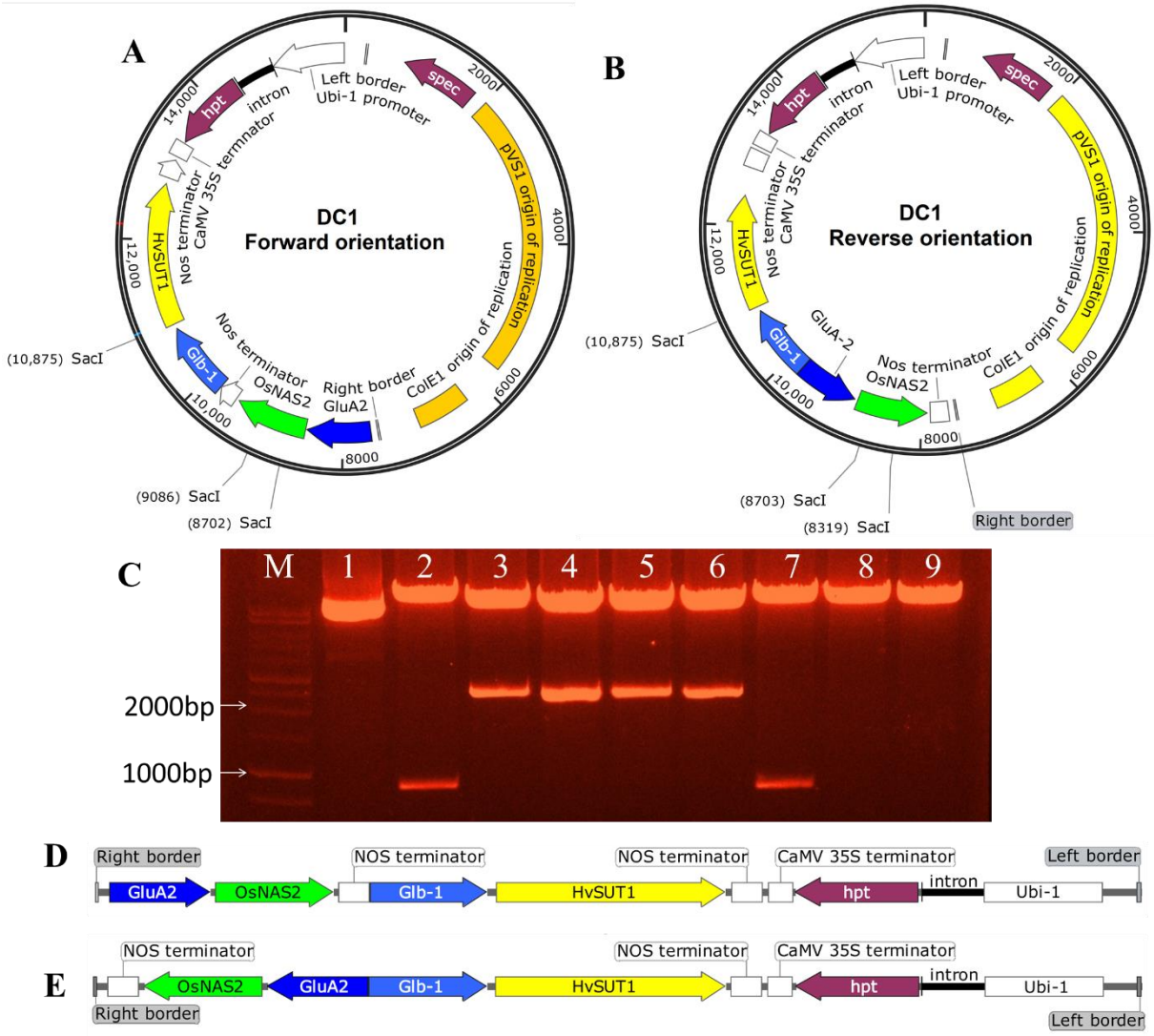

Figure 2.7. Digests to confirm of the DC1 construct containing the *GluA2:OsNAS2* and *Glb-1:HvSUT1*. **A** and **B**. The representative schemes of plasmid pIPKb001 containing the *GluA2:OsNAS2* and *Glb-1:HvSUT1* with a T-DNA in forward and reverse orientations, respectively. There were three sites of *Sac*I restriction enzyme. **C**. Digests with *Sac*I to confirm identity of cloned destination plasmids. M: marker; Lane 1: undigested the recombinant plasmid containing the recombination vector of DC from *E. coli*; Lane 2 and 7, the recombinant plasmid containing *GluA2:OsNAS2:NosT* and *Glb-1:HvSUT1:NosT* with a T-DNA in forward orientation from colony 1 and 10; Lane 3, 4, 5, and 6: digested the recombinant plasmid in reverse orientation

was found in colony 3,6,7, and 8; Lane 8 and 9: digested the recombinant plasmid of *Glb-1:HvSUT1* with single *Sac*I digestion site. **D** and **E**. T-DNA regions of the DC construct in forward and reverse orientations, respectively.

2.3.2. Generation of transgenic rice lines with three constructs

To examine the effect of nicotianamine synthase (NAS) and sucrose transporter (HvSUT1) protein in increasing of Fe and Zn levels in the rice endosperm, three constructs, namely *Glb-1*:*HvSUT1* (SC1), *GluA2*:*OsNAS2* (SC2) and *GluA2:OsNAS2-Glb-1:HvSUT1* (DC1) were designed (Figure 2.8) and then transfected into *A. tumefaciens* strain AGL1 for rice transformation.

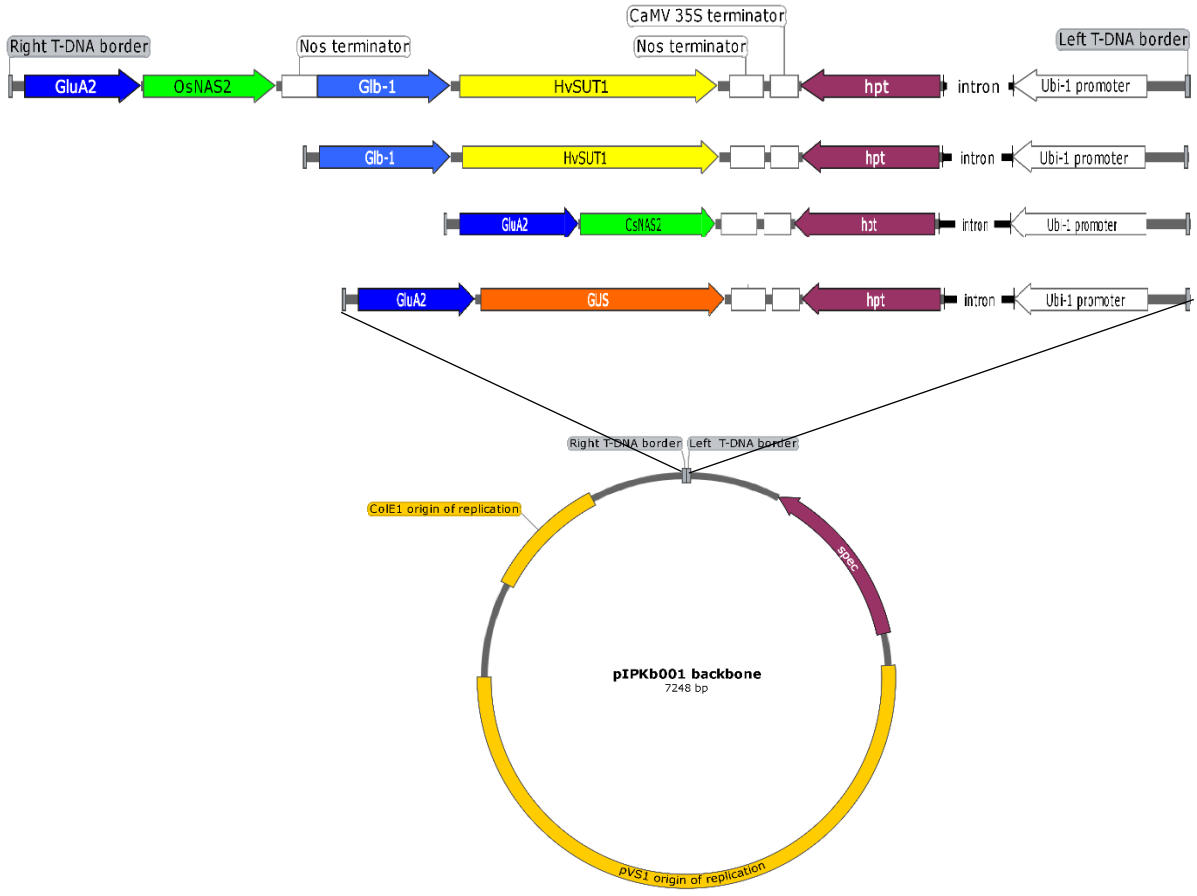

Figure 2.8. Schematic representation of the four T-DNA constructs for rice transformation. A. T-DNA construct containing *Glb-1*:*HvSUT1* in combination with *GluA2*:*OsNAS2* ; T-DNA

construct containing *Glb-1*:*HvSUT1* only (Huynh 2015); T-DNA construct containing *OsNAS2* *GluA2*:*OsNAS2* only; T-DNA construct containing β-glucuronidase gene (*uidA*), *GluA2*:*uidA*. *Glb1* and *GluA2*: endosperm specific promoter *Globulin 1* and *Glutelin A2*; T-DNA of GUS construct; *HvSUT1*: barley sucrose transporter 1, *OsNAS2*: rice nicotianamine synthetase 2. B. Backbone of expression binary plasmid.

2.3.2.1. Electroporation of the plasmid SC1, SC2 and DC1 into *Agrobacterium tumefaciens* strain AGL1

Verified plasmid DNA of SC1, SC2 and DC1 was electroporated into the *A. tumefaciens* strain AGL1. A single colony of *Agrobacterium* for each of the constructs was grown for storage and plasmid DNA extraction. Plasmid DNA extracted from *Agrobacterium* was re-transformed back into DH5α cell by heat-shock. Plasmid DNA was extracted for restriction enzyme digestion and compared to the DNA from the original DH5α colonies. The patterns of bands for SC1 and SC2 and DC1 DNAs passed through AGL1 and back into DH5α were identical to that donor DH5α plasmid DNAs. No structural changes were found in any of the constructs and thus the sequence was assumed to be fully intact. The *Agrobacterium* strains were now used for rice transformation.

2.3.2.2. Unsuccessful *Agrobacterium* transformation used mature embryos as starting material

Because IR64, an Indica rice, is a recalcitrant cultivar for *Agrobacterium*-mediated transformation and tissue culture, this study used mature and immature embryos as starting materials for transformation. The study started with the use of mature embryo of IR64 for

Agrobacterium transformation according to the method of Sahoo *et al.* (2011) and Sahoo and Tuteja (2012). Initial efforts using this transformation protocol were unsuccessful.

As a result, a protocol for *Agrobacterium* transformation of immature embryos as starting material was used, based on the protocol published by Slamet-Loedin *et al.* (2014) with several modifications outlined in the sections below: namely, co-cultivation with less overgrowth of *Agrobacterium*, multiple transgenic events from a single IE, consistent growth conditions from callus induction to root induction, and no non-transgenic shoot escape.

2.3.2.3. *Agrobacterium* transformation used immature embryos as starting material

Less overgrowth of Agrobacterium strain AGL1 in the cocultivation step

Immature seeds at 8 – 12 DAA provided the optimal material for embryo isolation and successful *Agrobacterium* transformation. Younger and older embryos were less successful as they were less intact, and survival was poor after isolation. After infection with 5 µl of *Agrobacterium* suspension (OD_{600nm} = 0.3), the embryos were incubated for 7 days at 29^0C. Overgrowth of *Agrobacterium* covering the whole embryos was observed if the infected embryos were not transferred into fresh cocultivation media (Figure 2.10 A, B and C). The embryos would turn brown and stop growing and consequently, no hygromycin-resistant callus was obtained after 3 selection rounds. However, if the infected embryos were rolled on the surface of the plate around the *Agrobacterium* inoculum and transferred onto fresh cocultivation medium, the overgrowth of *Agrobacterium* after cocultivation was minimised (Figure 2.10 D, E and F. This modification prevented the infected embryos from being overgrown with *A. tumefaciens*, leading to a poor transformation outcome. This step did not only reduce the overgrowth of *Agrobacterium*, but also growth of the infected embryos remained healthy during the 7-day

period of incubation. The infected immature embryos were split into 3-4 small pieces, and as a result, 3-4 independent transgenic lines were generated from a single embryo. In most of the experiments, the cocultivation step was incubated at 25^0C under dark conditions. Furthermore, two experiments were able to obtain hygromycin-resistant calli after the cocultivation step at 23^0C. However, there was no comparison made between the transformation efficiency between the two different temperature conditions for cocultivation.

Figure 2.9. Preparation of starting materials. A. Panicle of IR64 harvested, B. Immature IR64 seeds C. Immature IR64 dehusked. D. Immature embryos isolated

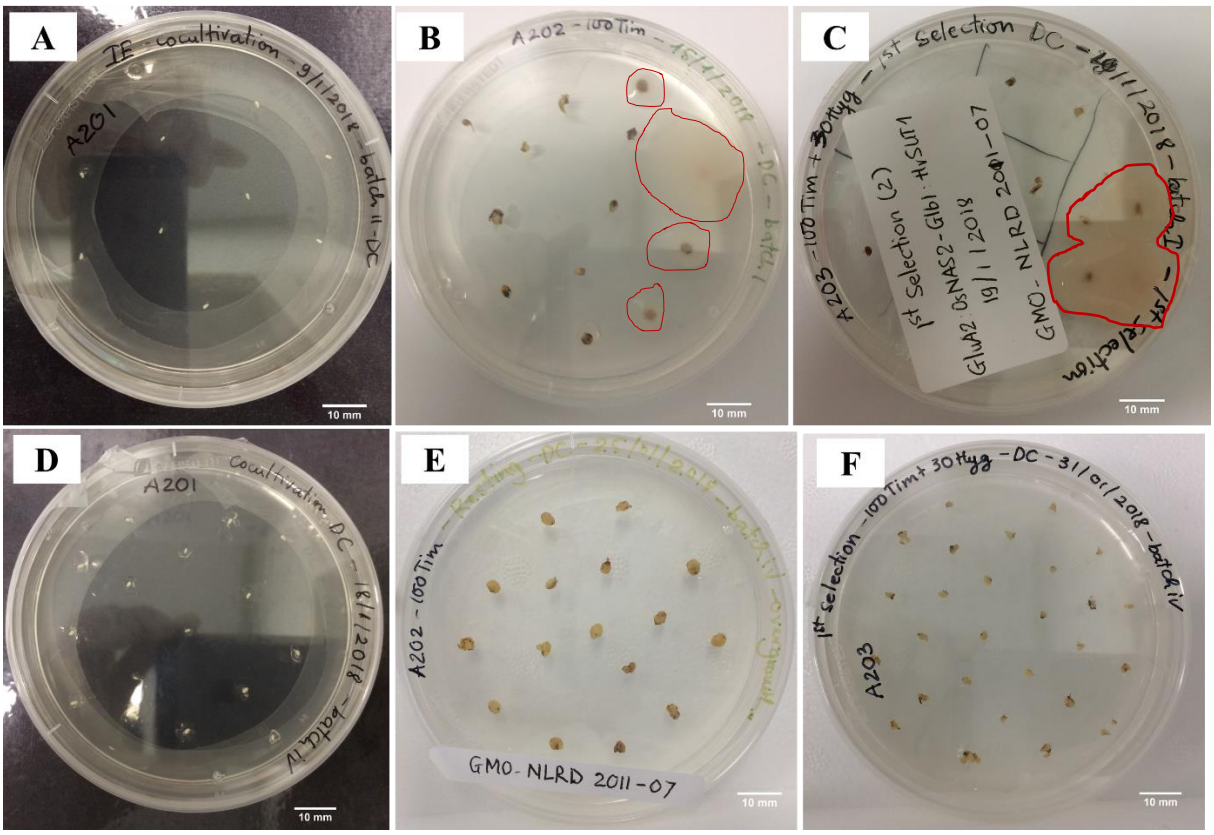

Figure 2.10. *Agrobacterium* infection and cocultivation for rice immature embryos. A 5µl aliquot of *Agrobacterium* suspension was dropped directly onto the embryos (A); the infected embryos incubated on the resting medium (B), then transferred onto the selection medium (C). A 5µl aliquot of *Agrobacterium* suspension was dropped directly onto the embryos and allowed to soak in for 15 minutes, then the infected immature embryos were rolled on the surface of the plate around *Agrobacterium* inoculum and transferred onto the fresh cocultivation medium (D), then transferred on the resting medium for 10 days (E), on the selection medium (F). The sections of the plates outlined in red indicate overgrowth of *Agrobacterium*. In all cases these embryos died and did not yield any transgenic tissue.

Consistent growth condition from callus induction to root induction

To generate high numbers of transgenic events with different transgene constructs, consistent growth chamber conditions for callus induction to root induction was important. In this study, seven batches of immature embryos were done in one month. With the exception of the cocultivation step, the calli were incubated at 30^0C under the continuous light in all following steps in the same growth chamber. This differs from the report of Slamet-Loedin *et al.* (2014) where the temperature for root induction was reduced to 25^0C..

Table 2.1. All transformation experiments

Construct	Batch number	Immature embryos	hygromycin-resistant calli	Designated
Glb1:HvSUT1:NosT (SC1)	6	78	25	SC1.1 to SC1.25
	2	Failed in *Agrobacterium* co-cultivation		
GluA2:OsNAS2:NosT (SC2)	4	46	10	SC2.1 to SC2.34
	7	110	24	
GluA2:Gus:NosT (GUS)	3	27	6	Gus1 to Gus39
	8	61	33	
GluA2:OsNAS2:NosT-Glb1:HvSUT1:NosT (DC1)	1	54	10	DC1.1 to DC1.21
	5	61	11	
Total		**437**	**119**	

Hygromycin selection rooting medium caused a very low possibility to get non-transgenic events

To preferentially promote transgenic shoots development, hygromycin continued to be used for selecting shoot growth in the rooting induction medium. An example of non-transgenic calli and regenerating shoots is shown in Figure 2.11 A and C. The non-transgenic calli were placed on the regeneration media A205 with 50 µg/ml of hygromycin. After 10 days, 7 out 8 calli were completely dead and 1 out of 8 calli showed some shoots with very poor growth, compared to healthy and vigorous growth of the shoots from transgenic calli (Figure 2.12 A and B). In spite of poor growth, the non-transgenic shoot was able to recover and develop into a full plantlet after 10 days in the root induction media MS0 without hygromycin. Therefore, adding hygromycin (30 µg/ml) into the root induction media MS30 was helpful to screen the non-transgenic shoots. Similarly, the heathy non-transgenic shoot died in the media MS30 with hygromycin after 10-day root induction (Figure 2.12B and D). The regenerated non-transgenic shoots on the media with hygromycin turned brown and had a very poor growth and died after 3 weeks, whereas on the media with no hygromycin, all the non-transgenic shoots grew vigorously. Therefore, the root induction medium was modified by adding hygromycin to screen non-transgenic shoot development.

For hygromycin-resistant shoots regenerating from three selection rounds, all grew vigorously into full plantlets after 2 weeks. Plantlets derived from separate hygromycin-resistant calli were designated as independent transgenic events, whereas regenerated shoots and seedlings from the same callus were considered to be potentially the same event. In this study, a total of 119 independent lines were produced from 119 different hygromycin-resistant calli. One experiment failed in the *Agrobacterium* co-cultivation step and seven successful transformation experiments

were carried out in this study.

Four populations, representing the 4 constructs, SC1, SC2, DC1 and GUS, of the putative T0 transgenic plantlets (119 independent lines in total) were generated from the seven successful transformation experiments (Table 2.1). These plantlets were transferred to soil and grown in a PC2 glasshouse. A population of 25 independent transgenic lines transformed with *Glb-1*:*HvSUT1* were designated from SC1.1 to SC1.25, 35 independent transgenic lines transformed with *GluA2*:*OsNAS2* were designated SC2.1 to SC2.35, 39 independent lines carrying *GluA2*:*uidA (GUS)* were designated GUS1 to GUS39, and 21 independent lines carrying *GluA2:OsNAS2:NosT-Glb1:HvSUT1:NosT* were designated DC1.1 to DC1.21. Plantlets regenerated from the same callus belonged to one line and had the same designation, for example, DC1.1-1 and DC1.1-9 were two plantlets from the line DC1.1. More than 95% of hygromycin-resistant plants had normal morphology and were fertile and there were only 5/119 (4.2%) with abnormal phenotype of either albinos, dwarfs (stunted height and small leaves) and/or were infertile.

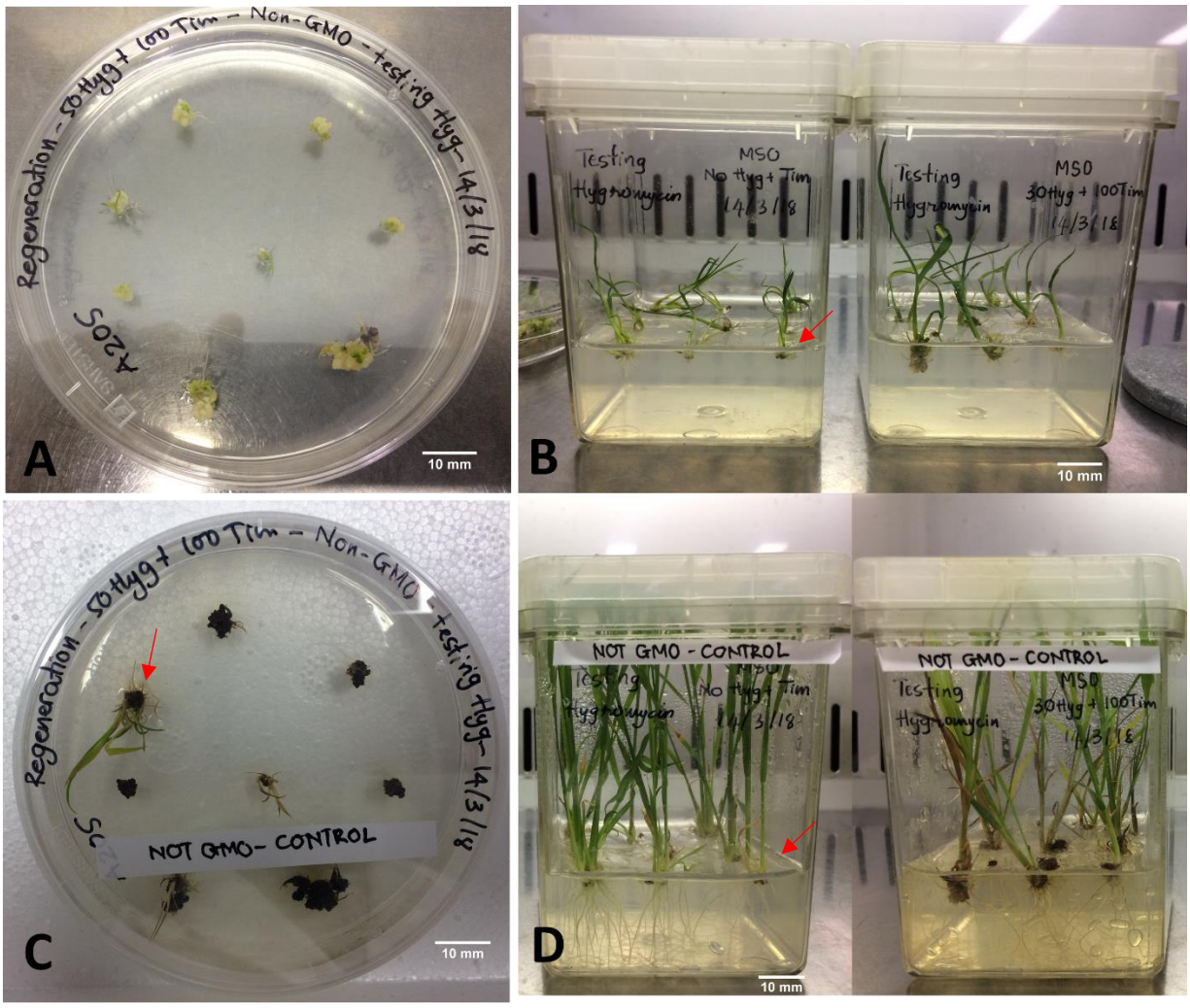

Figure 2.11. Non-transgenic calli and shoots in hygromycin selection medium at the regeneration and rooting induction steps. Non-transgenic calli transferred on the regeneration media with hygromycin (A) and after 10-day regeneration (C). Regenerated shoots from non-transgenic calli transferred on the root induction media without hygromycin (left) or with hygromycin (right) (C), after 10-day root induction media without hygromycin (left) and with hygromycin (right) (D). Red arrow showed a shoot regenerated from non-transgenic callus on hygromycin-regeneration media and this non-transgenic shoot was heathier on root induction media without hygromycin.

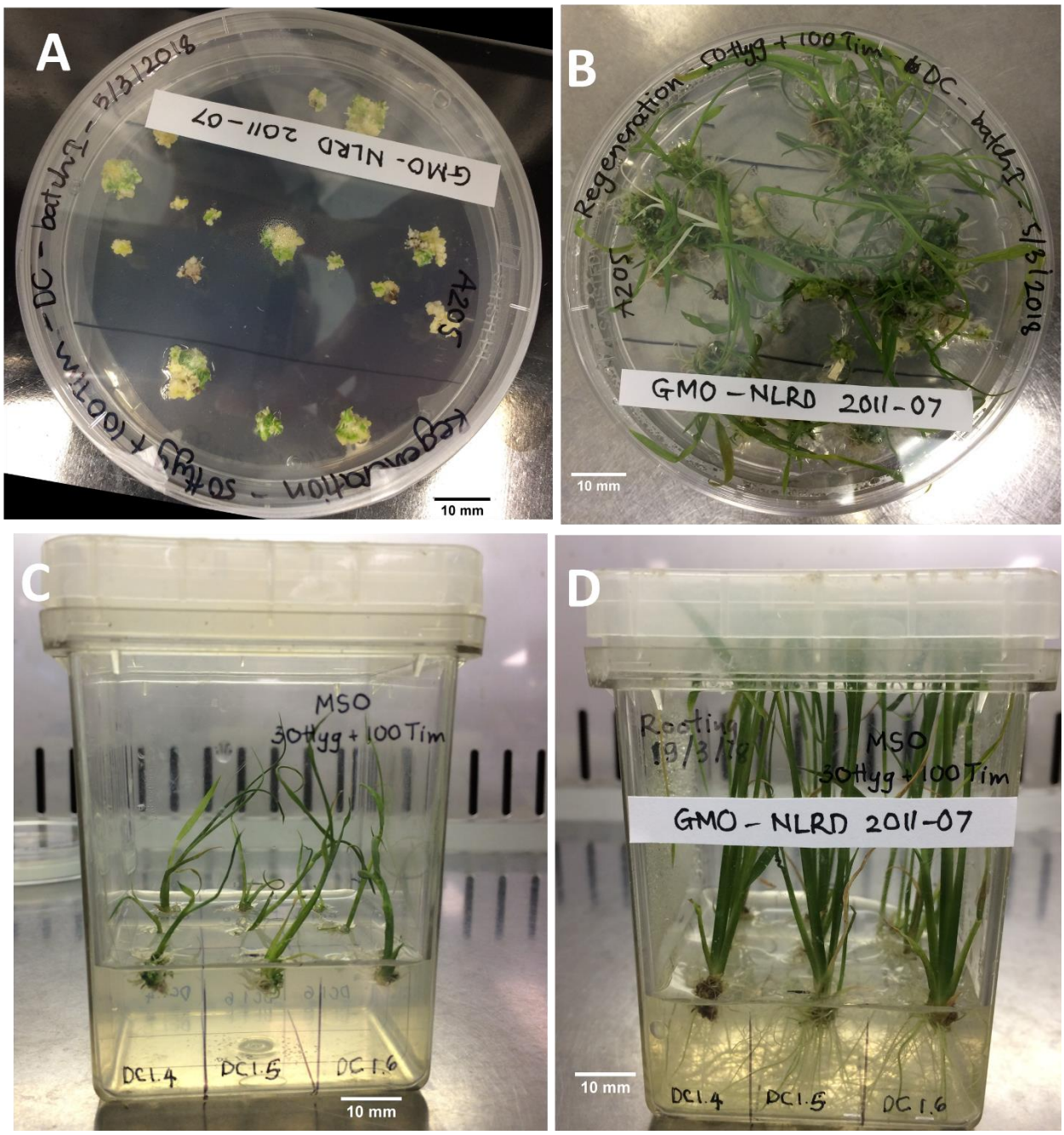

Figure 2.12. Representatives of the putative transgenic lines carrying the DC1 construct. A hygromycin resistant calli transferred on the regeneration medium (A) and after 10-day regeneration (B). Regenerated shoots transferred on the root induction medium (C), after 10-day root induction (D).

2.3.3. Transgene copy number analysis in T0 transgenic rice

Genomic DNA extracted from the putative transgenic lines was used for PCR to confirm the presence of the transgene (Figure 2.6). Genomic DNA extracted from the leaves of two plants derived from the same callus for each independent T0 transgenic event was isolated using a BIOLINE kit (ISOLATE II Plant DNA kit). The primers using for PCR were designed to be specific for each construct. For the SC1 and SC2 constructs, the forward primers were targeted in the coding region of transgenes and the reverse primers were targeted to the *nos* terminator. The PCR products of SC1 and SC2 lines were 974 bp and 992 bp in length, respectively. The primer pair for the DC construct amplified the region from *OsNAS2* gene to the *HvSUT1* gene (1728 bp in length). Primers targeting the unique adjacent arrangement of *OsNAS2* and *HvSUT1* ensured that no amplification would be predicted when genomic DNA from the SC1 and SC2 lines was used as templates. In non-transgenic rice (WT), no PCR product was amplified using all three sets of primer pairs. All the putative transformants from the populations were positive for the transgenes (Figure 2.9). All putative transformants with the GUS construct were positive by GUS staining. Based on the PCR analysis, the successful integration of the transgenes into the genome of all the putative transformant can be assumed.

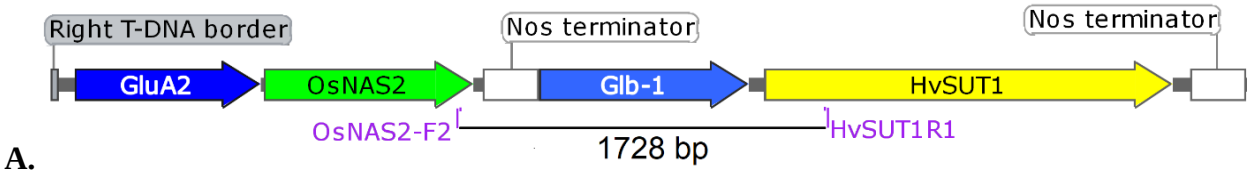

A.

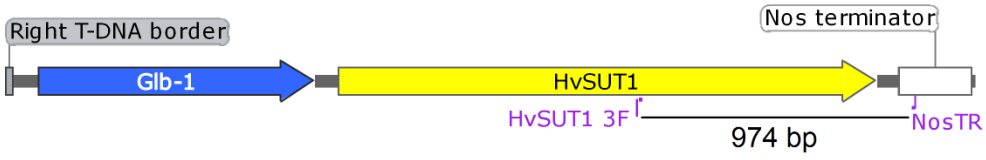

B.

C.

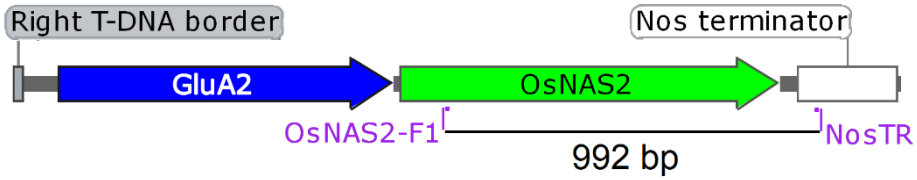

D.

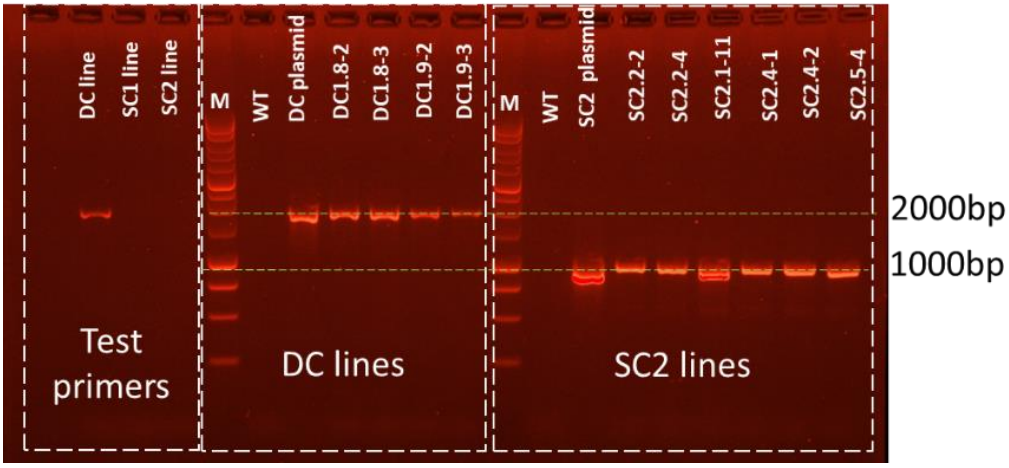

E.

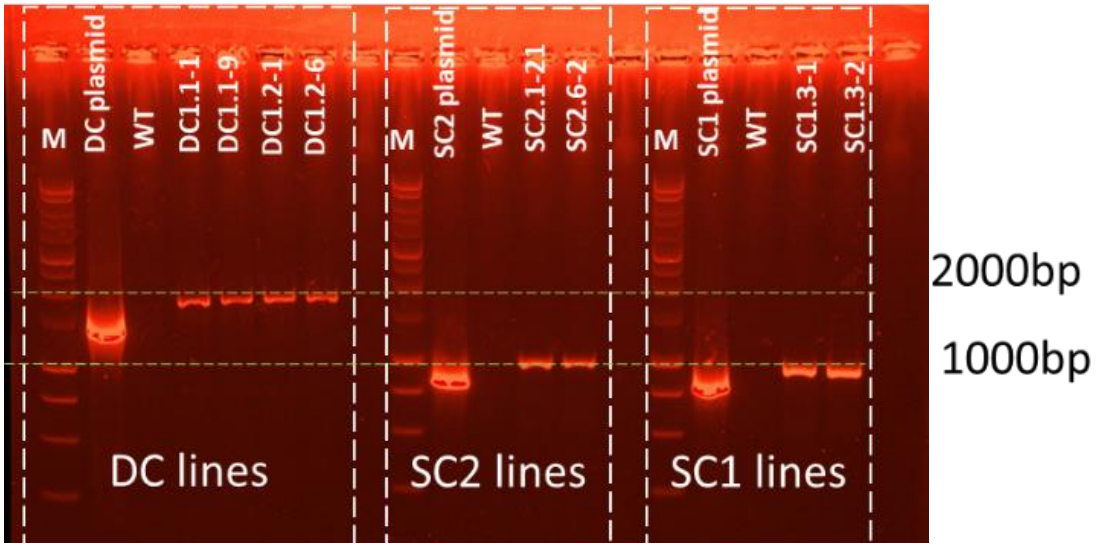

Figure 2.13. Three T-DNA maps and validation of transgenic lines through genomic PCR in T0 generation. A. T-DNA map (DC1) with specific primers for amplifying 1728 bp PCR product; B. T-DNA map (SC1) with specific primers for amplifying 974 bp PCR product; C. T-DNA map (SC2) with specific primers for amplifying 992 bp PCR product.; D. Representative gel for testing specificity of DC1 primers, for screening DC1 and SC2 lines. E. Representative gel for screening DC1, SC2 and SC1 lines.

2.3.4. Efficiency of IR64 rice transformation using immature embryos

Table 2.2. Efficiency of IR64 rice transformation using immature embryos

Construct	Batch number	IEs (A)	Hygromycin -resistant calli	Lines with positive PCR results (*) (B)	Efficiency of transformation (B/A) x100%	Average
Glb1:HvSUT1:NosT (SC1)	6	78	25	25	32.0%	32.0%
	2	Failed in *Agrobacterium* co-cultivation				
GluA2:OsNAS2:NosT (SC2)	4	46	10	10	21.7%	21.79%
	7	110	24	24	21.8%	
GluA2:uidA:NosT (GUS)	3	27	6	6	22.2%	44.32%
	8	61	33	33	54.1%	
GluA2:OsNAS2:NosT-Glb1:HvSUT1:NosT (DC1)	1	54	10	10	18.5%	18.26%
	5	61	11	11	18.0%	
Total		**437**	**119**	**119**	**27.2%**	

(*): the transgenes from SC1, SC2 and DC1 were confirmed by PCR, GUS lines were confirmed by GUS staining in grains. IEs: immature embryos

Seven separate experiments of immature embryos of IR64 (from 27-110 embryos for each batch) were used for *Agrobacterium* transformation. Four constructs were used to generate transgenic rice (T0 plants) (Table 2.2) with the resulting transformation efficiency ranging from 18% to 54.1%. Transformation efficiency of the GUS construct reached the highest percentage in batch 8 (54.1%) with all optimised conditions, which had higher efficiency than for batch 3 with 22.2% transformation. Average efficiency of transformation with the GUS construct was higher than for the other constructs, followed by SC1 (32%). A large variation in transformation efficiency was attained in the experiments with the GUS construct, whereas smaller variation was found in experiments with construct SC2 (from 21.7-21.8%) and DC1 (18.5-18.0%).

2.3.5. Determining copy number of transgenes in T0 plants using qPCR

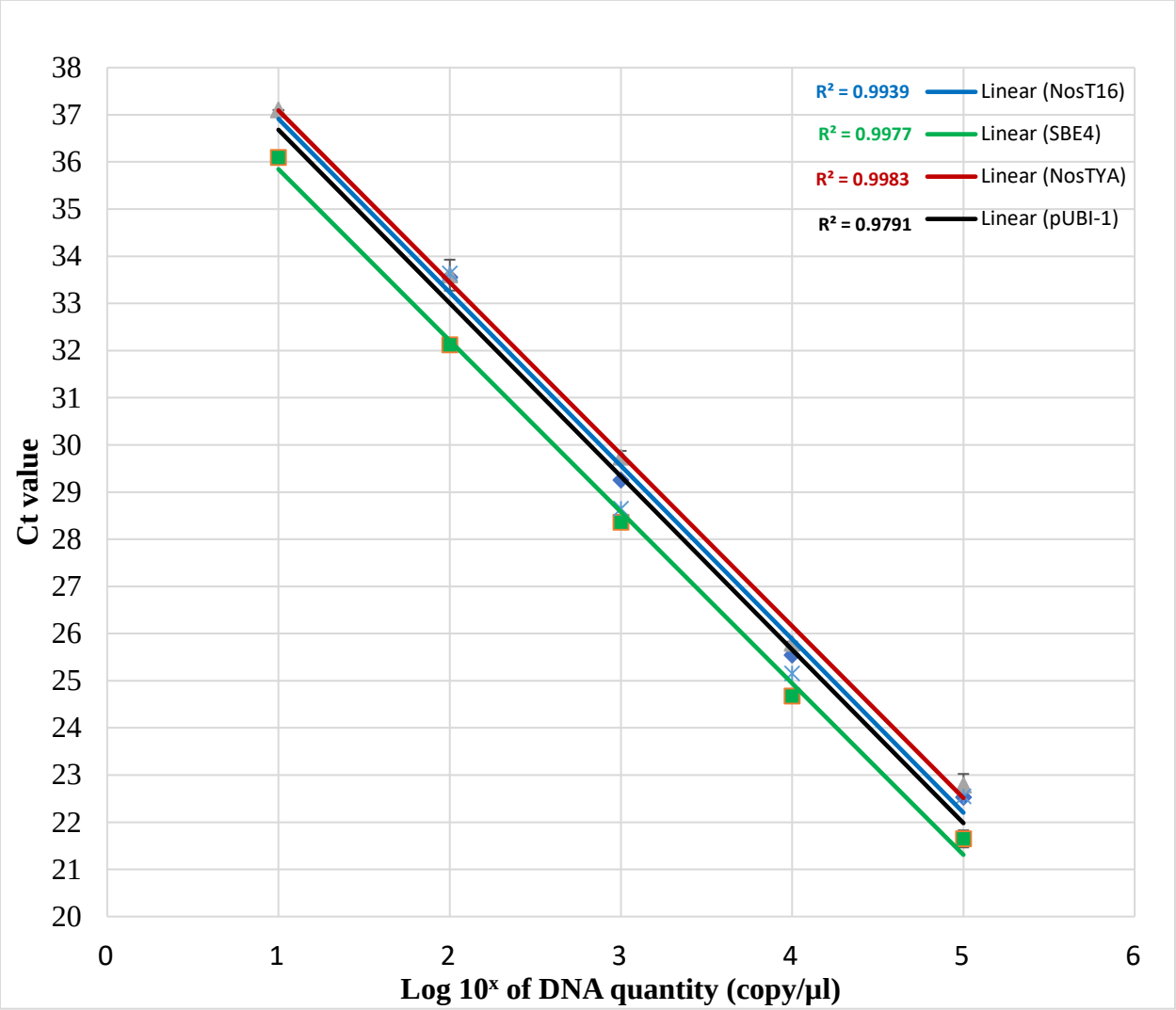

Figure 2.14. Comparison in amplification efficiency of SBE4, pUBI-1, NosT16 and NosTYA primers. Genomic DNA from a transgenic plant with a single copy was serially diluted by 10-fold dilutions (10^1 10^2, 10^3, 10^4 and 10^5 copies/µl). A standard curve for each primer pair was prepared by plotting average Ct value of three replicates for each dilution against the $\log_{10}$ of the DNA starting quantity (copy/µl). The green, black, blue, and red regressions wit R^2 values are 0.9977, 0.9791, 0.9939, and 0.9983 for SBE4, pUBI-1, NosT16 and NosTYA primer pairs, respectively.

Transgene copy number in the putative transformants was determined by qPCR assay with two well-matched and specific primer pairs, one designed to target the *nos* terminator of the transgenes, and the other to target an endogenous reference gene, the starch branching enzyme 4 gene (*SBE4*), which is present in two copies in the rice genome (Mizuno *et al.* 2001; Wang *et al.* 2015b). A calibrator sample was a hemizygous, single T-DNA insert plant confirmed by Southern blot, qPCR and segregation analysis (Schramm 2015; Tran 2015).

In this experiment, four primer pairs were used for the qPCR assay, including the *SBE4* primer pair and two (NosT16 and NosTYA primer pairs) targeting the *nos* terminator region of the transgene and a pUBI-1 primer pair targeting the promoter *ubi-1* upstream of the *hpt* gene (hygromycin resistance). The assay requires that the primers are used to amplify the transgene and the reference gene with similar efficiencies, as close to 100% as possible. A serial 10-fold dilution of genomic DNA from the calibrator (10^1 10^2, 10^3, 10^4 and 10^5 copies/µl) was conducted for comparison in the standard curves (including the slope of the line, average correlation coefficients (R^2), and PCR amplification efficiency) of the four primer pairs (Section 2.2.6, Section 2.2.7 and Figure 2.14). The standard curves for SBE, NosT16 and NosTYA primer pairs were well-matched and close to 100%. The difference in Ct values at each dilution between SBE primer pair and NosT16 and NosTYA primer pairs was consistently 1 cycle. Therefore, the three primer pairs were used for the qPCR assay to determine copy number of transgenes per genome in the putative transgenic lines.

In the T0 generation, the transgenes in all the putative transgenic lines exist in a hemizygous state. For single-insert lines, Ct value of NosTYA or NosT16 primer pair (~ 25) was higher by around 1, compared to the Ct value of reference SBE4 primer pair (~ 24) (Figure 2.14). The result was similar with the calibrator. Based on the $2^{-\Delta\Delta Ct}$ value (Section 2.2.6 and Section

2.2.7) of each putative transgenic line in the T0 generation, the copy number of transgenes were determined, with 1 for hemizygous single insertion, 2 for hemizygous two insertion, etc. The results are summarized in Table 2.3, with the putative transgenic events showing single insertions was most frequently found in all the three populations. A high percentage (25.9 %) of the transgenic lines contained a single insertion per genome in the SC1 population ($2^{-\Delta\Delta Ct}$ value of 0.8 -1.0), 47.8% was attained from the SC2 population with the $2^{-\Delta\Delta Ct}$ value of 0.7 -1.1.

Table 2.3. Summary of transgene copy number in two populations of transgenic rice lines (the T0 generation).

Construct	Copy number of transgenes	Two-fold difference value	Number of lines	Percentage
SC1	1	0.8-1.00	7	25.9%
	2	2.1 – 2.5	6	22.2%
	3	3.3 -3.5	2	7.4%
	4	3.6-3.8	4	14.8%
	>=5		7	25.9%
	Abnormal line		1	3.8%
SC2	1	0.7-1.1	11	47.8%
	2	1.5-1.9	2	8.7%
	3	2.6	1	4.3%
	4	3.5-4.00	3	13.1%
	>=5		4	17.4%
	Abnormal line		2	8.7%

For T0 transgenic lines carrying the DC1 construct, Ct value of NosTYA or NosT16 primer pairs were similar with that of the reference SBE4 primer pair, around 24, because in this case there were two *nos* terminator regions (Figure 2.13). The $2^{-\Delta\Delta Ct}$ value was ~ 2 for single-insert lines, ~ 4 for two-insert lines, etc. The result, shown in Table 2.4, indicates seven of 21 putative transgenic lines (33.3%) from the population DC1 were determined to carry a single insertion of the transgene with the $2^{-\Delta\Delta Ct}$ value of 1.8 – 2.2 while the transgenic lines with two insertion accounted for 28.7%, and the remaining transgenic events were with more than 3 copies per genome (28.7%). In general, a greater proportion of the putatively transgenic events carrying a single insert were attained in this study. The putative transgenic lines (T0) with single or two copies of transgene were selected for development of homozygous plants in the T1 generation.

Table 2.4. Summary of transgene copy number in the population of DC1 transgenic rice lines (the T0 generation).

Construct	Copy number of transgenes	Two-fold difference value	Number of lines	Percentage
DC1	1	1.8 – 2.2	7	33.3%
	2	3.3-4.4	6	28.7%
	3	5.2-6.9	2	9.5%
	4	7-7.7	2	9.5%
	>= 5		2	9.5%
	Abnormal line		2	9.5%

2.3.6. Detection of homozygous single -insert lines in the T1 generation

The T0 lines with single insertion were grown and used to screen for homozygous plants in the T1 generation. The theoretical segregation of the transgene in single-insert lines would be consistent with a Mendelian ratio of 1:2:1 for homozygous plants with 2 copies, hemizygous plants with 1 copy and null plants with 0 copy, respectively. Seeds from 13 independent transgenic events in the T0 generation, identified by the qPCR to have a single insertion, were grown to detect the zygosity using the qPCR described in Table 2.5. A total of 40 homozygous plants (T1) were attained from the qPCR assay, 22 plants from 6 independent events transform with the DC1 construct, 11 plants from 3 independent events transform with the SC1 construct and 7 plants from 4 independent lines transform with the SC2 construct. Chi squared (χ^2) analysis was used for analysing segregation ratios of T1 progeny based on the qPCR results. In all cases, there was no significant difference between with the observed ratios and that of the expected Mendelian ratios. The frequencies of 2-copy (homozygous) plants in the SC1 (26.8%) were much closer to the expected frequency of 25% and there were lower frequencies in the SC2 lines (only 10.4%). There were no plants with more than 2 copies identified by the qPCR.

All materials, including immature and mature grains from all the homozygous plants in the T1 generation were used for further analysis. Starting with a unique insert and the standardized procedures for DNA isolation, universal primer pairs and qPCR assay greatly assisted in fast-tracking the development of homozygous lines with single insertion.

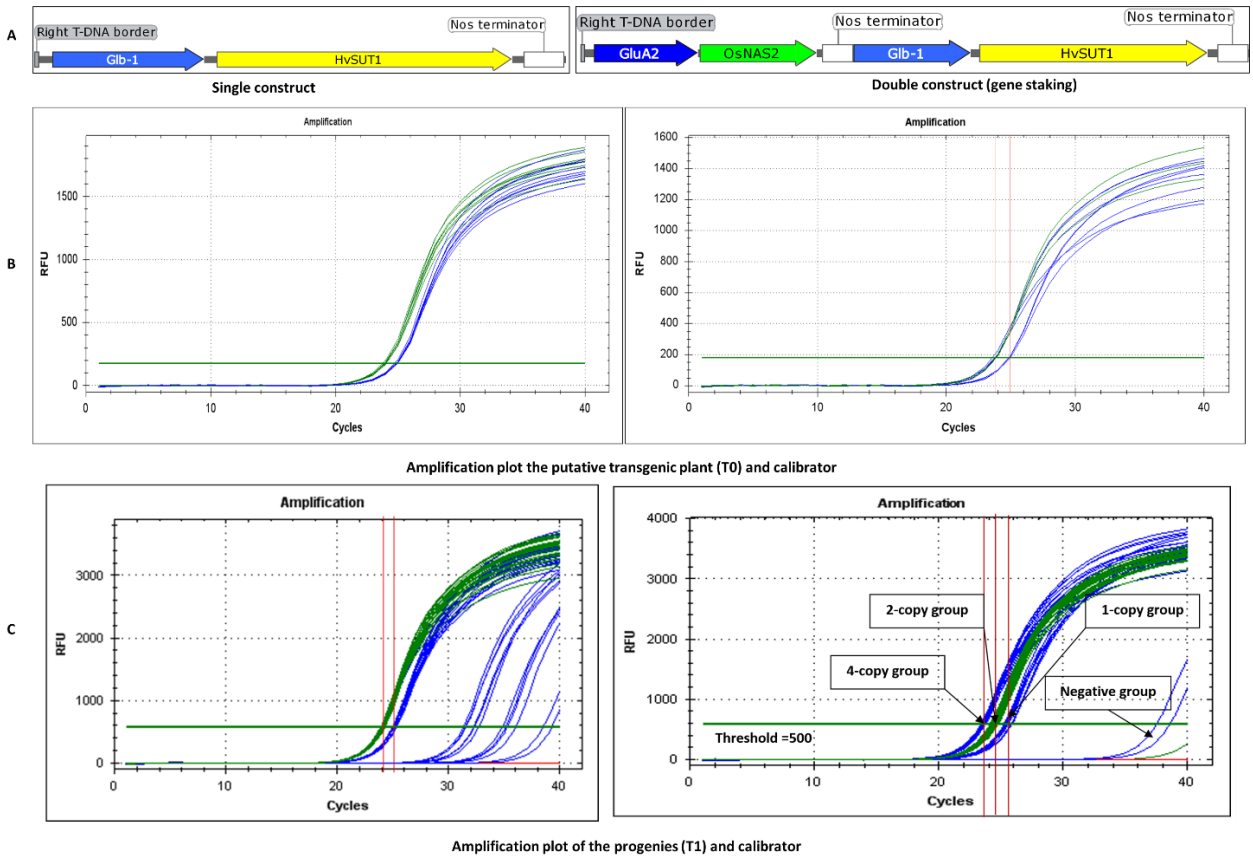

Figure 2.15. Performance of the qPCR assay to determine the zygosity of transgenic plants. **A**. T-DNA carrying a single gene cassette with a single *nos* terminator (Left), and T-DNA carrying double gene cassettes with two *nos* terminator regions (gene stacking) (Right); B. Amplification plot of a single-insert line and gene-stacking line in the T0 generation. C. Amplification plot of T1 offspring of the T0 generation. Blue and green curves presented for PCR amplifications of NosTYA and SBE4 primer pairs, and red curve showed the no template control. The calibrator is a single-insert, hemizygous plant verified by Southern blot, qPCR assay, and segregation testing.

Table 2.5. Transgene segregation analysis of T1 plants from T0 plants carrying single insert based on the qPCR.

Line	Total plants	T1 segregation (2:1: 0 copy)	Chi-square (χ^2) value	p value	Percentage of 2-copy plant (%)
DC1.21	22	2:12:8	3.45	0.178	9.1%
DC1.1	20	4:10:6	0.40	0.819	20%
DC1.5	24	5:8:11	5.67	0.059	20.8%
DC1.9	17	1:10:6	3.47	0.176	5.9%
DC1.13	38	7:19:12	1.32	0.518	18.4%
DC1.2	16	3:7:6	1.37	0.503	18.75%
Total for DC1	**137**	**22:66:49**	**10.82**	**0.004***	**16.06%**
SC1.22	16	5:8:3	0.50	0.779	31.2%
SC1.21	17	3:7:7	2.41	0.299	17.6%
SC1.12	8	3:4:1	1.00	0.606	37.5%
Total for SC1	**41**	**11:19:11**	**0.22**	**0.896**	**26.8%**
SC2.15	21	2:14:5	3.19	0.200	9.5%
SC2.31	25	2:17:6	4.52	0.104	8%
SC2.14	8	1:6:1	2.00	0.368	12.5%
SC2.32	13	2:6:5	1.46	0.481	15.4%
Total for SC2	**67**	**7:43:17**	**8.37**	**0.015***	**10.4%**
Total	**245**	**40:128:77**	**11.67**	**0.003***	**16.3%**

The copy number of transgene was estimated by the qPCR assay using the set of NostYA/NosT16 and SBE4 primers. $\chi 2$ test ($\chi 2_{0.05}$ =5.99; dF=2) for goodness of fit was applied to compare whether significant difference between the observed segregation and expected segregation at $p < 0.05$. In case of single insert, the segregation of transgene is 1: 2: 1 for 0: 1: 2 copies, respectively.

Table 2.6. Transgene segregation analysis of T1 plants from T0 plants carrying two insertions based on qPCR.

Line	Total plants	T1 segregation (4: 3: 2: 1: 0 copy)	Percentage of 4-copy plants	Note
DC1.16	42	3: 10: 26: 0: 13	7.1%	
DC1.19	5	1: 1: 1: 1: 1	20%	
SC1.16	10	3: 0: 5: 0: 2	30%	
SC1.13	11	1: 0: 5: 0: 5	9.1%	
Total	**68**			

In case of two copy events, the independent segregation of two inserts is expected to be 1: 4: 6: 4: 1 for **4: 3: 2: 1: 0** copies, respectively.

A population of 68 transgenic T1 offspring from 4 independent T0 events with two inserts were also analysed to detect homozygous plants (Table 2.6). Homozygous two-insert plants should carry 4 copies of the transgene, compared to 1 copy in the calibrator and 2 copies in their parent plants. According to Mendel's law of two-insert segregations, there should be only 6.25% of the offspring with 4 copies of transgene. It can be seen in DC1.16, in which 3/42 T1 plants were detected to carry 4 copies and double the copy number of its parent plant. There was no progeny detected any plant with more than 4 copies of the transgene cassette. Small numbers of the T1 plants were screened to select homozygous plants for downstream analysis; 1/5 of DC1.19, 3/10 of SC1.16, and 1/11 of SC1.13 (Table 2.7). In the T2 generation, 100% of their progeny were confirmed for the presence of transgene by end-point PCR (10/10 for DC1.16, 9/9 for DC1.19 and 9/9 for SC1.13) (Table 2.7).

2.3.7. Reliable qPCR assay for homozygous plants (T1) identification validated in the T2 generation

Table 2.7. Summarising end-point PCR results of T2 plants from T1 homozygous plants

Line	Insert number	Plant number	PCR result	Percentage
DC1.1	1	10	10	100%
DC1.5	1	8	8	100%
DC1.9	1	9	9	100%
DC1.13	1	10	10	100%
DC1.16	2	10	10	100%
DC1.19	2	9	9	100%
SC1.22	1	10	10	100%
SC1.21	1	6	6	100%
SC1.12	1	10	10	100%
SC1.13	2	9	9	100%
SC2.32	1	7	7	100%
SC2.15	1	10	10	100%
SC2.14	1	7	7	100%
SC2.31	1	9	9	100%
Total	-	124	124	100%

All T2 progeny from T1 homozygous plants were confirmed the presence of transgene by endpoint PCR.

To verify the reliability of the qPCR assay to determine the homozygous plants with single insertion, 124 progeny plants from 14 homozygous single-insert plants determined in Section 2.3.6

were analysed for the presence of the transgenes by end-point PCR using the specific primer pairs (Section 2.3.3). No plant with a negative result was observed among all the independent lines (6-7 plants per line). The results indicated (Table 2.7) that 100% of the progenies from the single-insert homozygous plants were correctly scored as homozygous, demonstrating 100% accuracy for identifying homozygous plants with a single insert attained from this qPCR assay in the T1 generation. A similar result was also achieved for the transgenic plants, determined by the qPCR to have two inserts. Therefore, all materials from those homozygous plants and their progenies can be confidently used for further phenotypic, molecular, and physiological analysis presented in this study.

2.4. Discussion

Rice (particularly the Indica cultivars) is one of the best candidates for Fe and Zn biofortification because it is a major staple food for people in undeveloped and developing countries where Fe and Zn deficiencies are very serious problems. The used of genetic engineering has been successful in Fe and Zn biofortification over the last few years (Masuda *et al.* 2013a; Sperotto *et al.* 2012). To develop Fe and Zn-enriched transgenic rice, promising gene engineering constructions, a high efficiency method of transformation, and stable inheritance of target genes, are decisive steps to achieve success. Here, this study reported an improved transformation method for Indica rice, and a practical application of accurate and fast-tracking generation of homozygous plants with low insert copy in the T1 generation carrying a novel combination of *HvSUT1* and *OsNAS2* overexpression driven by two endosperm-specified promoters.

2.4.1. A novel combination of *HvSUT1* and *OsNAS2* overexpression under the control of endosperm-specified promoters for Fe and Zn biofortification

Here the strategy of *HvSUT1*-mediated Fe and Zn biofortification is expanded to include *OsNAS2* overexpression, with both the transgenes under the regulation of two endosperm-specific promoters. Similar to Huynh (2015), *HvSUT1* was under the control of the *Glb-1* promoter for overexpression specific to the endosperm cells (Huynh 2015; Qu & Takaiwa 2004). The sequence of the *Glb-1:HvSUT1* construct was designed to direct the *HvSUT1* expression in the rice endosperm.

Overexpression of *NAS* genes have been demonstrated to increase Fe and Zn concentration in monocotyledonous crops (Johnson *et al.* 2011; Masuda *et al.* 2008). In most of the previous studies of *NAS* overexpression, constitutive promoters were used to regulate *NAS* genes (Beasley *et al.* 2019a; Boonyaves *et al.* 2017; Johnson *et al.* 2011; Lee *et al.* 2009b; Masuda *et al.* 2009; Trijatmiko *et al.* 2016; Wu *et al.* 2018; Wu *et al.* 2019). Amongst the *OsNAS* gene family, *OsNAS2* was considered as the best candidate to enhance Fe and Zn levels (Johnson *et al.* 2011). Although the constitutive overexpression of *NAS2* was successful in increasing Fe and Zn concentration in rice grains, a potential effect of *NAS* on accumulation of toxic heavy metals such as Ni and Cd in the grains was seriously considered (Kyriacou 2013; Wu *et al.* 2018; Wu *et al.* 2019). In addition, a growth inhibition was observed in constitutive overexpression of *OsNAS1* in rice, compared to non-transgenic controls and transgenic rice with endosperm-specific overexpression of *OsNAS1* (Zheng *et al.* 2010). Because *OsNAS1* shares the same function with *OsNAS2*, *OsNAS2* was designed in this study with regulation from the *GluA2* promoter for endosperm-specified expression, which was expected to eliminate the negative effects as mentioned above. Based on the hypothesis mentioned in Chapter 1, this promoter highly active during the early stages of grain

development will increase expression of *OsNAS2* leading to the metal chelating properties of its products, NA or/and DMA. The presence of these chelators could facilitate Fe and Zn mobilization from the aleurone layers into the starchy endosperm. Through GUS activity reported by Qu *et al.* (2008), the *GluA2* promoter was demonstrated to be active in the early stage of Japonica rice grain development, at 7 days after anthesis (DAA), and with strong expression in the outer layer of the endosperm (Qu *et al.* 2008).

The combined overexpression of *GluA2:OsNAS2* and *Glb-1:HvSUT1* is a new strategy to enhance Fe and Zn in the rice grain. To examine the beneficial effects of this new combination of *genes*, many IR64 transgenic events overexpressing *Glb1:HvSUT1* (SC1), *GluA2:OsNAS2* (SC2), and the combination of *GluA2:OsNAS2* and *Glb-1:HvSUT1* had to be generated. The SC1 and SC2 transgenic events were used to monitor the individual effects of the transgenes and as controls to the effects found in the DC1 transgenic plants. To confirm specific expression of the *GluA2* promoter, IR64 transgenic events carrying *GluA2: uidA* (GUS) were also required in this study. Obviously, a robust and highly efficient protocol for IR64 transformation was very critical to generate enough rice transgenic events for further analyses.

2.4.2. A highly efficient and productive protocol for IR64 transformation, mediated by *Agrobacterium*.

Agrobacterium-mediated transformation is a very popular method used for generating rice transgenic events (Hiei *et al.* 2014), due to its accessibility and high frequency of transgenic events with intact low- or single-copy insertion(s) of the transgene. IR64 (Indica rice) is a recalcitrant cultivar for *Agrobacterium*-mediated transformation and tissue culture (Tie *et al.* 2012), thus this study used rice mature and immature embryos as starting materials for transformation. The starting material for *Agrobacterium*-mediated transformation is one of the most important factors for successful generation of transgenic rice, particularly Indica rice (Hiei *et al.* 1994). In this study, mature seeds of IR64 were also used for *Agrobacterium*-mediated transformation, but no transformants were obtained. This supports the very low transformation efficiency of IR64 from embryos of mature seeds reported by (Hiei & Komari 2008). For the *Agrobacterium*-mediated transformation using immature embryos as starting material, the low availability of immature embryos for transformation throughout the year, and the labour-intensive process are limitations mentioned by many previous reports (Belide *et al.* 2017; Sahoo *et al.* 2011; Sahoo & Tuteja 2012). Following the first two reports of *Agrobacterium*-mediated transformation using rice IEs (Hiei & Komari 2008; Slamet-Loedin *et al.* 2014), this transformation method offered several advantages in terms of high efficiency, lower copy number of transgenes, stable transgene expression, and the short period of tissue culture relative to other methods. In addition to these advantages, the transformation protocol was improved with several modifications reported in this study: including less over-growth of *Agrobacterium* after the 7-day cocultivation, multiple transgenic events from a single immature embryo to achieve higher efficiency, consistent growth condition from callus induction to root induction, and no non-transgenic shoot escape. Here, this protocol yielded up to

54.1% transformation efficiency, which is slightly higher, compared to 40% reported by Slamet-Loedin *et al.* (2014) (Table 2.8).

In the recent protocol of IR64 transformation, a time-consuming step is preparation of donor plants to collect immature embryos, which usually take around three months until flowering. To save time, the donor plants used here were grown under greenhouse conditions. However, using IEs for *Agrobacterium*-mediated transformation would not require a callus induction step like the method using mature seeds, which took at least 20 days (Sahoo *et al.* 2011; Sahoo & Tuteja 2012). The protocol used in this study avoided somaclonal variations or mutations which accompany long periods of tissue culture (Carsono & Yoshida 2007; Stroud *et al.* 2013; Toki *et al.* 2006). Only a small number of transgenic lines with abnormal phenotypes were found in this study. Most of transgenic lines (over 90%) had normal morphology and were fertile.

Using the current transformation method, this study generated 119 independent transgenic lines from 437 infected IEs giving an average transformation efficiency of 27.2%. Ideally, the transformation efficiency means that one relatively small experiment of 50 or 100 IEs is sufficient to produce about 10 or 20 independent lines. It can be seen in this study (Table 2.2), four transformation experiments generated about 10 transgenic lines from roughly 50 infected IEs, two transformation experiments of 100 IEs produced over 20 transgenic lines, and one experiment of 27 IEs had 6 putative transgenic lines. To achieve the ideal efficiency of rice transformation, all infected IEs should be recovered after the 7-day cocultivation. In this method, the infected IEs were rolled on the surface of the plate around the *Agrobacterium* inoculum then transferred onto a fresh cocultivation medium (A201) before the dark incubation at 25^0C. This could prevent the overgrowth of *Agrobacterium*, ensuring that the infected IEs remained healthy during the 7-day period of the *Agrobacterium* cocultivation. The infected IEs were heathy enough to split into 3-4

small pieces, and as a result, every IE could generate up to 3-4 independent transgenic lines. This contributed to the enhanced transformation efficiency.

Using the transformation protocol reported here, 100% of the plants transferred into soil were verified to have the transgene integrated into the genome. Non-transgenic escapes were not found as plantlets were regenerated and roots were induced in hygromycin-containing media. This was different to the protocols reported by Slamet-Loedin *et al.* (2014), in which hygromycin was not added into the root induction medium.

In addition, the transformation protocol was more straightforward than the protocols of Hiei *et al.* (2006) and Hiei and Komari (2008) because steps of heat treatment at 46^0C and centrifugation of immature embryos at 20,000 xg were skipped. In this transformation protocol, the growth chamber was set up for a consistent condition at 30^0C and under continuous light for most of steps, excluding the cocultivation. Therefore, multiple experiments with different steps could be incubated in the same growth chamber. This saved facilities and space for research.

However, transformation efficiencies for the four T-DNA constructs were variable (see Table 2.2), with a higher efficiency attained from short size T-DNA constructs, namely GUS (6286 bp), SC1 (6531 bp), and SC2 (5428 bp), and lower efficiency attained from the large T-DNA construct (DC1 with 8701 bp in length). Although the larger-sized T-DNAs were demonstrated to result in lower transformation efficiency (Xi *et al.* 2018), it is difficult to conclude that the difference in the transformation efficiencies was accorded to the size of T-DNA in this study, because there were not large differences in the size of four T-DNA constructs and were routine size of a natural T-DNA in the wild-type Ti-plasmid (5-30 kbp) (Gelvin 2003). Any leaky activity of the promoters during regeneration and plant growth may impact on transgene expression and

thus transformation efficiency. This is highly speculative and would require more thorough investigation.

Table 2.8. Several modifications of the transformation protocol of Slamet-Loedin *et al.* (2014) and Hiei and Komari (2008)

Step	**This transformation protocol**	**Original protocol**	**Difference**
Agrobacterium culture	A 200 µl aliquot of frozen AGL1 cells harbouring the correct destination plasmid on LB medium with 25 µg/ml Spec and 20 µg/ml Rif.	AB medium	LB medium
Transformation	Dropping 5 µl of *Agrobacterium* suspension onto each IE, then incubated for 15 min at room temperature. Before transferring IEs, they were rolled on the surface of the plate around the *Agrobacterium* inoculum to eliminate overgrowth of *Agrobacterium*.		Less over-growth of *Agrobacterium* No treatment of immature embryo with heat and centrifugal force before inoculation
Co-cultivation	Under dark condition at 23-25^{0}C for 7 days.	25^{0}C for 7 days	Wider range of 23-25^{0}C
1st Selection	Each IE was cut into 4 equal pieces. Transferred onto A203 selection medium under continuous light at 30^{0}C for 10 days	Consistent growth condition at 30^{0}C under continuous light condition, but inconsistent with the stop of root induction	Multiple transgenic events from single embryo. It was mentioned by Slamet-Loedin *et al.* (2014) Consistent growth condition at 30^{0}C under continuous light condition with all steps
2nd selection	Transferred onto A203 selection medium under continuous light at 30^{0}C for 10 days		
3rd selection	Transferred onto A203 selection medium under continuous light at 30^{0}C for 10 days		
Pre-regeneration	Transferred onto A204 selection medium under		

	continuous light at 30^0C for 10 days		
Regeneration	Transferred onto A204 selection medium under continuous light at 30^0C for 10 days		
Root induction	Transferred regenerated plantlets (shoots) to MS30 root induction medium at 30^0C for 10 - 14 days under continuous light condition	Transferred regenerated plantlets (shoots) to MS0 without hygromycin root induction medium at 25^0C for 10 days.	Keep adding selective agent (hygromycin). 100% plantlets were transformed plants. Consistent growth condition at 25^0C under continuous light condition
Transformation efficiency	18-54.1%	20-40%	Higher efficiency
Single insert lines	25.9-47.8%	~ 40%	Slightly higher percentage of single insert events

2.4.3. A fast-tracking development of homozygous transgenic rice

In most studies on genetic transformation and molecular plant breeding, development of homozygous transgenic lines is required prior to a downstream application. With a high-throughput *Agrobacterium*-mediated transformation used in this study, a large number of transgenic lines transformed with different gene expression cassettes can be generated. A method of fast-tracking of homozygous plants is therefore essential to accelerate the downstream analyses and applications. In previous studies, the qPCR assay based on the method of Mieog *et al.* (2013) was well-established to reliably and precisely identify the zygosity of transgenic rice (Nipponbare cultivar) (Schramm 2015; Tran 2015). Here, this study rapidly developed many homozygous single-or two-insert IR64 rice plants in the T1 generation by the qPCR assay. To achieve the fast-tracking development of homozygous lines, the single- and two-insert T0 transgenic lines in this study were used as the founding plants for developing homozygous lines carrying low insert-copy

plants. The results of the assay indicated that single-insert lines had one copy of transgene like the calibrator (a hemizygous, single-insert sample), while the double-insert lines contained two copies of insert, which doubled the insert number in the calibrator. Because the T0 transgenic lines with a single insert are hemizygous, their segregation results in progeny where 25% are homozygous for the transgene, 50% are hemizygous and 25% are nulls. Neither end-point PCR or Southern blotting shows a radical distinction between a homozygous and hemizygous plants. The aim was to identify the homozygotes in this generation (T1) for further analyses without the need of a further generation to confirm zygosity. The qPCR assay reached 100% accuracy of determining homozygous and null plants from the segregants of single-insert and two-insert line. The accuracy of the assay was similar or even higher, compared to the previously reported qPCR protocol (Bubner & Baldwin 2004; Ingham *et al.* 2001; Mieog *et al.* 2013; Song *et al.* 2002; Wang *et al.* 2015b; Yang *et al.* 2005).

In addition, the qPCR assay was straightforward to apply to different gene expression cassettes in different rice cultivars, or even different crop plants which share the same regulatory elements (for instance terminators or promoters). Here, the transgenic Indica rice in this study contained the same construct (SC1), the same standard sequence elements such as the n*os* terminator (SC2). In addition, the reference gene (*SBE4*) is single copy gene and shows no difference between IR64 and the Nipponbare cultivars studied by Schramm (2015) and Tran (2015). Because the qPCR assay was designed to be straightforward and universal, it could screen multiple lines with different T-DNA constructs at the same time without any adaption. The standard curves indicated that the primer pairs and the qPCR assay was robust, reliable and repeatable for determination of transgene copy number.

Furthermore, the results in this study indicated that the qPCR assay was effective and accurate at identifying homozygous plants carrying the two gene cassettes of the DC1 lines (gene stacking). The previous study of Wang *et al.* (2015b) reported that the qPCR protocol was successful in identifying homozygous lines stacked with three different gene cassettes at different loci in rice. Meanwhile, the qPCR protocol used here with universal primer pairs was employed to detect the homozygous lines stacked with two different genes at the same locus. However, the qPCR assay was only used for single- and double-insert lines. The assay may become less accurate and more complicated when used for multiple-insert lines.

2.4.4. Potential application to large-scale production of transgenic rice

With a routine transformation efficiency in Indica rice of 27%, and the high percentage of transgenic events containing low insert numbers, this protocol is a very reliable and a powerful tool for larger-scale production of transgenic rice in functional genomics. Although Japonica cultivars were not investigated in this study, the efficiency maybe even higher in Japonica cultivars, compared to Indica cultivars. Many previous studies of *Agrobacterium*-mediated transformation using immature embryos of Japonica cultivars showed very high efficiency (>90%) (Hiei *et al.* 2006; Hiei & Komari 2008; Slamet-Loedin *et al.* 2014). With a better efficiency of transformation in Indica rice, more opportunities are offered to conduct genetic research on the Indica genotype, compared to the past when the protocol for Indica transformation had very low efficiency.

A combination of the *Agrobacterium*-mediated transformation protocol and the qPCR assay provides a very reliable, fast-tracking, and powerful tool for larger-scale production of homozygous rice plants with low insert number in the T1 generation. Starting with low insert copy number lines, a standardized procedure of qPCR assay, and universal primer pairs of the *nos*

terminator can be used to identify the homozygous plants transformed with different gene expression cassettes in different rice cultivars in the T1 generation. The assay successfully worked for two stacked genes sharing the same common element – *nos* terminator in rice. In this study, end-point PCR analysis was also used to screen transgenic plants from null plants, before the qPCR was used to distinguish homozygous plants from hemizygous. This accelerated the determination of homozygous plants. The materials from the homozygous plants (T1) would be used for further analysis, such as protein expression in grains, in this study.

2.5. Conclusion

This study attempted to fast-track the development of many homozygous transgenic lines in the T1 generation with low insert copy of transgenes for further analyses. Using the robust *Agrobacterium* transformation system and a reliable and accurate qPCR assay, this study demonstrated the capacity to generate multiple independent homozygous transgenic events carrying *Glb-1:HvSUT1*, *GluA2:OsNAS2*, and the novel combination of *Glb-1:HvSUT1* - *GluA2:OsNAS2* in a short turn-around time. Both the high-throughput rice transformation protocol and the universal qPCR assay are likely to accelerate the production of large numbers of homozygous transgenic plants with low copy of transgene. The grains from the homozygous plants were used for further phenotypic and molecular and micronutrient analyses and all non-transgenic IR64 plants used as controls in this study were regenerated from the calli through tissue culture, the results of which are presented in Chapters 3 and 4.

CHAPTER 3: CHARACTERISATION OF *HvSUT1* AND *OsNAS2* EXPRESSION IN HOMOZYGOUS TRANSGENIC RICE

3.1. Introduction

The rice grain is an important storage organ for starch, proteins, and other nutrients, and is a staple food of more than half of the world's population. Improvements in the nutrient level and quality of rice grains therefore have far reaching implications for human health. The grain is composed of maternal tissues (pericarp, testa, and nucellus) and filial tissues (the endosperm and embryo) which is isolated from the maternal tissues by an apoplasmic space. Endosperm development undergoes four successive stages, including coenocyte (1-2 days after anthesis (DAA)), cellularization (3-5 DAA), storage product accumulation (6-20 DAA), and maturation (21-30 DAA) (Wu *et al.* 2016b). During these stages, assimilates and nutrients are dominantly transported to support developing rice grains via vascular bundles, mainly on the dorsal side (Krishnan & Dayanandan 2003; Wu *et al.* 2016a). Transport of assimilates, mineral nutrients, and water are from an ovular vascular trace into nucellar cells. From the nucellar cells, solutes efflux into the apoplasmic space and subsequently influx in to the aleurone cells via specific transporters for each solute. For instance, sucrose transporters (OsSUT1 and OsSWEET 11/15) play a role in sucrose transport (Aoki *et al.* 2003; Furbank *et al.* 2001; Ma *et al.* 2017; Scofield *et al.* 2007; Scofield *et al.* 2002; Yang *et al.* 2018). Manipulating gene expression of nutrient transporters is a promising strategy for improving yield and grain quality in cereals and several examples of this exist in the literature (Saalbach *et al.* 2014; Weichert *et al.* 2017; Weichert *et al.* 2010).

Under the control of a constitutive promoter, like the cauliflower mosaic virus 35S promoter element, transgenes can be continuously expressed in all, or most, cells at a strong level during the life cycle of a plant. For Fe and Zn biofortification in the grain, constitutive expression

of many transgenes may be unnecessary and even detrimental for vegetative growth or other traits. For instance, soybean ferritin can store large amount of Fe, but its constitutive expression in rice and wheat led to higher Fe levels in vegetative tissues but not in the grain (Drakakaki *et al.* 2000). Furthermore, rice nicotianamine synthase 1 (*OsNAS1*), which catalyzes the biosynthesis of nicotianamine (NA) was constitutively expressed in rice with the aim to increase Fe and Zn concentrations in grains (Zheng *et al.* 2010). Unfortunately, the constitutive overexpression of *OsNAS1* was correlated with inhibition of rice growth, a trait not seen in endosperm-specific overexpression (Zheng *et al.* 2010). Also NA is a ubiquitous chelator for other micronutrients in the plant, including Fe, Zn, Cu, Mn (Anderegg and Ripperger, 1989, Husted et al., 2011, Pich et al., 1994, von Wiren et al., 1999) and heavy metals such as Ni (Douchkov *et al.* 2005; Kim *et al.* 2005; Weber *et al.* 2004) and Cd (Kyriacou 2013; Slamet-Loedin *et al.* 2015). Although no report of transgenic rice with constitutive expression of *NAS* genes has led to high accumulation of toxic heavy metals in the grains, careful consideration to this factor should be considered in the constitutive expression of *NAS* genes in rice and other grains.

To control the expression of one or multiple transgenes in the rice endosperm, biotechnological techniques can be employed to develop expression cassettes under the regulation of endosperm-specific promoters. Based on expression of the *uidA* reporter gene (GUS activity), multiple promoters of rice grain storage protein genes have been characterised, namely a 26kDa globulin (*Glb-1*), multi-gene family of glutelin, prolamin genes, and allergenic protein genes (Kawakatsu *et al.* 2008; Qu & Takaiwa 2004; Qu *et al.* 2008; Wu *et al.* 1998). The 26 KDa globulin accounts for 8% of the total endosperm protein and is encoded by a single copy gene, while the rice glutelin proteins comprising about 75% of the total seed protein are encoded by a multi-gene family (Hwang *et al.* 2002). The expression pattern of these promoters was shown to differ, for

example a *Glb-1:uidA* gene fusion showed GUS activity in the inner starch endosperm, whereas the GUS activity under the regulation of the glutelin gene promoters was observed in the outer layer of the endosperm (Qu & Takaiwa 2004; Qu *et al.* 2008). The promoters of globulin and glutelin genes were reported to be endosperm-specific because no GUS activity was observed in embryo and vegetative tissues, while a similar analysis of prolamin gene promoters showed they were not tightly specific for the rice endosperm (Qu & Takaiwa 2004).

Depending on the objectives of the study, potential promoters with desired specificities needs to be carefully selected and confirmed in the target crops (Furtado *et al.* 2008). In most studies, the expression of transgenes has been targeted to the rice grains. The most well-known example of this is Golden Rice where two transgenes, phytoene-synthase (*Psy*) and carotene-desaturase (*crtI*), were both expressed in rice grains under the control of seed specific promoters (Paine *et al.* 2005). Another consideration in targeted multiple-gene expression is the use of endosperm-specific promoters with diverse sequences so as to avoid potential homology-dependent gene silencing, and thus ensure stable transgene expression (Charrier *et al.* 2000; Kooter *et al.* 1999; Matzke *et al.* 1994; Matzke & Matzke 1995; Vaucheret *et al.* 1998).

In this study, the rice endosperm was the focus for Fe and Zn biofortification, thus the objective was to successfully and specifically express the *HvSUT1* and *OsNAS2* in the rice endosperm under the control of the *Glb-1* and *GluA2* promoters, respectively. Furthermore, this work also demonstrated temporal patterns of OsNAS2 and HvSUT1 expression during important stages of nutrition uptake in immature grains from three populations of transgenic lines, SC1, SC2 and DC1 via immunoblot analysis. Finally, a better growth performance of transgenic lines was investigated.

3.2. Methods

3.2.1. Plant growth

Transgenic rice seeds were dehusked and then sterilised by rinsing with 70% ethanol for 30 seconds, then in 50% commercial bleach with a drop of Tween-20 for 20 min with shaking. The seeds were then rinsed five times with Milli-Q water and left to germinate on moist Whatman paper at 29^0C for 36 h in dark conditions, and then with a photoperiod of 14h day/10h night for further 5 days.

An agar transferring hydroponic system was used prior to potting into soil. Eppendorf tubes (1.5 ml) were used with the bottom cut off. A 200-µl volume of 0.8% agar was filled into the tubes, and germinated seeds were placed on the agar. The root should be in contacted with the agar. The hydroponic system was maintained at 25-29^0C and the photoperiod was 14h light /10h dark for further 7 days. Then the seedlings were transferred into Jefferies® soil mix for 3 days before they were transplanted into 3 L pots of Jefferies® soil mix and placed in the greenhouse under the same photoperiod conditions.

3.2.2. Histochemical analysis

Roots (root tips including hair zone), young leaves of primary tillers and immature seeds from the top of the panicles of the primary tillers were harvested at 5-6, 10-11, 15-16 and 20-21 DAA from three independent lines (Gus 1.1, Gus 3.1, and Gus 4.4) (see Section 2.3.2.3, Chapter 2) and then placed in a solution of 90% cold acetone for 2 hours. The seeds were sectioned longitudinally with a razor blade and incubated in the fixative solution of 4% formaldehyde for 30 minutes and then transferred into phosphate buffer (50 mM NaH_2PO_4 and 50 mM Na_2HPO_4) for 1 hour. Subsequently, these seeds were incubated in 1mM X-Gluc (5-bromo-4-chloro-3-indolyl-β-

D-glucuronic acid, sodium salt), phosphate buffer, 1mM potassium ferrocyanide, 1mM potassium ferricyanide, and 0.05% (w/v) Triton X-100 pH 7.0 and incubated overnight at room temperature. After staining, these sections were washed in 100% ethanol for one day to remove chlorophyll and maintained in 70% ethanol until observed. These GUS-stained sections were imaged by an Olympus SZX10 Stereoscope connected with DPL20 Camera.

For paraffin sections, the GUS-stained sections were fixed in FAA solution (50% (v/v) ethanol, 3.7% (v/v) formaldehyde and 5% (v/v) acetic acid) for 30 minutes. The sections were dehydrated by incubation in a series of ethanol solutions (70%, 80%, 90% and 100%, 30 minutes for each solution) and the dehydration was completed by incubating in 100% tert-butanol for 15 minutes (2 times). Before the sections were embedded in paraffin wax, they were embedded in melted paraffin wax at 62^0C for 90 minutes. Slices (8 µm in thickness) of these sections were obtained using a Leica RM2135 rotary microtome and then mounted in DEPEX mounting medium (Merck). Specimens were observed and imaged with Brightfield BX53 Microscope connected with DP27 colour camera (Olympus).

3.2.3. Antibody production for HvSUT1 and OsNAS2 protein detection

A polyclonal anti-HvSUT1 antibody produced and characterized by Huynh (2015) was used for HvSUT1 detection. For polyclonal anti-OsNAS2 antibody production, a peptide of the antigen, 14 amino acids in length (KADPRRGGGLAGAR), was designed by NovoFocus™ and manufactured by NovoPro. The antigen was mixed with NovoBoost™ and then was used to immunize rabbits for 6 rounds. Affinity-purified rabbit polyclonal antibody was then validated by ELISA titre using the designed antigen (≥1:50000). Before the anti-OsNAS2 antibody was used to detect OsNAS2 protein, the concentration of the antibody was titrated against serial dilutions of

the unconjugated peptide antigen by dot blot analysis to determine antibody dilution for use in immunoblotting analysis.

3.2.4. Protein extraction

Immature grains from homozygous plants (the T2 generation) at 3, 5, 7, 10, 15, 20 days after anthesis (DAA) were dehulled to remove the glumes, lemma and palea (Figure 3.1) and then frozen in liquid nitrogen. The grains were ground into a fine powder in liquid nitrogen and then stored at -80^{0}C. A 400 µl-volume of extraction buffer (250mM Tris-HCl (pH 8.0), 25mM ethylenediamine-tetraacetic acid (EDTA), 30% w/v sucrose, 5mM DDT, 1mM PMSF and benzamidine and 1X proteinase inhibitor cocktail (Roche) was added to 100 mg of ground grain tissue, and then thoroughly mixed by vortexing. Samples were centrifuged at 3,000 g for 10 minutes at 4^{0}C to remove all cell debris, then aliquots of 100 µl of supernatant were carefully transferred into 1.5 ml Eppendorf tubes. The aliquots of supernatant were centrifuged at 15,800 g for 120 minutes at 4^{0}C to separate soluble protein from membrane protein. An 80-µl aliquot of the supernatant with soluble proteins was transferred into a fresh tube and the pellets with membrane proteins were suspended on ice in 30 µl of sample buffer [50 mM N-(2-hydroxyethyl) piperazine-N′-(2-ethanesulfonic acid) (HEPES) (pH 7.5) with 2% SDS, 5 mM EDTA, 2 mM DTT and protease inhibitors as described above]. All protein samples were stored at -80^{0}C.

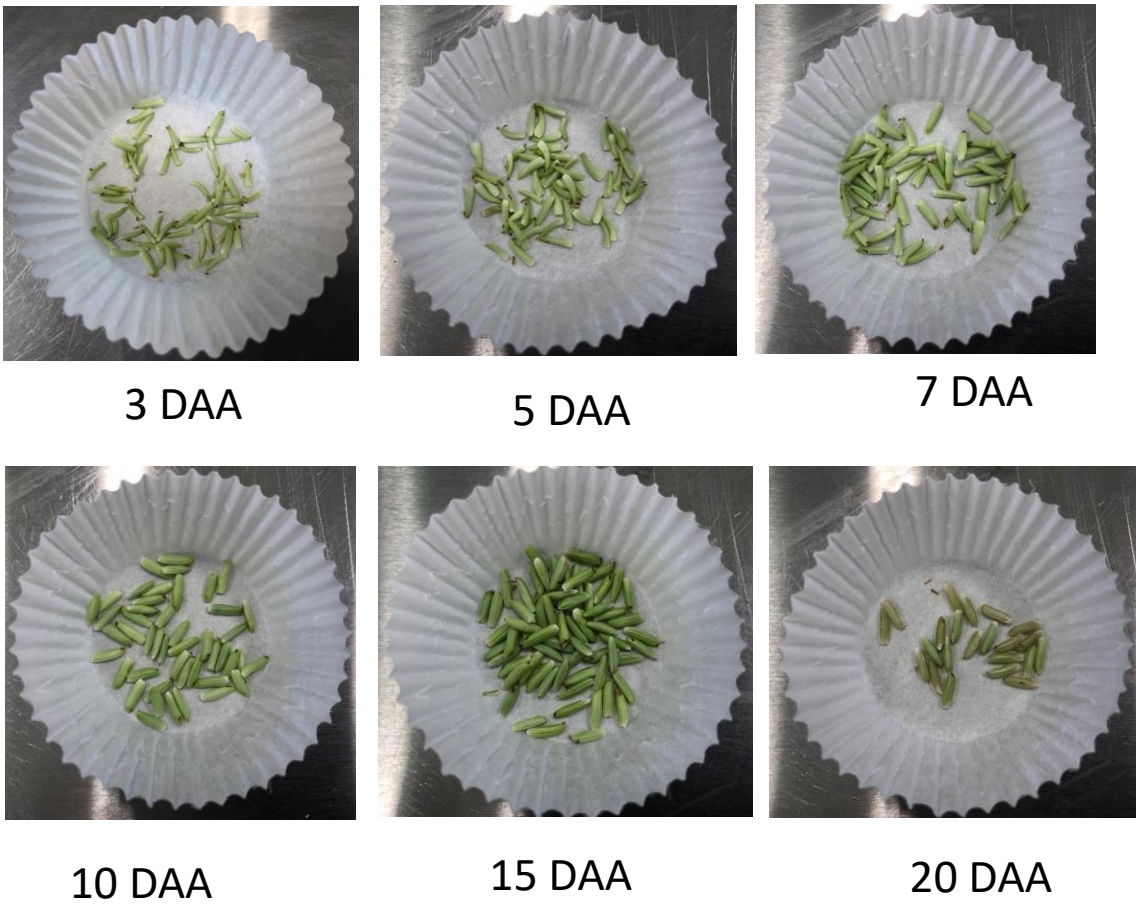

Figure 3.1. Immature grains at 6 different stages of grain development; at 3, 5, 7, 10, 15, and 20 DAA were collected for protein extraction using for immunoblotting.

3.2.5. Protein electrophoresis on SDS-PAGE and immunoblotting

For OsNAS2 detection, the 80 µl aliquot of the supernatant with soluble proteins were added with 20 µl of 5X Urea sample buffer (6M urea) and 1.25 µl mercapto-ethanol 98%. For HvSUT1 detection, a 30 µl-aliquot of total membrane proteins was added to 7.5 µl of 5X Urea sample buffer. The total protein samples were incubated at 37^0C for 30 minutes. A 15-µl aliquot of the protein sample was loaded and separated on a 10% SDS-polyacrylamide gel at 170V for 60 minutes in 1X gel electrode buffer (pH 8.3), and then transferred onto nitrocellulose membrane (GE Healthcare Amersham^{TM}) by electro-blotting at 60V for 90 minutes in 1X transfer buffer (pH

8.3). A duplicate gel was run at the same time for Coomassie staining to determine equivalent loading of samples. After transfer, blots were blocked at room temperature for 1 hour in 1X blotto buffer (20mM Tris-Base, 150mM NaCl, 5% skim milk powder, and 0.1% Tween 20, pH 7.4). The blots were incubated with HvSUT1 primary antibody at a 1:500 dilution, or OsNAS2 affinity purified primary antibody at a 1:1000 dilution, in blotto buffer overnight (~14 hours) at 4^0C. The membranes were then washed 3X for 5 minutes in 1X blotto buffer, followed by incubation at 4^0C for 1 hour with Goat anti-rabbit IgG-horseradish peroxidase (HP) conjugated secondary antibody (Rockland Immunochemicals, Inc.) diluted 1:5000 in blotto. The membranes were rinsed in 1X TBS (20mM Tris-Base, 150mM NaCl, and 0.1% Tween 20, pH 7.4 for washing (3X) for 5 minutes each time. The blots were developed in Western Star Chemiluminescent substrate (BioRad) and imaged with the Chemidoc CCD camera (Biorad). QuantityOne software (Bio-Rad) was used to determine the intensity of detected protein bands. All buffer components are listed in Table 6.13.

3.2.6. Growth and yield parameters

Height (cm) and tiller number of the transgenic lines and the non-transgenic control, IR64 were recorded at 0.5, 1, 2 and 3 months after germination. Grain weight and dry weight of biomass (gram) were recorded after harvesting.

Percentages difference in plant height and tiller number (%) relative to the non-transgenic control were calculated using the equation below

$$\boldsymbol{Difference}\ (\%) = \frac{\boldsymbol{H_{Sample}} - \boldsymbol{H_{Control}}}{\boldsymbol{H_{Control}}} \times \mathbf{100}$$

where $\boldsymbol{H_{Sample}}$ is plant height or tiller number of transgenic plants and $\boldsymbol{H_{Control}}$ is plant height or tiller number of non-transgenic control.

3.2.7. Statistics

The means and standard error of the height, tiller number, yield, and plant biomass of transgenic lines and the non-transgenic IR64 were calculated. The results were expressed as mean ±SE. The ANOVA analysis with a Waller-Duncan post-hoc test was performed for the comparison of the difference in the mean of the height, tiller number, yield and plant biomass from transgenic lines and the wild type between each of the transgenic lines. Differences were considered significant at $p < 0.05$ and $p < 0.01$. All statistical analyses were done with R or IBM SPSS statistics 25.

3.3. Results

3.3.1. Spatial and temporal control of GUS expression under the regulation of endosperm-specific promoters (*GluA2* and *Glb-1*) during grain development and early grain germination

To test the specificity of the *GluA2* promoter, the roots, leaves, and immature grains from T0 *GluA2:uidA* transgenic lines were harvested at different stages from 5 DAA to 21 DAA for histochemical assay with X-Gluc. GUS activity was detected in the endosperm tissue at all the time-points of the developing grain, even the grains at earlier stages (3-4 DAA) (data not shown due to the difficulty of working with this tissue). For the whole grains, the GUS staining was located along the dorsal vascular bundle of the grain at 10-11 DAA (Figure 3.2B) and 15-16 DAA (Figure 3.2C), but inside the grain at 5-6 DAA (Figure 3.2A). In longitudinal section, the grains at all different time-points showed strong GUS staining in the endosperm with dark blue staining in the outer layers, and light blue inside of the endosperm, but not in the embryos (Figure 3.2 E, F, G, and H). Furthermore, darker staining was seen on the ventral side of the longitudinal sections. For non-transgenic rice, no GUS activity was observed in both the section and dissection grains

(Figure 3.2 I, J, K, and L). Non-seed tissues, including roots and leaves, showed no detectable GUS staining in both transgenic and non-transgenic control tissue (Figure 3.2 M, N, O, and P).

No GUS staining was detected in the maternal tissues in the grain, namely the nucellus projection, nucellus epidermis, ovular vascular trace, epicarp, mesocarp and spikelet hull), GUS staining was only detected in the aleurone and the endosperm, but not present in the embryo of the filial tissues in grains (Figure 3.3). Moreover, no GUS staining was observed in the root and leaf tissues and in the non-transgenic IR64. The results indicated that the regulation of the *GluA2* promoter is, to the level of sensitivity of the GUS assay, endosperm-specific and expresses in the grains at 5-6 DAA.

Another analysis of GUS activity in the Nipponbare mature grains (over 5 years old) carrying *Glb-1:uidA* or *Act-1:uidA* from Huynh (2015) and the IR64 mature grains (over 1 year old) carrying the *GluA2:uidA* construct was carried out covering the early period of grain germination between 0 day after germination (DAG) and 3 DAG (Figure 3.4). GUS staining was detected in all the mature grains at 0 DAG. For the *uidA* gene under control of a constitutive promoter *Act-1*, the GUS activity was detected in the whole grain at 0 DAG, including the embryo and endosperm. From 1-3 DAG, the staining was still seen in the whole grain, and was especially evident in the embryo, while staining was still detected in the coleoptile and root developing from the embryo at 3 DAG.

For the endosperm-specific promoters of *Glb-1* and *GluA2*, the GUS activity was only seen in the rice endosperm, but the GUS activity regulated by the *Glb-1* promoter was seen in the central region of the endosperm (Huynh 2015), while the GUS staining of the grains carrying *GluA2:uidA* was seen in the outer layer of the endosperm. No GUS activity was detected in the embryo, the coleoptile, and the developing root from the embryo during grain germination. Furthermore, no

GUS staining was observed in the endosperm, embryo, the coleoptile, and the root developing from the embryo in the germinating from non-transgenic seed. Based on the sensitivity of the GUS assay, the regulation of the *Glb-1* promoter confers endosperm-specific expression in Nipponbare transgenic rice, and the GUS protein remains very stable in the transgenic grains.

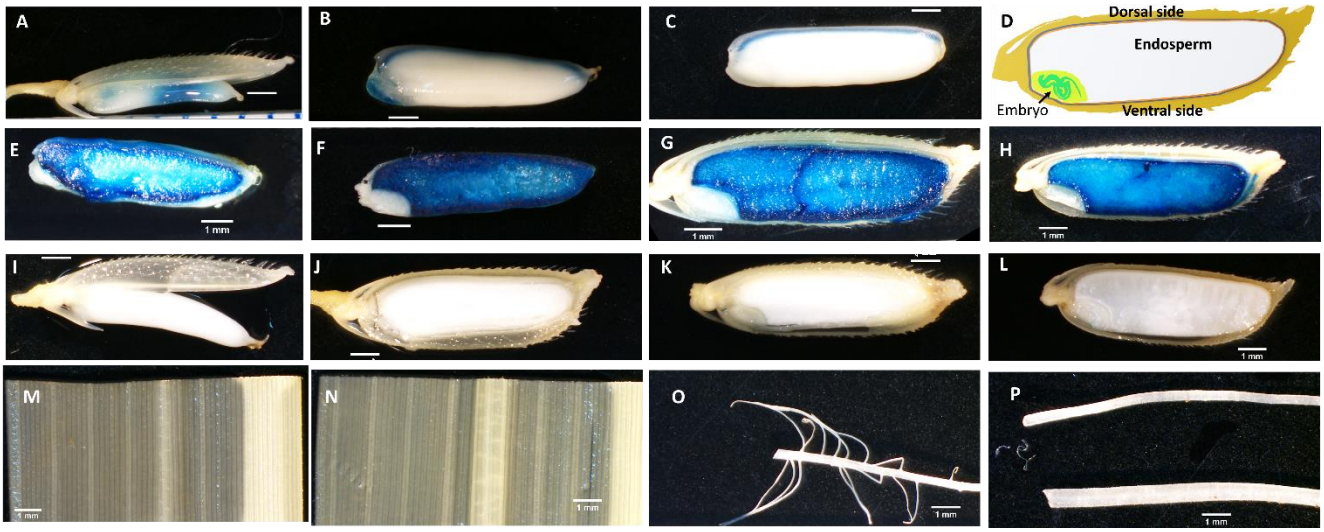

Figure 3.2. Histochemical analysis of GUS expression under the control of promoter *GluA2* at four different timepoints of seed maturation. (D) Scheme of longitudinal section of rice grains. GUS protein was detected by incubating in X-Gluc solution in the whole grain at 5-6 DAA (A), at 10-11 DAA (B) and at 15-16 DAA (C), in hand-cut longitudinal sections at 5-6 DAA (E), 10-11 DAA (F), 15-16 DAA (G) and 20-21 DAA (H), and on control non-transgenic rice at 5-6 DAA (I), 10-11 DAA (J), 15-16 DAA (K) and 20-21 DAA (L). No GUS was detected on the leaf and root of transgenic plants (M and O) and non-transgenic plants (N and P). Scale bar: 1 mm.

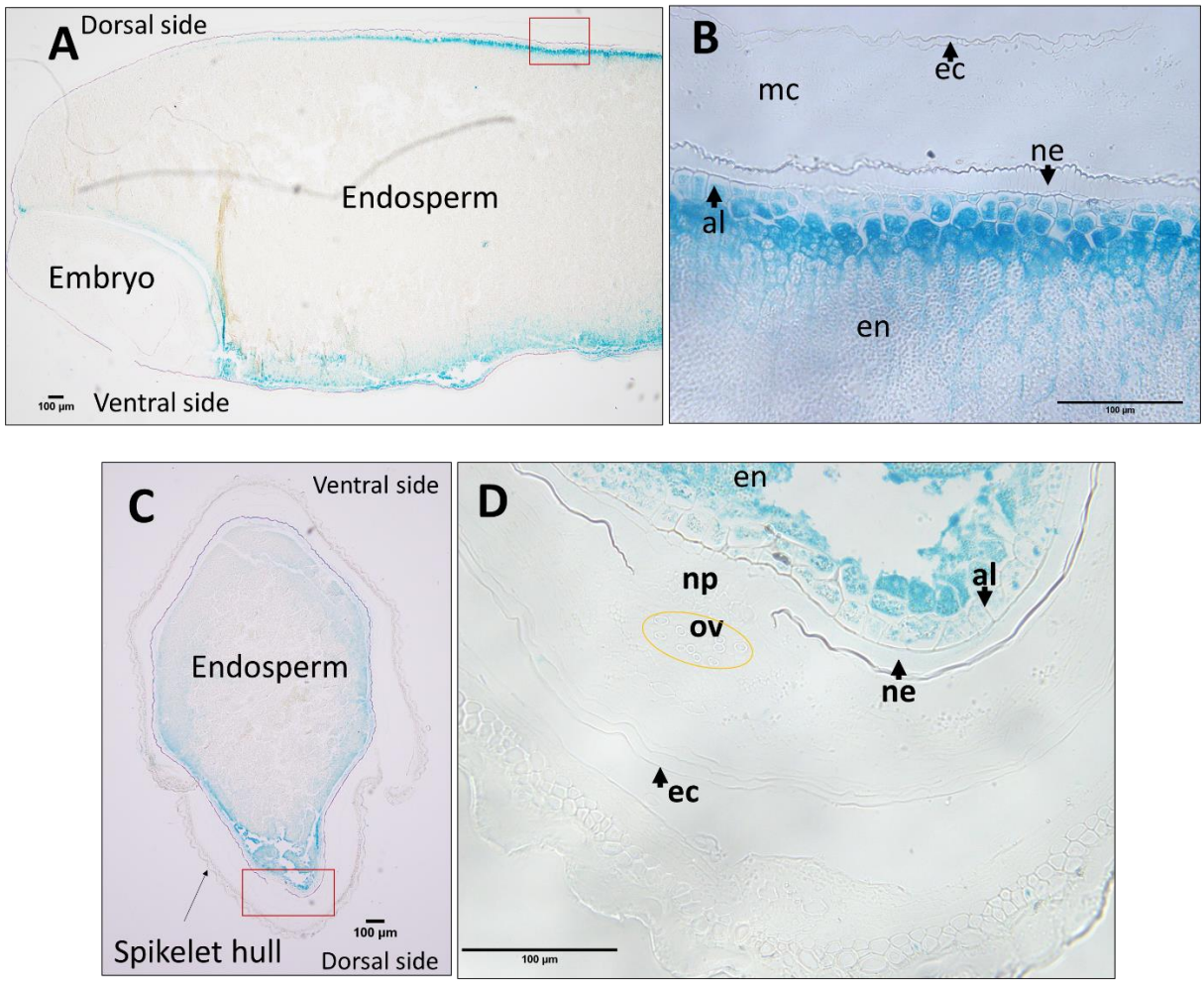

Figure 3.3. Histochemical analysis of GUS representing the expression of GUS under the control of promoter *GluA2*. A. Longitudinal section of the immature rice grains at 18 DAA carrying *GluA2:uidA*; B. Red box area in A, showing GUS activity detected in aleurone and endosperm cells. C. Transverse section of the immature grains at 10 DAA; D. Red box area in C, showing GUS activity. No GUS staining was detected in the maternal tissues (np: nucellus projection, ne: nucellus epidermis, ov: ovular vascular trace, ec: epicarp, mc: mesocarp and spikelet hull), GUS staining was detected on the filial tissues (al: aleurone and en: endosperm).

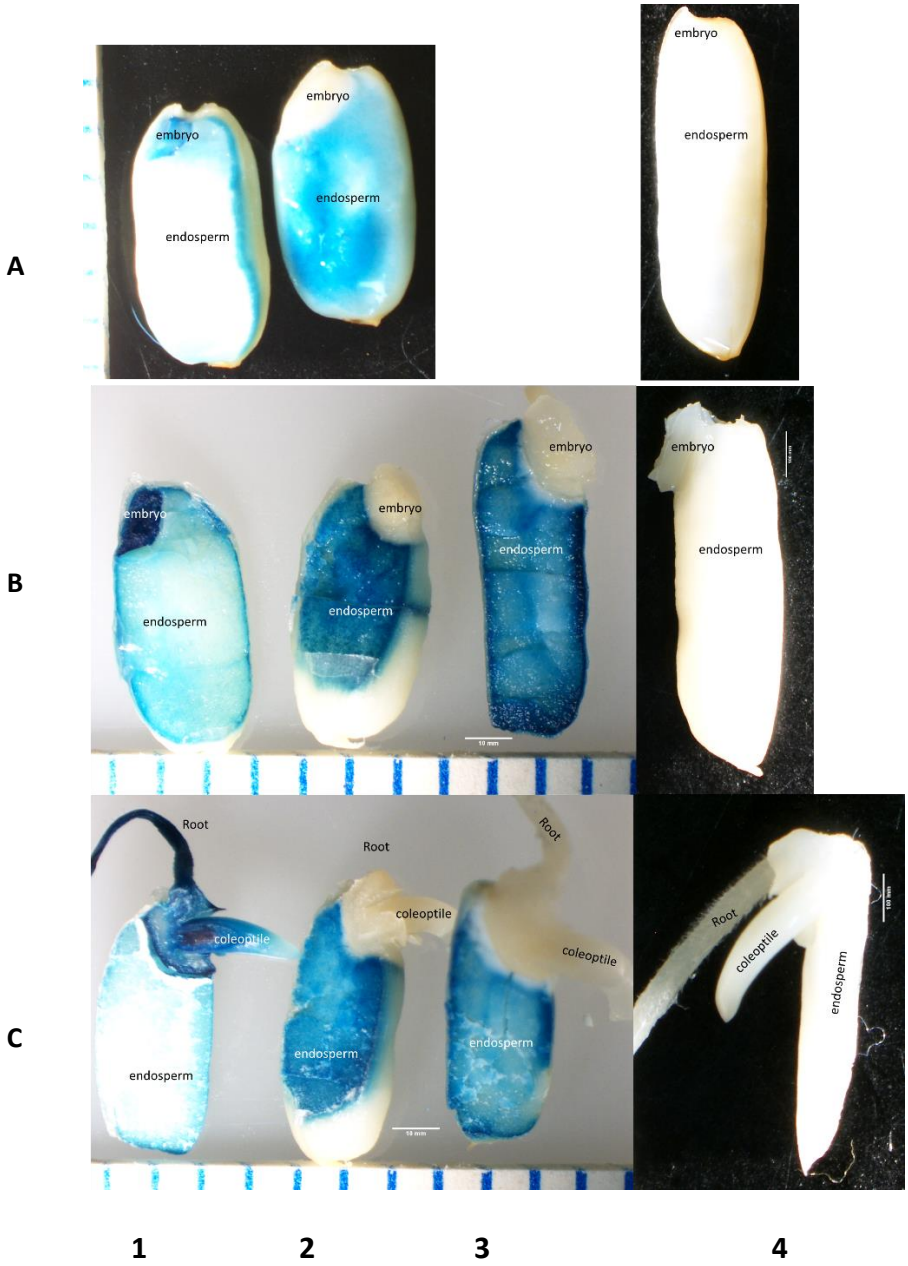

Figure 3.4. Histochemical analysis of GUS activity during grain germination. A. 0 day after germination (DAG); B. 1 DAG and C. 3 DAG. **1:** *Act-1:uidA* expressed in Nipponbare obtained from Huynh (2015); 2. *Glb-1:uidA* expressed in Nipponbare grains obtained from Huynh (2015); 3. *GluA2:uidA* expressed in IR64 and 4. the non-transgenic control IR64.

3.3.2. Antigen design for anti-OsNAS2 production

In order to follow the expression of the NAS2 protein during grain filling, a polyclonal antibody was raised to a unique region of the OsNAS2 protein. A multiple sequence alignment of NAS1 (Q0DSH9-332 aa), NAS2 (Q10MI9 -326 aa), and NAS3 (Q0D3F2 – 343aa) from Japonica rice and three amino acid sequences of NAS1 (A2XFU4-332 aa), NAS2 (A2XFU5-326 aa), and NAS3 (A2YQ58 -343) from Indica rice were aligned by GeneDoc and GenomeNet (Kyoto University Bioinformatics Center) (Figure 3.5). The amino acids derived from the cloned OsNAS2 generated here had 100% identity to the Japonica OsNAS2 (Q10MI9). The amino acid sequences of three NAS proteins were very similar between two rice cultivars with 100% identity for NAS1 and NAS3 and 99.08% for NAS2. It can see that the NAS3 protein had the sequence of amino acid sharing 60.54 % similarity with NAS1 and 61.96% similarity NAS2. NAS1 and NAS2 shared higher identity with over 88%. There was only one region from aa 278 to the N terminus, which was divergent and therefore suitable for antigen production.

A peptide antigen Design Tool (NovoFocus^{TM}) was used to choose the best antigen for anti-OsNAS2 production. There were 36 potential antigens with scores from 13 to 20.2 (Table 3.1). To ensure anti-OsNAS2 to be specific for NAS2, the best antigen peptide would be derived from aa 278 to the N terminus. The sequence of KADPRRGGGLAGAR with score of 14.4 was selected to be synthesized and used as antigen for anti-NAS2 production.

Table 3.1. Potential antigens for anti-OsNAS2 production.

An antigen design software (NovoFocus^{TM}, Novopro company in China) was used to design potential peptides for anti-OsNAS2 production. An ideal antigen with high score (>13) and position in the region from aa 278 to the N terminus of the OsNAS2 protein was the final choice to synthesise and raise polyclonal antibodies in rabbit production (Figure 3.5).

Sequence	**Score**	**Position**	**Sequence**	**Score**	**Position**
NERARRLFRGADEG	20.2	163-176	GFLYPIVDLEDIRR	14.4	241-254
AANERARRLFRGAD	20.2	161-174	DLEDIRRGGFDVLA	14.4	248-261
ANERARRLFRGADE	20.2	162-175	**KADPRRGGGLAGAR**	**14.4**	**278-291**
ERARRLFRGADEGL	18.6	164-177	SVIVARKADPRRGG	14.2	272-285
DNYDRCGAANERAR	18.2	154-167	AVFDNYDRCGAANE	14.2	151-164
PIVDLEDIRRGGFD	17.8	245-258	IRRGGFDVLAVYHP	14.2	252-265
FDNYDRCGAANERA	17.8	153-166	RRGGFDVLAVYHPD	14.2	253-266
YPIVDLEDIRRGGF	17.4	244-257	IVARKADPRRGGGL	14	274-287
IVDLEDIRRGGFDV	17.2	246-259	VARKADPRRGGGLA	14	275-288
GAANERARRLFRGA	17	160-173	RGFLYPIVDLEDIR	14	240-253
VFDNYDRCGAANER	16.4	152-165	GARGFLYPIVDLED	14	238-251
VDLEDIRRGGFDVL	15.4	247-260	ARRLFRGADEGLGA	13.6	166-179
LYPIVDLEDIRRGG	15.4	243-256	RGGFDVLAVYHPDD	13.4	254-267
RARRLFRGADEGLG	15	165-178	LSKLEYDLLVRYVP	13.2	108-121
VIVARKADPRRGGG	15	273-286	EDIRRGGFDVLAVY	13.2	250-263
NYDRCGAANERARR	14.8	155-168	HGARGFLYPIVDLE	13	237-250
ARGFLYPIVDLEDI	14.4	239-252	ARKADPRRGGGLAG	13	276-289
FLYPIVDLEDIRRG	14.4	242-255	DIRRGGFDVLAVYH	13	251-264

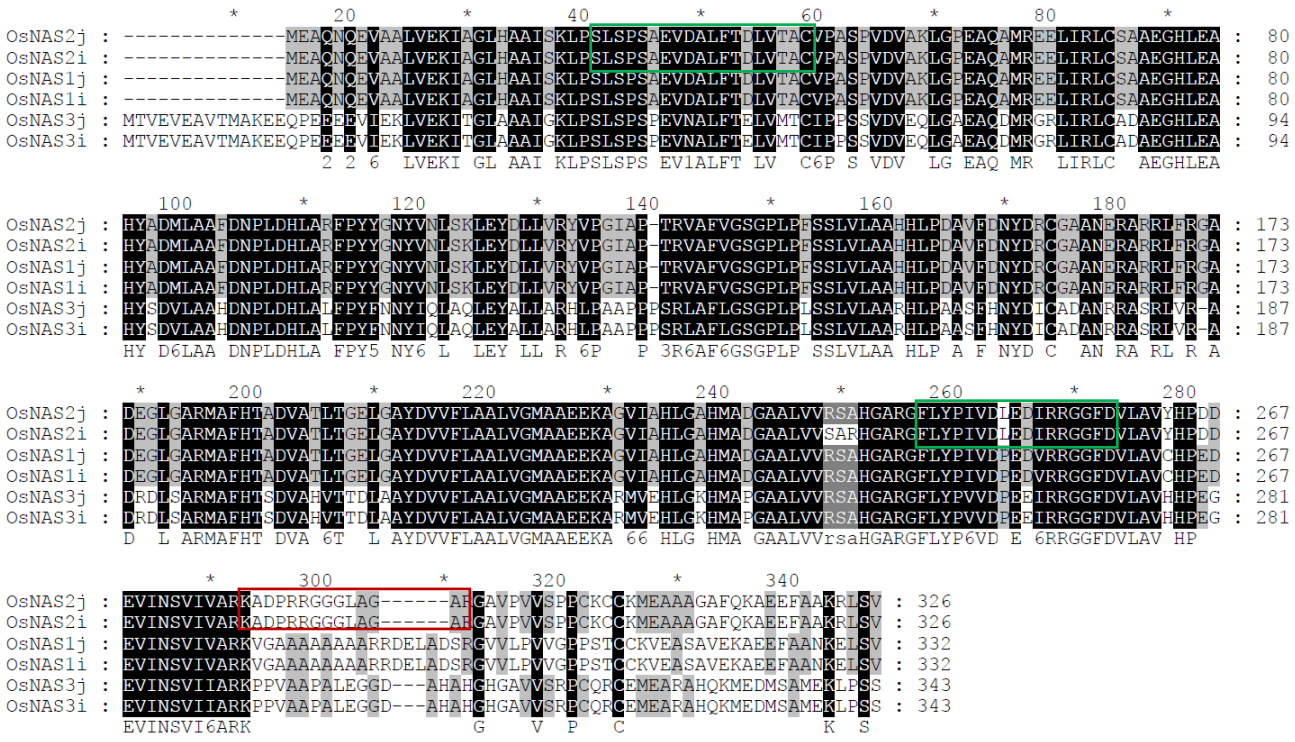

Figure 3.5. Alignment of amino acid sequences of OsNAS1, OsNAS2, and OsNAS3 from Indica rice and Japonica rice was performed by GeneDoc and GenomeNet. The three shade levels represent conservative degrees of 100, 80 and 60% similarity. Based on the sequence of OsNAS2, two transmembrane helices with N-terminus in outside of vesicle were predicted by TMpred program (https://embnet.vital-it.ch/software/TMPRED_form.html), numbered in Latin. The sequence of antigen for anti-OsNAS2 production is indicated in the red box close to the C terminus. The sequences of antigens published by Nozoye *et al.* (2014a) in green boxes.

3.3.3. Verifying specificity of the anti-OsNAS2

Because the specificity of the anti-HvSUT1 was confirmed by Huynh (2015), the focus of this work was to validate specificity of the anti-OsNAS2 purified antibody. Firstly, dot blots were performed to optimise the concentration of anti-OsNAS2 (primary antibody). Four different dilutions of purified anti-NAS2 (1µg/ml), namely 1:500, 1:1000, 1:1500, and 1:2000 were carried

out to detect a dilution series of the NAS2 peptide antigen (0.2, 2, 20, and 200 ng). The anti-OsNAS2 could detect all the concentrations of the peptide except down to 0.2 ng. Intensities of different concentrations of the NAS2 peptide were black to grey, corresponding to the highest to lowest concentration (Figure 3.6A). In the highest concentration of anti-OsNAS2, higher background appeared around all of the peptide concentrations, whereas at dilutions of 1:1500 and 1:2000, the aliquots for 0.2 and 2 ng were not detected. The dilution of 1:1000 showed less background and was able to detect the dots of 0.2ng (Figure 3.6B). From these analyses a 1:1000 dilution of anti-NAS2 was used in subsequent immunoblot analysis.

To determine the specificity of the anti-OsNAS2 antibody to endogenous NAS2 protein, an immunoblot analysis was done on leaf and root tissues of non-transgenic IR64 and Nipponbare grown under Fe-deficient and Fe-sufficient conditions (Figure 3.7A). This was done because OsNAS2 is expressed in Fe-sufficient root, but not in leaf tissue, and its expression increases significantly in roots and leaves in response to Fe deficiency. Therefore, Fe-sufficient leaves and Fe-deficient leaves were considered as negative and positive controls, respectively. The same amount of total protein from cell lysates was loaded into the SDS gel (Figure 3.7C). Multiple bands were observed on the blot (Figure 3.7B) and the pattern of the bands from the same tissue with Fe-condition treatments was almost identical. However, in the Fe-deficient tissues, there were multiple bands in the roots (lane 2 and 4) and leaves (lane 1 and 2), yet one band of around 34 kDa was more prominent in the roots, compared to the leaves, and a similar pattern was found in both cultivars (Nipponbare and IR64). However, this peptide was not detected in Fe-sufficient leaves and endosperm, and present in small amounts in the Fe-sufficient roots. The molecular weight of this peptide was consistent with to that of OsNAS2 protein (34-35 kDa).

The pattern of bands in the immature grains was different with that in the leaves and roots. A prominent band of roughly 75 kDa still appeared in all the immature grain from transgenic rice and non-transgenic rice and persisted in all the immunoblots of rice protein preparation (Figure 3.8 C). The band of roughly 35kDa only appeared in transgenic immature grains with different intensity at 5 different stages of the grain filling but was absent in the non-transgenic immature grain samples. The identity of the 75kDa immune-reactive peptide is unknown, and the 35kDa peptide was assumed in all subsequent experiments to be the OsNAS2 protein.

The anti-OsNAS2 was used to examine the NAS2 expression in the grain tissue of OsNAS2-overexpressing transformants and non-transgenic IR64 (control), in which no OsNAS2 protein was expected to be present. For total protein preparation from the grains, two fractions of native protein extract, namely supernatant and pellet were separated by high speed centrifugation at 15800 g for 2 hours at 4^0C. The immunoblotting analysis of the two fractions of protein extracts from the T1 grains of multiple transgenic lines (T0) carrying the double gene construct (DC1) was probed with the anti-OsNAS2 antibody. The pellet samples showed only one consistent band of roughly 75 kDa, and no band at 35 kDa in all transgenic lines and the non-transgenic control. Meanwhile, the supernatant samples showed three consistent bands from 75-150 kDa, which were seen in all transgenic line and non-transgenic control (Figure 3.8 A, B, and C). A band of ~ 35kDa was present in the supernatant samples of all transgenic lines, with no signal of this band in the non-transgenic control. The band of ~ 35kDa was assumed to be the peptide of OsNAS2. The pattern of this band in protein samples extracted from the immature grains of DC1.9 at 5, 7, 10, 15, and 20 DAA showed a strongest signal at 5 DAA and gradual decrease during different stages of grain development consistent with the expression pattern predicted from the *GluA2* promoter driven expression (Figure 3.8 C). The non-specific bands did not interfere with detection of target

proteins, hence, further immunoblot images are presented showing only the bands of the target protein.

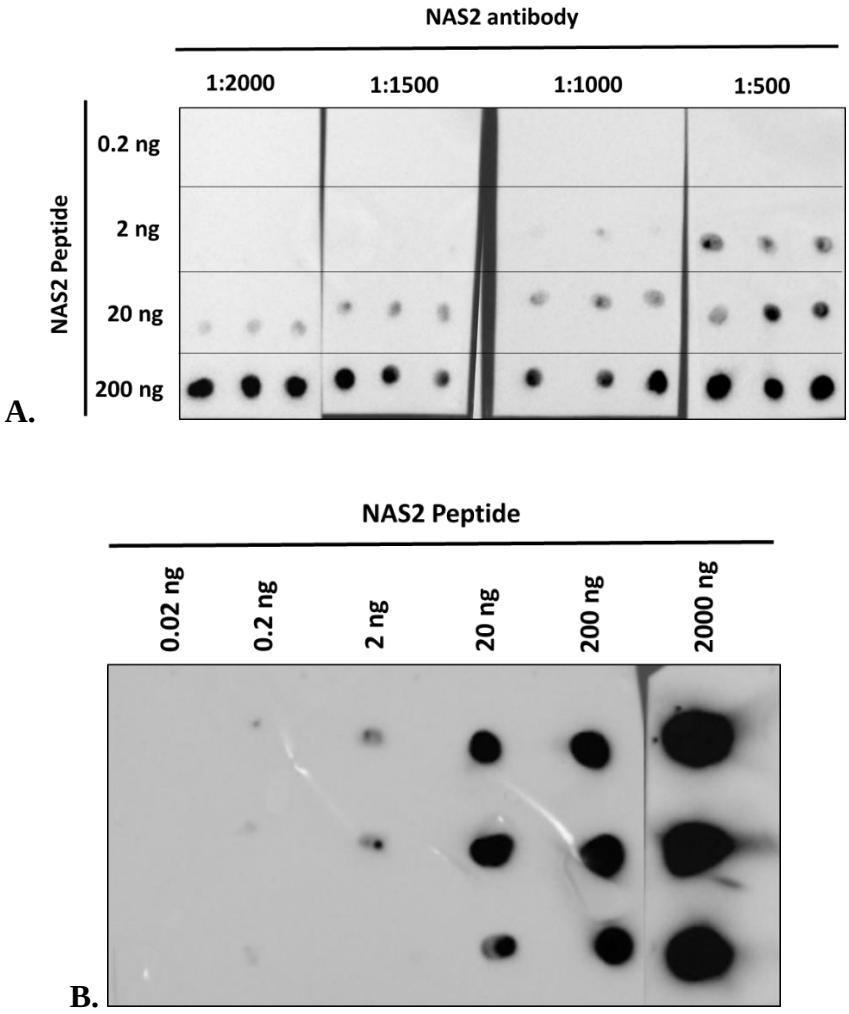

Figure 3.6. Dot blots for optimizing the concentration of anti-OsNAS2. A: Four different dilutions of anti-OsNAS2 from left to right (1:2000, 1:1500, 1:1000, and 1:500) against dilution series of the peptide (0.2 ng, 2 ng, 20 ng and 200 ng) from top to bottom on nitrocellulose membrane and secondary antibody (1:10000). B. Optimised concentration of primary antibody (anti-OsNAS2) (1:1000) and secondary antibody (1:10000) against a range of the NAS2 antigen amount (0.02, 0.2, 2, 20, 200, and 2000 ng).

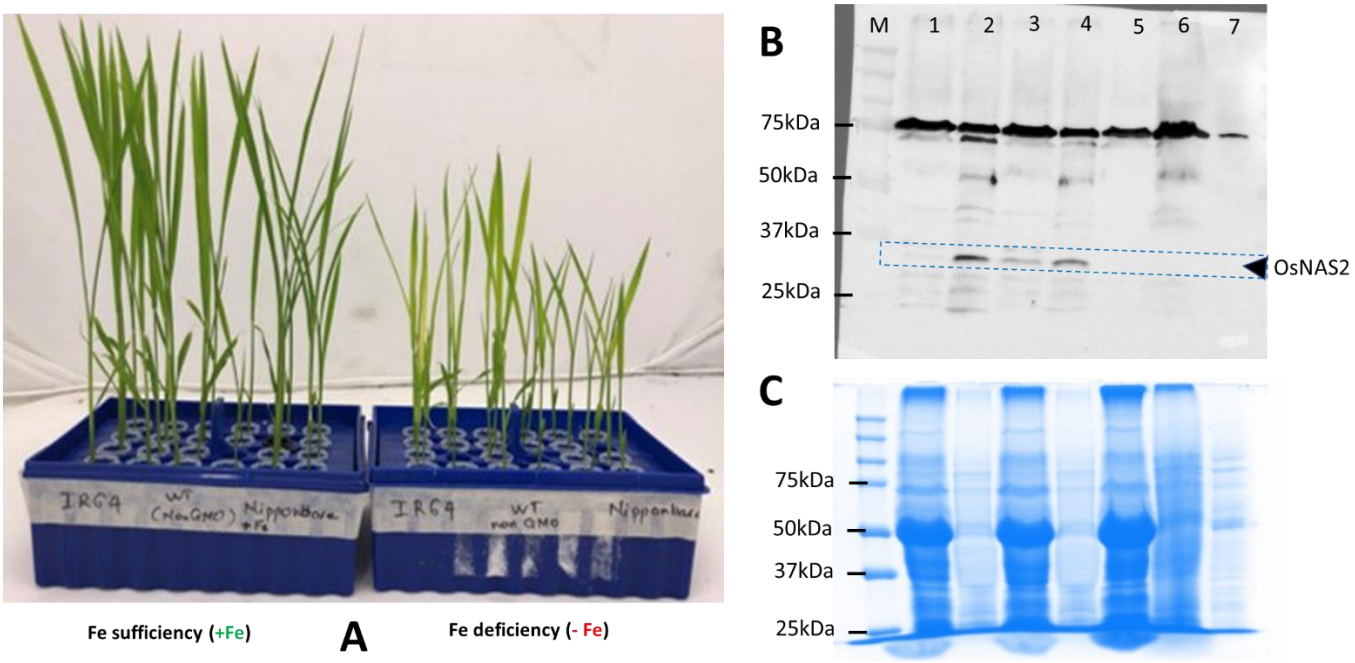

Figure 3.7. Immunoblot analysis for testing specificity of antiOsNAS2. Protein extractions according to Laemmli protocol (Table 6.13) were separated on SDS-PAGE gel (10%). A. Seedlings (Nipponbare and IR64) grown under Fe-sufficient (Left) and Fe-deficient (Right) conditions. B. Blot probed with anti-OsNAS2 (1:1000), followed by goat anti-rabbit IgG-horseradish peroxidase HP conjugated secondary antibody (1:10000). C. A replica SDS-PAGE gel was stained with Coomassie Brilliant Blue G-250. Lane 1 and 2: IR64 leaves and roots suffering Fe deficiency; Lane 3 and 4: Nipponbare leaves and roots suffering Fe deficiency. Lane 5, 6, and 7: IR64 leaves, roots and immature grains grown Fe-sufficient condition, respectively. M: Marker.

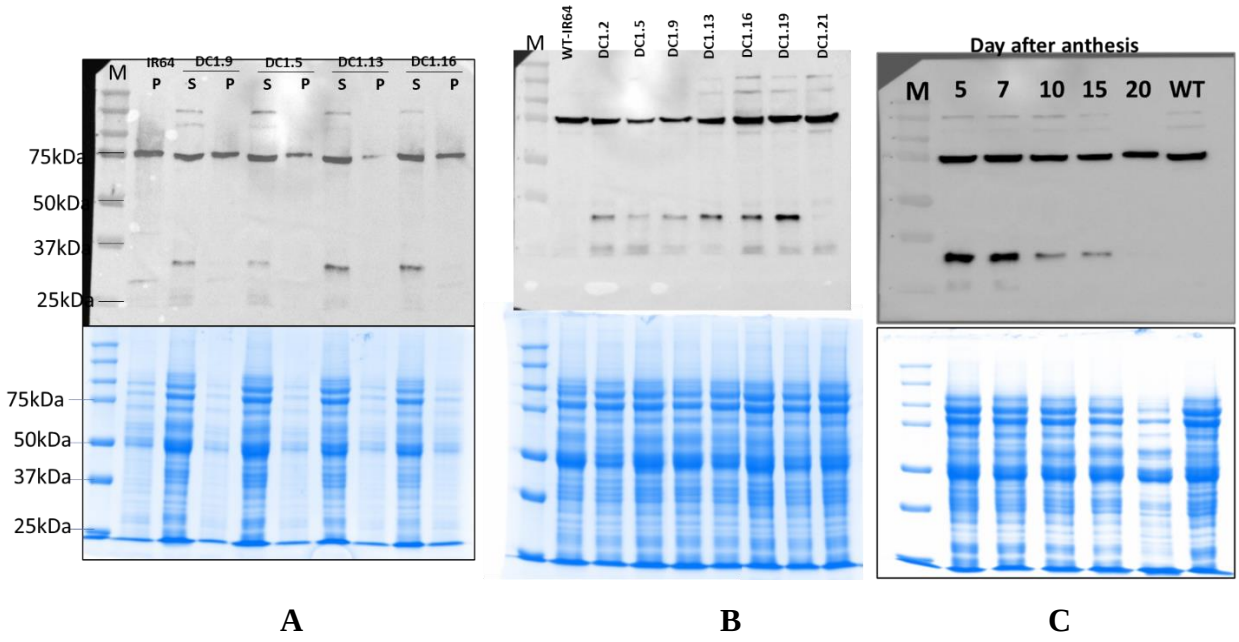

Figure 3.8. Immunoblotting analysis of NAS2 expression in immature grains from transgenic lines. Top: Blot probed with anti-OsNAS2 (1:1000), followed by goat anti-rabbit IgG-horseradish peroxidase HP conjugated secondary antibody (1:10000); Bottom: A replica SDS-PAGE gel at bottom stained with Coomassie Brilliant Blue G-250 was used as loading control. A. Crude protein of pellet (P) and supernatant (S) fractions extracted from immature grains of multiple independent lines of the DC1 construct in the T0 generation. B. Crude protein of supernatant fraction extracted from multiple independent lines of the DC1 construct in the T0 generation. C. Total crude proteins extracted (supernatant fraction) from immature grains at 5, 7, 10, 15 and 20 from *OsNAS2*-overexpressed transgenic line (DC1.9) in the T1 generation. M: marker, WT-IR64: non-transgenic control.

3.3.4. Temporal overexpression of *HvSUT1* and *OsNAS2* during rice grain development

Total proteins (supernatant fractions) were extracted from the immature grains of three homozygous and single-insert lines, namely SC2.14, SC2.15, and SC2.31, to determine the expression pattern of OsNAS2 protein in immature grains at 3, 5, 7, 10, 15, and 20 DAA (Figure 3.9). The results indicated that OsNAS2 protein was expressed at all stages of grain development (between 3 and 20 DAA). OsNAS2 protein was detected at 3 DAA and then reached a peak at 5 DAA, followed by a gradual decrease from 7, 10, 15, and 20 DAA. The three independent lines showed a consistent pattern of this temporal OsNAS2 expression during grain filling.

For the SC1 population of *HvSUT1*-overexpressing transgenic lines, four independent lines, namely SC1.16 (homozygous, two-insert line), SC1.17 (multiple-insert line), and SC.21 and SC1.22 (homozygous, single- insert lines) were analysed for temporal expression during grain development. To analyse the expression pattern of HvSUT1 protein in immature grains at 5, 7, 10, 15, and 20 DAA, total membrane protein (pellet fractions) extracted from four transgenic lines carrying *Glb1:HvSUT1* construct were probed with anti-HvSUT1 (Figure 3.10). A total protein sample from Nipponbare rice grains transformed with a *Glb-1:HvSUT1* reported by Huynh (2015) and non-transgenic IR64 rice grains were used for positive control and negative control in all immunoblots, respectively. A strong immune-reactive peptide of ~50 kDa was detected, consistent with the expected size of the HvSUT1 protein in the positive sample and was absent in the non-transgenic control sample. This peptide was detected in all immature grains at 5, 7, 10, 15, and 20 DAA with different intensity. HvSUT1 expression was detected at 5 DAA, and reached a peak at 7 or 10 DAA, then decreased at 15 ana 20 DAA. HvSUT1 expression in SC1.16 was similar with that in the positive control and remained strong expression until 15 DAA.

For the DC1 lines, three homozygous, single insert lines (DC1.13, DC1.5, and DC1.9) and two homozygous, double-insert lines (DC1.16 and DC1.19) were used for immunoblotting analyses of HvSUT1 and OsNAS2 expression in their immature grains at 5, 7, 10, 15 and 20 DAA. The signals of HvSUT1 and OsNAS2 were detected in immature grains at all stages of grain development (Figure 3.11 and Figure 3.12), but with lower intensity than the positive control (*Glb-1:HvSUT1* transgenic Japonica immature grains obtained from Huynh (2015)). The expression patterns of OsNAS2 and HvSUT1 proteins in DC1 lines were consistent with the OsNAS2 and HvSUT1 in the SC2 and SC1 lines, respectively. DC1.16 showed a steady increase in HvSUT1 expression from 5 DAA until 15 DAA (Figure 3.11) and a high intensity of protein signal, compared to the other lines. For OsNAS2 expression was strongest at 5 DAA, reducing as the grain matured. At 3 DAA OsNAS2 was identified but at a lower level that at 5 DAA (Figure 3.13B).

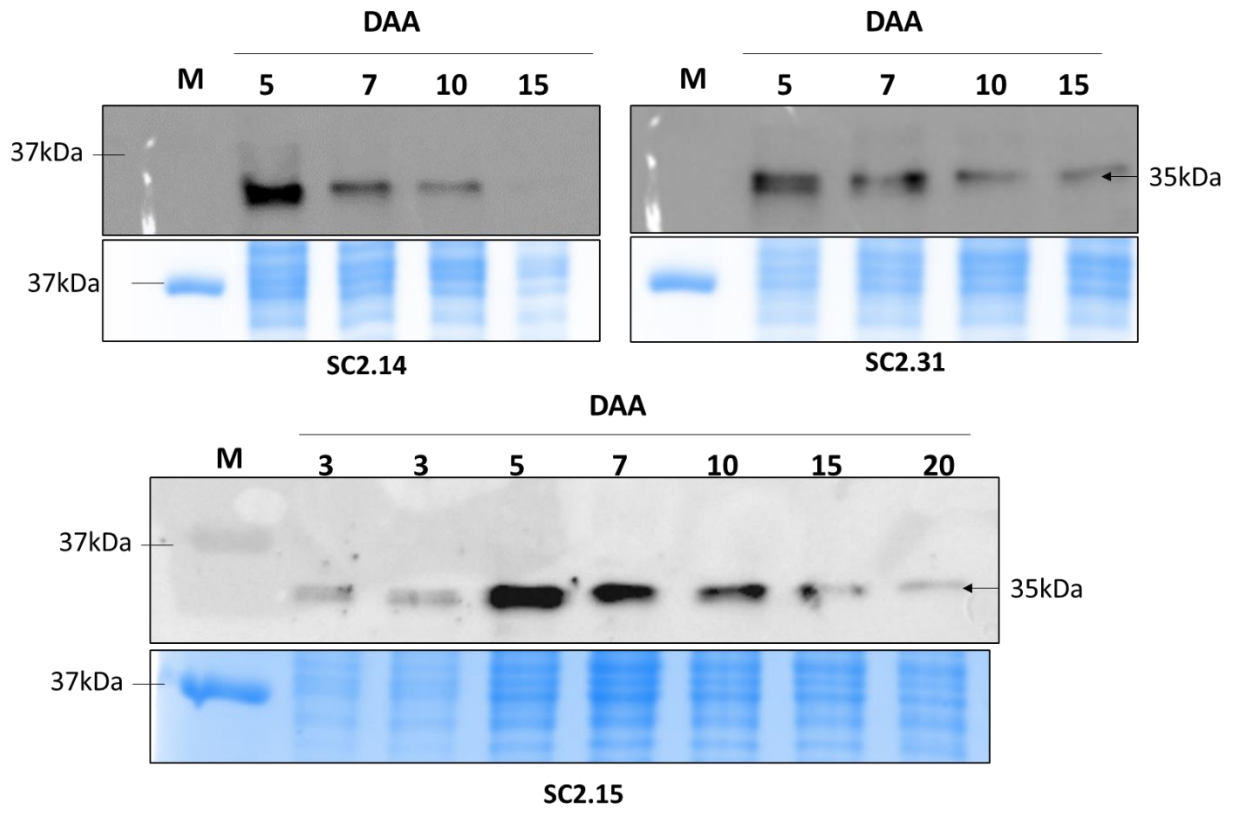

Figure 3.9. Temporal expression of OsNAS2 protein in three independent transgenic lines (SC2) carrying *GluA2:OsNAS2* during grain development. Bands of interest at ~35kDa (OsNAS2) were observed in SC2.14, SC2.15 and SC2.31. Immunoblots of crude total protein preparation of the immature grains at 3, 5, 7, 10, 15, and 20 DAA probed with anti-OsNAS2, followed by Goat anti-rabbit IgG-horseradish peroxidase HP conjugated secondary antibody (1:10000). Immunoblots were visualized using a chemiluminescent substrate and captured with a CCD camera at the optimum exposure time (16 seconds). A replica SDS-PAGE gel at the bottom stained with Coomassie Brilliant Blue G-250 was used as a loading control. M: Marker presents a protein of 37 kDa.

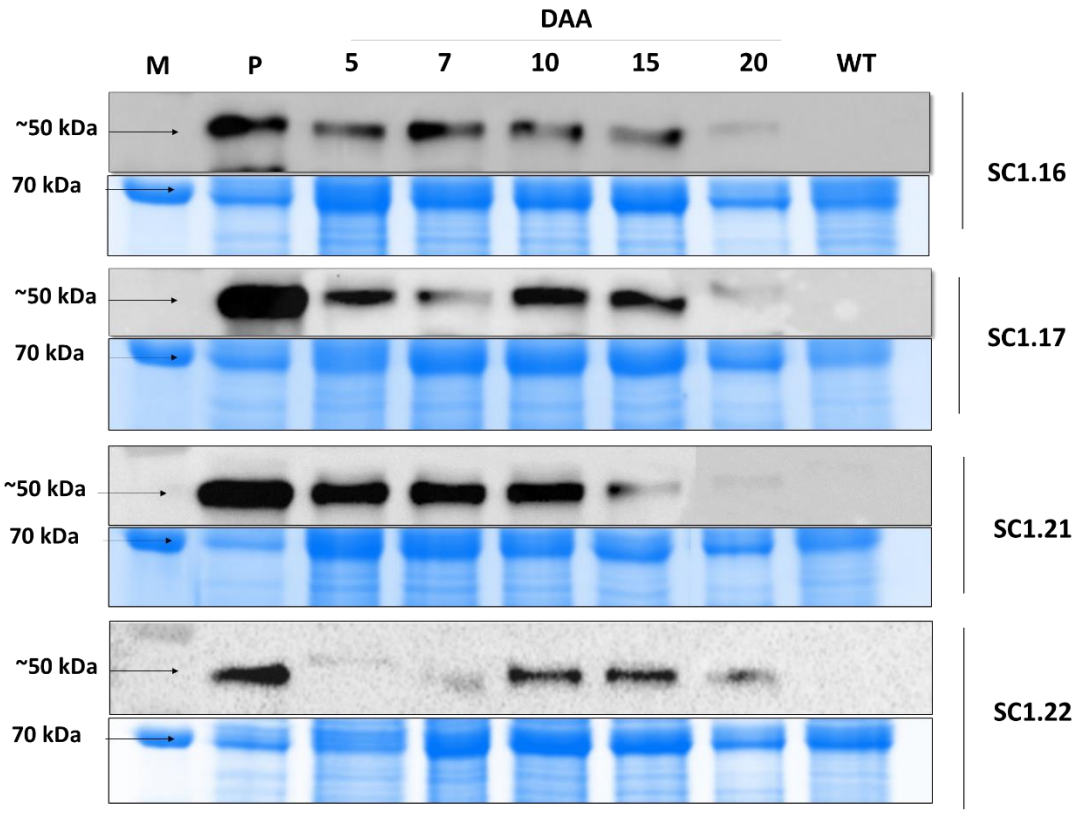

Figure 3.10. Temporal expression of HvSUT1 protein in four independent transgenic lines (SC1) carrying *Glb1:HvSUT1* during grain development. Bands of interest at ~50kDa (HvSUT1) were observed in SC1.16, SC1.17, SC1.21, and SC1.22. Immunoblots of crude total protein preparation of the immature grains at 5, 7, 10, 15, and 20 DAA probed with anti-HvSUT1, followed by Goat anti-rabbit IgG-horseradish peroxidase HP conjugated secondary antibody (1:10000). Immunoblots were visualized using a chemiluminescent substrate and captured with a CCD camera at the optimum exposure time (16 seconds). A replica SDS-PAGE gel at the bottom stained with Coomassie Brilliant Blue G-250 was used as the loading control. P: Crude total membrane protein sample from *HvSUT1*-expressing Japonica rice immature grains (Nipponbare). WT-IR64: Non transgenic IR64 control. M: Marker presents a protein of 70 kDa.

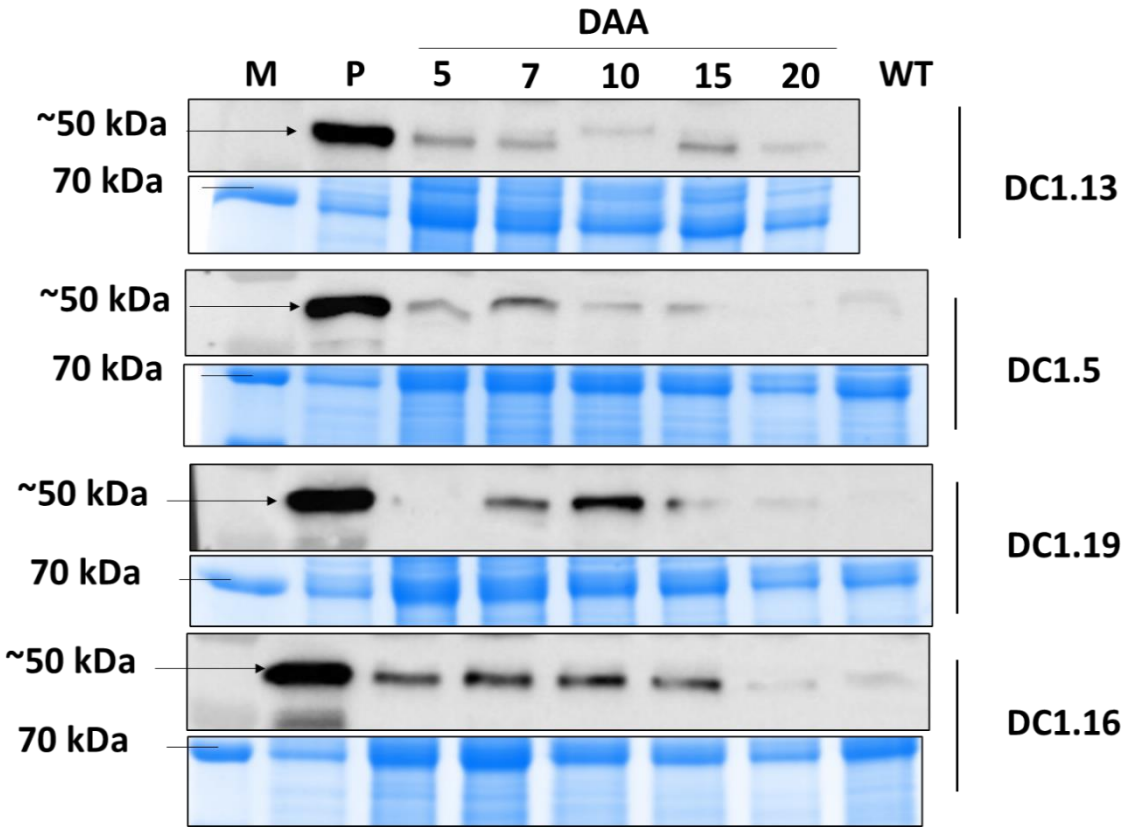

Figure 3.11. Temporal expression of HvSUT1 protein in four independent transgenic lines (DC1) carrying *GluA2:OsNAS2-Glb1:HvSUT1* during grain development. Bands of interest at ~50kDa (HvSUT1) were observed in DC1.13, DC1.5, DC1.16, and DC1.19. Immunoblots of crude total protein preparation of the immature grains at 5, 7, 10, 15, and 20 DAA probed with anti-HvSUT1, followed by Goat anti-rabbit IgG-horseradish peroxidase HP conjugated secondary antibody (1:10000). Immunoblots were visualized using a chemiluminescent substrate and captured with a CCD camera at the optimum exposure time (16 seconds). A replica SDS-PAGE gel at the bottom stained with Coomassie Brilliant Blue G-250 was used as the loading control. P: Crude total membrane protein sample from *HvSUT1*-expressing Japonica rice immature grains (Nipponbare). WT-IR64: Non transgenic IR64 control. M: Marker presents a protein of 70 kDa.

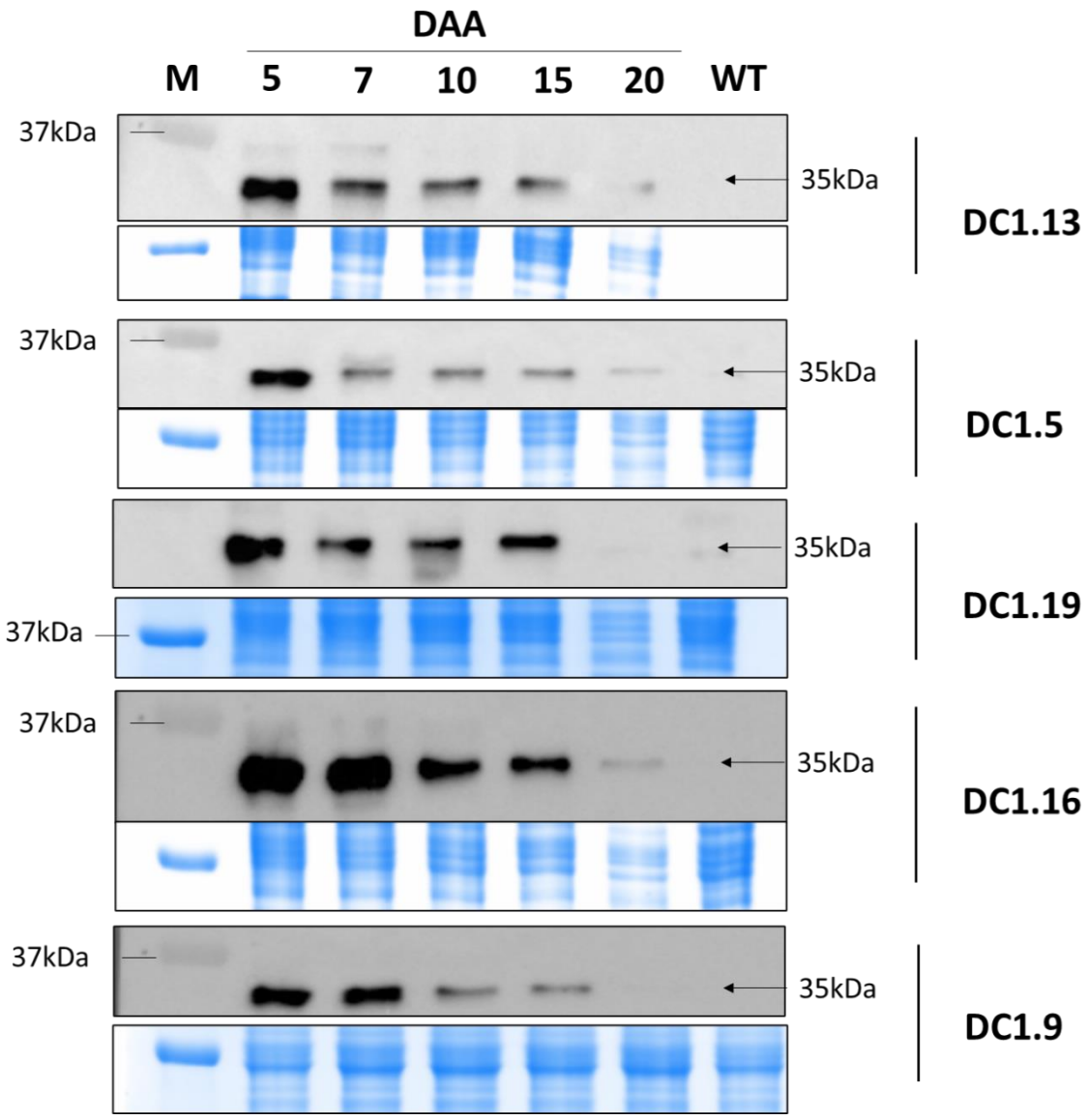

Figure 3.12. Temporal expression of OsNAS2 protein in four independent transgenic lines (DC1) carrying *GluA2:OsNAS2-Glb1:HvSUT1* during grain development. Bands of interest at ~35kDa (OsNAS2) were observed in DC1.13, DC1.5, DC1.19, DC1.16, and DC1.9. Immunoblots of crude total protein preparation of the immature grains at 3, 5, 7, 10, 15, and 20 DAA probed with anti-OsNAS2, followed by Goat anti-rabbit IgG-horseradish peroxidase HP conjugated secondary antibody (1:10000). Immunoblots were visualized using a chemiluminescent substrate and captured with a CCD camera at the optimum exposure time (16 seconds). A replica SDS-

PAGE gel at the bottom stained with Coomassie Brilliant Blue G-250 was used as the loading control. M: Marker presents a protein of 37 kDa.

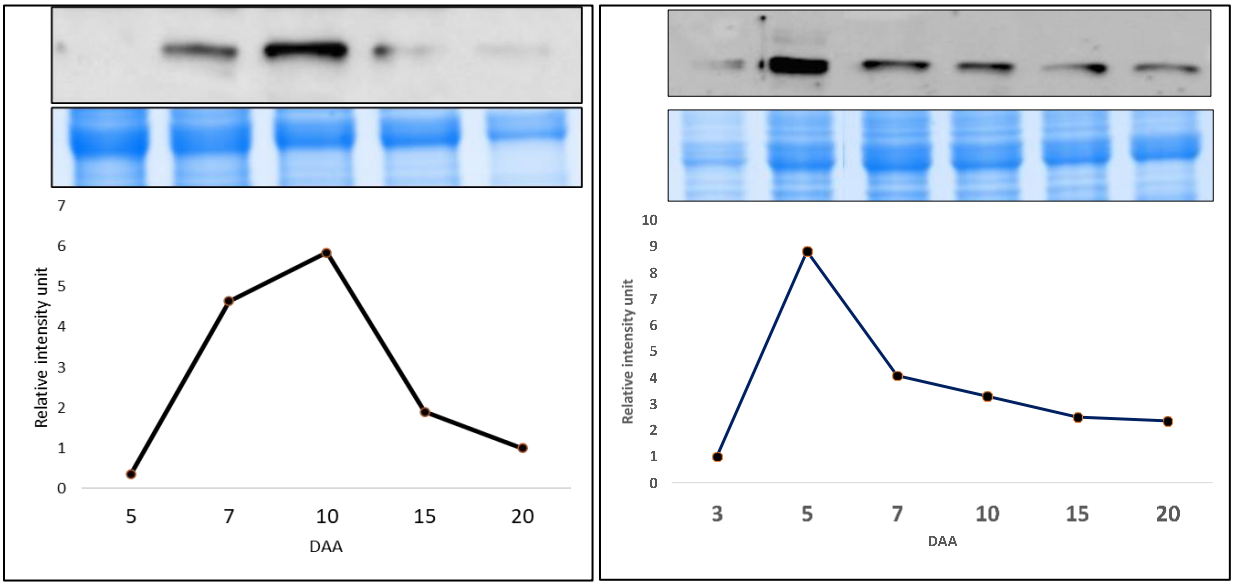

A **B**

Figure 3.13. Temporal expression patterns of HvSUT1 and OsNAS2 protein during the grain development from DC1.5. A. Highest expression of HvSUT1 protein under *Glb-1* at 10 DAA. B. *OsNAS2* detected the highest at 5 DAA

3.3.5. Comparison of HvSUT1 and OsNAS2 protein expression in independent lines

To examine differences in HvSUT1 and OsNAS2 expression between 5 independent-transgenic DC1 lines, two immunoblots were carried out to detect the expression of HvSUT1 and OsNAS2 proteins at their highest expression levels in immature grains. Total protein extracts were from the same tissue samples previously analysed. This represents 10 DAA for HvSUT1 (Figure 3.14) and 5 DAA for OsNAS2 (Figure 3.15). All the five DC1 lines had different expression levels of OsNAS2 protein, with stronger expression in homozygous, two-insert lines, namely DC1.16 and DC1.19 (Figure 3.14C), compared to three homozygous, single-insert lines and three SC2 lines which were homozygous, single insert lines. For the HvSUT1 expression, the signal of HvSUT1

in all the DC1 lines were much lower than that in the positive control but not markedly different between lines (Figure 3.15C).

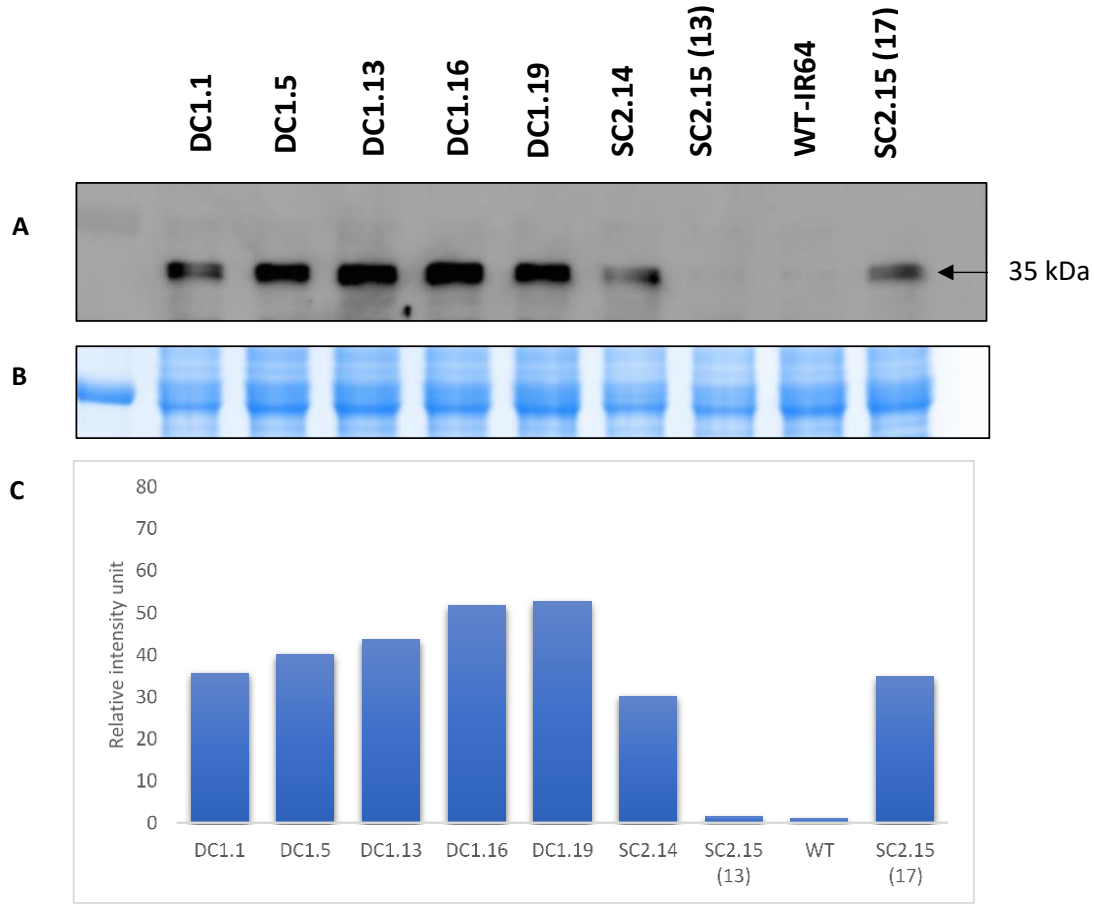

Figure 3.14. A comparison in OsNAS2 protein expression in grains at 5 DAA. A. Immunoblots of crude total protein preparation of the immature grains at 5 DAA probed with anti-OsNAS2 showed the band of interest at ~35kDa (OsNAS2). B. A replica SDS-PAGE gel stained with Coomassie Brilliant Blue G-250 was used as the loading control. C. Comparison in the intensity of OsNAS2 signal relative to the background control (WT-IR64) between multiple transgenic lines presenting a variation in protein expression of OsNAS2 at 5 DAA of grain filling.

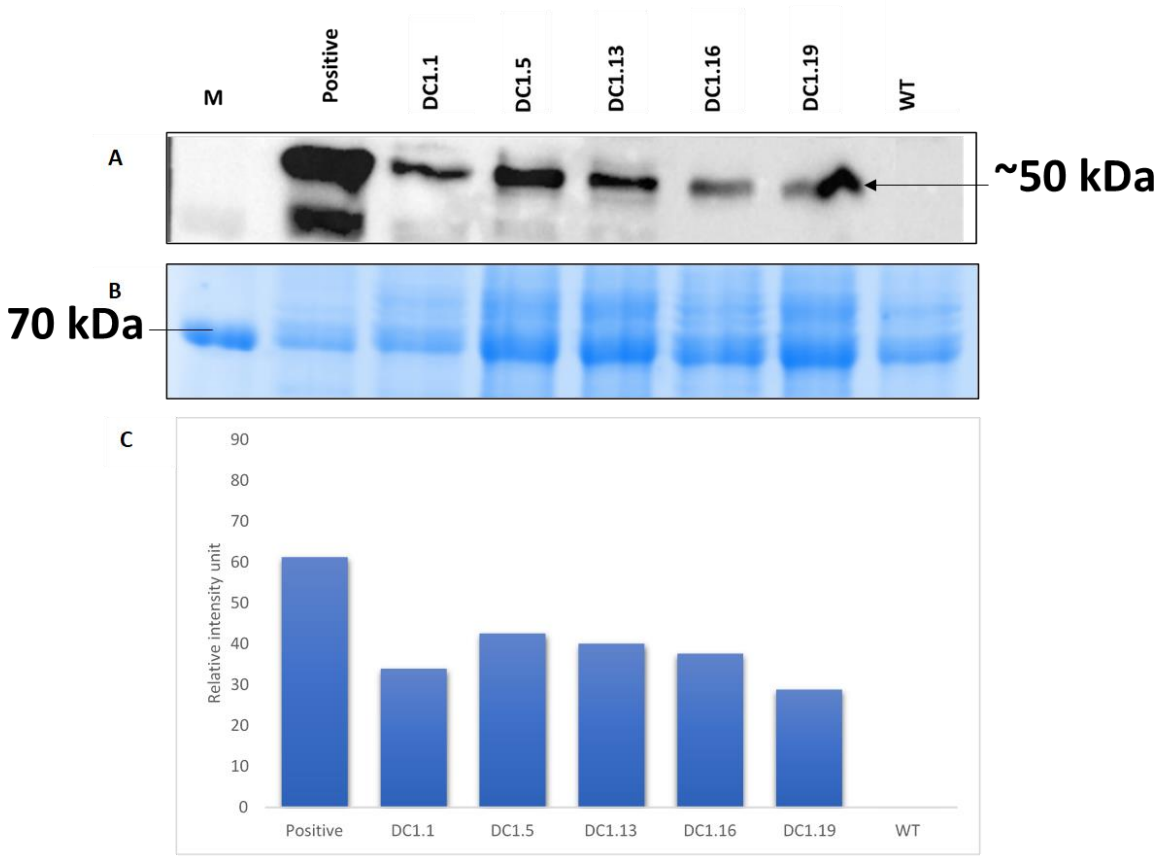

Figure 3.15. A comparison in HvSUT1 protein expression in grains at 10 DAA. A. Immunoblots of crude total protein preparation of the immature grains at 10 DAA probed with anti-HvSUT1 showed the band of interest at ~50kDa (HvSUT1). B. A replica SDS-PAGE gel stained with Coomassie Brilliant Blue G-250 was used as the loading control. C. Comparison in the intensity of HvSUT1 signal relative to background control (non-transgenic IR64) between multiple transgenic lines presenting a variation in protein expression of HvSUT1 at 10 DAA of grain filling.

3.3.6. Growth parameters of the transgenic lines

A surprising and unexpected result came from measuring the height and tiller number in the transgenic rice from 7 independent DC1 lines, 4 independent SC1 lines, and 4 independent SC2 lines, compared to non-transgenic IR64 control plants (WT-IR64). The height (Figure 3.16) and tiller number (Figure 3.17) were recorded from the stage of two-week-old seedlings until the plants were fully matured at 3 months old. At 2 weeks, the height of the transgenic lines was around 30 cm, with no different between the transgenic plants and non-transgenic control. The difference in height of transgenic plants at 1 month was insignificant, but differences began to emerge from this point on. At 2 months, four of the SC2 lines were shorter with an average height of 78 cm, reaching a maximum height of 85 cm at 3 months. In comparison, the height of the SC1 and DC1 lines was 95 cm and 96 cm at 2 months, respectively and reached approximately 110 cm at 3 months. There was insignificant difference in the plant height between SC1 and DC1 lines compared with non-transgenic control (91 cm at 2 months and 101 cm at 3 months), but both were significantly taller than SC2 (Figure 3.16B).

Tiller number of the transgenic plants showed high variation (Figure 3.17). At the seedling stages (2-week-old and 1-month-old age) the number of tillers in SC1, SC2, DC1 and non-transgenic control (WT-IR64) were not significantly different. When the transgenic plants were older than 1 month, the tiller number significantly increased from 2 -3 tillers to 7-8 for SC2 lines, and up to 10 tillers for SC1 and non-transgenic control, and to 14 tillers for DC1. The tiller number of DC1 transgenic lines were highest at 3 months and significantly higher than the other lines, followed by SC1 and non-transgenic control, with the lowest number tillers in the SC2 lines.

Differences in plant height and tiller number at 2 and 3 months is summarised in Figure 3.18. All four transgenic plants of the SC2 lines had a significant reduction in plant height by 12.1-

19.4% at 2 months old and 14.1 -19.0% at 3 months old, compared to the non-transgenic control. This is stark contrast to the SC1 and DC1 lines where an increase was seen in comparison to the non-transgenic control plants, especially DC1.1, DC1.13, DC1.16, DC1.9, and SC1.21. For the tiller number, a significant increase was seen in the DC1 lines, with 40-60% increase (excepting DC1.5 with an insignificant increase), compared to the control. Excepting SC1.13 with over a 50% increase, most of the transgenic SC1 and SC2 had reduction in the tiller number. In general, a significant difference in tiller number was found in the DC1 transgenic line overexpressing the combination of *HvSUT1* and *OsNAS2*. A clear trend from this data indicated that *HvSUT1* expression is correlated with taller plants, but *OsNAS2* expression alone is correlated with shorter plant. Furthermore, the positive growth effects associated *Glb-1:HvSUT1* transgenic plants is epistatic to the negative growth effects associated with *GluA2*:*OsNAS2* transgenesis.

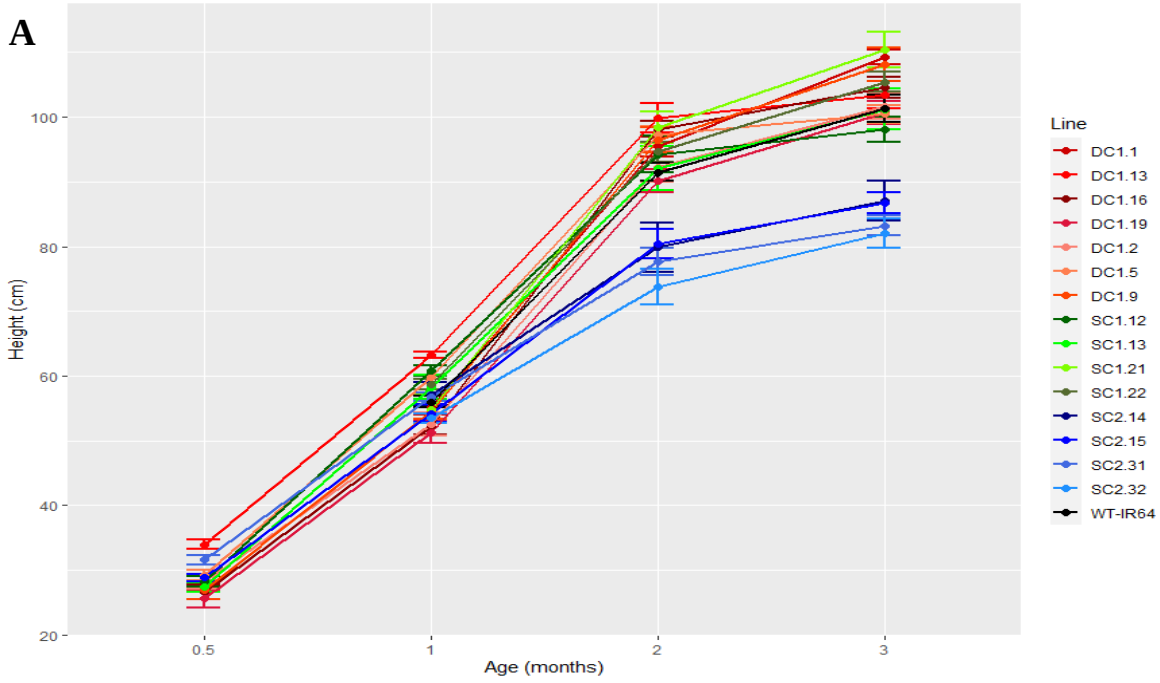

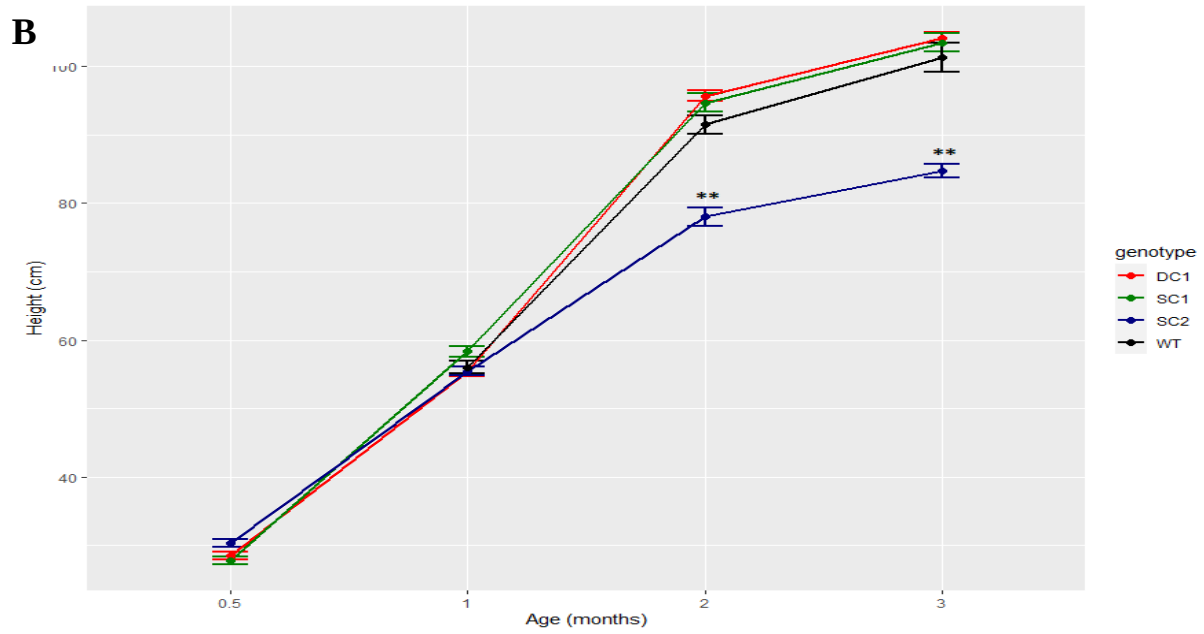

Figure 3.16. Plant height (cm) of transgenic lines in the T2 generation, compared to WT (non-transgenic IR64) between 0.5 month and 3 months. A. Fifteen independent lines of three transgenic populations were seperatly compared to the non-transgenic control. Lines in shades of red, blue and green for DC1, SC1 and SC2, respectively were compared to the non-transgenic control (black line); B. Grouping into three transgenic populations DC1, SC1 and SC2 was compared to the non-transgenic control. Each stage of plant growth represents mean ± SE value. Asterisks denote the significance between the non-transgenic control and independent transgenic events for $p < 0.05$ (*) and $p \leq 0.01$ (**) as analysed by one-way ANOVA. Biological replicates were 7-10 plants per each line.

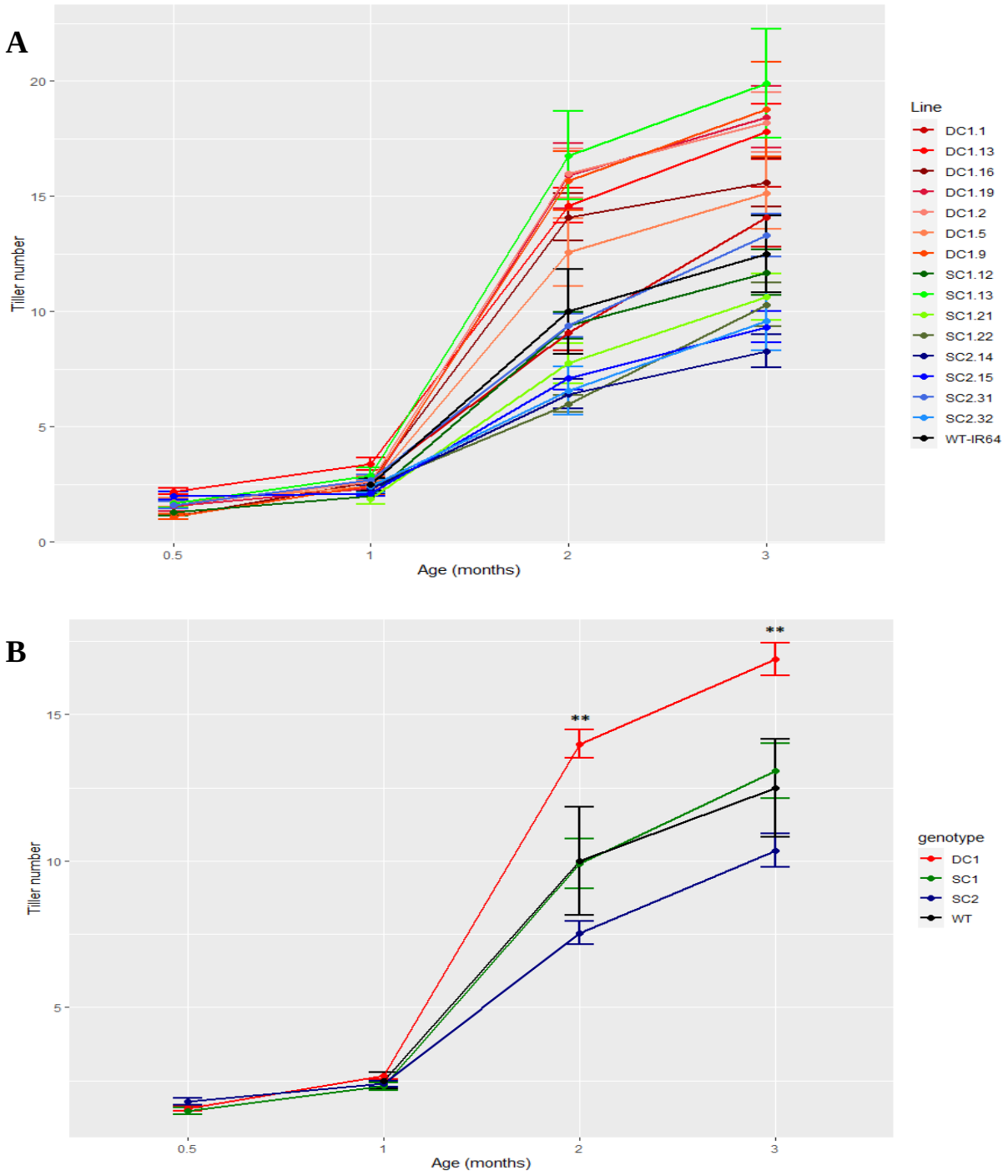

Figure 3.17. Tiller number of transgenic lines in the T2 generation, compared to WT (non-transgenic IR64) between 0.5 month and 3 months. A. Fifteen independent lines of three transgenic populations were seperatly compared to the non-transgenic control. Lines in shades of red, blue and green for DC1, SC1 and SC2, respectively were compared to the non-transgenic

control (black line); B. Grouping into three transgenic populations DC1, SC1 and SC2 was compared to the non-transgenic control. Each stage of plant growth represents mean ± SE value. Asterisks denote the significance between the non-transgenic control and independent transgenic events for $p < 0.05$ (*) and $p \leq 0.01$ (**) as analysed by one-way ANOVA. Biological replicates were 7-10 plants per each line.

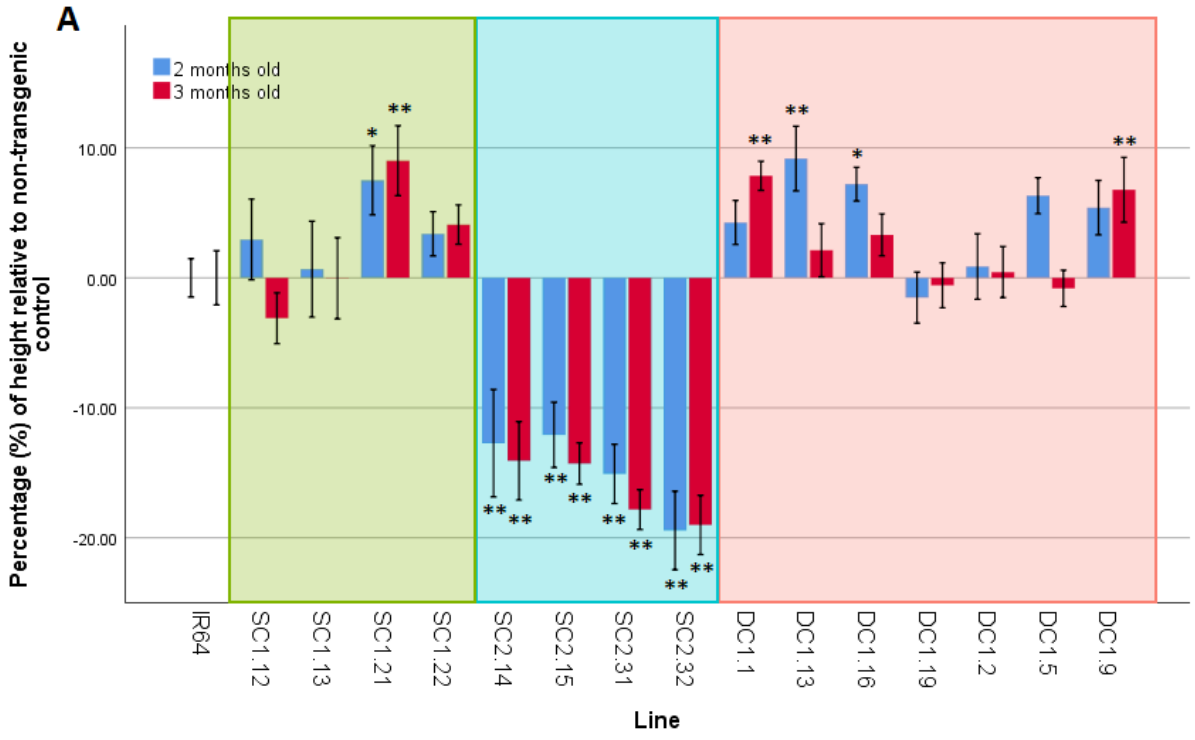

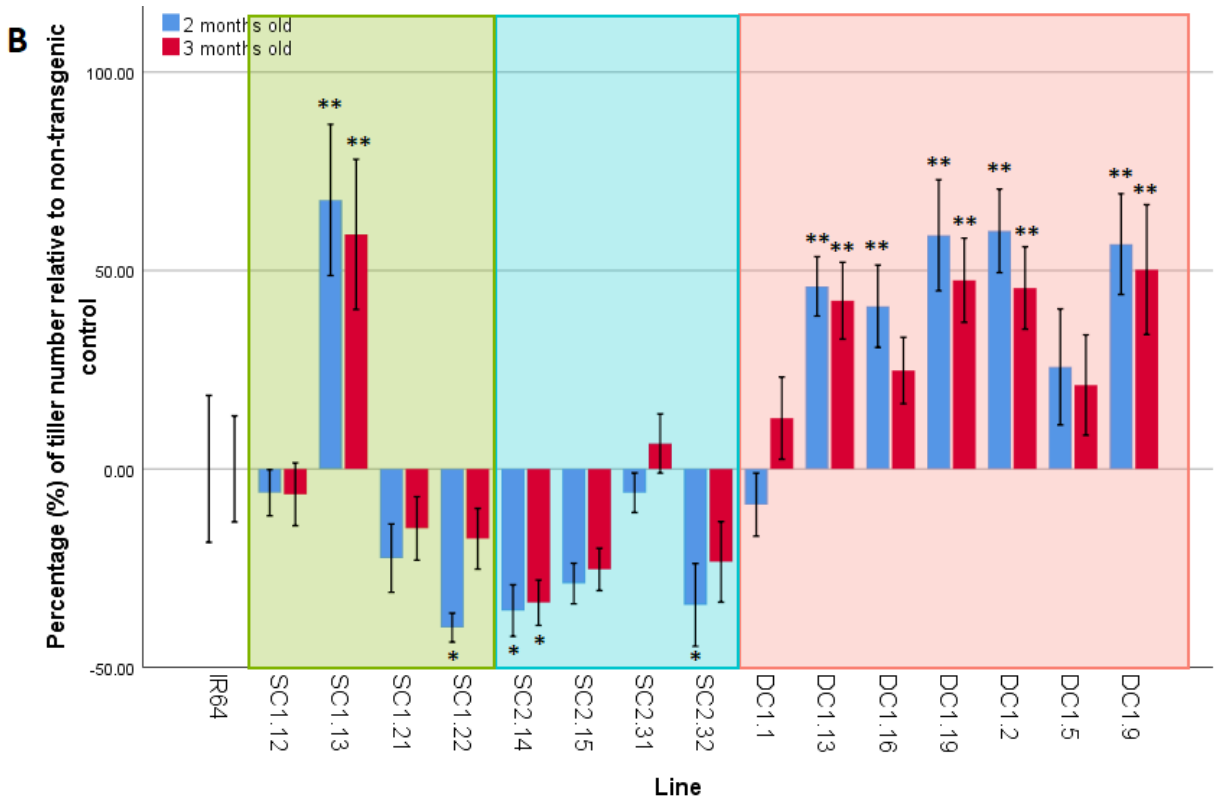

Figure 3.18. Percentage of height and tiller number of transgenic plants in the T2 generation relative to non-transgenic control (IR64). A. Bars represent average percentage of difference in the plant height (± SE) at 2 months old (blue) and 3 months old (red); **B**. Bars represent average percentage of difference in the tiller number (± SE) at 2 months old (blue) and 3 months old (red). The non-transgenic control (IR64) was 0 % difference. Asterisks denote the significance between the non-transgenic control and independent transgenic events for $p < 0.05$ (*) and $p \leq 0.01$ (**) as analysed by one-way ANOVA. Biological replicates were 7-10 plants per each line. Multiple independent transgenic lines overexpressing *HvSUT1* alone (SC1), *OsNAS2* alone (SC2) and the combination of *HvSUT1* and *OsNAS2* (DC1) were represented in green, blue, and red boxes, respectively.

3.3.8. Yield and dry biomass weight

An analysis of dry weight per plant (g) was evaluated over multiple independent SC1, SC2 and DC1 transgenic lines grown under greenhouse conditions (Figure 3.19). The DC1 and SC1 lines showed a significant increase in the dry weight compared with the SC2 lines and non-transgenic control, with more than 70 g per plant, compared to 56.14 g for the SC2 lines and 52.36 g for the control. In the SC2 lines, SC2.32 showed a reduction of 50% in the dry weight, compared to the non-transgenic control. A further analysis of grain weight per plant was also examined to see whether there was an increase in grain weight in multiple transgenic lines, compared to the control (Figure 3.20). Unfortunately, during grain filling the plants were infected with a fungal pathogen, most likely *Neovossia horrida,* the causal agent of rice kernel smut. No significant difference in the grain weight per plant was seen between transgenic and non-transgenic lines, however this experiment needs to be repeated given the confounding effects of the fungal infection. Higher biomass weight was however seen in the DC1 and SC1 lines, but whether this translates into higher yield is not clear.

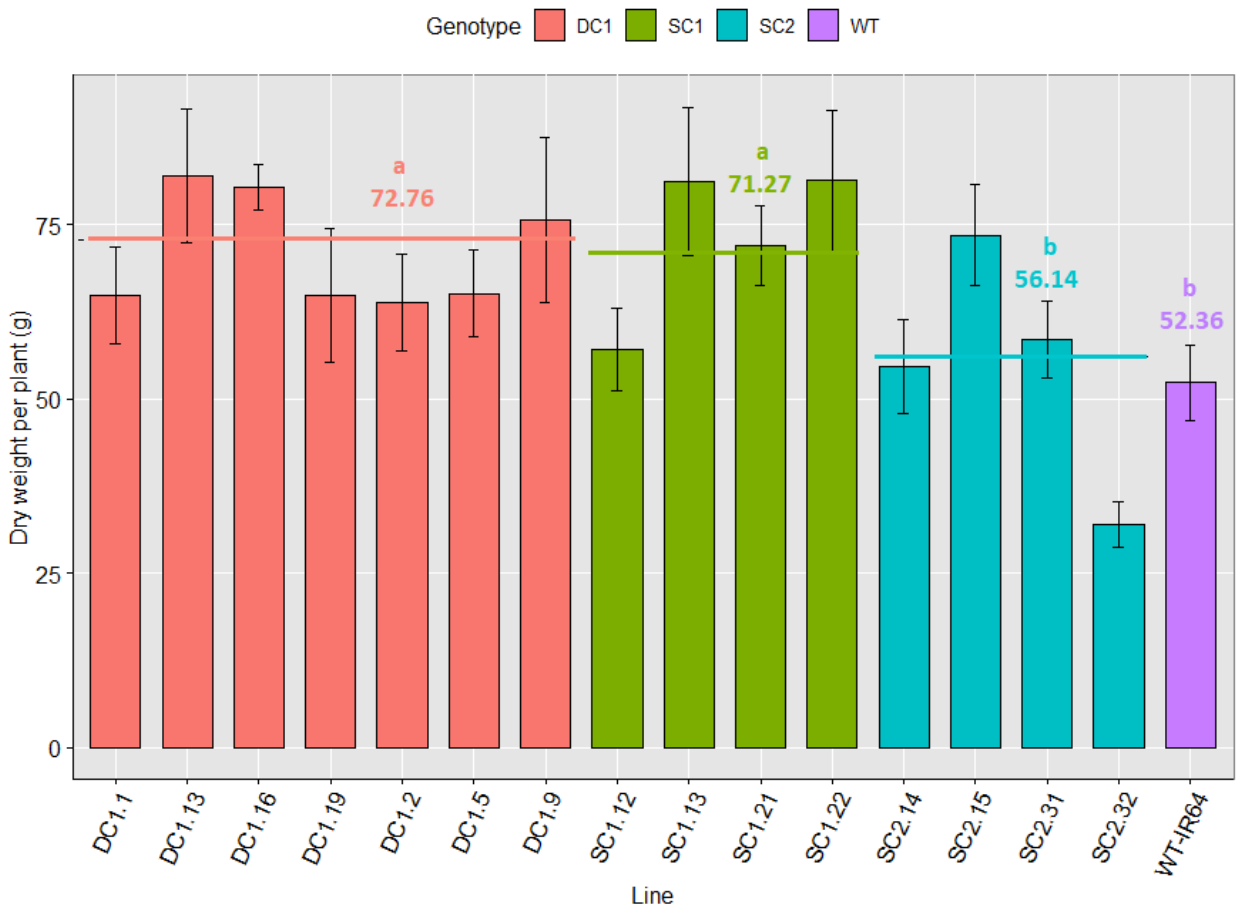

Figure 3.19. Dry weight (gram) per plants of transgenic lines in T2 generation, compared to WT (non-transgenic IR64) grown under greenhouse condition. Bars represent mean values of dry weight per plant (± SE) of 7-10 biological replicates of the DC1 (orange), SC1 (green) and SC2 (blue) lines, compared to the non-transgenic control (purple). Asterisks denote the significance between the transgenic lines and the control for $P < 0.05$ (*), $P \leq 0.01$ (**), $P \leq 0.001$ (***) as determined by student's t-test. Orange, green and blue lines represent means of 7 independent DC1 lines, 4 the independent SC1 lines and 4 the independent SC2 lines, compared to the non-transgenic control. The differences with the same letter are not significant.


SC2.14
SC2.32
WT
DC1.1
SC1.21
SC1.22


WT
DC1.5
DC1.16

Figure 3.20. Difference in rice plant growth between transgenic and non-transgenic rice for 3 months after sowing as grown under greenhouse condition. Representative plants of the transgenic rice overexpressing *HvSUT1* with or without *OsNAS2* (DC1.1, DC1.5, DC1.16, SC1.21 and SC1.22 lines) had vigorous growth, compared to the transgenic rice overexpressing *OsNAS2* alone (SC2.14 and SC2.32 lines) with growth inhibition and non-transgenic IR64 (WT) 3 months after germination.

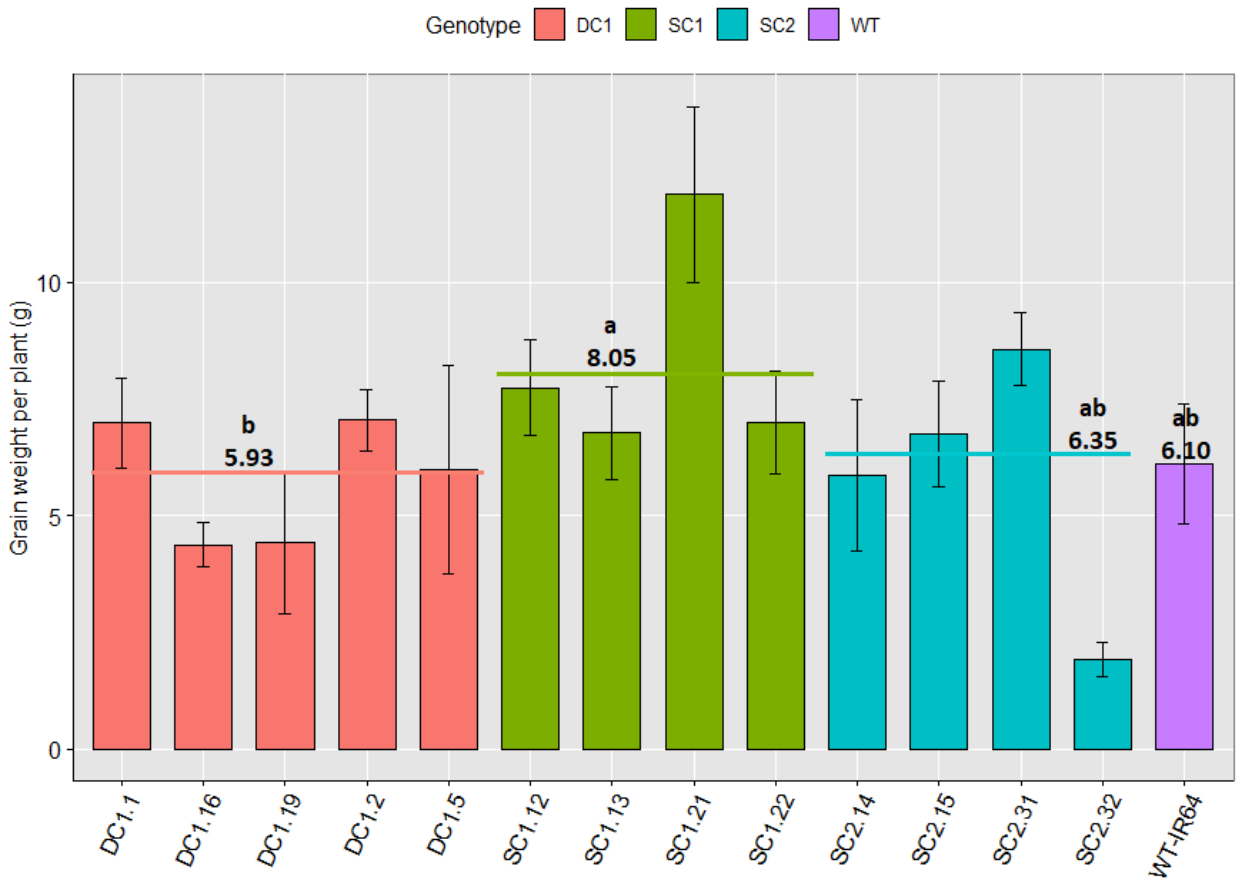

Figure 3.21. Grain weight per plant (gram) of independently transgenic lines in the T2 generation, compared to WT (non-transgenic IR64) grown under greenhouse condition. Bars represent mean values of grain weight per plant (± SE) of 7-10 biological replicates of the DC1 (orange), SC1 (green) and SC2 (blue) lines, compared to the non-transgenic control (purple). Asterisks denote the significance between the transgenic lines and the control for $P < 0.05$ (*), P

≤ 0.01 (**), P ≤ 0.001 (***) as determined by student's t-test. Orange, green and blue lines represent means of 5 independent DC1 lines, 4 the independent SC1 lines and 4 the independent SC2 lines, compared to the non-transgenic control. The differences with the same letter are not significant.

3.4. Discussion

The stable and successful expression of the *HvSUT1* and *OsNAS2* transgenes in the early stages of grain filling was demonstrated in this research. Along with copy number and the zygosity of transgenes as shown in Chapter 2, homology-dependent gene silencing in transgenic plants with multiple traits (gene stacking) needs to be carefully considered to ensure the success of any transgene expression. In this study, the rice endosperm was the focus for Fe and Zn biofortification, thus the objective in this chapter was to confirm *HvSUT1* and *OsNAS2* overexpression in the rice endosperm. Here, the successful expression of *HvSUT1* and *OsNAS2* during grain development, regulated by the *GluA2* and *Glb-1* promoters, respectively, was shown. The endosperm-specific expression of the transgenes was expected to affect only the grain-filling stage; however, a vigorous growth phenotype of *HvSUT1*-overexpressing transgenic rice line was an interesting and unexpected observation in this study. Also, a clear increase in tiller number was observed in *HvSUT1/OsNAS2* overexpression, but it is still unclear if this translates into higher yield.

3.4.1 Specific-endosperm *GluA2* and *Glb-1* promoters were confirmed by GUS analysis

The promoters of rice storage protein genes have been demonstrated to show endosperm-specific expression in the rice grain, for instance globulin, glutelin, prolamin, and allergenic protein gene *RAG-1* (Furtado *et al.* 2008; Kawakatsu *et al.* 2008; Qu & Takaiwa 2004; Qu *et al.* 2008; Wu *et al.* 1998). Multiple promoters for seed-specific expression were characterized to provide alternative options for gene-stacking in rice (Qu & Takaiwa 2004; Qu *et al.* 2008; Wu *et*

al. 1998). Diverse sequences of the promoter used in gene stacking is desirable to avoid homology-dependent gene silencing in transgenic plants (Kooter *et al.* 1999; Matzke *et al.* 1994; Matzke & Matzke 1995; Vaucheret *et al.* 1998; Vaucheret *et al.* 2001). The *GluA2* and *Glb-1* promoters have been cloned and well-characterized in transgenic Japonica rice (Qu & Takaiwa 2004; Qu *et al.* 2008), but very few studies have focused on Indica rice. Based on the analysis of GUS activity on the transgenic Japonica rice transformed with *GluA2:uidA* and *Glb-1:uidA*, the *GluA2* and *Glb-1* promoters were indicated to regulate the endosperm-specific expression of the transgenes. Here, along with the *Glb-1* promoter cloned to regulate the *HvSUT1* gene from the previous study (Huynh 2015), the *GluA2* promoter from Nipponbare rice was cloned to regulate the expression of *OsNAS2* in the IR64 rice endosperm, and the specificity of these promoters to regulate levels of transgene expression in the IR64 endosperm was confirmed. As shown in Chapter 2, the cloned *Glb-1* and *GluA2* promoters in this work had all the essential elements for endosperm-specific expression as demonstrated by the endosperm-specific expression of GUS in transgenic rice. These findings are consistent with most of previously reported findings (Hwang *et al.* 2002; Qu & Takaiwa 2004; Qu *et al.* 2008; Wu *et al.* 1998; Wu *et al.* 2000).

The *GluA2* and *Glb-1* promoters for gene-stacking expression did not share sequence homology to each other, and the *cis*-elements of the two promoters required for endosperm-specific expression are different (see Section 2.3.1.3 in Chapter 2). The *cis*-elements in the cloned *GluA2* promoter were identical to the 1 kb region of the *refGluA2* promoter upstream from the transcription start site (Qu *et al.* 2008), which contained all crucial *cis*-elements for endosperm-specific expression, namely the GCN4, AACA, ACGT, and prolamin box as reported in the *GluB1* promoter (Wu *et al.* 2000). In the case of the *Glb-1* promoter, the cloned sequence was the same as that published by Nakase *et al.* (1996), Hwang *et al.* (2002), and Qu and Takaiwa (2004). A

difference in *cis*-elements involved in regulation of endosperm-specific expression in the rice grain was seen in the *Glb-1* promoter, compared to the *GluA2* promoters (Furtado *et al.* 2008). The promoters of glutelin contained the GCN4 motif, whereas the promoter of globulin gene contained a A+T rich sequence absent in the *GluA2* promoter (Hwang *et al.* 2002; Nakase *et al.* 1996). The arrangement or diversity of *cis*-elements was assumed to lead the differences in the timing of expression of globulin and glutelin genes during grain filling (Kawakatsu & Takaiwa 2010; Kawakatsu *et al.* 2008). In general, this sequence analysis supports the cloning of intact sequences of the *GluA2* and *Glb-1* promoters with all essential *cis*-elements for endosperm-specific expression and nearly 100% similarity with their reference promoters. However, analyses of reporter gene (*uidA*) and transgene expression were still performed to confirm the specificity of the *GluA2* promoters in an Indica background. Huynh (2015) had already shown endosperm specific expression of the *Glb-1* promoter in a Japonica background.

The spatial and temporal patterns of *uidA* expression by these promoters shown here and by Huynh (2015) was determined in the rice endosperm only, with no expression in the embryo as determined by the analysis of GUS activity, which is consistent with previous reports (Furtado *et al.* 2008; Qu & Takaiwa 2004; Qu *et al.* 2008). Under the control of the *GluA2* promoter, GUS activity was seen in the whole endosperm with a strong signal in the aleurone and subaleurone cells and weaker signal in the inner starchy endosperm, which is consistent with the distribution pattern of glutelin A protein (Takahashi *et al.* 2019). In addition, the expression of glutelin A protein was found to be stronger on the ventral side than the dorsal side of the rice grain (Takahashi *et al.* 2019). This was also be seen in this study as GUS staining was localised to the ventral side, compared the dorsal side of the transgenic grain. In the embryo and maternal cells, such as nucellus layer, no *uidA* expression was detected. To my knowledge, this study shows the first cell-by-cell

observation of *GluA2* promoter activity in the developing rice grain and demonstrates that the promoter is active in the aleurone/subaleurone and outer part of the starchy endosperm, but not in maternal tissue like the nucellus cell layer.

There was no detectable GUS activity in vegetative tissues such as the root and leaf tissue under stereoscopic examination. For the *Glb-1* promoter Huynh (2015) showed GUS activity was confined to the rice endosperm and staining in other tissues was not reported. Therefore, the same expression pattern was presumed to occur in an Indica rice background as Oliva *et al.* (2014) did not report any GUS expression in IR64 rice under the control of Nipponbare globulin and glutelin B promoters in tissue other than the endosperm.

Opposite to the effect with the *GluA2* promoter, the GUS activity driven by the *Glb-1* promoter was strongest in the central part of endosperm and lower in the outer part of the rice endosperm in Nipponbare rice grains generated by the study of Huynh (2015) that were over 5 years old. Interestingly, the product of *uidA* gene, β-glucuronidase (GUS), is extremely stable in the rice grain, as the strong GUS staining was detected in the mature grain stored at room temperature for over 5 years. Due the strong stability of GUS, it is difficult to observe temporal change of *uidA* gene expression during grain development directed by the early promoter activity. The *GluA2* promoter is a clear example of this. In this study, very strong GUS activity under the regulation of the *GluA2* was able to be detected in immature grains as early as 5 DAA, and no change was observed at later stages of grain development. Similarly, no difference in GUS activity at three different stages of immature grains (7, 12 and 17 DAA) was seen in the investigation of the *GluA2* promoter by Qu *et al.* (2008). A temporal pattern of GUS expression under the control of the *Glb-1* promoter was strongest in the grain from 10-15 DAA (Furtado *et al.* 2008; Oliva *et al.* 2014; Qu & Takaiwa 2004). The results indicated the cloned *GluA2* and *Glb-1* promoters were

endosperm-specific, but this type of GUS reporter gene analysis of a promoter is qualitative and therefore, although, no GUS activity in other organs of vegetative tissues was detected at stage of grain filling, a more thorough quantitative analysis would be needed at the stages of plant growth to confirm no ectopic promoter activity is occurring. The phenomenon of leaky expression was observed in rice when using foreign promoters from other species such as wheat or barley (Furtado *et al.* 2008), but no findings regarding this phenomenon of ectopic expression of rice promoters used between Japonica and Indica varieties has been reported in the literature.

Although the effects of the *Glb-1* and *GluA2* promoters reported some weak or background GUS activity in vegetative tissues of transgenic plants, no mRNA was detected by the authors (Qu & Takaiwa 2004; Qu *et al.* 2008). Unfortunately, the specific stages of plant growth were not reported in their works, but probably at the grain filling stage. This may be due to the leaky expression in very low level at a particular time-point and possibly in very specific cell types in vegetative tissue. Hence, a detailed, quantitative, and sensitive cell specific analysis of the Nipponbare *Glb-1* and *GluA2* promoters in IR64 background should be done, perhaps using a more sensitive reporter gene such as the green fluorescent protein (GFP) is warranted, but unfortunately this was beyond the scope of this study. It is plausible that the activity of the *GluA2* and *Glb-1* promoters to produce storage proteins can be temporally expressed in other vegetative organs (leaves or stems) (Scofield *et al.* 2009) before their role in the grain-filling stage. However, all studies regarding glutelin and globulin proteins have focused on the grains (Chen *et al.* 2018; Takahashi *et al.* 2019).

A proteomic survey of metabolic pathways in rice had detected five glutelin proteins in rice leaves and seeds, whereas globulins were detected in only the rice seed (Koller *et al.* 2002). However, the expression level of these proteins in the leaves was not mentioned. In addition, the

GluA2 and *Glb-1* promoters were cloned from the Japonica genomic DNA, so several SNP variations were present in the *GluA2* and *Glb-1* promoters between Indica and Japonica rice, as observed in this study (Figure 2.4 in Chapter 2). Furthermore, although it was evident that SNP variation presents in the *GluA2* promoter in Indica and Japonica which is correlated with grain protein content diversity (Yang *et al.* 2019), any effects of the ectopic expression regarding natural SNP variation in the promoter region has not been reported. Using the endosperm-specific promoter originating from a different rice cultivar in rice transformation has been carried out in several studies. For instance, the globulin and glutenin B1 cloned from rice cultivar Kitaake (Japonica) were introduced into an Australia rice cultivar Jarrah (Furtado *et al.* 2008; Qu & Takaiwa 2004) or the glutelin B and globulin-1 cloned from Nipponbare genomic DNA was transformed into IR64 rice genome (Oliva *et al.* 2014). Although the ectopic expression was not mentioned, its possibility should not be ignored. A complementary analysis should be performed, especially information for Indica the *Glb-1* promoter available for alignment analysis. There is only one sequence of Indica globulin promoter (NCBI accession no. KX018119) from long-grain rice available to date, and unfortunately no original publication is available to compare with IR64. In general, the ectopic expression in other organs is not always poor, it may depend on location or stage.

3.4.2. Successful overexpression of *HvSUT1* and *OsNAS2* during rice grain development

In this study, the expression of HvSUT1 and OsNAS2 proteins in immature grains of the transgenic lines was investigated. Two polyclonal antibodies of OsNAS2 (anti-OsNAS2 developed in this study) and HvSUT1 (anti-HvSUT1 developed by Huynh (2015) were used in immunoblot assays to detect the expression of OsNAS2 and HvSUT1 proteins, respectively. Although multiple polypeptides were detected in all immunoblots using the anti-HvSUT1 and the

anti-OsNAS2 antibodies, there were always consistent bands of the correct size for HvSUT1 and OsNAS2 in all rice grain protein samples from the appropriate transgenic plants that were absent in non-transgenic controls. These antibodies were designed to recognize and bind to their target epitope of 6-7 amino acids in the antigens of 17 or 14 amino acids, respectively. The other immunoreactive protein bands were found in both transgenic and non-transgenic tissues. These most likely represent other proteins that share the same or similar target epitope. There was a strong band of ~50 kDa on the immunoblot against the anti-HvSUT1 and a band of ~ 35 kDa on the immunoblot against the anti-OsNAS2, which were only present in rice grain protein samples of the transgenic plants, but no signal for any of the non-transgenic control samples. Furthermore, the signal of the HvSUT1 and OsNAS2 proteins at different stages of rice grain development changed consistent with the expected activity of the respective promoters. These results indicate that these antibodies were specific to detect and to compare the target proteins in the immature rice grains.

The HvSUT1 protein was an exogenous protein, and its alignment of primary sequence with the OsSUT1 peptide showed little similarity at the region from which the antigenic peptide was synthesised (Huynh 2015). OsSUT1 shares a key role in transport of sucrose during grain development. The predicted molecular mass of OsSUT1 and HvSUT1 proteins calculated from the amino acid sequence is 55 kDa, slightly different with the HvSUT1 immunoreactive band of ~50kDa. This result is consistent with that found by (Lemoine 2000; Lemoine *et al.* 1996), because the mobility of plasma-membrane proteins could be increased in the SDS-PAGE gel. Based on the positive control of *HvSUT1*-expressed grain protein sample from Huynh (2015) and the non-transgenic control, we confirmed the anti-HvSUT1 targeted the HvSUT1 protein at the putative band of ~50kDa.

For the transgenic OsNAS2 protein, the primary amino acid sequence converted from the cDNA had nearly 100% identity with the endogenous OsNAS2, while it has low similarity with the endogenous OsNAS1 and OsNAS3 but is different in the region of the C termini. The anti-OsNAS2 was designed to bind this region for specific detection of OsNAS2, which is different from OsNAS1 and OsNAS3. The anti-OsNAS2 recognized the putative band of OsNAS2 with a molecular mass of 34 kDa on the immunoblots, which is very close to the calculated molecular mass of 35 kDa. Here, OsNAS2 was expressed in the rice endosperm, where the endogenous OsNAS2 is not present (Sato *et al.* 2010; Sato *et al.* 2012). Thus, no signal of the OsNAS2 protein was detected in the non-transgenic control. The result was consistent with the report of Nozoye *et al.* (2014a). However, two antibodies of OsNAS2 in the study of Nozoye *et al.* (2014a) targeted in the regions identical with OsNAS1, so it was challenging to distinguish OsNAS2 from OsNAS1 protein. In this study, the anti-OsNAS2 targeted the specific region of only OsNAS2, so no band of ~34 kDa was present in the non-transgenic control.

These antibodies were used to investigate the expression of HvSUT1 and OsNAS2 proteins in the immature grains from the homozygous plants in the T1 generation. The results of this study demonstrated the successful expression of the OsNAS2 and HvSUT1 under the control of the *GluA2* and *Glb-1*, respectively, during grain development. The expression pattern of the OsNAS2 and HvSUT1 proteins in the immature grains was slightly different from each other due to the regulation of the two different endosperm-specific promoters. Under the control of the *GluA2* promoter, the OsNAS2 protein was expected to express at an early stage of rice grain development. Here we found that the *GluA2* promoter was active at 3 DAA, which was also found from GUS staining in the *GluA2:uidA* transgenic grain. Qu *et al.* (2008) reported *GluA2* promoter activity as early as 7 DAA, so data presented here, extends the knowledge of this promoter's temporal activity

during grain development. Furthermore, these data show here the expression of the *GluA2* promoter dramatically increases and reaches the highest level at 5 DAA, then gradually decreases until 20 DAA. Interestingly, monitoring the temporal expression pattern of the *GluA2* promoter was not possible using the GUS assay, because the β-glucuronidase (GUS) product is extremely stable, with early expression masking the decline in expression at later times of development. This would explain the consistent level of GUS activity reported by Qu *et al.* (2008) in the endosperm tissue at all stages of grain development.

Under Fe-sufficient conditions, *OsNAS1* and *OsNAS2* are expressed in the roots, but not in leaves. This was confirmed by immunoblot assays with the anti-OsNAS2 where no OsNAS2 protein was detected in the Fe-sufficient leaves and immature grains, but signal of OsNAS2 was detected in the roots. No previous study has investigated the expression of the three *OsNAS* genes in the rice endosperm during grain development, excepting the rice expression profile database (RiceXPro) published by Sato *et al.* (2011) and Sato *et al.* (2012). The database showed that there was no transcript of OsNAS2 and OsNAS3, but a weak signal of *OsNAS1* expression in the rice endosperm. Although the role of OsNAS1 in the rice endosperm during grain filling has not been characterized, it might be involved in metal chelation via NA/DMA biosynthesis (Nozoye *et al.* 2007). Furthermore, very little information or analysis of rice nicotianamine synthases protein has been investigated, only in root cells reported by Nozoye *et al.* (2014a). Rice OsNAS2 protein was predicted to be monomeric protein of 34-35 kDa with two transmembrane helices, which was consistent with the results and prediction of this work (see Figure 1.9 in Chapter 1). Furthermore, according to Nozoye *et al.* (2014a) and Nozoye *et al.* (2014b), OsNAS2 protein was proposed to localize to vesicles in the cytoplasm of the root cell, which originate from the rough endoplasmic reticulum (rER). The rER derived vesicles are supposed to not fuse directly with cell plasma

membrane, thus NA/DMA may be synthesized in the vesicles and then transported into the cytoplasm of root cells. It is not known whether trafficking pathway is similar in the rice endosperm cells where OsNAS2 was expressed in this work.

Compared to the *GluA2* promoter, a slightly different expression pattern of the HvSUT1 protein under the control of the *Glb-1* promoter was observed in the immature grains during grain-filling. The HvSUT1 expression was also detected at early stages of grain development, increased gradually and then reached the highest level at 10 DAA, and was still detectable in the immature grains at later stages up to 20 DAA. A similar pattern of expression was also observed in Nipponbare rice grains (G1.4, a well-characterized line used as the positive control in this work) overexpressing *HvSUT1* under the regulation of *Glb-1* promoter (Huynh 2015). The immunoreactive band of HvSUT1 was most abundant at 10 DAA, like in the pattern of expression of endogenous OsSUT1 in other Japonica rice (Taipei 309) (Furbank *et al.* 2001), but a little later than the result in Nipponbare rice reported by Aoki *et al.* (2003). The exogenous HvSUT1 and the endogenous OsSUT1 share the same role in sucrose transport in the endosperm during grain filling (Aoki *et al.* 2003; Furbank *et al.* 2001; Weschke *et al.* 2000). In this study, although the expression of endogenous OsSUT1 in the IR64 transgenic grains was not investigated, the expression of exogenous HvSUT1 is likely to extend sucrose transport into grains during the storage stage in rice (Huynh 2015) or increase sucrose uptake by expressing *HvSUT1* in wheat (Weichert *et al.* 2010).

The results indicated that the HvSUT1 and OsNAS2 proteins were expressed in all the immature grains from 5 DAA to 20 DAA, when the rice endosperm turns to the nutrient storage phase (Wu *et al.* 2016b). Particularly, the peaks of the OsNAS2 and HvSUT1 expression were at 5 DAA and 10 DAA, respectively. In the time from 6-10 DAA, the inner endosperm cells are still

alive to transport the nutrients from the outer layer cells (the aleurone, the subaleurone and the outer endosperm) (Wu *et al.* 2016b). This suggests that both proteins were expressed at the critical stage of nutrients storage in developing grains. The expression pattern of HvSUT1 and OsNAS2 proteins in the transgenic plants DC1 were identical to that of HvSUT1 in SC1 lines and OsNAS2 in SC2 lines.

Furthermore, to compare the levels of transgene expression between multiple independent transgenic lines, the HvSUT1 and OsNAS2 protein at the stage of highest expression was investigated. The transgenic IR64 rice overexpressing HvSUT1, including both the SC1 lines and DC1 lines, showed a consistently lower HvSUT1 levels in 10 DAA immature grains than the transgenic Japonica rice expressing HvSUT1 (the positive control) (Huynh 2015). This could be explained by the *Glb-1* promoter from Nipponbare rice not being fully recognized and regulated in an Indica rice background. Based on the immunoblotting analysis, four lines (SC1.16, SC1.21, DC1.16, and DC1.5) had the highest level of HvSUT1 expression and the HvSUT1 level remained relatively constant throughout the period of grain filling. No transgenic Indica rice with stronger HvSUT1 protein level had been detected from a small number of transgenic lines (8/45). The result suggests that the natural variation of the *Glb-1* promoter between Indica and Japonica might lead to the difference in HvSUT1 expression. It is noticeable that the OsNAS2 level in DC1.16 and DC1.5 was stronger at 5 DAA and remained relatively constant throughout the period of grain filling, compared to the others. The events with high expression of HvSUT1 and OsNAS2 were expected to have a clear effect on the grain during the period of grain filling. Therefore, these transgenic lines were used for further micronutrient analysis, which will be discussed in Chapter 4.

3.4.3. Vigorous growth in the *HvSUT1*- overexpressing transgenic lines, but growth inhibition in single *OsNAS2*-overexpressing events.

Huynh (2015) reported that the endosperm-specific overexpression of the barley sucrose transporter *HvSUT1* in rice enhanced sucrose uptake capacity and potentially modifies the sucrose flux potential. However, better growth and development of *HvSUT1*-overexpressing Japonica rice was not reported in the study of Huynh (2015). Here, a very interesting observation of vigorous growth and development was found in the IR64 transgenic events expressing the *HvSUT1* construct as reported by Huynh (2015). This includes the SC1 lines overexpressing only *HvSUT1* and the DC1 lines overexpressing *HvSUT1* and *OsNAS2*. To show the vigorous growth and development, the height and tiller number of multiple independent transgenic lines in the T2 generation were recorded from 2-week-old seedlings to maturity at 3 months old. The better growth and development became evident at 2 months and continued to increase over the next month of growth. Three-month-old *HvSUT1* transgenic plants were taller and had an increased tiller number per plant. These results were consistent with the previous work on *HvSUT1* expression in wheat grains (Saalbach *et al.* 2014; Weichert *et al.* 2017), but only with panicle number in Nipponbare rice plant expressing *HvSUT1* (Huynh 2015).

The vigorous growth associated with *Glb-1:HvSUT1* transgenic plants may be due to ectopic expression of *HvSUT1*, which was also considered by Huynh (2015), but it was not confirmed. This means that *HvSUT1* maybe expressed in other organs of the plant other than the developing grain, and preferentially in young vegetative tissues. As a consequence, increased sucrose transport and partitioning into these tissues may be occurring leading to more tillers/roots or taller plant height. An ectopic expression of *HvSUT1* was suggested as a possible explanation

for the better performance in plant growth of transgenic wheat transformed with *HvSUT1* controlled by the barley hordein promoter (Weichert *et al.* 2017).

In this study, although the increased grain yield per plant was not tested due to fungal infection, the vigorous growth phenotype may lead to a potential increase of grain yield. Similar findings were reported in *HvSUT1*-expressing wheat in larger scale study under field-like conditions (Saalbach *et al.* 2014; Weichert *et al.* 2010), where more nutrients potentially could be available to supply plant growth. The experiment reported here needs to be repeated and then conducted under field conditions

Furthermore, the *OsNAS2*-expressing lines (SC2), were consistently shorter than their non-transgenic control plants. A growth inhibition in transgenic Japonica rice was previously reported by Zheng *et al.* (2010) when *OsNAS1* was constitutively expressed. These authors argue that high Fe accumulation in the leaves via increased NA concentration can explain the growth inhibition. In other studies, a growth inhibition of transgenic rice constitutively expressing *OsNAS2* has not been reported (Beasley *et al.* 2019a; Johnson *et al.* 2011; Kyriacou *et al.* 2014; Trijatmiko *et al.* 2016). However, in the present study, a negative effect on plant growth was observed at the vegetative stage of rice despite the intended endosperm-specific expression of *OsNAS2* under the control of the *GluA2* promoter. This result suggests that the Japonica *GluA2* promoter may also be miss-regulated in Indica rice, leading to ectopic expression in vegetative tissues and toxicity due to excess Fe accumulation. An alternative explanation maybe that ectopic expression of NAS and hence biosynthesis leads to a carbon limitation and hence a growth penalty. Interestingly, a vigorous growth phenotype was seen in the DC1 lines expressing the combination of *OsNAS2* and *HvSUT1*. If both the Japonica *Glb-1* and *GluA2* promoters are miss-regulated in an Indica background leading to ectopic expression, then the increased growth associated with *HvSUT1* may

create a greater demand for metal ions than that evinced by the ectopic expression of *OsNAS2*. Although this explanation is highly speculative, it is an intriguing observation and one that requires more study.

3.5. Conclusions

The transgenic events of overexpressing *OsNAS2* or/and *HvSUT1* under the control of the *GluA2* and *Glb-1* promoters, respectively, were examined for transgene expression in the immature grains. The results reveal that the OsNAS2 and HvSUT1 proteins were successfully expressed during the critical stage of storage in developing grains between 5 and 20 DAA. *HvSUT1* expressing lines showed a vigorous growth phenotype, whereas single *OsNAS2*-expressing lines showed a slight growth inhibition. The results may be explained by leaky expression of both promoters in other younger vegetative tissues. It was noticeable that the transgenic events with the *OsNAS2* and *HvSUT1* combination showed the additional benefit of *HvSUT1* expression, without inhibition as seen in the single *OsNAS2*-expressed lines.

To examine the relationship of HvSUT1 and OsNAS2 expression with nutrition in mature grains, the transgenic events from the three populations (SC1, SC2 and DC1) with strong expression of the transgenes were the focus of further study reported in Chapter 4.

CHAPTER 4: NUTRITION ANALYSIS AND BIOAVAILABILITY

4.1. Introduction

Recent efforts in biofortification have focused on increasing the Fe and Zn levels and bioavailability in the rice endosperm (Bashir *et al.* 2013b; Masuda *et al.* 2013a; Sperotto *et al.* 2012). During grain filling, the sink for nutrients shifts from the vegetative to reproductive tissues, and thus mass flow of nutrients is translocated to the grain (Zhang *et al.* 2007). In general, rice grain development progresses though cell division and expansion at early stages, before a storage stage from 7- 20 DAA, and then to the maturation stage (Wu *et al.* 2016a; Wu *et al.* 2016b). Nutrient loading rates are synchronised with increasing grain volume during the cell division and expansion stage, remaining constant during the storage product accumulation stage, before declining as grain maturation approaches. The developing grain takes up sucrose, amino acid and other nutrients from the phloem (Weber *et al.* 2005; Zhang *et al.* 2007) and probably some micronutrients from the xylem (Palmgren *et al.* 2008; Stomph *et al.* 2011; Stomph *et al.* 2009).

Transport of sucrose into developing seeds occurs via sucrose transporters located on the surface of endosperm cells. Sucrose is not only known to be a key component in translocation and storage in developing grains, but it is also involved in regulation of source-sink relations (Braun *et al.* 2014; Yu *et al.* 2015). Manipulating gene expression of nutrient transporters is a promising strategy for improving uptake capacity and nutrient partitioning. For instance, a higher protein level was reported in pea seeds overexpressing a potato sucrose transporter (*StSUT1*) in pea cotyledons (Rosche *et al.* 2002; Rosche *et al.* 2005) and vegetable peas (*Pisum sativum* L.) overexpressing an endogenous sucrose transporter SUT1 (Lu *et al.* 2020). Similar results were found when the barley sucrose transporter gene (*HvSUT1*) was expressed in wheat controlled by the barley endosperm-specific Hordein B1 promoter (Weichert *et al.* 2010). Along with an increase

in grain protein content, increasing Fe and Zn by 20-40% in transgenic wheat grain with higher sink strength was reported, compared to non-transgenic wheat grain (Saalbach *et al.* 2014). Huynh (2015) partially replicated the works of Weichert *et al.* (2010) and Saalbach *et al.* (2014) in Nipponbare transgenic rice overexpressing *HvSUT1*, but not under field evaluation. In the wheat and rice studies, the expression of the *HvSUT1* gene was designed to achieve a predominant sink strength in the grain by the control of an endosperm-specific promoter. Several successful results obtained from the transgenic rice lines overexpressing *HvSUT1* by Huynh (2015) has reinforced this hypothesis. These rice grains had increased Fe and Zn concentrations in the rice endosperm, and gave more promising results than those with constitutive expression of the *HvSUT1* gene (Huynh 2015). However, a significant accumulation of phytate was also found in the *HvSUT1*-expressing grain and was assumed to prevent mineral mobilization into the inner endosperm region, especially for Fe. Furthermore, this increased phytate is likely to inhibit micronutrient bioavailability.

Phytate is an insoluble salt form of phytic acid (myo-inositol 1,2,3,4,5,6-hexakisphosphate) bound with various mineral cations such as magnesium (Mg), K, calcium (Ca), manganese (Mn), Fe, and Zn (Bohn *et al.* 2007; Bohn *et al.* 2008; Cegłowski *et al.* 2016). The insoluble form of these salts results in reduced mineral availability for their absorption in the human intestine (Bohn *et al.* 2008). Phytic acid also serves as a major storage form of phosphorus (P) in cereal grains, which accounts for 65- 85% of the total grain P (Raboy 2003). Two other forms of P in cereal grains are soluble inorganic phosphate (P_i) (less than 5%) and other organic phosphates (10-20%) which are found in DNA, RNA, free nucleotides, phospholipid sugar phosphates, etc (Larson *et al.* 2000). In mature rice grains, the majority of phytic acid is localized in the aleurone cell layer, with trace amounts in the rice endosperm (Iwai *et al.* 2012; Yoshida *et al.* 1999). During rice grain

development, phytic acid is more likely to be immediately converted from the translocated Pi in the rice aleurone at the early stage of grain filling, rapidly increasing during the storage phase from 7-25 DAA. Like P, other nutrients are taken up into the rice aleurone/subaleurone cells. Before the minerals are mobilized into the endosperm cells, several minerals (especially Fe) can often be sequestered in the aleurone/subaleurone cells, binding with phytic acid, and leading to their low bioavailability.

To increase the bioavailability of minerals, breeding of food crops with low phytic acid by generating mutations in one or several genes responsible for phytic acid synthesis has been attempted (Gupta *et al.* 2015; Perera *et al.* 2018; Welch & Graham 2004). However, reducing the level of phytic acid in plant seeds needs very careful consideration, because of the many valuable properties it has for plant health. During germination, phytate is a major source of P for seedling growth and therefore a penalty in seed germination and seedling growth are often found in low-phytate crops (Raboy 2007; Sparvoli & Cominelli 2015). Furthermore, from a human health perspective, phytic acid is a natural antioxidant, linked to cancer prevention (Graf & Eaton 1993; Graf *et al.* 1987; Vucenik & Shamsuddin 2006).

An alternative and more promising approach than reducing the phytic acid levels in grains, is to mobilise essential micronutrients in the endosperm region by the use of other competing mineral chelators (Iwai *et al.* 2012). Nicotianamine (NA) and 2'-deoxymugineic acid (DMA) are two natural chelators of multiple metal cations, including Fe and Zn in plants (Takahashi *et al.* 2003; von Wirén *et al.* 1999). In rice, NA is a non-protein amino acid, synthesized by the trimerization of three molecules of S-adenosylmethionine (SAM). The reaction is catalyzed by nicotianamine synthase (NAS), a product of three *OsNAS* genes (*OsNAS1*, *2* and *3*) (Inoue *et al.* 2003). Increasing NA or/and DMA by constitutive overexpression by any of the three *OsNAS*

genes has been a popular strategy for Fe biofortification in multiple crops (Beasley *et al.* 2019a; Johnson *et al.* 2011; Kyriacou *et al.* 2014; Lee *et al.* 2012; Singh *et al.* 2017b; Trijatmiko *et al.* 2016; Wu *et al.* 2019). Furthermore, the presence of higher levels of NA and DMA has been shown to improve bioavailability of Fe, and possibly Zn (Aung *et al.* 2019; Beasley *et al.* 2019b; De Schepper *et al.* 2013; Eagling *et al.* 2014; Lee *et al.* 2012; Nozoye 2018; Zheng *et al.* 2010). However, because NA/DMA can chelate various metal cations, it has the potential to bind toxic metals in the grains, such as nickel (Ni), cadmium (Cd), and arsenic (As) (Norton 2019), as reported in transgenic rice overexpressing either *OsNAS1*, *OsNAS2*, or *OsNAS3* using a constitutive promoter (Kyriacou 2013). Although no evidence has yet shown a clear relationship between *OsNAS1*, *OsNAS2*, or *OsNAS3* expression and toxic metal accumulation in the grains (Slamet-Loedin *et al.* 2015; Wu *et al.* 2018; Wu *et al.* 2019). This possibility still remains and important consideration.

To examine the effects of the combined overexpression of *HvSUT1* and *OsNAS2* on the Fe and Zn mobilization into the inner endosperm and their bioavailability, in this chapter, the concentration of a range of minerals were measured in the polished and unpolished grain derived from multiple independent transgenic lines carrying *HvSUT1* and/or *OsNAS2*, the development and characterization of which is described in Chapter 2 and 3. The data revealed a positive correlation between transgene expression and Fe and Zn concentrations in the rice grain. Striking results of Fe and Zn distribution showed levels expanding into the endosperm region from both ventral and dorsal sides of the grain in the transgenic lines expressing the combination of *HvSUT1* and *OsNAS2*, particularly DC1.16. Based on Fe and Zn to phytate ratios, an improved mineral bioavailability is a likely result and no evidence of higher levels of toxic metal accumulation in the transgenic rice grain are also presented.

4.2. Methods

4.2.1. Transgenic plant materials

Mature T2 seeds (Indica rice, *Oryza sativa* L. cv. IR64) were harvested from the homozygous transgenic lines overexpressing *HvSUT1* and/or *OsNAS2*. Seed from non-transgenic IR64 plants were harvested at the same time. All plants were grown under similar conditions in a PC2 greenhouse in Jefferies® soil mix with added fertilizer for nutrient supplement (see Section 3.2.1).

4.2.2. Optimising condition for polishing

A commercial bench-top miller (Kett Electrical Laboratory, Tokyo, Japan) was used to polish rice grains, modified to prevent metal contamination. To establish an optimised condition for polishing, 50 brown rice grains (*O. sativa* cv. IR64) were milled for 60, 90, 120, 150 and 180 seconds. To visualise the remaining aleurone left after the different milling conditions, the polished grains and unmilled grains were incubated in a 1:3 solution of 100% ethanol and 2% potassium hydroxide (KOH) for 15 minutes. Under these conditions, the aleurone will stain dark yellow (Singh *et al.* 2017a; Vanangamudi *et al.* 1988).

4.2.3. Nutrient analysis in mature grains by ICP-MS

Following optimization of the polishing step, T2 mature grains from homozygous plants were analysed by Inductively Coupled Plasma Mass Spectrometry (ICP-MS), as described by Wheal *et al.* (2011). In short, the polished and unpolished rice grains were dried at 80^0C overnight. Approximately 250 mg of sample was prepared and then transferred into a 50 ml CELLSTAR® polypropylene tube (Greiner Bio-one). Digestion was initiated by adding 2.5ml nitric acid and 0.5ml hydrogen peroxide into each sample tube. Tubes were vortexed to ensure the entire sample

was fully wetted and then placed in a fume hood overnight at room temperature for pre-digestion. Two blank digests without sample and two reference digests with plant material of known mineral content (String Bean Pods) were prepared as controls. The tubes were vortexed again before being placed onto the Digi-Prep digestion block at room temperature and heated according to the digestion program. The program was set up with 4 steps: including 15 minutes for warming up to 80^0C, 30 minutes for stable heating at 80^0C, 15 minutes for increasing temperature to 125^0C, and 120 minutes for stable digestion at 125^0C. Pressure build-up in the tubes during the initial 30 minutes warming period was released by loosening each cap sufficiently to equalize pressure, then immediately re-tightened firmly and replaced back in the digestion block. When finished, tubes were allowed to cool to room temperature overnight. Milli-Q water was added to the tubes to make up to a final volume of 25ml. Multiple elements in the plant materials were then determined by ICP-MS.

4.2.4. Phytate extraction and quantitation by high-pH anion-exchange chromatography with pulsed electrochemical detection.

Mature polished and unpolished rice grains from the transgenic plants in Section 4.2.2 were used for phytate analysis. Fine flour was prepared from samples of unpolished and polished rice by grinding 90 grains for 2 minutes/each time (3X) in a bench top mill (Mini-Mill, Fritsch PULVERISETTE 23). The samples were then incubated in an oven at 80^0C for 24 hours. Approximately 200 mg of the flour samples was weighed and transferred into a fresh 15 ml CELLSTAR® polypropylene tube (Greiner Bio-one) for digestion with 10ml of 1.25% (v/v) sulphuric acid solution (H_2SO_4). The tubes were placed on a rotary shaker for 2 hours at room temperature, followed by centrifugation at 3500 g for 10 minutes at room temperature. A 1-ml aliquot of supernatant was transferred into a 1.5ml Eppendorf tube, then centrifuged at 13300 g

for 10 minutes at room temperature. A 1:100 dilution of the supernatant with MilliQ water was prepared using an auto dilutor. Phytate concentration, in the form of myo-inositol hexaphosphate (IP-6) was quantitated by high-pH anion-exchange chromatography (HPAEC) and pulsed electrochemical detection.

4.2.5. Microscopic section preparation

Twenty unpolished mature grains of three transgenic lines (SC2.15, SC1.16, and DC1.16) and non-transgenic IR64 were placed on a 100 mm square dish spread with epoxy glue (Selley® Araldite, Australia). The grains of similar size were selected for microscopic section preparation. Once the glue was dry, the grains were shaved open with a commercial sander (Ryobi, USA; 50–60 Hz max. 11000 rpm) attached with a fine sanding disc (Nortons, Australia; p240 grade). The slowest speed was used until half of each grain was removed. The remaining part of the grain was vacuum-infiltrated with a fixation solution containing 2% paraformaldede and 1% glutaraldehyde in 0.1M phosphate buffer (pH 7.0) for 30 minutes and then incubated overnight in the same solution. The fixed sections were rinsed in 0.1M phosphate buffer (pH 7.4) three times before the dehydration steps. The sections were dehydrated by sequential immersion in a graded ethanol series (50, 70, 80, 90, and 100%) for 45 minutes, followed by tert-butanol:ethanol (1:1) for 45 minutes, and finally 2X 100% tert-butanol for 30 minutes. Then the dehydrated sections were embedded in paraffin. Slide sections of 9-µm in thickness were obtained with a Leica RM2135 rotary microtome. The slide sections were deposited on glass slides and then incubated in a 37^0C incubator overnight. Before staining, paraffin was removed from the sections by immersion in xylene for 4 minutes two times and the rehydrated in an ethanol series of 100, 90, and 70% for 2 minutes/each.

4.2.6. Perl/DAB/$CoCl_2$ staining for Fe visualization in mature grains.

Perl's Prussian Blue (PPB) solution was freshly prepared by mixing in a 1:1 ratio, 142mM Potassium hexacyanoferrate (Sigma Aldrich) and 4% (v/v) HCl solution, according to the procedures of Choi *et al.* (2007). The slide sections were incubated in the PPB solution for 30 minutes at room temperature and then rinsed 3 times with high purity water to stop the reaction. The sections were treated in a methanol solution containing 0.01M NaN_3 and 0.3% (v/v) H_2O_2 for 1 hour, then rinsed in 0.1M phosphate buffer (pH 7.4) 3 times. An intensification reaction was performed by incubating the slide sections in 0.1M phosphate buffer (pH 7.4) containing 0.025% (w/v) 3,3-diaminobenzidine (DAB), 0.005% H_2O_2 and 0.005% $CoCl_2$ (added freshly; 500 µl of 1% $CoCl_2$ in 100 ml of 0.1M phosphate buffer). The sections were incubated in MilliQ water to stop the intensification reaction. The stained slide sections were mounted in dibutylphthalate polystyrene xylene (DPX) mounting medium (Merck). Images of stained sections were captured by the Brightfield BX53 Microscope connected with the DP27 colour camera (Olympus). DC1.16 sections (background control) were carried out as described above but without the staining in PPB solution.

4.2.7. Dithizone (DTZ) staining for Zn visualization in mature grains.

Dithizone (DTZ) staining solution was freshly prepared by dissolving 1,5-diphenyl thiocarbazone (Merck), 500 mg/l, in analysis-grade pure methanol, according to the procedures of Choi *et al.* (2007). The sections were incubated in the DTZ solution for 30 minutes. The stained sections were rinsed in MilliQ water and quickly mounted in DPX mounting medium (Merck). Images of stained sections were captured as described in Section 4.2.6. DC1.16 sections (background control) were carried out as described above but without the staining in DTZ solution.

4.2.8. Image analysis

All images of the stained slide sections were imported into the Image Sequence tool. The images were used to conduct colour deconvolution to separate up to three levels of stains by the ImageJ software (Crowe & Yue 2019; Varghese *et al.* 2014). The result of the colour deconvolution separated three images with different colours, namely brown for DAB stain, purple for DAB/$CoCl_2$ stain and a complimentary image. Brown and purple images were used for image analysis. The pixel intensity values of staining ranged from 0 to 255, wherein 0 represents the strongest intensity of staining and 255 represents the lightest intensity. A "Interactive 3D surface plot" function of ImageJ was used to create 3D surface plots of the staining distribution. The staining intensity value of each pixel in the image was interpreted by the height for the plot. The plot was displayed in different LUT schemes. A polygon selection tool was used to cover the entire area of the seed. The images of the negative control section were the pixel intensity values of the background.

For the images of the Zn-DTZ staining, the tool for colour deconvolution was also used to separate the three colour images. In the image of colour 1 (purple), the Zn-DTZ staining was separated from the background and turned into white. To compare intensity of the Zn-DTZ staining, a reversed image was created for image analysis. The "interaction 3D surface" plot was utilised as described above for the Fe/DAB/$CoCl_2$ staining. An area (69.83 µm x 206.90 µm = 486000 pixels) covering the aleurone layer and the endosperm, was selected to count the number of stained pixels with 0 value of intensity by an IHC Profilter tool of ImageJ software. An average percentage of stained pixels per area was calculated based on four replicates.

4.2.9. Calculation of molar ratios of phytate to iron, zinc, and calcium.

Molar ratios of phytate to iron (Phytate:Fe), zinc (Phytate:Zn), and calcium (Phytate:Ca) were calculated to estimate their relative bioavailability. Based on 1 kg of sample, the molar ratios Phytate:Fe, Phytate:Zn and Phytate:Ca were calculated to the following formula:

$$\frac{M_{PA}/MW_{PA}}{M_{mineral}/MW_{mineral}}$$

where: M_{PA} and $M_{mineral}$: Phytate and mineral content (g) in 1 kg of sample. MW_{PA} and $MW_{mineral}$: Phytate and mineral molecular weight with 660.8 g/mol for phytate, 55.845 g/mol for Fe, 65.38 g/mol for Zn, and 40.078 g/mol for Ca.

4.2.10. Statistical analysis.

The means and standard deviation of all minerals (Fe, Zn, copper (Cu), Mn, Ca, P, sulphur (S), Mg, and K and phytate contents of the mature grains were calculated. The results were expressed as mean ± SE of at least three biological replicates from separate the T2 plants of the same transgenic line. The ANOVA analysis with a Waller-Duncan post-hoc test was performed for comparison of the difference in the phytate and mineral contents between any two of the transgenic lines. Differences were considered significant at $p < 0.05$. All statistical analyses were done with R or IBM SPSS 25.

4.3. Results

4.3.1. Optimising conditions for grain polishing

To determine the mineral concentration in the starchy endosperm of rice grains, it was first necessary to remove the aleurone and pericarp, known as the bran. To achieve this, and also minimize the amount of broken grains during the milling process, it was important to optimise the polishing procedure. One hundred brown rice grains were milled for 60, 90, 120, 150, and 180 seconds using a commercial bench-top miller (Figure 4.1). A KOH staining method was used to visualise any aleurone retention (Kyriacou 2013; Singh *et al.* 2017a; Vanangamudi *et al.* 1988). KOH produced a yellow-brown colouring when in contact with the aleurone (Figure 4.1). The retention of aleurone strands was observed in the polished grains after milling for 60, 90, and 120 seconds. No aleurone tissue was observed in polished grains with a milling time of 150 and 180 seconds; however, around 53% of the polished grains were broken after 180-second milling, and this compares to 19% being broken when milled for 150 seconds (Figure 4.2). Based on these data, a milling time of 150 seconds was employed.

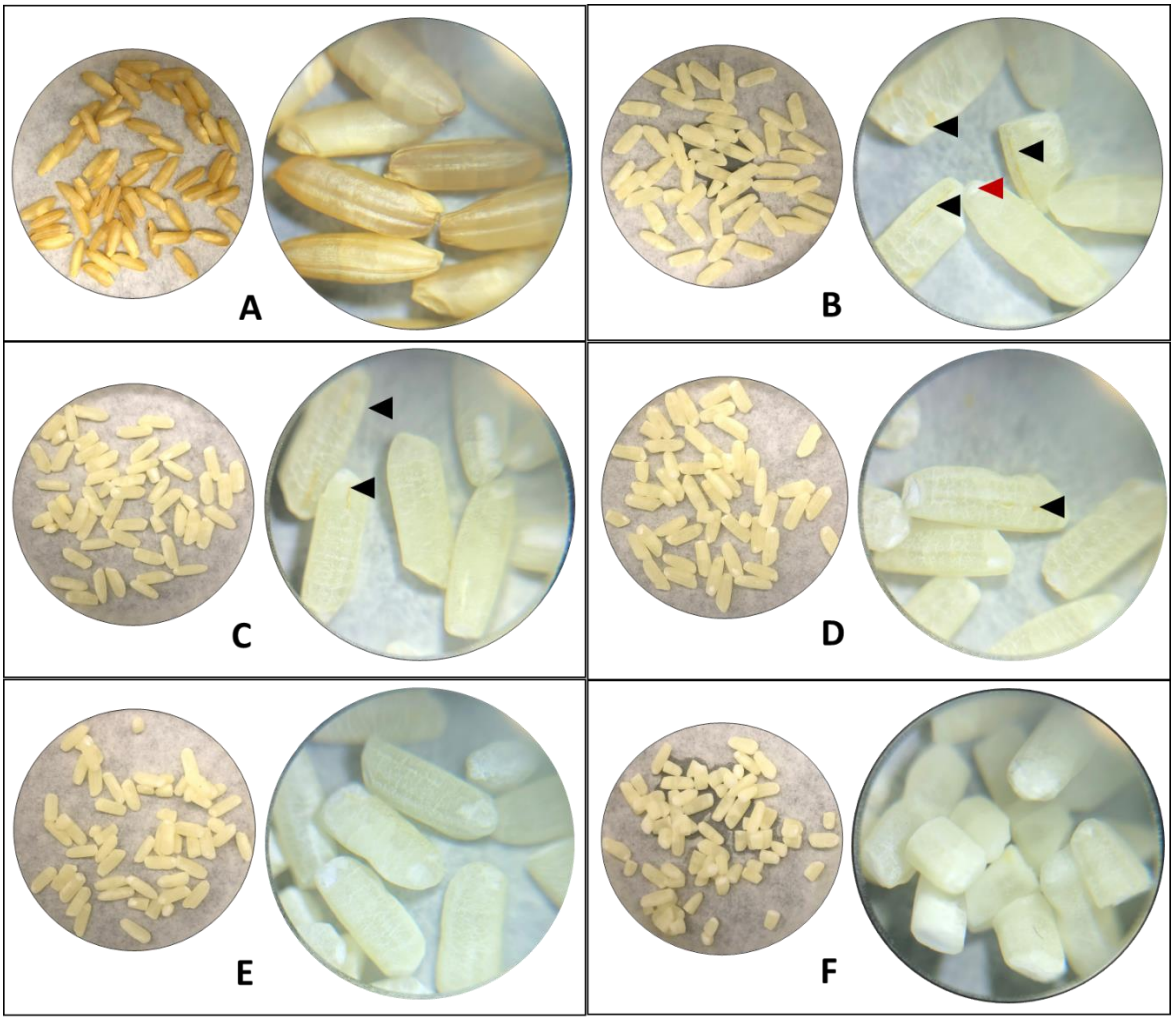

Figure 4.1. Optimising time of rice grain polishing by staining with 2% potassium hydroxide for visualising aleurone retention. A: 0 second (brown rice), B: 60 seconds, C: 90 seconds, D: 120 seconds, E: 150 seconds, and F: 180 seconds. Red triangle showed the embryo remaining in polished grains and black triangle showed the aleurone remaining in the polished grains.

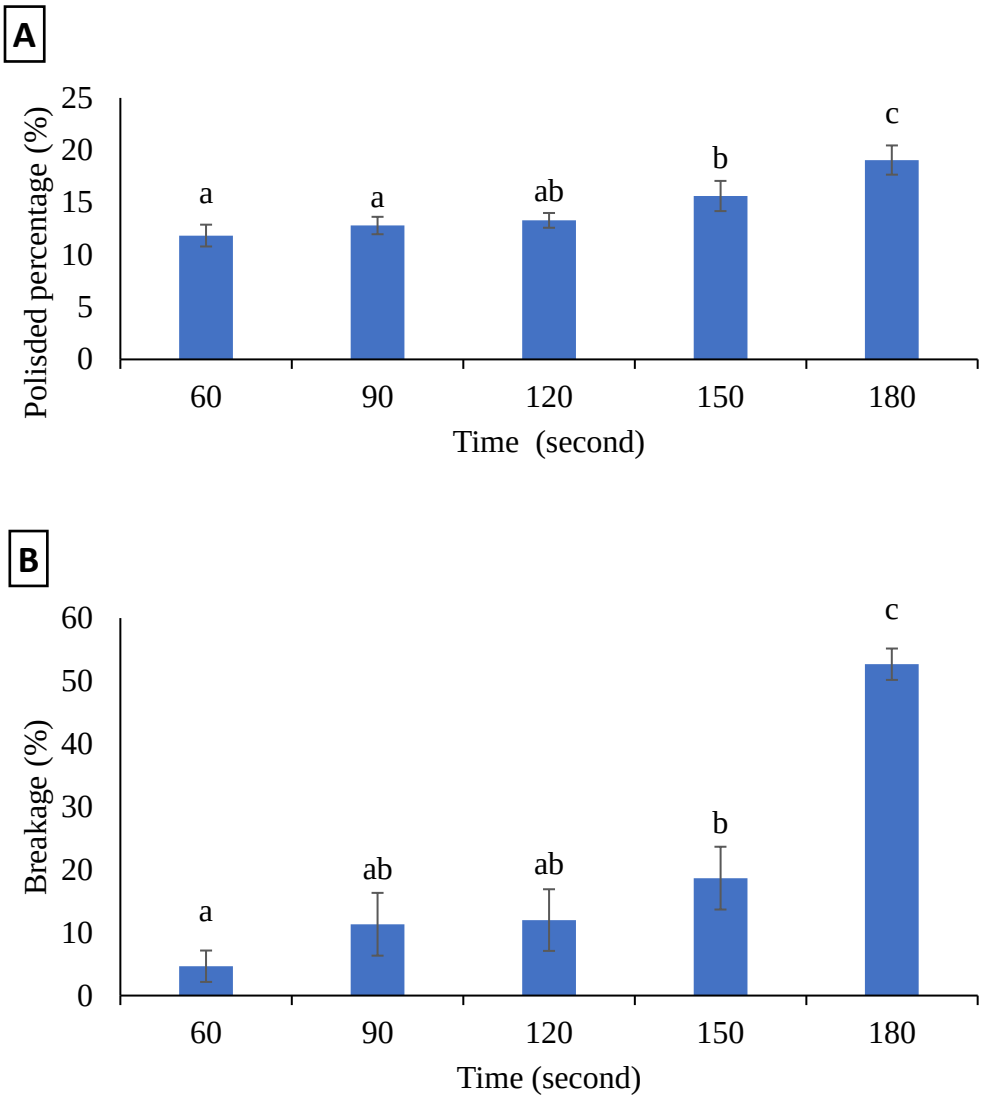

Figure 4.2. Average polished percentage (A) and breakage (B) of five different time conditions of grain milling. N = 3 replicates, error bar is ± SE. Treatments with the same letter are not significantly different.

Table 4.1. A summary of elemental analysis in polished and unpolished grains of T1 transgenic plants by ICP-MS.

Samples of ~250mg polished or unpolished grains from each homozygous transformant of DC1, SC1, SC2 (T1) and non-transgenic control were analysed by ICP-MS. Asterisks denote the significance between the transgenic lines and the control for $p < 0.05$ (*) and $p \leq 0.01$ (**) and ns presents for non significance as determined by student's t-test.

			Fe (mg/kg)		Zn (mg/kg)		P (mg/kg)		S (mg/kg)	
Sample	**Line**	**Gene**	**Average ± SE**	**Range**	**Average ± SE**	**Range**	**Average ± SE**	**Range**	**Average ± SE**	**Range**
Unpolished grain	**WT-IR64**		**12.1** ± 2.9	9.2-15.0	**39.3** ± 5.0	34-44	**5033** ± 586	4600-5700	**1737^{ns}** ± 145	1590-1880
	SC1.12	***Glb1:HvSUT1***	**20.0**** ± 3.0	17.0-23.0	**51.7*** ± 9.5	42-61	**4867^{ns}** ± 58	4800-4900	**1930^{ns}** ± 157	1790-2100
	SC1.13		**18.5**** ± 0.7	18.0-19.0	**80.5**** ± 16.3	69-92	**5700*** ± 141	5600-5800	**2150**** ± 71	2100-2200
	SC1.16		**18.3**** ± 1.0	17.0-19.0	**50.3^{ns}** ± 2.9	48-54	**4550^{ns}** ± 58	4500-4600	**1735^{ns}** ± 24	1710-1760
	SC1.17		**18.8**** ± 1.3	18.0-21.0	**52.2*** ± 6.2	48-63	**4700^{ns}** ± 424	4400-5400	**1748^{ns}** ± 143	1650-2000
	SC1.21		**17.8**** ± 1.9	15.0-20.0	**56.3**** ± 11.3	46-78	**4833^{ns}** ± 151	4700-5000	**1823^{ns}** ± 75	1700-1920
	SC1.22		**14.8^{ns}** ± 2.2	12.0-17.0	**45.3^{ns}** ± 3.8	40-49	**4725^{ns}** ± 443	4300-5200	**1680^{ns}** ± 107	1570-1820
	SC1.25		**15.0^{ns}** ± 0.0	15.0-15.0	**53.5*** ± 2.1	52-55	**4750^{ns}** ± 495	4400-5100	**1640^{ns}** ± 57	1600-1680
	SC2.14	***GluA2:OsNAS2***	**18.0*** ± 2.8	16.0-20.0	**52.0^{ns}** ± 4.2	49-55	**4850^{ns}** ± 354	4600-5100	**1965^{ns}** ± 191	1830-2100
	SC2.15		**17.0*** ± 2.8	15.0-19.0	**55.5*** ± 3.5	53-58	**4950^{ns}** ± 212	4800-5100	**1810^{ns}** ± 28	1790-1830
	SC2.31		**13.3^{ns}** ± 1.2	12.0-14.0	**51.0^{ns}** ± 7.0	43-56	**4967^{ns}** ± 208	4800-5200	**1867^{ns}** ± 111	1750-1970
	DC1.1	***GluA2:OsNAS2 - Glb1:HvSUT1***	**15.3^{ns}** ± 1.5	14.0-17.0	**58.3**** ± 9.5	50-67	**5000^{ns}** ± 337	4500-5200	**2010**** ± 180	1740-2100
	DC1.13		**15.7^{ns}** ± 2.6	11.0-19.0	**55.3*** ± 5.0	49-64	**4657^{ns}** ± 251	4200-4900	**1693^{ns}** ± 166	1460-1910
	DC1.16		**19.7**** ± 2.5	17.0-22.0	**58.0**** ± 9.2	48-66	**4800^{ns}** ± 100	4700-4900	**1573^{ns}** ± 100	1470-1670
	DC1.19		**11.5^{ns}** ± 2.2	9.9-13.0	**55.5*** ± 2.1	54-57	**5150^{ns}** ± 212	5000-5300	**1795^{ns}** ± 21	1780-1810
	DC1.5		**18.6**** ± 4.3	14.0-24.0	**63.2**** ± 5.3	58-69	**4820^{ns}** ± 390	4200-5200	**1686^{ns}** ± 75	1610-1810
	DC1.9		**18.5**** ± 2.1	17.0-20.0	**60.0**** ± 0.0	60-60	**5000^{ns}** ± 141	4900-5100	**1790^{ns}** ± 28	1770-1810
Polished grain	**WT-IR64**		**2.2** ± 0.5	1.9-2.8	**38.7** ± 10.6	29-50	**1333** ± 161	1150-1450	1460 ± 111	1340-1560
	SC1.12	***Glb1:HvSUT1***	**4.4**** ± 0.4	4.0-4.8	**42.7^{ns}** ± 8.0	35-51	**1680**** ± 101	1590-1790	**1843**** ± 129	1750-1990
	SC1.13		**4.7**** ± 1.7	3.5-5.9	**62.0**** ± 9.9	55-69	**1985**** ± 445	1670-2300	**1870**** ± 99	1800-1940

SC1.16		**4.8****	± 0.7	4.3-5.8	**45.3**^{ns}	± 1.9	44-48	**1600***	± 59	1530-1670	**1675***	± 26	1650-1710
SC1.17		**4.9****	± 0.5	4.5-5.8	**47.4**^{ns}	± 5.7	41-55	**1622****	± 160	1490-1880	**1634***	± 77	1550-1740
SC1.21		**4.5****	± 0.6	3.7-5.0	**51.8***	± 10.7	42-70	**1647****	± 152	1490-1780	**1770****	± 91	1660-1930
SC1.22		**3.0**^{ns}	± 0.6	2.4-3.6	**39.3**^{ns}	± 3.6	34-42	**1463**^{ns}	± 104	1330-1560	**1615**^{ns}	± 99	15401750
SC1.25		**2.9**^{ns}	± 0.5	2.5-3.2	**41.5**^{ns}	± 2.1	40-43	**1470**^{ns}	± 184	1340-1600	**1495**^{ns}	± 78	1440-1550
SC2.14	***GluA2:OsNAS2***	**3.7***	± 0.7	3.2-4.2	**39.5**^{ns}	± 0.7	39-40	**1500**^{ns}	± 42	1470-1530	**1695***	± 92	1630-1760
SC2.15		**3.5***	± 0.2	3.3-3.7	**46.0**^{ns}	± 8.7	36-52	**1530**^{ns}	± 60	1470-1590	**1710****	± 147	1580-1870
SC2.31		**4.0****	± 0.1	3.9-4.1	**46.5**^{ns}	± 3.5	44-49	**1610***	± 28	1590-1630	**1625**^{ns}	± 49	1590-1660
DC1.1	***GluA2:OsNAS2 - Glb1:HvSUT1***	**3.2**^{ns}	± 0.5	2.7-3.8	**54.5****	± 11.9	42-67	**1590***	± 131	1450-1760	**1853****	± 157	1620-1960
DC1.13		**3.0**^{ns}	± 0.7	2.0-4.0	**45.7**^{ns}	± 5.4	41-56	**1497**^{ns}	± 117	1380-1680	**1560**^{ns}	± 126	1380-1710
DC1.16		**5.4****	± 0.2	5.2-5.6	**47.0**^{ns}	± 9.5	36-53	**1747****	± 176	1560-1910	**1457**^{ns}	± 118	1320-1530
DC1.19		**3.1**^{ns}	± 0.1	3.0-3.2	**43.5**^{ns}	± 2.1	42-45	**1620***	± 14	1610-1630	**1535**^{ns}	± 106	1460-1610
DC1.5		**4.6****	± 1.1	3.3-5.5	**53.4****	± 4.5	48-58	**1472**^{ns}	± 77	1370-1570	**1538**^{ns}	± 77	1480-1670
DC1.9		**3.8***	± 0.3	3.6-4.0	**50.0**^{ns}	± 0.0	50-50	**1540**^{ns}	± 85	1480-1600	**1620**^{ns}	± 71	1570-1670

To assess the effect of transgene expression on mineral accumulation in rice grains, mature grains from six independent DC1 lines overexpressing *OsNAS2* and *HvSUT1*, seven SC1 lines overexpressing *HvSUT1*, three SC2 lines overexpressing *OsNAS2* and three non-transgenic IR64 plants were prepared for elemental analysis by ICP-MS (Table 4.1). Fe concentration in the grains from non-transgenic IR64 plants was 12.1 mg/kg. Fe concentration in the three transgenic lines transformed with the SC2 construct ranged from 13.3 – 18 mg/kg. SC2.14 and SC2.31 had a significant increase in grain Fe concentration. In the DC1 lines over-expressing *OsNAS2* and *HvSUT1*, Fe concentration in all the transgenic lines ranged from 15.7 mg/kg to 19.5 mg/kg, all significantly higher compared to non-transgenic grains (p=0.04, student t-test), with the exception of DC1.19 with only 11.5 mg/kg. Transgenic events of the SC1 population had Fe concentrations ranging from 14.8 – 20.0 mg/kg, significantly higher than non-transgenic grains (p=0.001). In polished (white) grains, Fe concentrations in SC1.12, SC1.13, SC1.16, SC1.17 and SC1.21 were up 2.2-fold higher, compared to the non-transgenic control (2.2 mg/kg). DC1.16, DC1.5, and DC1.9 had up to 2.4-fold higher Fe concentrations relative to the non-transgenic control. Three lines of the SC2.14, SC2.15 and SC2.31 ranged from 3.5-4.0 mg/kg Fe.

For Zn concentration in brown grains, a significant increase was observed in all transgenic lines, with 52.6 mg/kg in the SC2 lines, 54.0 mg/kg in the SC1 lines and 58.3 mg/kg in the DC1 lines, compared to 39.3 mg/kg in non-transgenic control (IR64). For the Zn concentration in polished grains, SC1.13 (62 mg/kg), SC1.21 (51.8 mg/kg), DC1.1 (54.5 mg/kg), and DC1.5 (53.4 mg/kg) showed a significant increase, compared to the non-transgenic control of 38.7 mg/kg, while the other lines showed an increase in Zn concentrations from 39.3 -50.0 mg/kg but were not significant different to non-transgenic controls.

For macronutrient concentrations, the focus was on P and S as these potentially change phytate concentrations and protein bodies, which in turn influence Fe and Zn bioavailability. Differences for P in brown grains was insignificant in all transgenic events (4550 - 5700 mg/kg for SC1 lines, 4850-4967 mg/kg for SC2 lines and 4657-5150 mg/kg for DC1 lines), compared to the non-transgenic control (5033 mg/kg). However, the SC1.13 was an exception with a significant increase in S and P concentration, and SC1.16 had a significant decrease in P concentration. In the polished grains, P and S concentrations in the SC1 population were significantly higher than those in the non-transgenic control, and no significant increase was seen in the SC2 and DC1 populations.

Despite large variation in micro- and macronutrient content in independent lines transformed with the same construct, in general there was a correlation between nutrient content and transgene expression. This can be best exemplified by the following lines DC1.5, DC1.9 and DC1.16 for the DC1 population, SC1.16, SC1.21 and SC1.22 for the SC1 population and SC2.14, SC2.15 and SC2.31 for the SC2 population. These showed higher levels of Fe and Zn and immunoblot data showed higher levels of transgene expression (Section 3.3) In the subsequent sections to determine the distribution of Fe and Zn in the grain, data for these three lines will be presented.

4.3.2. Minerals changes in polished and unpolished grains.

The average concentrations of four micronutrients in the selected DC1 lines showed significant increases in unpolished grains by approximately 55% for Fe and Zn and around 25% for Cu and Mn, compared to the non-transgenic control (Figure 4.3). In unpolished grains, the SC1 and SC2 lines had increases in all four micronutrients but a significant difference was seen in only Fe concentration for the SC1 lines (17.07 mg/kg) and Zn concentrations for the SC2 lines (52.57

mg/kg). No significant differences in average concentrations of macronutrients (P, S, Mg, K, and Ca) in unpolished grains were found in all transgenic lines relative to the non-transgenic control, except for concentration of S from the DC1 lines where on average 1673 mg/kg was recorded, which is a decrease, compared to 1736.7 mg/kg for the non-transgenic control (Figure 4.4).

For polished grains, although all the transgenic lines had increased levels of micronutrients (Figure 4.5), the DC1 and SC1 lines were found to have significantly enhanced levels, compared to the non-transgenic control. Fe, Zn, Cu and Mn concentrations were increased by over 100%, 31%, 41%, and 34% in the DC1 populations with *HvSUT1* and *OsNAS2* expression, respectively. Fe concentration showed a significant increase, by around 65% and 85% in polished grains from the SC2 and SC1 lines, respectively, but there was no significant difference in Zn, Cu and Mn concentrations relative to the non-transgenic control. Contrary to the unpolished grains, the polished grains of the transgenic SC1 and SC2 lines had significant increases in P, S and Mg, while the DC1 lines showed a significant increase in P and Mg, but no difference in S concentration (Figure 4.6). Although no significant differences in K and Ca concentration were seen in the three transgenic populations, an opposite pattern of Ca and K was found, with an increase for Ca and a decrease for K.

To determine the proportion of minerals retained in the rice endosperm after polishing, the nutrient concentration in the polished relative to the unpolished grains was calculated as a percentage (Figure 4.7 and Figure 4.8). In general, Zn, Cu and S had very high retention with over 80% of these minerals retained in the endosperm. The opposite was found for Fe and Mg with low retention in the rice endosperm of approximately 20%. Medium retention, from 30 to 50% was found for Mn, P, Ca, and K. Furthermore, Cu, P and S in the three transgenic populations had significantly higher retention in the rice endosperm, compared to the non-transgenic control.

Increased retention of Fe was significantly different to the non-transgenic grains for the SC1 and DC1 lines, both expressing HvSUT1, but not for the SC2 lines overexpressing only *OsNAS2*. Zn and K retention of the non-transgenic control was slightly higher than that of transgenic lines.

A correlation between HvSUT1 and OsNAS2 protein expression and Fe and Zn concentration in polished grains was analysed (Table 4.2). The HvSUT1 signal on the immunoblots at 10 DAA relative to background (no signal in the non-transgenic control IR64) was calculated and recorded as a fold change of HvSUT1 protein expression. A similar calculation was made for the NAS2 protein at 5 DAA. The fold change values of HvSUT1 and OsNAS2 were correlated with the fold change in polished grain micronutrient and macronutrient concentrations. The results revealed that the HvSUT1 expression had a significantly positive correlation with the polished grain Fe concentration ($r=0.89$, $p=0.002$), but not significant for Zn ($r=0.54$, $p=0.08$), Cu ($r=0.36$, $p= 0.387$) and Mn concentrations ($r=0.50$, $p= 0.211$). For macronutrients, significant correlation with HvSUT1 expression was found for P ($r=0.77$, $p= 0.025$) and Mg ($r=0.78$, $p= 0.022$) and not for K. No correlations between the OsNAS2 expression with mineral concentrations were found in polished except for Mn and S. OsNAS2 expression had a negative correlation with Mn ($r= -0.62$, $p= 0.141$), but was positively correlated with S ($r=0.54$, $p= 0.21$).

Interestingly, DC1.16 and DC1.5 lines of the DC1 population, SC1.16 and SC1.21 of the SC1 population and the SC2.15 line of the SC2 population always showed the best performance in nutrition accumulation and the expression of their transgenes were at the highest levels (see Figure 3.14-Figure 3.15). Therefore, these events were the focus of further analysis of Fe and Zn localization presented in Section 4.3.3.

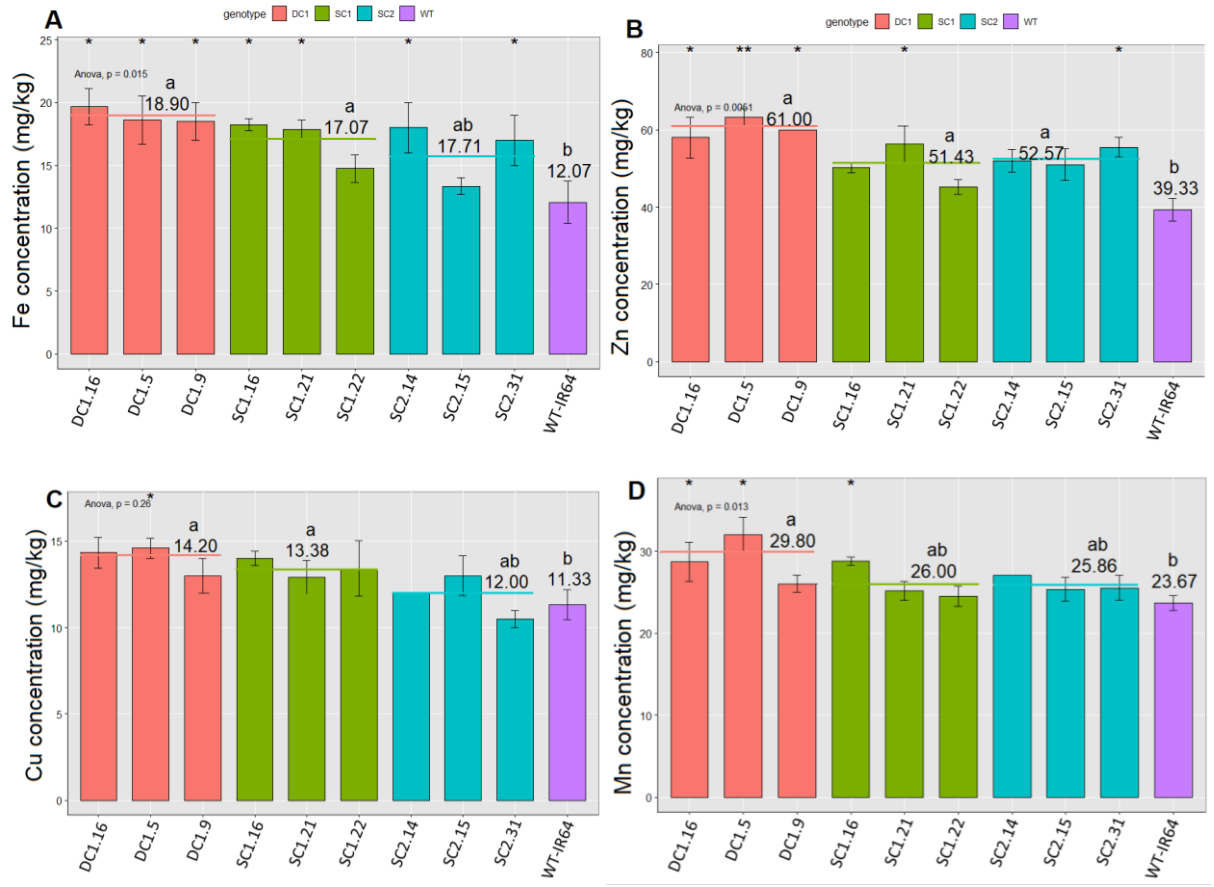

Figure 4.3. Analysis of micronutrient concentration (mg/kg) in unpolished grains, namely Fe (A), Zn (B), Cu (C), and Mn (D). Bars represent mean ± SE of at least 3 biological replicates of the DC1 (orange), SC1 (green) and SC2 (blue) lines, compared to the non-transgenic control (purple). Asterisks denote the significance between the transgenic lines and the control for $p < 0.05$ (*) and $p \leq 0.01$ (**) as determined by student's t-test. Orange, green and blue horizontal lines represent means of 3 independent lines DC1, SC1 and SC2, compared to the non-transgenic control. The differences with the same letter are not significant.

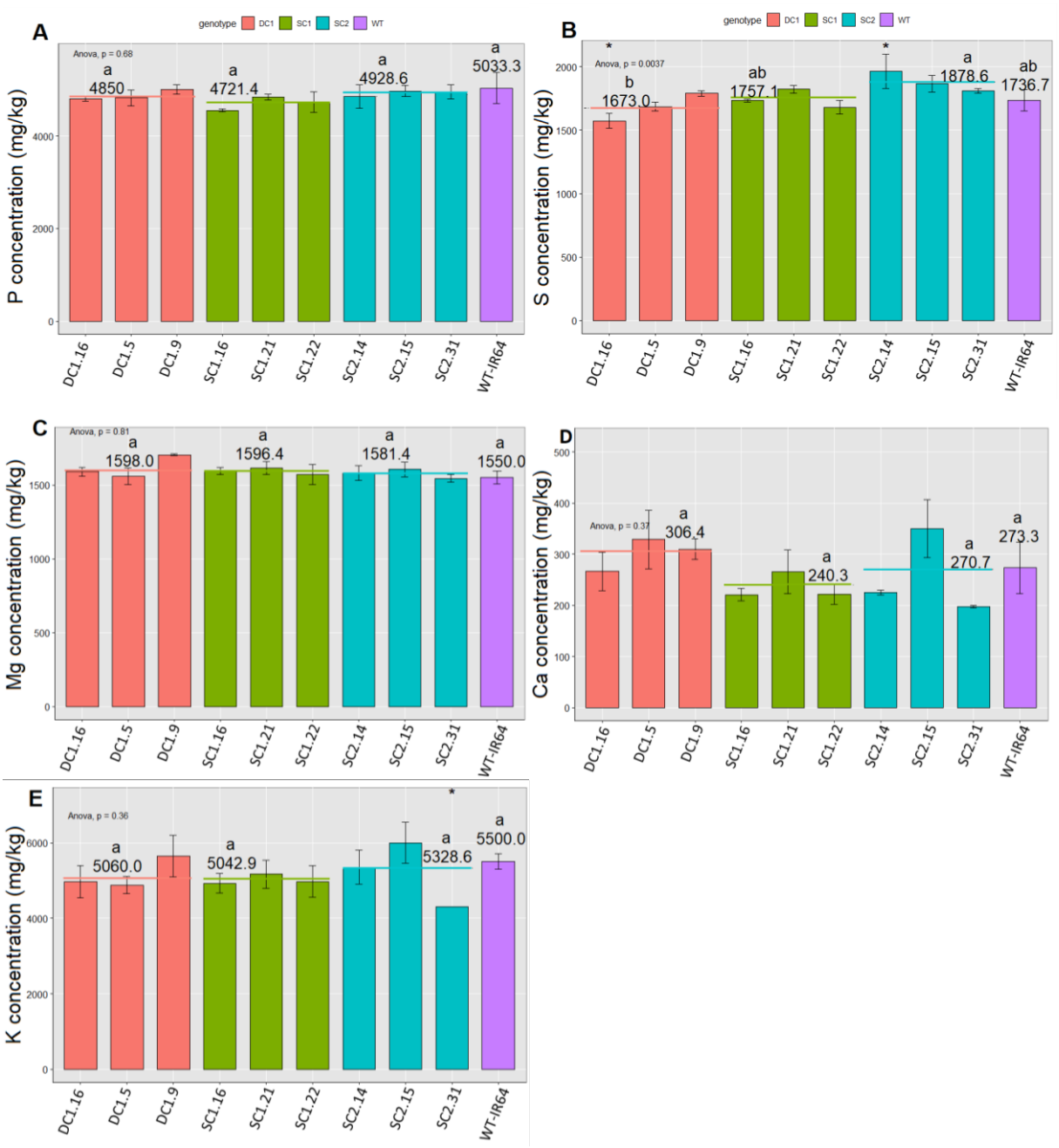

Figure 4.4. Analysis of macronutrient concentration (mg/kg) in unpolished grains, namely P (A), S (B), Mg (C), Ca (D), and K (E). Bars represent mean ± SE of at least 3 biological replicates of the DC1 (orange), SC1 (green) and SC2 (blue) lines, compared to the non-transgenic control (purple). Asterisks denote the significance between the transgenic lines and the control for $p < 0.05$ (*) and $p \leq 0.01$ (**) as determined by student's t-test. Orange, green and blue horizontal lines

represent means of 3 independent lines DC1, SC1 and SC2, compared to the non-transgenic control. The differences with the same letter are not significant.

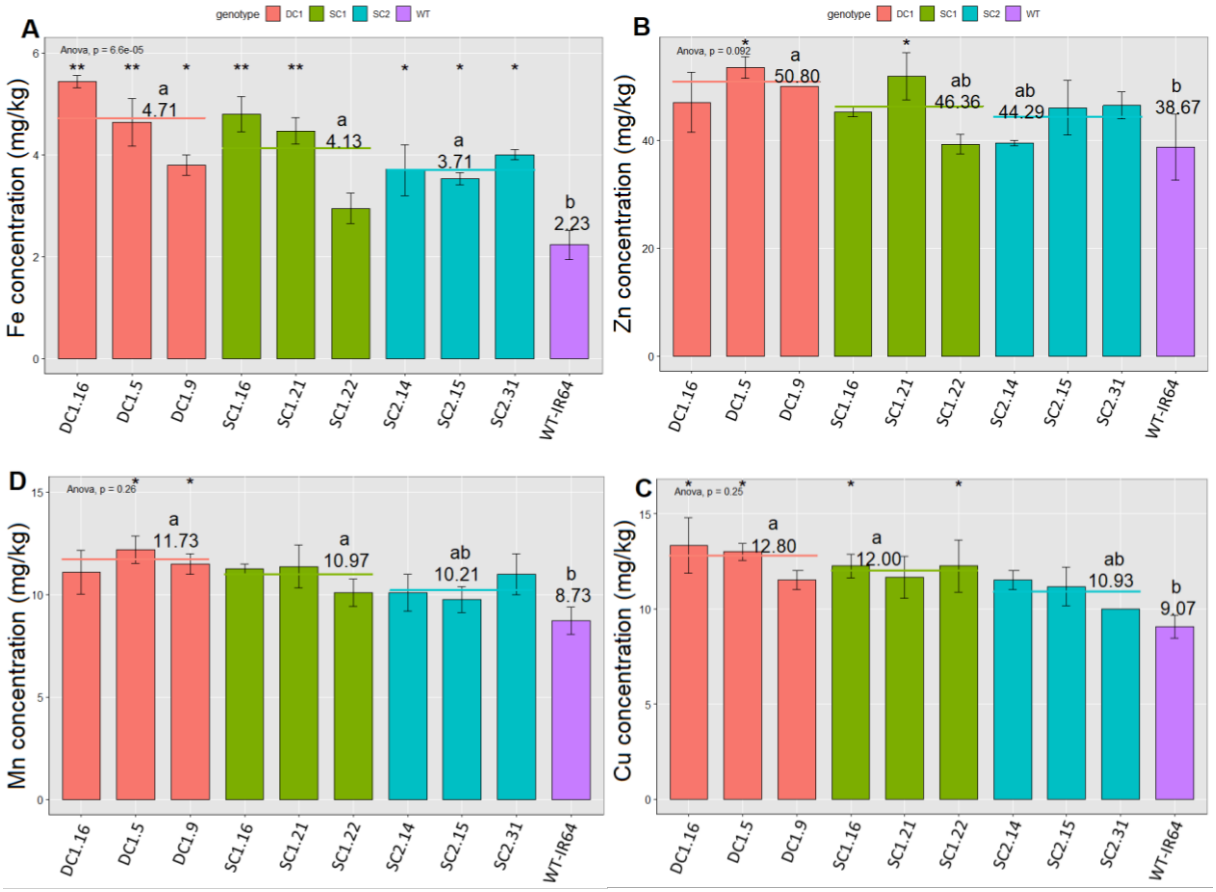

Figure 4.5. Analysis of micronutrient concentration (mg/kg) in polished grains, namely Fe (A), Zn (B), Cu (C), and Mn (D). Bars represent mean ± SE of at least 3 biological replicates of the DC1 (orange), SC1 (green) and SC2 (blue) lines, compared to the non-transgenic control (purple). Asterisks denote the significance between the transgenic lines and the control for $p < 0.05$ (*) and $p \leq 0.01$ (**) as determined by student's t-test. Orange, green and blue horizontal lines represent means of 3 independent lines DC1, SC1 and SC2, compared to the non-transgenic control. The differences with the same letter are not significant.

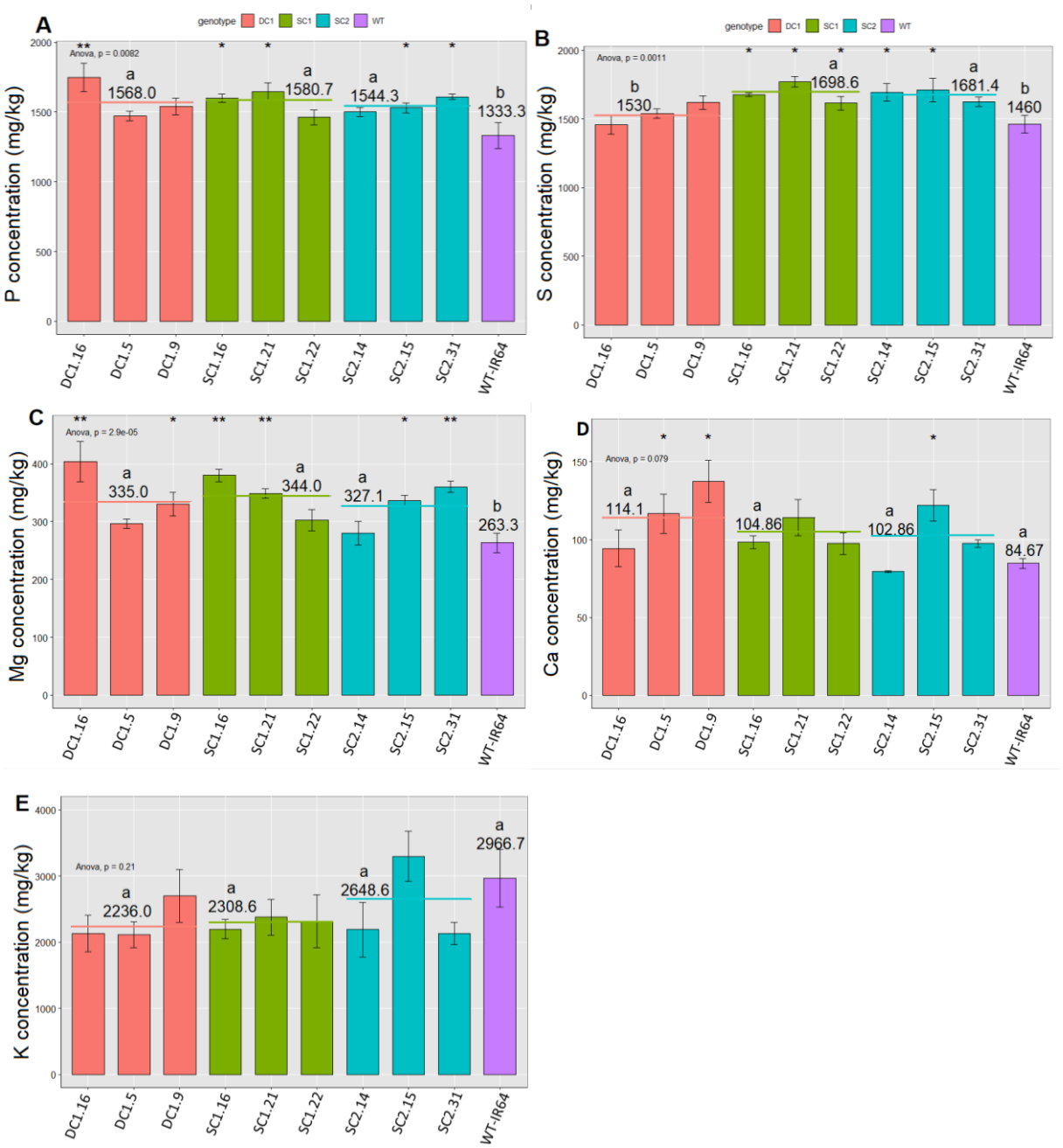

Figure 4.6. Analysis of micronutrient concentration (mg/kg) in polished grains, P (A), S (B), Mg (C), Ca (D), and K (E). Bars represent mean ± SE of at least 3 biological replicates of the DC1 (orange), SC1 (green) and SC2 (blue) lines, compared to the non-transgenic control (purple). Asterisks denote the significance between the transgenic lines and the control for $p < 0.05$ (*), $p \leq 0.01$ (**) as determined by student's t-test. Orange, green and blue horizontal lines represent means

of 3 independent lines DC1, SC1 and SC2, compared to the non-transgenic control. The differences with the same letter are not significant.

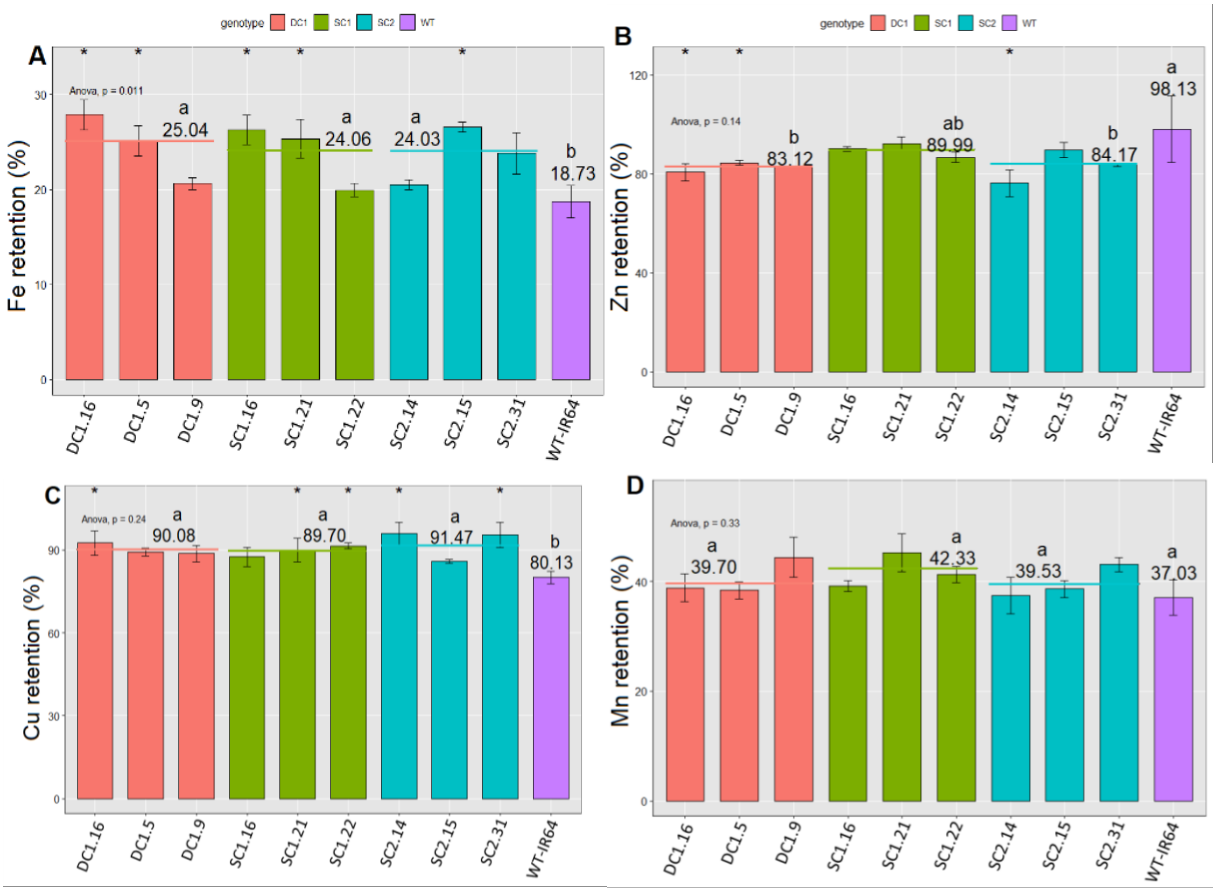

Figure 4.7. Analysis of micronutrient retention (%) in polished grains, namely Fe (A), Zn (B), Cu (C), and Mn (D). Bars represent mean ± SE of at least 3 biological replicates of the DC1 (orange), SC1 (green) and SC2 (blue) lines, compared to the non-transgenic control (purple). Asterisks denote the significance between the transgenic lines and the control for $p < 0.05$ as determined by student's t-test. Orange, green and blue horizontal lines represent means of 3 independent lines DC1, SC1 and SC2, compared to the non-transgenic control. The differences with the same letter are not significant.

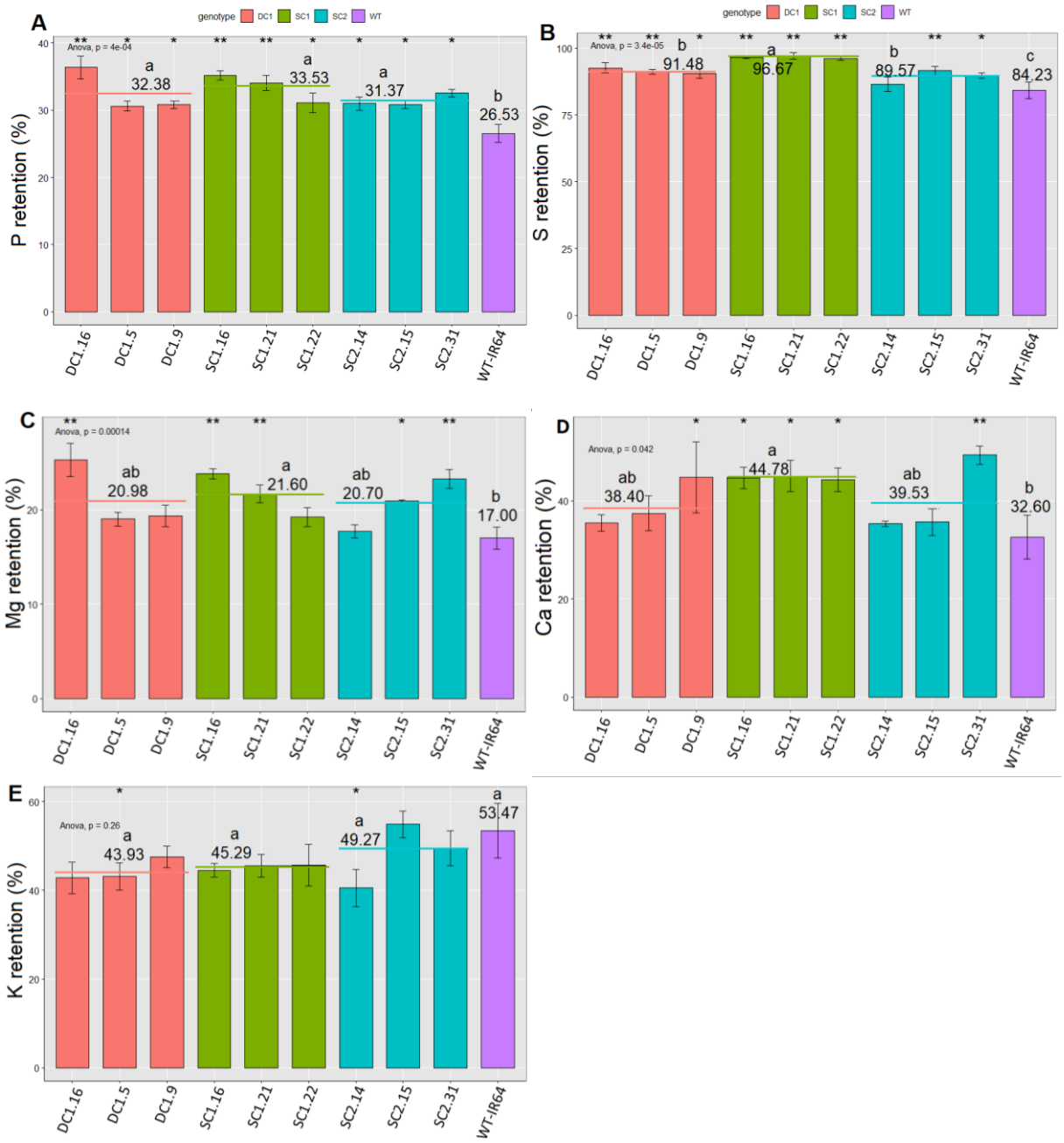

Figure 4.8. Analysis of macronutrient retention (%) in polished grains, namely P (A), S (B), Mg (C), and Ca (D). Bars represent mean ± SE of at least 3 biological replicates of the DC1 (orange), SC1 (green) and SC2 (blue) lines, compared to the non-transgenic control (purple). Asterisks denote the significance between the transgenic lines and the control for $p < 0.05$ (*), $p \leq 0.01$ (**) as determined by student's t-test. Orange, green and blue horizontal lines represent means of 3 independent lines DC1, SC1 and SC2, compared to the non-transgenic control. The differences with the same letter are not significant.

Table 4.2. Pearson's correlation analysis of protein expression and mineral concentrations in polished grains. (A) the correlation between fold change in HvSUT1 protein expression and polished grain mineral concentrations in four SC1 events (SC1.16, SC1.17, SC1.21, and SC1.22) and four DC1 events (DC1.5, DC1.13, DC1.16, and DC1.19). (B) the correlation between fold change in OsNAS2 protein expression and polished grain mineral concentrations in three SC2 events (SC2.14, SC2.15 and SC2.31) and four DC1 events (DC1.5, DC1.13, DC1.16, and DC1.19). **Bold** and small numbers represent Pearson's correlation coefficients (r) and p values, respectively.

A

HvSUT1	Fe	Zn	Cu	Mn	P	S	K	Mg
HvSUT1	**0.89****	**0.54**	**0.36**	**0.50**	**0.77***	**0.25**	**0.06**	**0.78***
	0.003	0.165	0.387	0.211	0.025	0.557	0.895	0.022
Fe	**1**	**0.59**	**0.72***	**0.56**	**0.62**	**0.02**	**0.09**	**0.70**
		0.123	0.045	0.151	0.104	0.969	0.836	0.053
Zn		**1**	**0.30**	**0.91****	**0.16**	**0.15**	**0.12**	**0.03**
			0.466	0.002	0.704	0.719	0.786	0.941
Cu			**1**	**0.27**	**0.13**	**-0.32**	**0.28**	**0.25**
				0.512	0.755	0.433	0.503	0.545
Mn				**1**	**0.08**	**-0.03**	**-0.19**	**0.04**
					0.856	0.943	0.645	0.932
P					**1**	**-0.06**	**-0.20**	**0. 90****
						0.893	0.634	0.003
S						**1**	**0.53**	**0.01**
							0.175	0.979
K							**1**	**-0.20**
								0.627

B

	OsNAS2	Fe	Zn	Cu	Mn	P	S	K	Mg
OsNAS2	**1**	**0.01**	**0.15**	**-0.13**	**-0.62**	**-0.27**	**0.54**	**-0.09**	**-0.31**
		0.992	0.756	0.776	0.141	0.552	0.210	0.853	0.497
Fe		**1**	**0.32**	**0.80***	**0.26**	**0.51**	**-0.49**	**-0.09**	**0.48**
			0.491	0.030	0.576	0.246	0.270	0.842	0.274
Zn			**1**	**0.72**	**0.13**	**0.15**	**-0.68**	**-0.91****	**-0.01**
				0.070	0.790	0.752	0.094	0.004	0.985
Cu				**1**	**0.44**	**0.28**	**-0.74**	**-0.49**	**0.17**
					0.318	0.545	0.060	0.266	0.714
Mn					**1**	**-0.19**	**-0.50**	**0.00**	**-0.12**
						0.686	0.252	0.994	0.804
P						**1**	**-0.55**	**-0.25**	**0.94****
							0.198	0.593	0.002
S							**1**	**0.63**	**-0.49**
								0.132	0.261
K								**1**	**-0.03**
									0.950

*. Correlation is significant at the 0.05 level (2-tailed).

**. Correlation is significant at the 0.01 level (2-tailed).

4.3.3. Fe and Zn localization in longitudinal section of mature grains

To investigate the distribution of Fe in mature grains, 9-µm thick sections of mature grains from DC1.16, SC1.16, SC2.15 lines and the non-transgenic control (IR64) were prepared and stained with Perls/DAB/$CoCl_2$, according to Roschzttardtz *et al.* (2009) and Meguro *et al.* (2007). Fe stained brown to dark brown, dependent on the concentrations, with dark brown indicative of higher concentrations. The images, captured under the Brightfield BX53 Microscope, were converted to a three-dimensional surface plot by the ImageJ software. The distribution pattern of Fe in longitudinal sections of mature grains is shown in Figures 4.9- 4.12. Fe was abundant in the outermost part of the rice endosperm and the scutellum of the embryo (Figure 4.9). In the non-transgenic control, Fe was confined to a thin line on the dorsal side of the grain, which was similar to the distribution pattern of Fe staining in the SC2.15 grains expressing only *OsNAS2*. A stronger intensity of Fe on the dorsal side was found in the longitudinal section of SC1.16 grain expressing only *HvSUT1*. Interestingly, a stronger signal of Fe was not only observed on the dorsal side, but also on the ventral side of the section of DC1.16 grain expressing *HvSUT1* and *OsNAS2*.

In the embryo section of the non-transgenic grains, as expected, the distribution of Fe was dominant in the scutellum of the embryo, especially very strong in the regions where the embryo and endosperm are in contact and around the radicle (Figure 4.10). Compared to the non-transgenic control, the embryo sections of SC2.15, SC1.16, and DC1.16 grains had very similar distribution patterns of Fe, but the DC1.16 grain section had stronger Fe staining.

Fe staining down to cellular resolution in rice grains is shown on the dorsal (Figure 4.11) and ventral side (Figure 4.12). From the seed coat, there was only one layer of stained aleurone cells on the ventral side, while multiple layers of the aleurone and subaleurone cells can be seen on the dorsal side. On the dorsal side of the non-transgenic grain section, the abundant signal of

Fe staining was in the single aleurone cell and with only slight staining in the subaleurone cell layer (Figure 4.11 D and E). There were two peaks of Fe signal in an area 40 µm from the seed coat (Figure 4.11 F). The distribution in *OsNAS2*-expressing grain (SC2.15) sections indicated Fe in both the aleurone and subaleurone layers and extended into the outer endosperm. Multiple peaks of Fe signal were seen 40 µm from the seed coat (Figure 4.11 I). A stronger intensity of Fe signal in both the aleurone and subaleurone layers was found in the SC1.16 and DC1.16, compared to the SC2.15 and non-transgenic control. In spite of the similarity in the distribution of Fe staining in the grain sections, the DC1.16 showed a much stronger intensity and wider extension into the endosperm layer. This was confirmed as the strong intensity of Fe staining extended between 40 µm to 100 µm from the seed coat in the DC1.16 grain, compared to 40 µm to 60 µm in the SC1.16 and 40 µm in the non-transgenic control grains.

On the ventral side, there was a single aleurone cell layer. Very low intensity of Fe staining localized on the ventral side of the longitudinal sections of mature grains in the non-transgenic control (Figure 4.12). There was no remarkable difference in Fe distribution on the ventral side of the SC2.15 and SC1.16 grain sections, compared to the non-transgenic control. The Fe staining mainly localized in the single aleurone cell layer between 20 µm and 30 µm from the seed coat (Figure 4.12 F, I, and L). A much stronger intensity of Fe was however detected in the ventral side aleurone layer at 20-30 µm and extended into 80 µm from the seed coat in the DC1.16 grain (Figure 4.12 M, N and O).

To determine the Zn distribution in mature grains, 9-µm thick sections as described above were prepared and then stained by DTZ (Choi *et al.* 2007; Ozturk *et al.* 2006). Zn staining appears from orange at lower concentrations to pink at higher concentrations. Irrespective of genotype, the embryo tended to stain pink and the endosperm orange (Figure 4.13). There was no intensification

step, thus the Zn staining had a relatively lower intensity, but these results were sufficient to visualise Zn distribution. The stained images were converted to a 3D surface plot by the ImageJ software. Similar to previous reports (Johnson *et al.* 2011; Kyriacou *et al.* 2014; Trijatmiko *et al.* 2016), the distribution of Zn staining was across the endosperm region and the embryo of the longitudinal sections of grains. The intensity of Zn staining in the SC2.15, SC1.16 and DC1.16 were far stronger, especially on the ventral side of grains (Figure 4.13 D, E and F), compared to the non-transgenic grain. Interestingly, the Zn staining in the DC1.16 grain was strongest on both the ventral and dorsal sides (Figure 4.13 F).

There was no difference in the distribution pattern of Zn staining in the rice embryo between the non-transgenic and transgenic grains (Figure 4.14). The Zn staining was localized to the scutellum and the plumule of the embryo. Compared to the non-transgenic grains, stronger Zn staining was found in the transgenic grains, especially in the DC1.16 line (Figure 4.14 K and L).

This work also focused on determining how Zn was distributed on both the ventral and dorsal sides of the rice endosperm (Figure 4.15). The Zn staining was mostly distributed across the endosperm region, with little Zn detectable in the aleurone and subaleurone cells from the seed coat of the grain in both the transgenic and non-transgenic grains. To compare Zn accumulation on ventral and dorsal sides of the rice endosperm, the Zn staining was calculated based on the percentage of Zn-stained pixels in a specific area from the seed coat to the endosperm (69.83 µm x 206.9 µm or 486000 pixels) and displayed in Figure 4.16. In the non-transgenic grains, the result revealed that the dorsal side of grain section (8.7%) accumulated more Zn staining than the ventral side (3.1%). Compared to the non-transgenic control, accumulation of Zn staining was significantly higher in the transgenic grains (Figure 4.15 and Figure 4.16). Increased accumulation of Zn was seen only on the dorsal side for the SC1.16 grain (over 23%) and only on ventral side

for the SC2.15 grain (17.4%). Consistent with the results for Fe, there was a significant increase in Zn staining both the ventral and dorsal sides of the DC1.16 grain, with 14.9% and 27.3 % respectively.

In summary, there was a clear increase in Fe and Zn on both the dorsal and ventral sides of mature grains in the DC1.16 line where *HvSUT1* and *OsNAS2* were overexpressed, while Fe and Zn accumulations were only seen on one side of mature grains (ventral or dorsal side) in the SC2.15 and SC1.16 events overexpressing single gene, respectively.

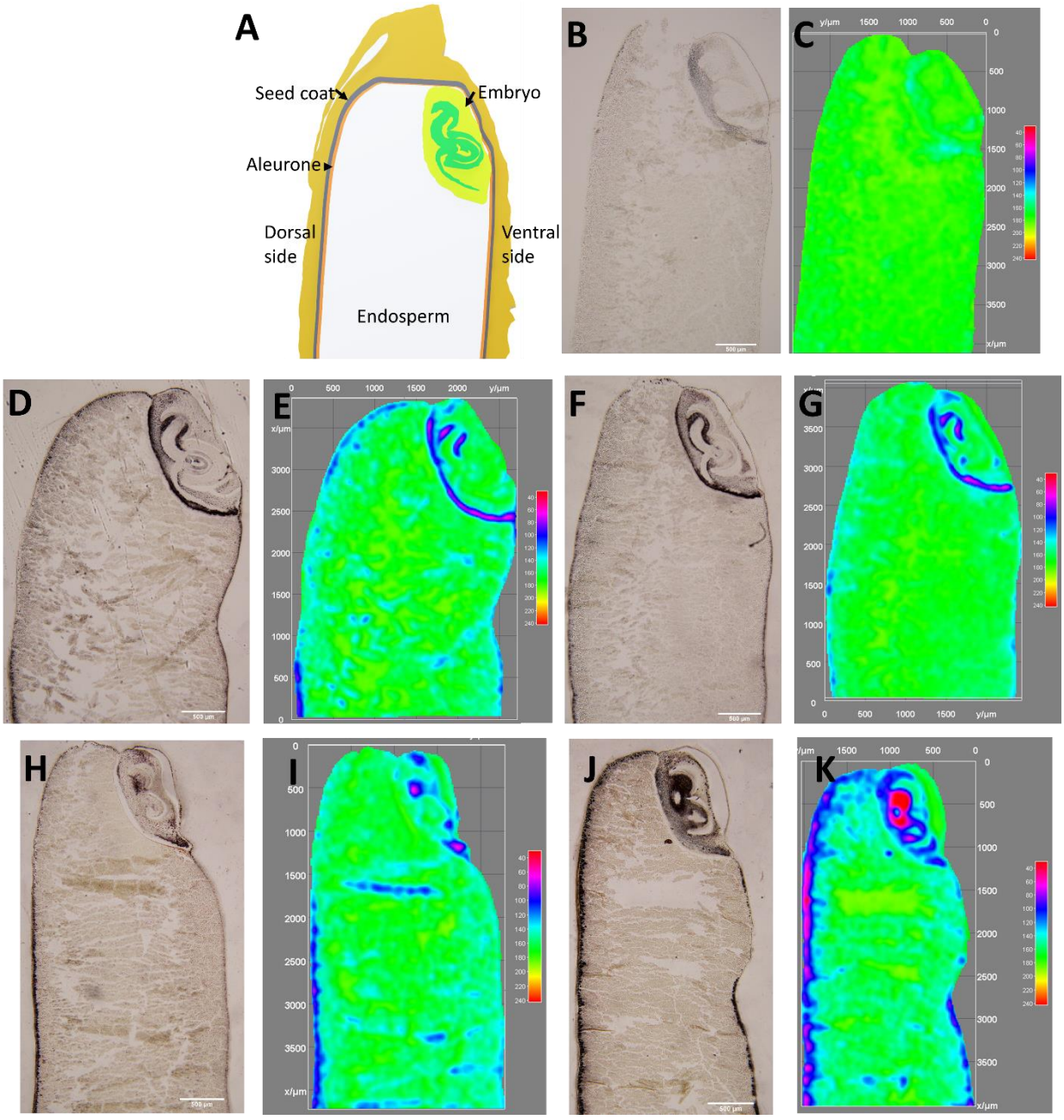

Figure 4.9. Fe accumulation and distribution in longitudinal section of mature grains. (A) Schematic of longitudinal sections of rice grains. The non-transgenic control (D and E), SC2.15 (F and G), SC1.16 (H and I) and DC1.16 (J and K) grains were embedded in paraffin and sectioned into 9 µm sections, then stained with Perls/DAB/$CoCl_2$ or DAB/$CoCl_2$ alone (B and C) as a background control. Fe staining appears as brown to dark brown, dependent on the Fe content. The

stained sections were observed under a light microscope (4X) (B, D, F, H, and J), the images of the stained sections were analysed for the stain intensity (C, E, G, J and K). Yellow to green represents the background, blue-pink represents low to high intensity of the stains. Scale bar = 500 µm.

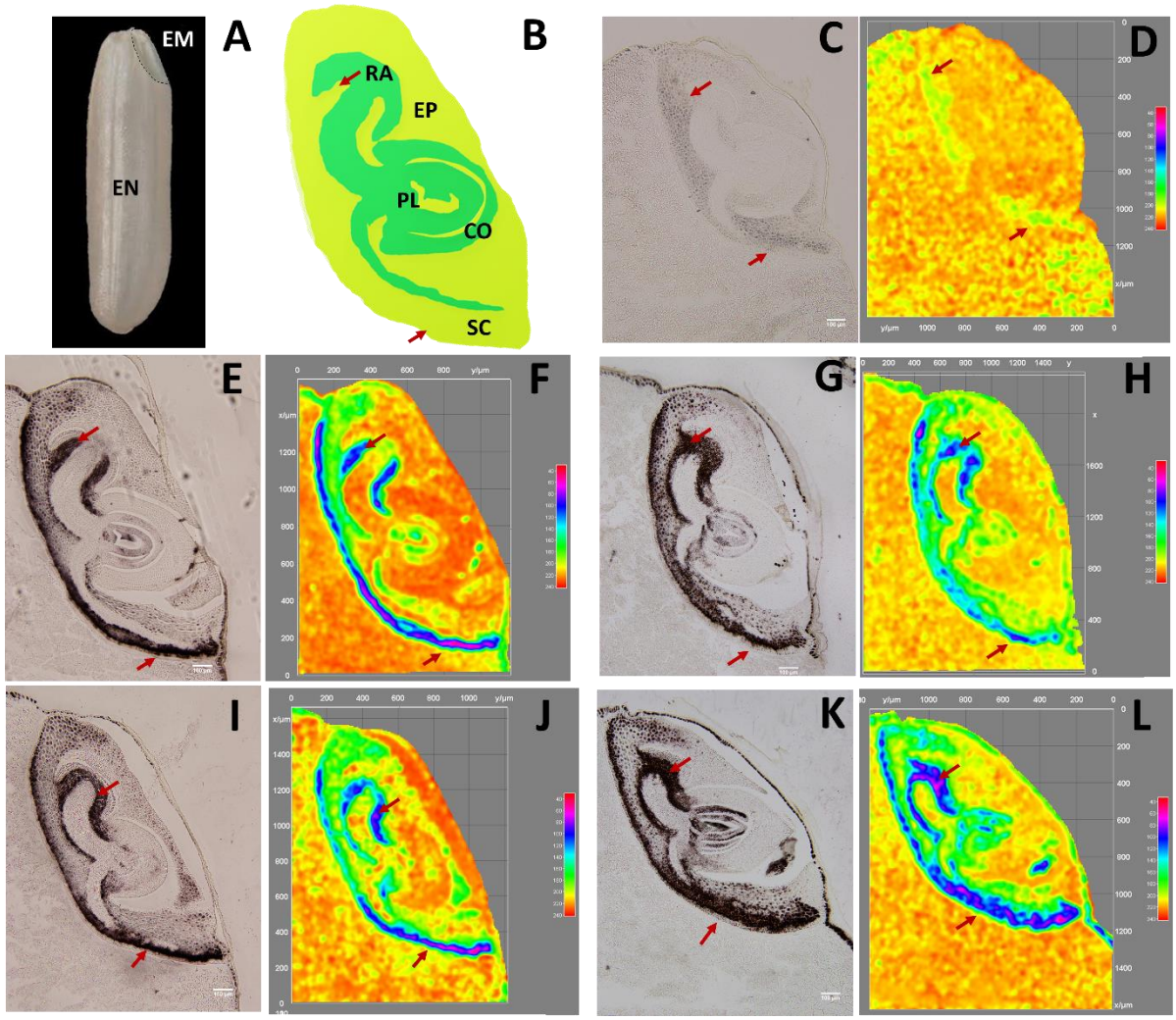

Figure 4.10. Fe accumulation and distribution in embryo sections of mature grains. (A) Morphology of a mature seed of rice. EM: embryo, EN: endosperm. (B) Schematic of longitudinal section of the rice embryo. SC: scutellum, CO: coleoptile, PL: plumule, EP: epiblast, and RA: radicle. The non-transgenic control (E and F), SC2.15 (G and H), SC1.16 (I and J) and DC1.16 (K

and L) embryo sections were embedded in paraffin and dissected into 9 µm sections, then stained with Perls/DAB/$CoCl_2$ or DAB/$CoCl_2$ alone (C and D) as a background control. Fe appeared as brown to dark brown, dependent on the Fe content. The stained sections were observed under light microscope (C, E, G, I, and K), the images of the stained sections were analysed for the intensity of stains (D, F, H, J and L). Orange to green represents the background, blue -pink-red represents the low to high intensity of Fe stains. The stained sections were observed under a light microscope (10X). Scale bar = 100 µm.

sc a s e

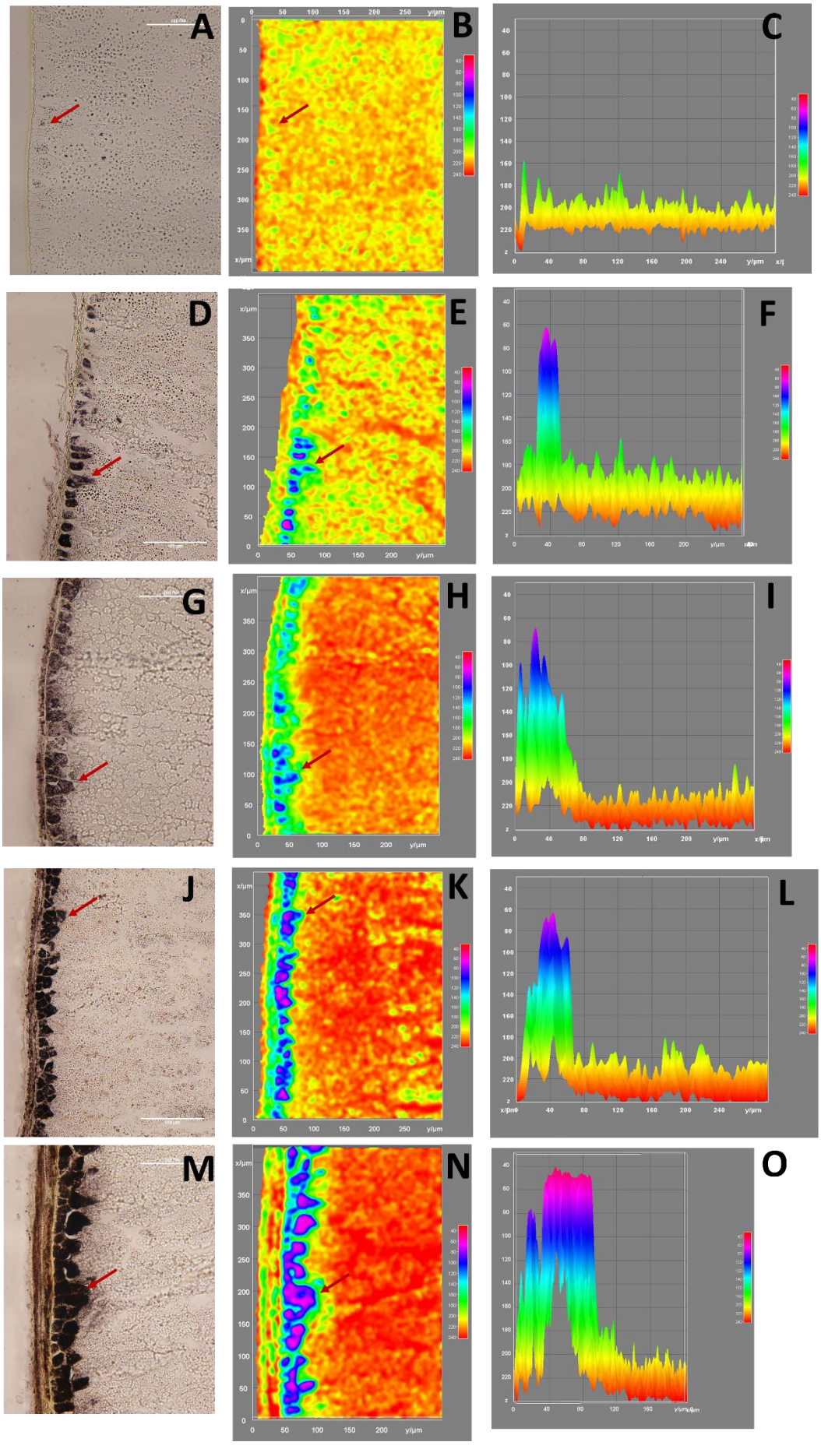

Figure 4.11. Fe accumulation and distribution on the dorsal side of mature grains. The non-transgenic control (D, E and F), SC2.15 (G, H and I), SC1.16 (J, K and L) and DC1.16 (M, N and O) dorsal side of grain longitudinal sections were embedded in paraffin and sectioned into 9 µm sections, then stained with Perls/DAB/$CoCl_2$ or DAB/$CoCl_2$ alone (A, B and C) as a background control. Fe stain appears as brown to dark brown, dependent on the Fe content. The stained sections were observed under a light microscope (40X) (A, D, G, J, and M), the images of the stained sections were analysed for the intensity of stains (B, E, H, K and N). Orange to green represents the background, blue-pink represents the low to high intensity of the stains. Scale bar = 100 µm. A plot of Fe distribution from the seed coat to the endosperm is shown in C, F, I, L and O. Scale bar = 100 µm. sc: seed coat, a: aleurone, s: subaleurone, and e: endosperm.

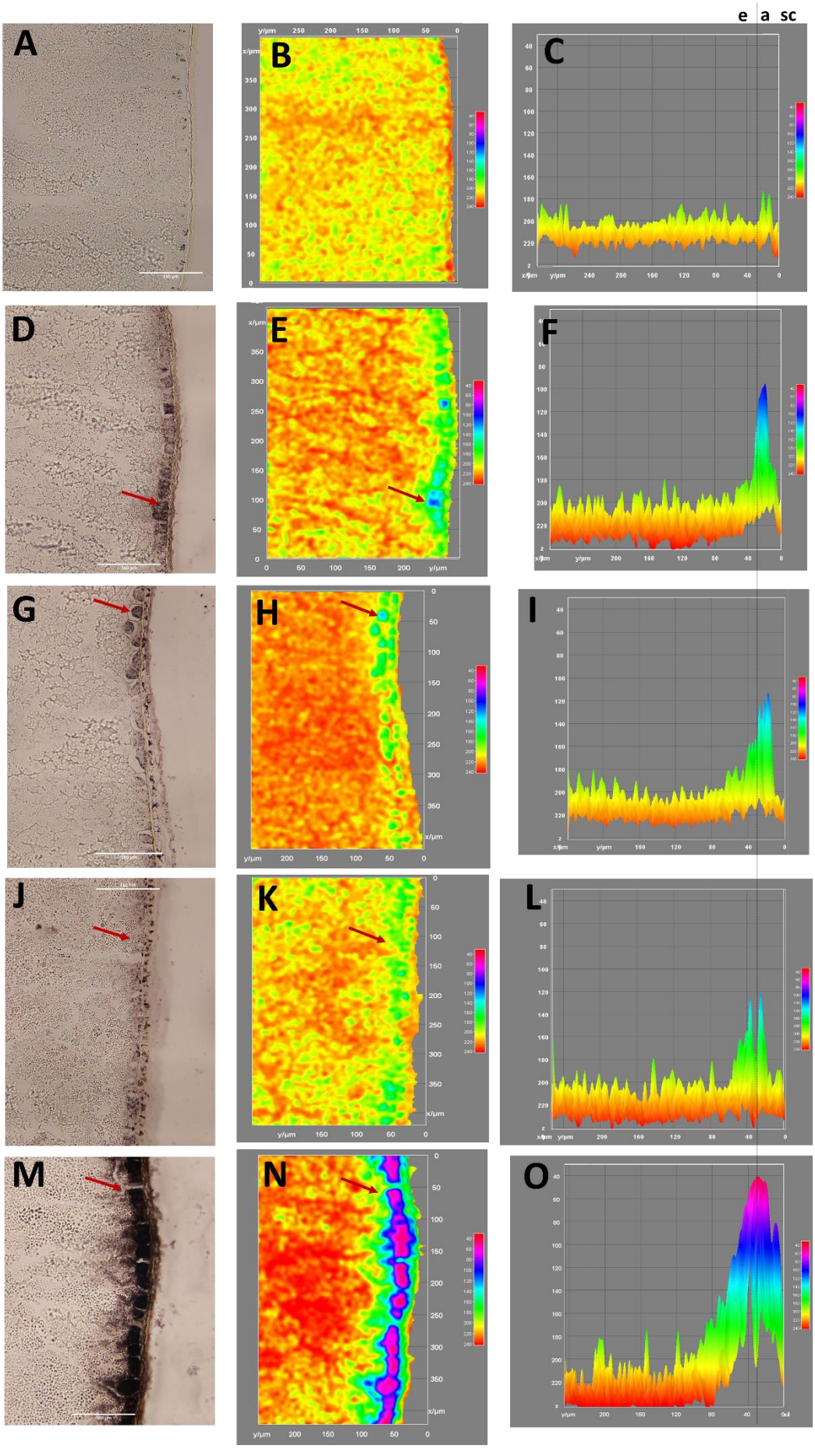
e a sc
A
B
C
D
E
F
G
H
I
J
K
L
M
N
O

Figure 4.12. Fe accumulation and location on the ventral side of mature grains. The non-transgenic control (D, E and F), SC2.15 (G, H and I), SC1.16 (J, K and L) and DC1.16 (M, N and O) ventral side of grain longitudinal sections were embedded in paraffin and sectioned into 9-µm sections, then stained with Perls/DAB/$CoCl_2$ or DAB/$CoCl_2$ alone (A, B and C) as a background control. Fe stain appears as brown to dark brown, dependent on the Fe content. The stained sections were observed under a light microscope (40X) (A, D, G, J, and M), the images of the stained sections were analysed for the intensity of stains (B, E, H, K and N). Orange to green represents the background, blue-pink represents the low to high intensity of the stains. Scale bar = 100 µm. A plot of Fe distribution from the seed coat to the endosperm is shown in C, F, I, L and O. Scale bar = 100 µm. sc: seed coat, a: aleurone, e: endosperm.

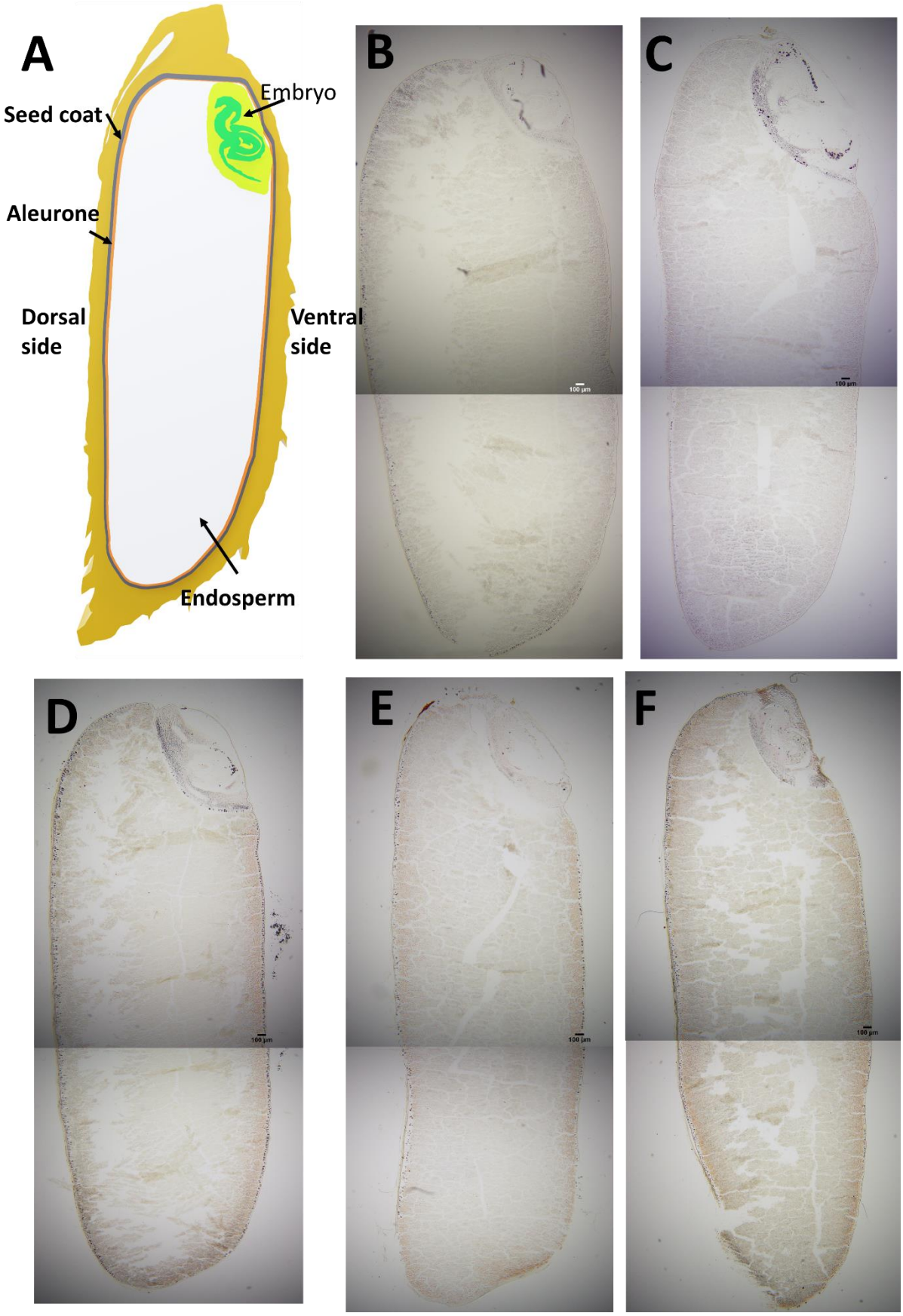
A
Embryo
Seed coat
Aleurone
Dorsal side
Ventral side
Endosperm
B
C
D
E
F

Figure 4.13. Zn accumulation and distribution in longitudinal sections of mature grains. (A) Schematic of the longitudinal section of rice grains. The non-transgenic control (C), SC2.15 (D), SC1.16 (E) and DC1.16 (F) grains were embedded in paraffin and sectioned into 9 µm sections, then stained with DTZ or without DTZ (B) as a background control. Zn staining appears from pink to orange. The stained sections were observed under a light microscope (4X). Scale bar = 100 µm.

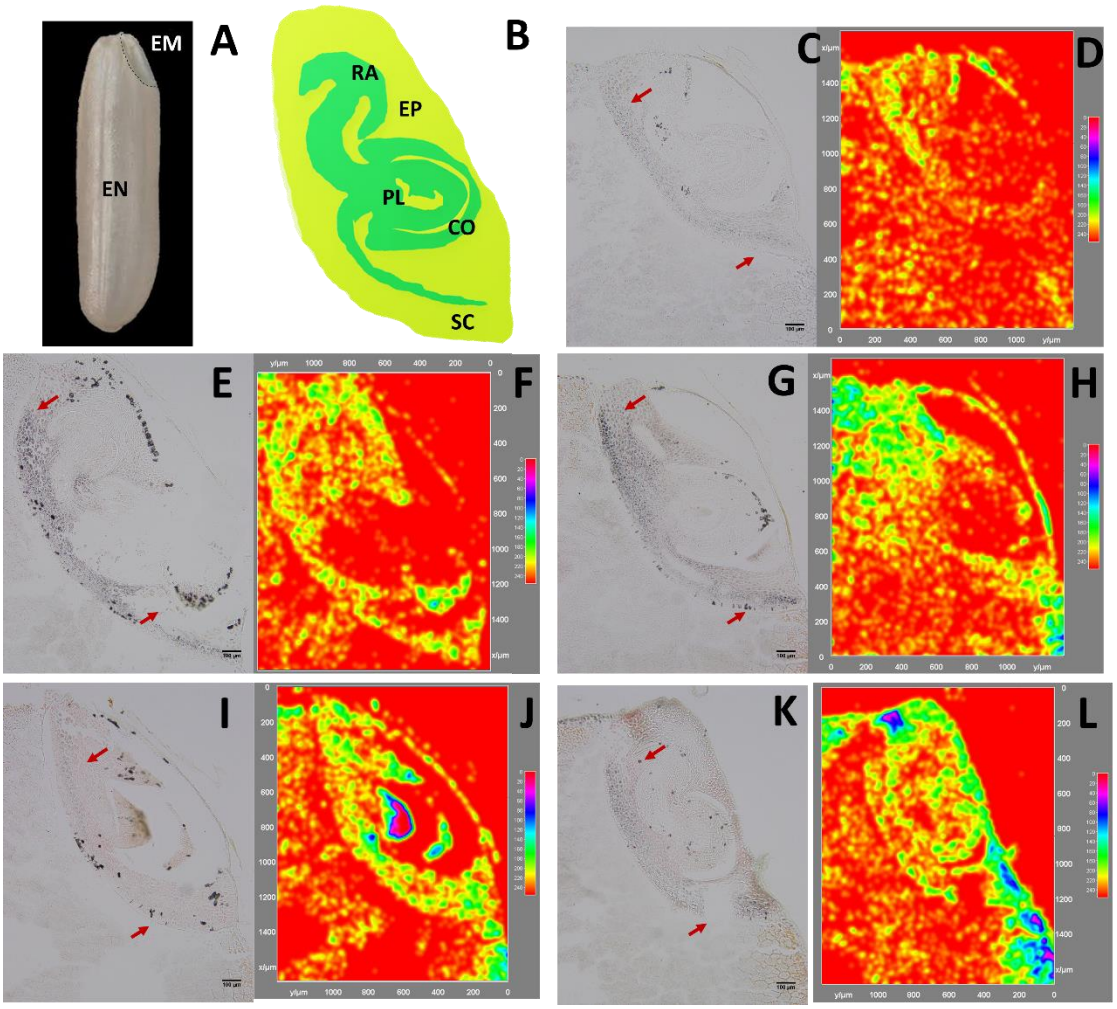

Figure 4.14. Zn accumulation and distribution in embryo sections of mature grains. (A) Morphology of a mature seed of rice. EM: embryo, EN: endosperm. (B) Longitudinal section of the rice embryo. SC: scutellum, CO: coleoptile, PL: plumule, EP: epiblast, and RA: radicle. The non-transgenic control (E and F), SC2.15 (G and H), SC1.16 (I and J) and DC1.16 (K and L)

embryo sections were embedded in paraffin and dissected into 9 μm sections, then stained with DTZ or without DTZ (C and D) as background control. Zn appeared as pink stain, which is dependent on Zn content. The stained sections were observed under a light microscope (10X) (C, E, G, I, and K), the images of the sections were analysed for stain intensity (D, F, H, J and L). Red to yellow represent the background, green-blue-pink represent low to high, respectively. Scale bar = 100 μm.

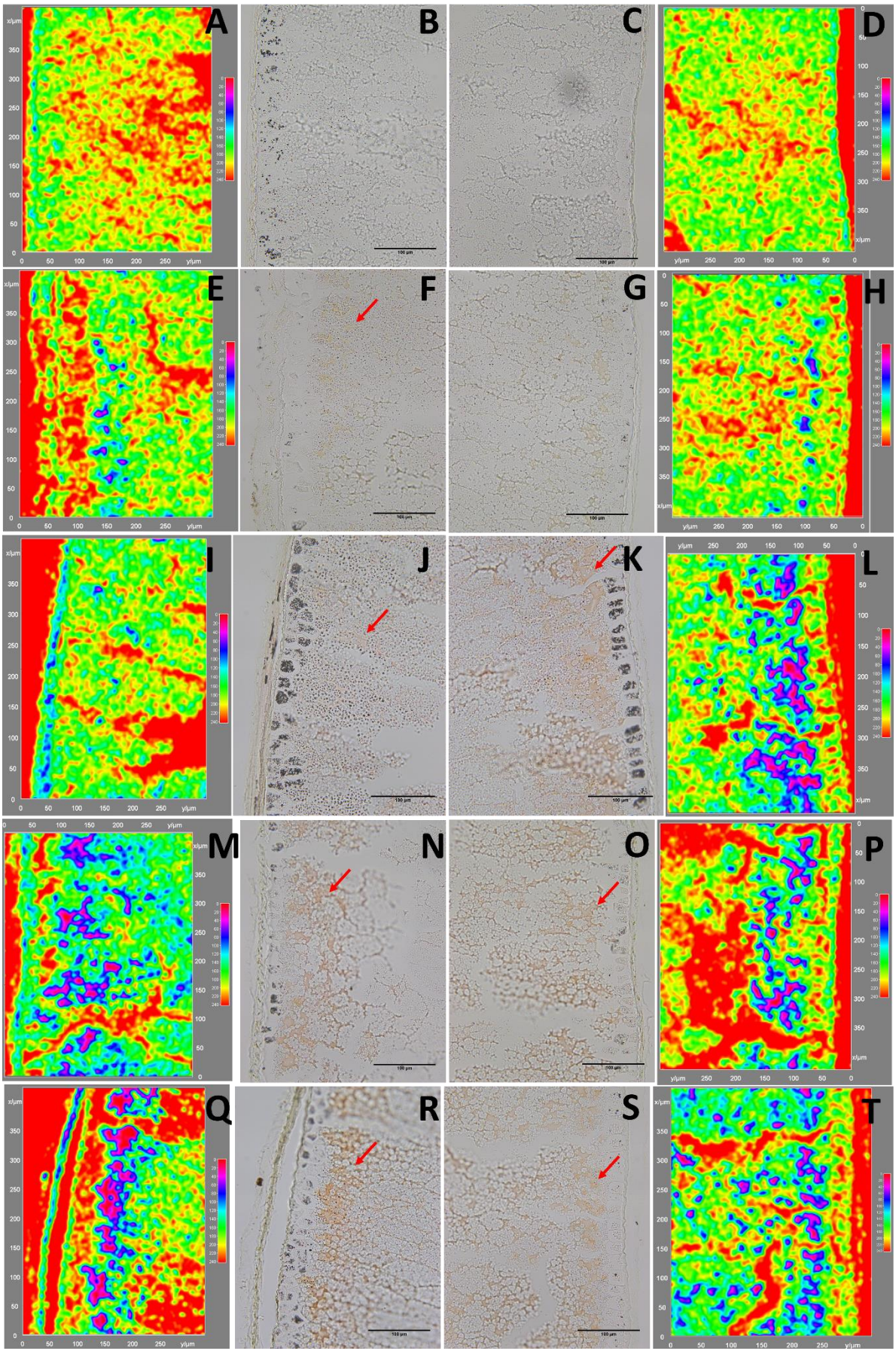
A
B
C
D
E
F
G
H
I
J
K
L
M
N
O
P
Q
R
S
T

Figure 4.15. Zn accumulation and localisation on the dorsal and ventral sides of mature grains. The non-transgenic control (E, F, G and H), SC2.15 (I, J, K and L), SC1.16 (M, N, O and P) and DC1.16 (Q, R, S and T) dorsal and ventral side of grain longitudinal sections were embedded in paraffin and sectioned into 9 µm sections, then stained with DTZ or without DTZ (A and B for dorsal side; C and D for ventral side) as a background control. Zn stain appears from orange to pink, dependent on the Zn content. The stained sections were observed under a light microscope (40X) (F, J, N, and R for dorsal side; G, K, O, and S for ventral side), the images of the sections were analysed for stain intensity (E, I, M, and Q for dorsal side; H, L, P, and T for ventral side). Red to green represent the background, blue to pink represent low to high intensity of the Zn stain. Scale bar = 100 µm.

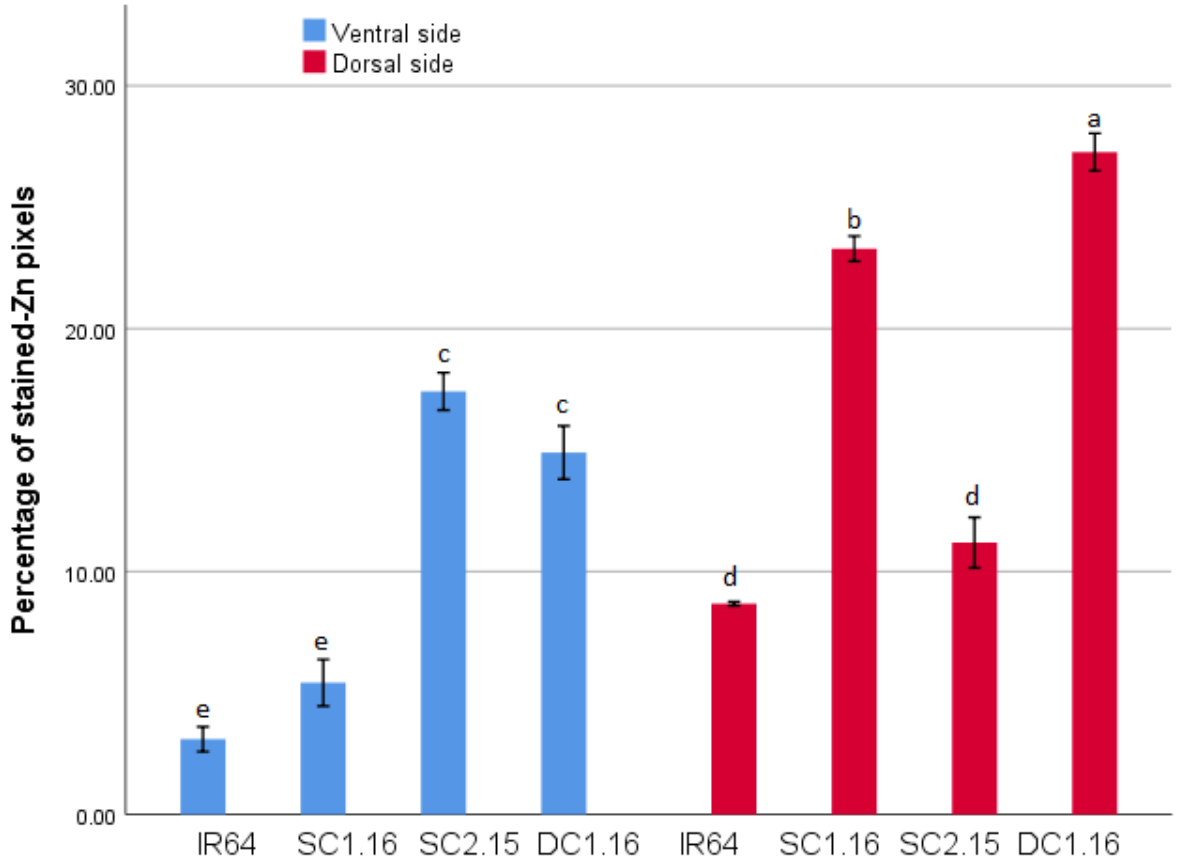

Figure 4.16. A comparison in percentage of stained-Zn pixels in the ventral (blue) and dorsal sides (red) of transgenic rice and non-transgenic IR64 grains. The stained pixels in three regions between the seed coat to the endosperm (69.83 µm x 206.9 µm or 486000 pixels) from the stained sections captured under a light microscope (40X) were counted. Bars represent average percentage of Zn-stained pixels (± SE) of 4 replicates. Significantly different levels are indicated by different letters as determined by a student's t-test.

4.3.4. Phytate to mineral ratios indicates improved bioavailability.

In humans, absorption of Fe and Zn from food is directly related to its phytate content (Brune *et al.* 1992). To gauge the bioavailability of Fe and Zn in the transgenic grains reported here, phytate concentration (Figure 4.17) and molar ratios of phytate to iron (Phytate:Fe), zinc (Phytate:Zn) and calcium (Phytate:Ca) (Figure 4.18) were calculated and compared to those ratios in non-transgenic control. The concentration of phytate levels in the non-transgenic control grains was measured to be 10.7 mg/g in unpolished, and 3.95 mg/g in polished grains. This was not significantly different than those in transgenic lines of the DC1, SC1 and SC2 populations. For unpolished grains, the average phytate concentration in the DC1 lines was 8.69 mg/g (from 6.73 mg/g to 11.19 mg/g), which was lower than those in the SC1 lines with 9.74 mg/g (from 5.30 mg/g to 12.97 mg/g) and higher than those in the SC2 lines with 7.17 mg/g. After milling for 150 seconds, approximately 30% of the phytate remained in the polished grains. The average phytate concentration was lowest in the DC1 lines, but there was no significant difference to that of the SC1 and SC2 grains. However, three independent DC1 lines, namely DC1.1, DC1.13 and DC1.5 were significantly lower than the non-transgenic control. Similarly, SC1.21, SC1.22 and SC1.25 had significantly lower phytate concentration than the controls.

Molar ratios of phytate to iron (Phytate:Fe), zinc (Phytate:Zn) and calcium (Phytate:Ca) were calculated to provide an indication of their bioavailability (Gibson *et al.* 2010; Ma *et al.* 2005). These results presented in Figure 4.18, indicate the likely improved bioavailability in all transgenic grains as they had lower Phytate:Fe, Phytate:Zn and phyate:Ca ratios, compared to non-transgenic control grains. In unpolished and polished grains, the molar ratios of phytate to Fe in the three transgenic populations were significantly lower than those in the non-transgenic control, except for the SC1.22 line where there was no significant difference. The phytate:Fe molar ratio

in all the transgenic lines and the non-transgenic control were higher than 1, where a ratio lower than 1 is an indication of high bioavailability (Hallberg *et al.* 1989).

For Zn bioavailability, a phytate:Zn molar ratio <18 is regarded as high (Gibson *et al.* 2010). Interestingly, along with the non-transgenic control, phytate:Zn molar ratios in all the transgenic lines were lower than 18, and significantly lower than the non-transgenic control. In unpolished grains, all transgenic lines overexpressing *OsNAS2* had phytate:Zn molar ratios of <18 which was significant lower, compared to the non-transgenic control, whereas the transgenic SC1 lines overexpressing *HvSUT1* only had phytate:Zn molar ratios of >18, which was not significantly lower than the non-transgenic control. For Ca bioavailability, phytate:Ca molar ratios >0.24 are considered indicative of good Ca bioavailability (Morris & Ellis 1985). Although none of the transgenic grains had phytate:Ca molar ratios of <0.24, the DC1 grains were significant lower than the non-transgenic control in both polished and unpolished grains (with 2 and 1.69, compared to 2.52 and 2.85 for the control). The SC1 events had significant lower phytate:Ca molar ratio in polished grains, but no significant difference in unpolished.

Analyses using the Pearson's correlation coefficient of fold change in Fe, Zn, Ca, P and phytate concentration relative to the non-transgenic control were conducted to see their relation in the rice grains from all the transgenic events from the three populations (Table 4.3). The results revealed that phytate change in polished and unpolished grains had a weak correlation with the changes in Fe, Zn, Ca, and P. Interestingly, there was a significant and strong correlation of P change with Fe, Zn and Ca in unpolished and polished grains, except for Fe in unpolished grains. The fold change in Zn significantly correlated with Fe and Ca in both polished and unpolished grains. In general, increased Fe and Zn concentrations were not related with phytate, but correlated with P.

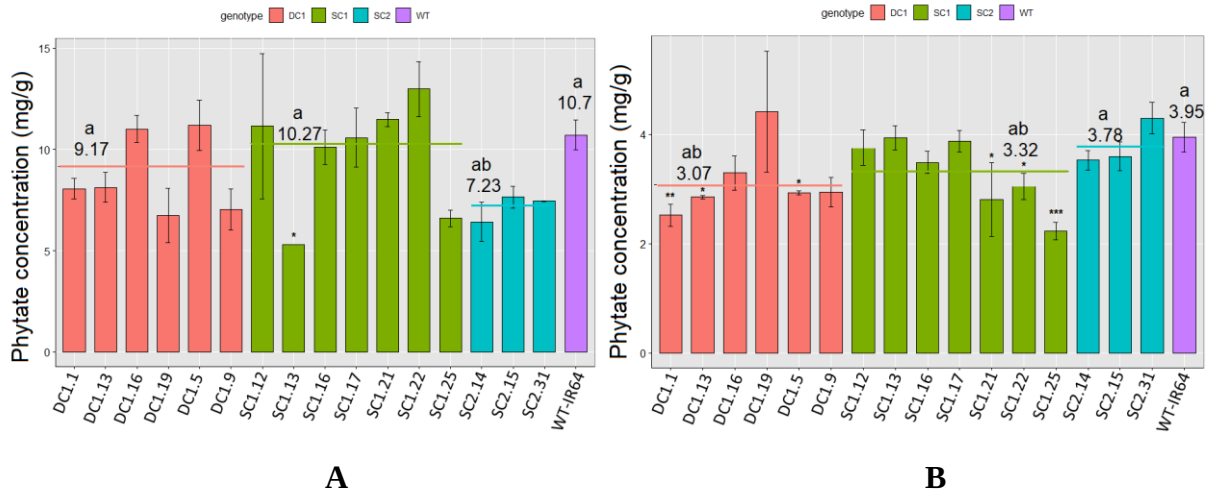

A **B**

Figure 4.17. Phytate concentration in unpolished grains (A) and polished grains (B). Bars represent mean ± SE of at least 3 biological replicates of the DC1 (orange), SC1 (green) and SC2 (blue) lines, compared to the non-transgenic control (purple). Asterisks denote the significance between the transgenic lines and the control for $P < 0.05$ (*), $P \leq 0.01$ (**), $P \leq 0.001$ (***) as determined by a student's t-test. Orange, green and blue horizontal lines represent means of 3 independent lines DC1, SC1 and SC2, compared to the non-transgenic control. The differences with the same letter are not significant.

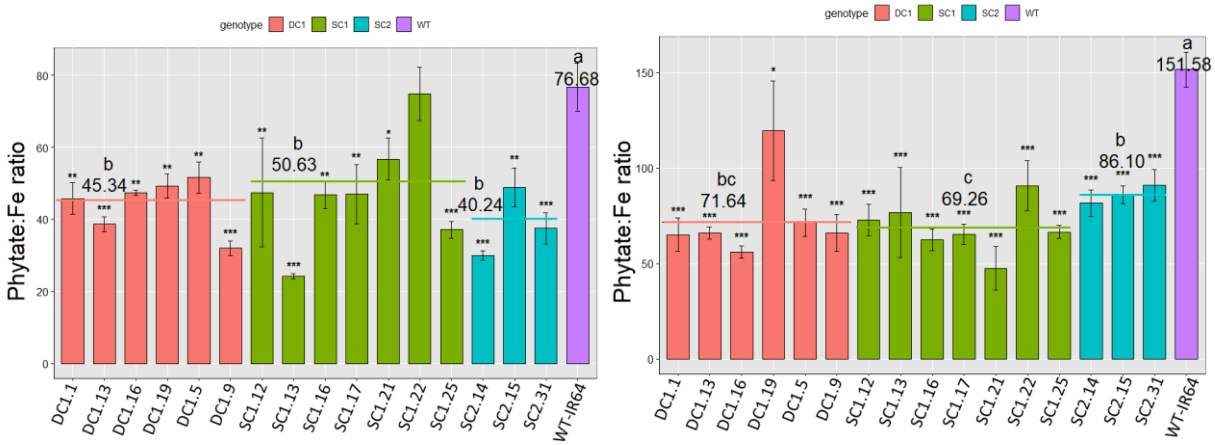

A **B**

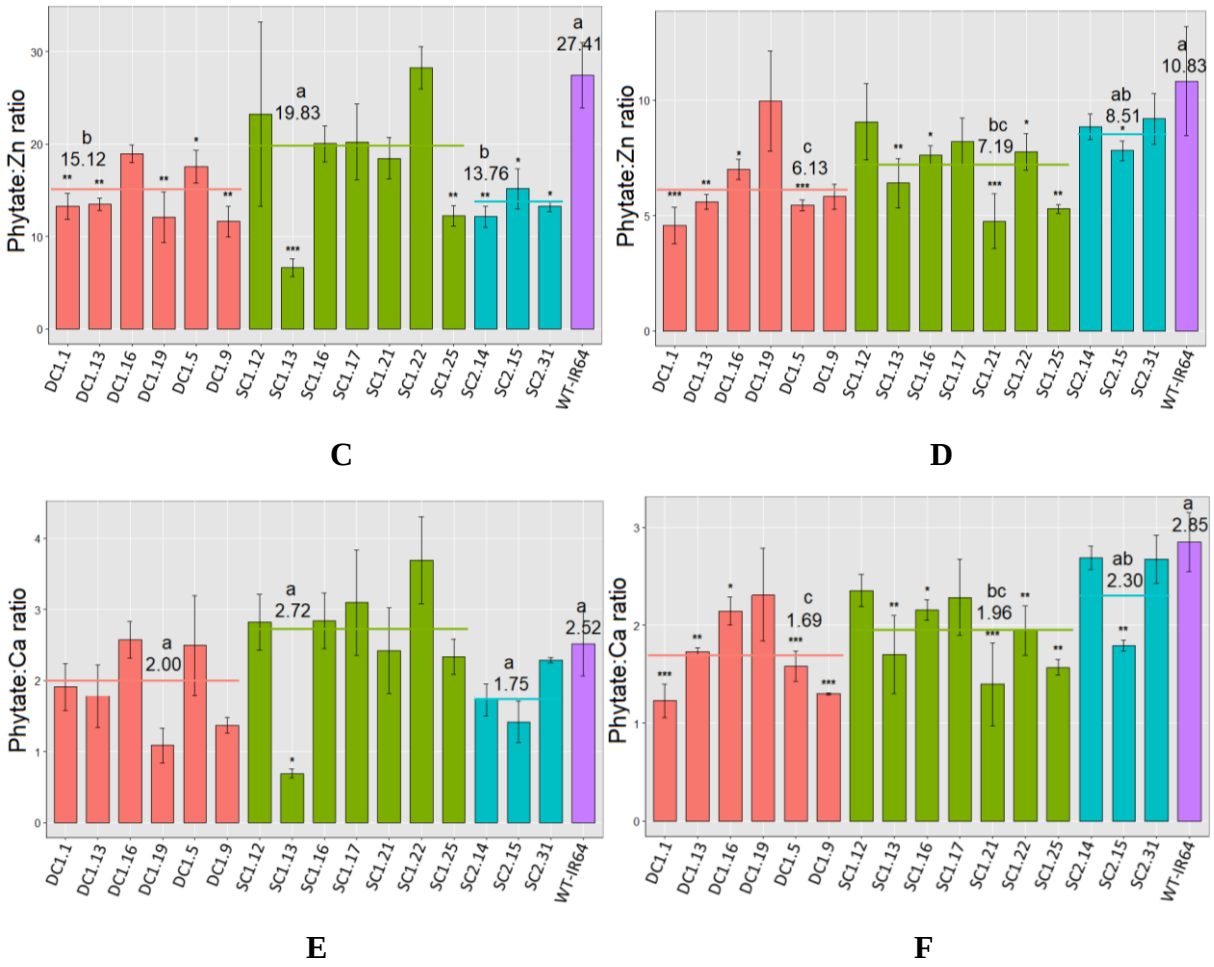

Figure 4.18. Molar ratios of phytate to iron (Phytate:Fe) in unpolished and polished grains (A and B), zinc (Phytate:Zn) (C and D) and calcium (Phytate:Ca) (E and F). Bars represent mean ± SE of at least 3 biological replicates of the DC1 (orange), SC1 (green) and SC2 (blue) lines, compared to the non-transgenic control (purple). Asterisks denote the significance between the transgenic lines and the control for $P < 0.05$ (*), $P \leq 0.01$ (**), $P \leq 0.001$ (***) as determined by a student's t-test. Orange, green and blue horizontal lines represent means of 3 independent lines DC1, SC1 and SC2, compared to the non-transgenic control. The differences with the same letter are not significant.

Table 4.3. Pearson's correlation analysis of fold change in Fe, Zn, Ca, P and Phytate concentrations (mg/kg) relative to the non-transgenic IR64 in unpolished (A) and polished grains (B). **Bold** and small numbers represent correlation coefficients (r) and p values, respectively.

A. Unpolished grain

	Zn	**Ca**	**P**	**Phytate**
Fe	**0.34****	**- 0.24**	**- 0.05**	**0.26**
	0.008	0.065	0.728	0.079
Zn		**0.48****	**0.45****	**- 0.29***
		0.000	0.000	0.047
Ca			**0.43****	**- 0.23**
			0.001	0.119
P				**- 0.21**
				0.154

B. Polished grain

	Zn	**Ca**	**P**	**Phytate**
Fe	**0.39****	**0.02**	**0.68****	**0.12**
	0.002	0.904	0.000	0.420
Zn		**0.62****	**0.60****	**- 0.19**
		0.000	0.000	0.203
Ca			**0.38****	**- 0.17**
			0.003	0.251
P				**0.05**
				0.733

*. Correlation is significant at the 0.05 level (2-tailed).

**. Correlation is significant at the 0.01 level (2-tailed).

4.3.5. Analysis of toxic metal elements

ICP-MS elementary analysis also enabled the examination of three toxic metal ions, including arsenic (As), nickel (Ni) and cadmium (Cd) in the transgenic grains of the SC1, SC2, DC1 lines and non-transgenic IR64 control plants grown in normal soil under greenhouse conditions (Figure 4.19). The As concentration of all transgenic lines was low (0.1 mg/kg) in unpolished grains and around 0.05 mg/kg in polished grains. Ni concentration was less than 0.2 mg/kg in unpolished grain and around 0.1 mg/kg in polished grains of all transgenic events, and Cd levels in the DC1 events were around 0.2 mg/kg in polished grains, which was not significantly different with Cd concentration in the non-transgenic control. Interestingly, the SC1 events with only *HvSUT1* overexpression had 50% lower Cd concentrations than the non-transgenic control grains although there was a high level of variation between independent SC1 events. All samples returned concentrations that were not higher than the recommended limits of 0.2, 1.0 and 0.2 mg/kg for As, Ni and Cd, respectively.

A comparison of arsenic (As), nickel (Ni) and cadmium (Cd) concentrations relative to the non-transgenic control was performed (Figure 4.20) with the non-transgenic control set at 0%. In unpolished and polished grains, accumulation of Cd and Ni in transgenic events was lower relative to the non-transgenic IR64. An opposite pattern was found in As accumulation with a significant increase of around 50% in the polished grains from the SC1 and SC2 events when compared to the non-transgenic control. The DC1 events showed a non-significant increase in As accumulation in the polished grains, excepting for DC1.16 with a significant difference.

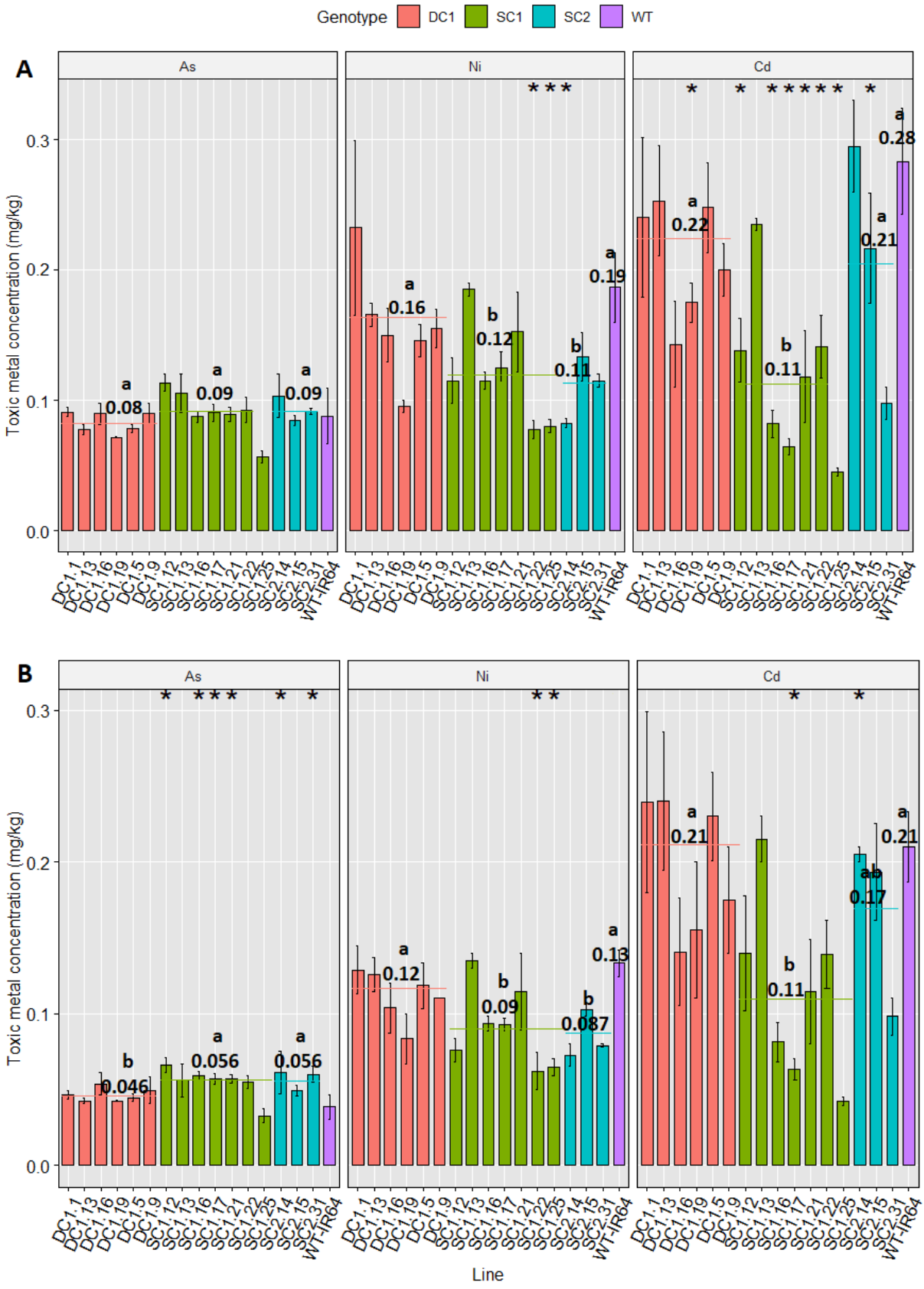
Genotype
DC1
SC1
SC2
WT
A
As
Ni
Cd
Toxic metal concentration (mg/kg)
0.0
0.1
0.2
0.3
a
0.08
a
0.09
a
0.09
a
0.16
b
0.12
b
0.11
a
0.19
a
0.22
b
0.11
a
0.21
a
0.28
B
As
Ni
Cd
b
0.046
a
0.056
a
0.056
a
0.12
b
0.09
b
0.087
a
0.13
a
0.21
b
0.11
ab
0.17
a
0.21
DC1.1
DC1.13
DC1.16
DC1.19
DC1.5
DC1.9
SC1.12
SC1.13
SC1.16
SC1.17
SC1.21
SC1.22
SC1.25
SC2.14
SC2.15
SC2.31
WT-IR64
Line

Figure 4.19. Analysis of toxic heavy metal concentrations, namely As, Ni and Cd. Bars represent means of at least 3 biological replicates (±SE) of the DC1 events (orange), SC1 events (green), SC2 events (blue), compared to the non-transgenic control (purple) in unpolished grains (A) and polished grains (B0. Asterisks denote the significance between the transgenic lines and the control for P < 0.05 (*), as determined by student's t-test. Orange, green and blue lines represent means of 3 independent lines DC1, SC1 and SC2, compared to the non-transgenic control. The differences with the same letter are not significant.

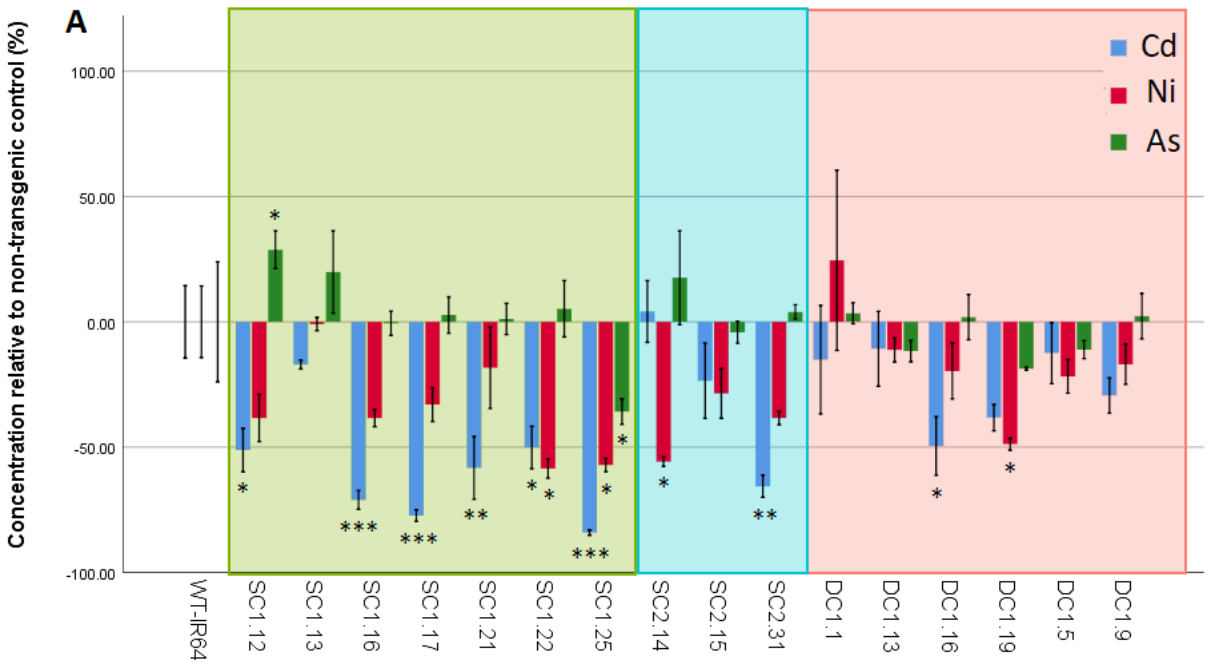

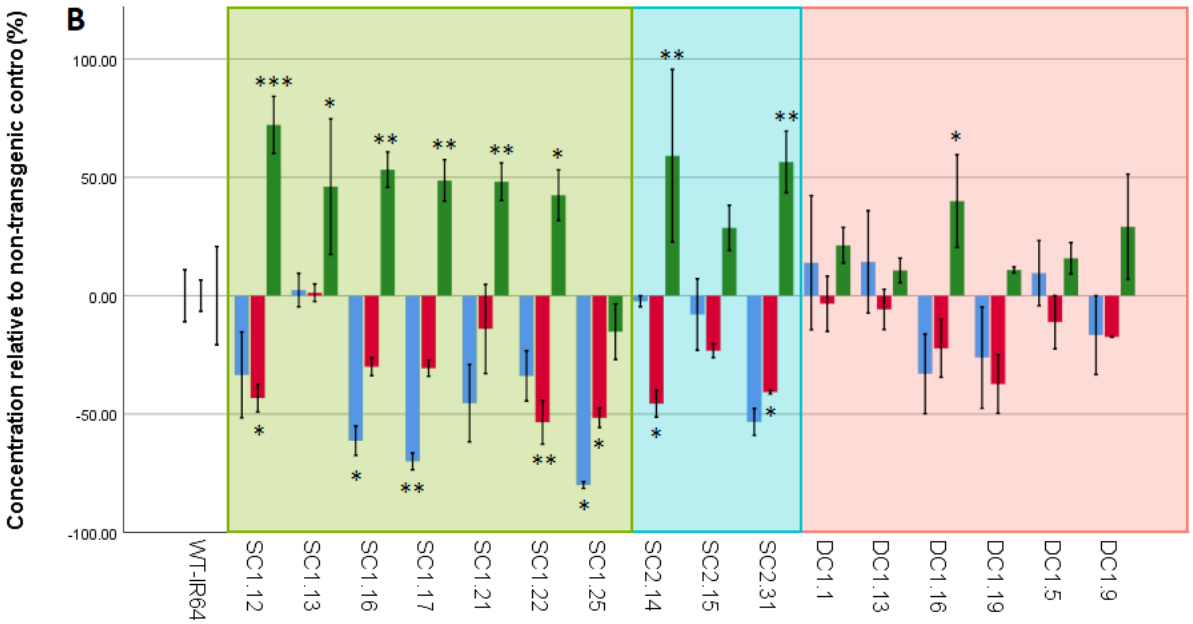

Figure 4.20. Toxic heavy metal concentration of T2 grains from the SC1, SC2 and DC1 events relative to the non-transgenic control. Bars represent means of at least 3 biological replicates (±SE) of Cd (blue), Ni (red) and As (green) in unpolished grains (A) and polished grains (B). Asterisks denote the significance between the transgenic lines and the control for $P < 0.05$ (*), $P \leq 0.01$ (**), $P \leq 0.001$ (***) as determined by student's t-test. Multiple independent transgenic lines overexpressing *HvSUT1* alone (SC1), *OsNAS2* alone (SC2) and the combination of *HvSUT1* and *OsNAS2* (DC1) were represented in green, blue, and red boxes, respectively.

4.4. Discussion

4.4.1. Semi-quantitative methods using histochemical analyses of Fe and Zn distribution in mature rice grains.

Histochemical analysis using Perl's Prussian blue stain (PPB) are commonly used to investigate *in situ* Fe localization and semi-quantitation in rice grains (Choi *et al.* 2007; Prom-u-thai *et al.* 2003). The Perls reagent stains free Fe on the surface of the sample and it reacts preferentially with ferric ions (Fe^{3+}) than ferrous ions (Fe^{2+}) (Meguro *et al.* 2007; Roschzttardtz *et al.* 2009; Roschzttardtz *et al.* 2013). The Perls method can stain tissues where Fe is heavily accumulated, so it is challenging to detect and quantitate Fe accumulation in the rice grain where it is in such low concentration. The threshold of Fe detection using the Perls method is therefore rarely reached in thin sections of rice grains. All past histochemical analyses with the Perls reagent to detect Fe accumulation in rice were performed on a half-grain section, failing to obtain stained images with cellular resolution.

In this study, the Perls method combined with a DAB/H_2O_2/$CoCl_2$ intensification step (termed Perls/DAB/$CoCl_2$ method) was used to visualise Fe distribution in 9-µm longitudinal sections of the rice grains. The Perls/DAB/$CoCl_2$ method had been described and applied for Fe staining in animal tissue (Meguro *et al.* 2007; Nguyen-legros *et al.* 1980), then adapted for Fe^{3+} and Fe^{2+} staining in *Arabidopsis* tissues (Roschzttardtz *et al.* 2009; Roschzttardtz *et al.* 2013). The Perls/DAB/$CoCl_2$ method was specified for Fe ions and stained most of the Fe in cells, excepting heme Fe which do not react with the reagents (Nguyen-legros *et al.* 1980). To my knowledge, the Perls/DAB/$CoCl_2$ method has not been used to detect Fe localization in a mature rice grain. Like the previous reports, this study yielded very high-resolution images of Fe localization with a cellular resolution. The pattern of Fe distribution in the whole grain was very consistent with the

results analysed by synchrotron X-ray fluorescence microscopy (SXRF) and LA-ICP-MS by Kyriacou *et al.* (2014) and Huynh (2015), respectively. In the reports of Meguro *et al.* (2007), Roschzttardtz *et al.* (2009) and Roschzttardtz *et al.* (2013), along with the major drawback that a portion of Fe in the central region of starch endosperm could be lost during the fixation and dehydration steps, no tool was used or suggested for statistical quantitation or comparison of staining intensity in the images. Here, this study demonstrated the adaption and utility of an open-source plugin (ImageJ) that is compatible with automating semi-quantitative analysis and scoring of the stained images. The semi-quantitative analysis was used for investigating Fe staining intensity and distribution pattern in the whole grain (see Figure 4.9 - Figure 4.12).

The product of Perls/DAB staining from brown to dark brown is dependent on the Perls Prussian blue colour corresponding to Fe content in tissues (Meguro *et al.* 2007; Roschzttardtz *et al.* 2009). It is difficult to distinguish the DAB intensity by human eye, but possible for several image processing programs, for example the ImageJ software. A common tool of colour deconvolution in ImageJ software was used in semi-quantitative Immunohistochemistry (IHC) to separate the DAB stain from the DAB-stained image and then used to automatically score and quantify the intensity of the DAB stain (Varghese *et al.* 2014). The Perls/DAB/$CoCl_2$ method shared the same DAB staining, thus the tool of colour deconvolution in ImageJ software was adapted to quantify the DAB intensity in this study.

Histochemical analysis of Zn using dithizone (DTZ) staining was also adapted to visualize the Zn distribution with cellular resolution in the rice grains via a light and electron microscopy, and the stained image was used for semi-quantitation analysis by ImageJ. DTZ staining is commonly used for detecting Zn in grain tissue (Cakmak *et al.* 2010; Choi *et al.* 2007; Duarte *et al.* 2016; Jaksomsak *et al.* 2014; Ozturk *et al.* 2006; Prom-u-thai *et al.* 2010). After reaction with

Zn, a red-coloured complex with DTZ is formed and the intensity of DTZ-stain is correlated to the grain Zn concentrations (Ozturk *et al.* 2006). Therefore, the DTZ-stained images were used here for semi-quantitation by comparison of the intensity level using ImageJ software. Unlike the method of Duarte *et al.* (2016), the DTZ stained images of 9-µm sections of unpolished mature rice grain captured under the Brightfield BX53 Microscope were analysed by the tool of colour deconvolution in ImageJ software to separate the red staining of Zn-DTZ complex. The map of Zn distribution in the rice grain was consistent with the results of Johnson *et al.* (2011) and Kyriacou *et al.* (2014) using synchrotron X-ray fluorescence spectroscopy, as Zn was abundant in the embryo tissue and distributed broadly in the whole grain, and was not limited to the aleurone layers.

This study confirms the use of these techniques as rapid and cost-effective tools to visualize and semi-quantitate Fe and Zn distribution with cellular localisation by using Perls/DAB/$CoCl_2$ and DTZ staining combined with analyses of the colour-stained images by ImageJ software. These techniques could be applied on a large scale in rice breeding programs for Fe and Zn biofortification where access to an inexpensive and relatively accurate method is required to analyse a large number of genotypes. Furthermore, these techniques could be adapted with immature grain tissues to investigate dynamic changes in Fe and Zn distribution during grain development. Like as for other histochemical analyses, only a single mineral element is visualized by one chemical staining, compared to multiple mineral elements, as for other higher cost technologies, such as transmission electron microscopy (TEM), scanning electron microscopy (SEM), Synchrotron X-ray fluorescence microscopy (SXRF), and high resolution nanosecondary ion mass spectrometry (nano-SIMS). Therefore, multiple chemical staining methods are required to detect multiple minerals. This is straightforward for a few elements but more complicated for

multiple elements because few specific chemical stains are available. Furthermore, weak and faint staining signals often result from 9 µm sections of grain tissues (which were often seen in the non-transgenic IR64 grain, see Figure 6.7 in Appendix D) because Fe and Zn concentrations are below the threshold of detection. Therefore, the intensification of the staining signal is required to enhance the sensitivity and definition of Fe detection in grain sections. Unfortunately, no method to intensify the Zn staining has been reported, so the Zn staining using the DTZ alone had a relatively weak signal, especially in the non-transgenic control. Another major drawback was that a small portion of Fe or Zn could potentially be lost or drained out of the section during the fixation and dehydration steps (Roschzttardtz *et al.* 2013).

The data for Fe and Zn staining partially supported the ICP-MS results in Table 4.2. The concentrations in the unpolished and polished grains of the DC1.16 line were higher, compared to the SC2.15 and SC1.16 grains overexpressing *OsNAS2* and *HvSUT1*, respectively, and the non-transgenic control. Much stronger intensity of Fe staining was observed in the DC1.16 grains than in SC1.16 grain, while only approximately 13% difference between the two lines was found in Fe concentration.

4.4.2. *HvSUT1* and/or *OsNAS2* expression altered mineral accumulation in rice grains.

In this study, endosperm-specific overexpression of *HvSUT1* in IR64 rice led to a significantly higher accumulation of micronutrients in unpolished grains (approximately 30-40% more Fe and Zn (see Figure 4.3)), consistent with that reported for wheat by Saalbach *et al.* (2014). Other micronutrients (Cu and Mn) increased, but statistically significant differences were not found. This result supports the hypothesis that *HvSUT1*-expressed rice enhances sucrose uptake capacity resulting in modification of mass flow of nutrients into the grain tissue during grain development (Huynh 2015; Saalbach *et al.* 2014; Weichert *et al.* 2010). An increase was also found

in macronutrient accumulation (P, S, Mg and K) in unpolished rice grains, but differences were not statistically significant, compared to the non-transgenic IR64. After milling to obtain polished grains, significant retention of Fe in the rice endosperm was found in the *HvSUT1*-expressing grain, consistent with the result of Nipponbare rice overexpressing *HvSUT1* under the control of the same endosperm-specific (*Glb-1*) promoter (Huynh 2015). In the SC1transgenic lines, the average concentrations of most micronutrients in the grain showed significant differences in Fe, Cu, and Mn, but non-significant differences in Zn. In particular, an increase in Fe accumulation of around 85% was found in the SC1 transgenic lines, whereas a non-significant increase was reported by Huynh (2015). However, in Huynh's study, only a single transgenic Nipponbare rice line (G1.4) was investigated. Meanwhile, multiple homozygous transgenic lines were investigated here, providing more confidence in assessing the effects of *HvSUT1* on grain nutrient accumulation. Other difference between this study and that of Huynh (2015) is the polishing conditions. Here grain polishing was optimized to remove over 15% of the outer layer of the mature rice grains and minimize grain breakage, with almost all the aleurone layer removed. There was not much difference to the polishing condition of Nipponbare grains with approximately 20% weight loss (Huynh 2015). Meanwhile, the commercial white (polished) rice is milled to remove approximately 10% of the outer layer and result in 60-80% losses of mineral elements, compared to the brown (unpolished) grains (Hansen *et al.* 2012). No difference in the ratio of mineral elements in polished grain relative to the unpolished grain was reported between the rice grain polished to remove 15% and 20% loss of weight (Ogiyama *et al.* 2008). IR64 and Nipponbare rice grains have differences in morphology, with long grain in IR64 and round grain in the Nipponbare cultivar. A discrepancy in the milling conditions would therefore not be unexpected. Collectively, these reasons, along with different instrumentation to measure mineral concentration, and different

growth conditions, may contribute to the differences in Fe concentration found in *HvSUT1* expressing Nipponbare rice (Huynh 2015) and IR64 reported here.

Despite these differences, multiple independent events with a similar pattern of Fe and Zn increase in the polished grains were seen in this study. This strongly supports the proposal that overexpressing sucrose transporter results in increasing Fe and Zn accumulation in rice. Furthermore, a similar pattern of increasing accumulation of macronutrients in the rice endosperm of IR64 with *HvSUT1* expression was found, including P, S, and Mg, whereas K concentration decreased.

The transgenic IR64 rice overexpressing *OsNAS2* under control of the endosperm-specific promoter (*GluA2*) also showed a pattern of increasing micronutrients in unpolished or polished grains (especially Fe and Zn). However, the only significant change in Fe was seen in polished grains, compared to the non-transgenic control. Furthermore, the micronutrient accumulation in *OsNAS2*-expressing IR64 grains was lower than the population of *HvSUT1*-expressing IR64 grains. In the previous studies of *OsNAS2* overexpression (Beasley *et al.* 2019a; Johnson *et al.* 2011; Kyriacou *et al.* 2014; Singh *et al.* 2017b; Singh *et al.* 2017c; Trijatmiko *et al.* 2016), gene expression was controlled by a constitutive promoter, making comparison with results presented here difficult. Regardless, all the SC2 lines showed lower Fe concentration in polished grains than transgenic rice with constitutive expression of *OsNAS2* (Trijatmiko *et al.* 2016). This discrepancy is likely due to difference in promoters regulating the expression of *OsNAS*, which is consistent with the results of Zheng *et al.* (2010) where higher Fe and Zn accumulated in transgenic rice grains expressing *OsNAS1* under regulation of the maize ubiquitin promoter, compared to the grains from the transgenic line expressing *OsNAS1* in an endosperm-specific manner. This suggests that increasing only *OsNAS2* in the grain sink has no clear beneficial effect on Fe

accumulation in the grain and should be coupled with an improvement in mineral transport at the source to the grain (Nozoye 2018; Oliva *et al.* 2014; Wirth *et al.* 2009). However, the result was not in conflict with the hypothesis tested as *OsNAS2* expression in the endosperm was aimed at enhancing Fe and Zn mobilisation and bioavailability in the rice endosperm tissue when combined with *HvSUT1* overexpression. This will be discussed now.

The transgenic IR64 rice lines with the combined overexpression of *HvSUT1* and *OsNAS2* in the endosperm tissue (designated DC1 lines) showed significantly higher accumulation of all micronutrients (Fe, Zn, Cu, and Mn) in unpolished and polished grains relative to the non-transgenic control grains. Instead of just Fe or Zn having significant changes as in the SC1 and SC2 lines, all four micronutrients showed significant increase in the DC1 lines, particularly DC1.16 and DC1.5. In summary, compared to the SC1 and SC2 lines, the micronutrient concentrations in the DC1 lines accumulated into the whole of the brown grains or the endosperm of the white grains. The results suggest that *HvSUT1* overexpression is causing increased sucrose uptake and resulting in increased nutrient influx into the endosperm, and when combined with *OsNAS2* overexpression, has enhanced micronutrient mobilization in the grains. This was supported by the correlation analysis (Table 4.2) which revealed that HvSUT1 protein expression was highly correlated with changes in most of minerals, excepting K (r=0.056) and S (r=0.246). A particularly significantly positive correlation was found between HvSUT1 protein expression and Fe (r=0.886), P (r=0.771) and Mg (r=0.782) contents. Furthermore, OsNAS2 expression was highly correlated with S content.

Collectively, these results indicate that the micronutrient concentrations (especially Fe and Zn) are correlated with the HvSUT1 protein expression; however, further analysis of sucrose uptake and gene expression related to sucrose metabolism in grains was not investigated in this

study. Using C^{14}-labelled sucrose, Huynh (2015) reported that in the grains of an *HvSUT1*-expressing rice line (G1.4), an increase in sucrose uptake occurred at an early stage of grain filling (7-13 DAA), which was a similar period of HvSUT1 protein expression. This timing of HvSUT1 protein accumulation was similar to that reported here (see Chapter 3).

Beside the contribution of the xylem (Stomph *et al.* 2011; Stomph *et al.* 2009), the transfer route of micronutrient translocation into the rice grains is thought to be similar to that of sucrose, that is via the phloem. Possibly, the increased sucrose uptake can direct an increased sucrose flux into the rice endosperm. Because sucrose accounts for a high proportion of the phloem sap (up to 25%) (Fukumorita & Chino 1982), the change in sucrose flux under these transgenic conditions may affect other minor components such as micronutrients in the phloem sap. The increased uptake of sucrose can result in upregulation of genes involved in sucrose metabolic activities for grain development and product synthesis for storage purposes (Braun *et al.* 2014). These activities in the grain sink can lead to higher nutrient demand in the grain sink (sink strength) to direct mass flow of nutrients into the grains. Along with sucrose, other nutrients, including micronutrients may respond to the increased grain sink strength of *HvSUT1*-expressed rice grain (Saalbach *et al.* 2014; Weichert *et al.* 2017; Weichert *et al.* 2010). The Zn uptake capacity into the grains is determined by the grain strength in rice (Stomph *et al.* 2011). There is a gap in our understanding about the network of metabolic and hormonal signals that follow sucrose uptake into the endosperm. This needs investigation via metabolic or/and transcriptomic profiling to support the effect of the sink strength manipulation on the mineral concentration. This will be discussed in Section 5.2.2 of the next chapter.

4.4.3. A combination of *HvSUT1* and *OsNAS2* expression modifies Fe and Zn accumulation in both dorsal and ventral sides of the grains, extending into the endosperm region.

The Perls/DAB/$CoCl_2$ staining method (Meguro *et al.* 2007; Roschzttardtz *et al.* 2009) was used to visualise the distribution of Fe in the mature grains from three transgenic events. This result focused on the best line from each transgenic population. A striking difference in Fe accumulation on both the dorsal and ventral sides and extending into the inner endosperm in the mature grains of the DC1.16 line was found, compared to the SC1.16 and SC2.15 lines where Fe was found mainly on the dorsal side of the grains (Figure 4.9 - Figure 4.12). The images generated by the Perls/DAB/$CoCl_2$ method showed that Fe distribution in rice grains was abundant in the aleurone cell layer on the dorsal side of the rice grain and the scutellum close to the endosperm. The images are in agreement with element maps of the rice grain in previous reports (Huynh 2015; Johnson *et al.* 2011; Kyriacou *et al.* 2014; Trijatmiko *et al.* 2016). In the embryo region, there was no dramatic difference in the pattern of Fe distribution between the non-transgenic and the transgenic grains, but higher intensity of Fe staining was found in the DC1.16 transgenic grains. Therefore, this study focused on the outer regions in both the dorsal and ventral sides of the DC1.16 grains where the greater differences for Fe staining intensity were observed, compared to the SC1.16, SC2.15 and non-transgenic plants.

The map of non-transgenic IR64 grains showed that the highest intensity of Fe staining was locked inside the aleurone/subaleurone cells, with very low Fe staining extending into the endosperm from the dorsal side. A lower peak of Fe intensity was found in the aleurone cells on the ventral side at 30 µm from the seed coat. This result suggests that Fe is more abundant in the aleurone cells on the dorsal side, which make sense as it is adjacent to the vascular bundles that acts as the major gate of nutrient translocation (Díaz-Benito *et al.* 2018; Huynh 2015; Iwai *et al.*

2012; Wu *et al.* 2016a). The aleurone cells of the rice grain accumulate phytic acid at very high levels during grain filling, which is a strong chelator of metal elements, especially Fe, to form insoluble salts (Iwai *et al.* 2012; Johnson *et al.* 2011; Kyriacou *et al.* 2014; Sakai *et al.* 2015). Thus, it is likely that Fe is restricted to the aleurone cells on the dorsal side and has less ability for mobilization to the other side of the grain. Based on the DTZ staining, the Zn signal had a broader distribution pattern over the whole of the endosperm region and was not as abundant in the aleurone layer as Fe. This was in agreement to the map of Zn distribution in the rice grain generated by µ-XRF by Johnson *et al.* (2011) and Kyriacou *et al.* (2014). In the study of Iwai *et al.* (2012), the Zn gradually decreased in the outer layers of the grain, indicating that it was actively mobilised into the inner endosperm during grain development, whereas Fe remained primarily in the aleurone layer on the dorsal side. This can be seen as very high retention of Zn (over 80%) in the polished grain (see Figure 4.8 B), while the retention of Fe was much lower, <20%. Like Fe, Zn accumulated more on the dorsal side than on the ventral side (Figure 4.16), which was consistent with the observations of Jaksomsak *et al.* (2014).

The SC2.15 grain expressing only OsNAS2 accumulated slightly higher Fe on the dorsal side, compared to the non-transgenic grain. Similar to the non-transgenic IR64, more Fe accumulated on the dorsal side of the SC2.15 grain; however, the Fe was not concentrated in the centre of the aleurone cell, but dispersed the whole aleurone cell, with more Fe extending into the second layer of aleurone cells. The peak of Fe intensity at 30 µm decreased gradually until 70 µm from the seed coat, instead of a sharp drop as observed in the control IR64 grain. For Zn distribution in the SC2.15 grain, there was significantly more on the ventral side, compared to the dorsal side as was observed in the non-transgenic IR64 grain. Several analyses of NA and/or DMA would be required to suggest an explanation for this observation, but the likely presence of NA,

an Fe and Zn chelator, could modify mobilisations of these minerals after translocating into the aleurone cells.

For the SC1.16 grain expressing the single *HvSUT1* construct, more Fe accumulated in the aleurone/subaleurone layers on the dorsal than the ventral side. Significantly more Fe was found on the dorsal side, compared to the non-transgenic grain. With this, more Fe extended into the endosperm, consistent with the Nipponbare rice grain expressing *HvSUT1* in the study of Huynh (2015). In the SC1.16 grain, Fe extended into the endosperm to 70 µm from the seed coat on the dorsal side; however, no difference was found on the ventral side of the SC1.16 grain, compared to the non-transgenic grain. Like Fe, Zn accumulation on the ventral side did not differ between the SC1.16 and the non-transgenic grain, but significantly higher Zn accumulation was seen on the dorsal side. This was consistent with the distribution map of Zn reported by Huynh (2015) of rice grain from the *HvSUT1*-expressing Nipponbare rice.

The image of the DC1.16 grain overexpressing the combination of *OsNAS2* and *HvSUT1* revealed three striking differences in Fe distribution and intensity, compared to the non-transgenic, SC2.15 and SC1.16 grains. A much stronger intensity of Fe staining on the dorsal side was observed and likely stronger than in the other grains as the peak of Fe staining reached its highest values. Normally, the intensity of Fe staining would be lowered after a peak in the aleurone/subaleurone layers as was found in the non-transgenic grain, but in DC1.16 grains it continued to peak progressively further from the aleurone, subaleurone and into the endosperm at 90 µm, and then decreased until 100 µm from the seed coat. Another remarkable difference was the high intensity of Fe staining localized in the aleurone and extending into the endosperm on the ventral side, in stark contrast to that seen in the non-transgenic grain and the SC1.16 and SC2.15 lines generated in this study. In fact, the Fe accumulation reached a peak in the aleurone layer and

extended at a lower level into the endosperm to 80 µm. More Fe extending into the endosperm region, where low phytic acid content is detected (Iwai *et al.* 2012; Johnson *et al.* 2011; Kyriacou *et al.* 2014), could minimize loss after polishing and have less chance to bind with phytic acid, resulting in better bioavailability. Like Fe, Zn accumulation in the DC1.16 grain was radically modified, as for both sides of the rice grain Zn levels were significant higher, compared to the non-transgenic control. Zn accumulation on the ventral side was less abundant than on the dorsal but significantly higher than the ventral side of the SC1.16 grain. Based on the results in this study, it is likely that NA and/or DMA provide an alternative chelator to Fe resulting in changes in Fe mobilization around the DC1.16 grain. This could be a possible explanation for the enhanced accumulation of Fe on the ventral side. Furthermore, the promoter *GluA2* that regulated the expression of *OsNAS2* gene is preferentially active on the ventral side, which is consistent with the GUS analysis (see Chapter 3) and the results of Chen *et al.* (2018) who showed that the protein glutelin A was more abundantly detected on the ventral side of the grain. In general, more Fe and Zn accumulated in the rice endosperm and products of the OsNAS2 protein are likely to be responsible for this altered distribution. Measurement of NA levels in the grain could assist in addressing this question, but unfortunately this assay was not possible at the time of this study.

4.4.4. Changed Fe and Zn concentrations were unlikely to be related to phytate change in grains expressing *HvSUT1* or/and *OsNAS2*.

In contrast to the previous study of Huynh (2015), where Nipponbare transgenic rice line expressing *HvSUT1* had a significant increase in phytate concentration (around 85%), no changes in phytate concentration were found in either polished or unpolished grains of any of the transgenic lines generated in this study. Phytate is a mixed salt of phytic acid and multiple minerals, such as K, Mg, Ca, Fe and Zn and is found in the aleurone/subaleurone layers of rice grains (Bohn *et al.*

2007; Bohn *et al.* 2008; Cegłowski *et al.* 2016). Phytic acid is a primary storage form of P, providing a source for seed germination and the emerging seedling (Raboy 2003). Increasing phytate content may be understandable when more micronutrients are loaded into the Nipponbare rice grain expressing *HvSUT1* (Huynh 2015), but this presents a problem for absorption of these minerals in the human intestine (Bohn *et al.* 2007; Bohn *et al.* 2008; Cegłowski *et al.* 2016). Sucrose is assumed to enhance loading into the rice grain expressing *HvSUT1*. Like other grain storage products, an intermediate product of sucrose, glucose-6-phosphate, is the substrate involved in the synthesis of phytic acid. However, an analysis of the phytate concentration was conducted here in multiple independent transgenic lines; the results showed a wide variation but no significant differences in phytate concentrations with approximately 10 mg/g in unpolished and 3.5 mg/g in polished grains, consistent with the phytate content naturally occurring in rice varieties (Liang *et al.* 2009; Ma *et al.* 2005; Rose *et al.* 2020). Genetic variation between IR64 and Nipponbare, or different environmental conditions during rice growth, could be factors that explain the discrepancy in the phytate levels in the rice grains of the work of Huynh (2015) compared that presented here. Grain phytate concentrations have found to vary among genotypes of rice (Glahn *et al.* 2002; Welch *et al.* 2000) and two QTLs affecting 15%-24% of total phytate content variation have been identified by Stangoulis *et al.* (2007). However, phytate concentration in rice grains is also known to be altered by the application of P fertilizers during grain filling in IR64 and Nipponbare rice cultivars (Rose *et al.* 2020; Wang *et al.* 2017). The present study demonstrates the low or non-significant correlations among the concentrations of phytate and Fe and Zn in polished grains of the transgenic rice expressing *HvSUT1* with or without *OsNAS2*. The weak correlation was intriguing and suggests that changes in Fe and Zn levels may be related to other chelators or storage components in the rice endosperm where trace of phytic acid are present (Iwai

et al. 2012; Sakai *et al.* 2015). In this study, NA and/or DMA may still be involved in this observation, and thus consistent with the hypotheses of this study. This is also consistent with the suggestions of Johnson *et al.* (2011) and Kyriacou *et al.* (2014) as Fe in the rice endosperm was seen to not localize with phytate. As mentioned, measurement of NA and DMA in the transgenic grains would be required to confirm the potential role of OsNAS2 protein in this study. Unfortunately, a NA assay, although currently being optimized, was not available during the course of this study.

Interestingly, despite no clear correlation with phytate, the change in Fe and Zn concentrations in the transgenic lines significantly correlated to the change in P concentration (see Table 4.3). As mentioned early, elevating levels of sucrose via *HvSUT1* expression may directly alter the P demand by expression of genes involved in P uptake, transport, and allocation in rice grains (Hennion *et al.* 2018; Kehr 2013; Lei *et al.* 2011) or ATP demand for hexose phosphorylation in sucrose metabolism (Braun *et al.* 2014; Ruan 2014).

The presence of phytate affects the bioavailability of essential mineral elements inhibiting their absorption in the human gut (Bohn *et al.* 2008; Ma *et al.* 2005; Welch & Graham 2004). The molar ratios of phytate to minerals provides an indication of their bioavailability; for instance, molar ratios of phytate:iron <1 and phytate:Zn <18 suggest they are in a form available for absorption (Gibson *et al.* 2010; Ma *et al.* 2005). The molar ratios of phytate to Fe and Zn significantly decreased in the grains of transgenic plants in this study, although no transgenic line had a molar ratio of phytate to iron of <1. The ratios were significantly lower by approximately 50% in unpolished and 100% in polished grains, compared to the non-transgenic control (see Figure 4.19). Furthermore, the phytate:Zn ratio was lower in the transgenic lines expressing *OsNAS2*, including the DC1 and SC2 lines (15.12 and 13.76, respectively), compared to 19.83 and

27.41 for the SC1 lines and the non-transgenic control, respectively. As mentioned, NA and DMA concentrations in the transgenic rice grain expressing *HvSUT1* and *OsNAS2* should be examined to confirm the improved Fe and Zn bioavailability, because NA and DMA are suggested to be novel enhancers of Fe and Zn bioavailability (Beasley *et al.* 2019b; Eagling *et al.* 2014; Lee *et al.* 2012; Zheng *et al.* 2010), along with ascorbic acid and β-carotene from fruits and vegetables (White & Broadley 2009). To confirm Fe and Zn bioavailability in the transgenic grains, the *in vitro* Caco2 cell line model is recommended as a reliable tool.

4.4.5. Accumulation of potential toxic metals in the transgenic grains did not exceed guidelines.

As well as beneficial mineral elements (Fe and Zn), several heavy elements may potentially be altered in transgenic rice expressing *HvSUT1* or/and *OsNAS2*. These include As, Cd, lead (Pb), mercury (Hg) and Ni (Cao *et al.* 2017; Clemens *et al.* 2013; Huang *et al.* 2013; Meharg *et al.* 2013; Meharg *et al.* 2009; Norton *et al.* 2014). Accumulation of these potentially toxic elements in rice grains poses a risk to human health, which is more serious for populations who consume rice as a dietary staple. Therefore, monitoring these contaminating elements in rice, or rice products, is necessary to reduce the risk to human health. In this study, three potentially toxic elements, namely As, Cd and Ni showed no enhanced accumulation in polished and unpolished grains (see Section 4.3.5). No knowledge about the impacts of sucrose or sugar transport on Cd mobility into grains is available in the literature. Like Fe and Zn, Cd transport shares the same long-distance transport via phloem or xylem (Uraguchi *et al.* 2011; Uraguchi *et al.* 2009). Cd accumulation may increase as increasing sucrose uptake capacity into rice grains occurs. Here, no increase in Cd concentration in the transgenic rice expressing *HvSUT1* alone was found, in fact significantly lower levels were found compared to non-transgenic controls, despite increasing Fe and Zn levels. Furthermore, the

transgenic lines expressing endosperm-specific *OsNAS2* alone, or combined with *HvSUT1*, had higher concentrations of Cd in polished and unpolished grains than the transgenic lines expressed *HvSUT1* alone, but no difference with the non-transgenic control. Whilst it is interesting that Cd levels are lower in the SC1 lines but return to non-transgenic levels and the DC1 lines it is difficult to explain.

Similarly, the strategy of Fe/Zn biofortification exploiting genes involved in Fe and Zn translocation, for instance constitutive expression of *OsNAS* genes, often raises a concern about the possibility of toxic heavy metal accumulation in rice grains. Root-shoot translocation of Cd via xylem and phloem share many common mechanisms with Zn. Citrate is a common chelator for both Zn and Cd, which is transported by the NRAMP transporter family, so Cd can 'mimic' Zn and compete for binding affinity with chelating molecules and transporters to be mobilised into the shoots, and subsequently translocated into the rice grains (Kato *et al.* 2010; Olsen & Palmgren 2014). Most of the previous studies have reported no more Cd accumulation in Fe/Zn-enriched rice via a transgenic approach, but neither was this possibility mentioned (Johnson *et al.* 2011; Kyriacou *et al.* 2014; Lee *et al.* 2009b; Lee *et al.* 2012; Slamet-Loedin *et al.* 2015; Trijatmiko *et al.* 2016; Wu *et al.* 2018; Wu *et al.* 2019).

For As, although there was a significant difference in As accumulation in the grains expressing *HvSUT1* compared to the non-transgenic control, the total As concentration was far lower than the recommended limit for human intake of 0.2 mg/kg (FAO/WHO 2017). Arsenate is an inorganic form of As and its uptake and translocation in rice is through phosphate transporters, as arsenate is an analogue of phosphate. Whether or not the increased concentration of As results from an indirect effect of P demand in the transgenic lines presented in this study is unknown.

Interestingly P concentration in the rice grains was found to be higher in the SC1 and DC1 transgenic rice plants (see Figure 4.6).

Sucrose is a global signalling compound for plant responses to P deficiency, thus elevated levels of sucrose can directly enhance the demand for P by expression of genes involving in P uptake, transport, and allocation (Hennion *et al.* 2018; Kehr 2013; Lei *et al.* 2011). The following studies support this hypothesis. An effect of exogenous sugar supply in the response to phosphate starvation signalling was demonstrated in white lupin roots (Liu *et al.* 2005). In *Arabidopsis* roots the sucrose transporter 2 (*AtSUC2*) is linked to total P content, as an over-expressing SUC2 mutant had a higher sensitivity to P starvation (Lei *et al.* 2011; Liu *et al.* 2005). In the context of the results presented here, increasing sucrose uptake via endosperm specific overexpression of *HvSUT1* may alter the demand for P loading into the grains during the grain filling, though no information on P loading in the grain tissues is available. This indirectly may modify As translocation through increased the P demand, explaining the difference between As and Cd concentration in the grains.

Unlike Cd and As, less attention has been paid to Ni contamination in rice grains, but there have been several reports on the effects of diets with high Ni concentration, especially on Ni-sensitive patients. Ni-polluted rice is a serious problem in several countries, like China (Cao *et al.* 2017; Wang *et al.* 2020). The mechanism of Ni transport in plants has not been as thoroughly investigated as Cd and As, but Ni shares a common chelator (NA) with Fe and Zn (Callahan *et al.* 2007). Potential Ni accumulation in rice grains cannot be ruled out. In this study, there was no Ni accumulation in the grains of all the transgenic lines and far lower levels were observed than the grains of the non-transgenic IR64 control. Why there was lower Ni in the transgenic grains than in the control grains cannot be explained.

4.5. Conclusions

Endosperm-specific overexpression of a sucrose transporter might enhance sucrose uptake capacity into grains, resulting in an increase in nutrient accumulation. The results presented here indicate that *HvSUT1* expression altered Fe and Zn concentration in mature IR64 Indica rice grains. This was consistent with the previous study in wheat (Saalbach *et al.* 2014; Weichert *et al.* 2010) and Japonica rice (Huynh 2015). However, Fe distribution in the transgenic rice plants expressing *HvSUT1* alone was still limited to the aleurone/subaleurone layers on the dorsal side where Fe could be locked by the presence of phytic acid. In combination with the *OsNAS2* gene, the most striking finding of the DC1.16 transgenic grain was that Fe and Zn distribution and accumulation occurred on both dorsal and ventral sides, penetrating further into the rice endosperm, which was not seen in the SC1 and SC2 transgenic rice. This result supports the hypothesis of this study that the chelating products of *OsNAS2* expression (NA or/DMA) can modify Fe and Zn mobilization in the aleurone/subaleurone cells. However, further analyses of NA or/and DMA changes in these transgenic lines are needed to strengthen the hypothesis.

Molar ratios of phytate to Fe and Zn for predicting mineral bioavailability were consistent with the presence of the alternative chelators of NA and/or DMA, although the non-significant change in phytate in the SC1 lines in contrast to the work of Huynh (2015) requires further investigation and more replication. Future work should include testing Fe and Zn bioavailability using the Caco2 model system. Although the chelating products of *OsNAS2* expression (NA or/DMA) could result in improved Fe and Zn levels and bioavailability in this study, this is yet to be tested. Furthermore, it was comforting that no greater accumulation of potential toxic elements was found in any of the transgenic rice plants grown in this study under normal conditions.

CHAPTER 5. GENERAL DISCUSSION AND FUTURE WORK

Manipulating sucrose uptake capacity via seed or grain specific overexpression of a sucrose transporter has the potential to alter macronutrient and micronutrient contents in cereals (Huynh 2015; Saalbach *et al.* 2014; Weichert *et al.* 2010). Fe accumulation in rice is, however, often limited to the aleurone/subaleurone layers, because it is immediately bound to phytic acid to form an insoluble complex (phytate), preventing movement to the inner endosperm (Iwai *et al.* 2012). The mixed salt of phytate with Fe and Zn is usually removed after grain polishing, but regardless, Fe and Zn absorption in this form in the human gut is very limited. Ideally, Fe and Zn should be moved into the endosperm in a more bioavailable form, where less phytic acid is detected.

In this study, the objective was to expand on a previous biofortification strategy of Huynh (2015) whereby overexpression of *HvSUT1* was combined with endosperm-specific *OsNAS2* expression to enhance mobilisation of Fe and Zn into the rice endosperm of an Indica rice cultivar IR64. This rice is a mega-cultivar (Mackill & Khush 2018) but recalcitrant to *Agrobacterium*-mediated transformation. Endosperm-specific overexpression of *OsNAS2* was aimed to increase soluble complexes of Fe and Zn with NA and/or DMA in the outer endosperm to improve both mobilisation and bioavailability. To investigate whether this combined transgene expression would alter Fe and Zn distribution and accumulation, three major objectives were undertaken.

- First, multiple homozygous transgenic IR64 rice lines overexpressing *HvSUT1* or/and *OsNAS2* genes in the rice endosperm were generated by *Agrobacterium*-mediated transformation and their zygosity determined by the qPCR assay.
- Second, temporal patterns of OsNAS2 and HvSUT1 protein expression in the rice immature grains were analysed during grain development and two parameters of rice plant growth were measured from germination to full development.

- ❖ Third, nutrient content and Fe/Zn localisation were analysed to see the effect of single and combined *HvSUT1* and *OsNAS2* expression.

5.1. A summary of main results

The rice 26kDa globulin-1 (*Glb-1*) and glutelin A2 (*GluA2*) promoters cloned from the Japonica rice cultivar Nipponbare were redesigned for endosperm-specific expression of *HvSUT1* and *OsNAS2* in Indica rice cultivar IR64, respectively. The *Glb-1:HvSUT1* construct was made by Huynh (2015). Along with this construct, *Glb-1:HvSUT1* (SC1), a *GluA2:OsNAS2* (SC2), and a novel combination of *Glb-1:HvSUT1* and *GluA2:OsNAS2* were designed for *Agrobacterium* transformation in this study. Several modifications to the *Agrobacterium*-mediated protocol that used immature embryos led to a slight increase in transformation efficiency of 44 %, compared to 40% reported by Slamet-Loedin *et al.* (2014). This protocol has the potential for large-scale production of transgenic Indica rice hopefully prompting more genetic studies of this important rice cultivar.

In most molecular genetic studies, the selection of homozygous transformants is a crucial step when assessing transgene expression levels and any transgene- associated phenotype. With many independent transgenic events generated in this study, an accurate, rapid and reliable quantitative real-time PCR method (qPCR) was used to identify homozygous transgenic rice lines containing single or double inserts in the T1 generation. The qPCR protocol was optimised by Schramm (2015) and Tran (2015) in the transgenic Japonica rice cultivar Nipponbare. Accuracy of this qPCR method used here on IR64 transgenic Indica rice approached 100%. It is clear that the qPCR method can be used as a high-throughput method for fast-tracking identification of homozygous plants carrying single or double inserts. This method could easily be adapted to other transgenic rice plants, because all procedures described here are standardized, for example, the use

of inexpensive dye like SYBR Green, universal primers targeting common sequence elements of gene cassettes like the *nos* terminator, and standard qPCR reaction conditions. Moreover, this protocol successfully detected homozygous transgenic rice with multi-gene stacking, a feature likely to become more popular in future transgenic research.

In this study, grain material from multiple independent homozygous lines was used for further analyses. This provided the confidence to draw conclusions about the direct effects of transgene expression on plant phenotype and not the positional effects of the transgene. A routine transformation efficiency of up to 54.1% was found in Indica rice, with around half of the transgenic events shown to be single or double inserts. These results provide evidence for the application of this qPCR assay and improved transformation efficiency to large-scale production of transgenic rice.

Endosperm specificity of the *GluA2* promoter was verified by GUS staining that showed expression localised to the aleurone/sub-aleurone and outer cell layers of the endosperm with no detectable expression in the embryo and maternal tissues of rice grain and vegetative tissues. A novel polyclonal antibody raised to a unique 14 amino acid peptide within the OsNAS2 protein, and another polyclonal antibody reactive to the HvSUT1 protein developed by Huynh (2015), were used for immunoblot analysis to measure expression patterns of the HvSUT1 and OsNAS2 proteins during grain development. *OsNAS2* under the regulation of the *GluA2* promoter led to detectable protein 3 days after anthesis (DAA) at the early stage of grain filling, reaching a peak at 5 DAA and then remaining consistent until 20 DAA. Activity of the *Glu2A* promoter has not been reported as early as 3 DAA in the literature. Under control of the *Glb-1* promoter, HvSUT1 protein levels peaked at around 7-10 DAA and then declined but was still detectable at 20 DAA, constant with the findings of Huynh (2015).

A remarkable feature of the expression derived from the *Glb-1:HvSUT1* construct in IR64 was a vigorous growth phenotype with or without *OsNAS2*, whereas slight growth inhibition was observed in the single *GluA2*:*OsNAS2* transformed rice plants. Such an observation associated with the *Glb-1:HvSUT1* construct was not reported by Huynh (2015) apart from an increase in panicle number per plant. A possible explanation for these phenotypes could be ectopic expression of *HvSUT1* and *OsNAS2* in other tissues of transgenic IR64 rice. This possibility is discussed further below.

Fe and Zn levels in mature rice grains were measured by ICP-MS and their distribution determined by Perl/DAB/$CoCl_2$ and DTZ staining methods, respectively. More Fe and Zn were found in polished and unpolished grains overexpressing *HvSUT1* alone, thus reinforcing the strategy of Fe and Zn biofortification by sucrose transporter overexpression. The map of Fe distribution in mature grains showed remarkable accumulation on the dorsal side of the grain. When combined with *OsNAS2* overexpression in the endosperm, an even greater increase of over 100% for Fe and 30% for Zn in polished grains, was seen compared with non-transgenic IR64. A striking feature of the DC lines was the distribution of Fe and Zn on both dorsal and ventral sides of rice grains, whilst in rice expressing *HvSUT1* alone the distribution was mainly limited to the dorsal side of the grain. This result suggests that the chelating products of *OsNAS2*, NA or/and DMA, might modify the Fe and Zn mobilisation in the rice endosperm during grain development; a suggestion consistent with the hypothesis raised in this study.

In contrast to the findings of Huynh (2015) where Japonica rice grains overexpressing *HvSUT1* exhibited increased Fe and Zn levels along with that of phytate, this study found no accompanying increase in phytate content. Fe and Zn changes in polished grain of IR64 *HvSUT1* transgenic rice are likely to relate to other components, but not phytate. In addition to Fe and Zn,

no excessive accumulation of three potentially toxic elements was obtained in any of the transgenic rice grains on soil without toxic heavy metal contamination. This is a comforting finding for future implementation of this biofortification approach.

5.2. Discussion

5.2.1. Proposed mechanism of the role of *HvSUT1* and *OsNAS2* in modifying Fe and Zn mobilisation into the rice endosperm.

This study proposes three possible models for Fe and Zn translocation, along with sucrose translocation, from the dorsal vascular bundle into the rice endosperm for the three kinds of transgenic rice plants overexpressing *HvSUT1* or/and *OsNAS2* and a non-transgenic IR64 control. At this early stage of grain development, the primary flow of solutes is through the vascular bundle that runs the entire length of the dorsal side of the developing rice grains (Krishnan & Dayanandan 2003; Wu *et al.* 2016a). Following unloading from the phloem, solute move symplasmically through plasmodesmata to reach the nucellar projection cells abutting the filial aleurone. Because the filial tissues, including the rice endosperm and embryo, are isolated by an apoplasmic space, solutes move circumferentially in the nucellar epidermis around the developing endosperm and efflux cross the plasma membrane of the nucellar epidermis into the apoplasmic space (Furbank *et al.* 2001; Oparka & Gates 1981a; Oparka & Gates 1981b). Subsequently, solutes influx into the aleurone/subaleurone cells and further movement into the starchy endosperm cells is presume to occur primarily via symplasmic transfer (Wang *et al.* 1995). Transporters are required at the maternal/filial boundary to release sucrose from the nucellar epidermis and subsequently allow uptake into the aleurone cells. For sucrose transport from leaves to grains by the phloem pathway, SWEET11 or/and SWEET15, located on the nucellar epidermis are involved (Chen *et al.* 2012; Ma *et al.* 2017; Yang *et al.* 2018), and SUT1 present on the membrane of the aleurone cells (Aoki

et al. 2003; Furbank *et al.* 2001; Hirose *et al.* 1997; Oparka & Gates 1981a; Scofield *et al.* 2002) is proposed to facilitate further transport into the grain endosperm. Like sucrose, translocation of mineral nutrients from leaves to rice grains is proposed to occur through the phloem. Furthermore, due to the absence of xylem discontinuity in rice grain (Krishnan & Dayanandan 2003), any minerals are thought to load directly into the vascular bundle to the nucellar epidermis and aleurone cells (Stomph *et al.* 2011; Stomph *et al.* 2009). Through the phloem, NA is a major chelator for Fe and Zn translocation into the rice grains (Nishiyama *et al.* 2012; von Wirén *et al.* 1999). However, after unloading, a mechanism of Fe or Zn mobilisation from the maternal tissues into filial tissue remains unclear.

After unloading into the rice endosperm through specific transporters, for example *OsYSL2* and *OsZIP* for Fe and Zn, respectively (Bashir *et al.* 2012; Ishimaru *et al.* 2010; Ishimaru *et al.* 2007; Koike *et al.* 2004), movement and distribution of Fe and Zn, along with other minerals, differ. In the study of Iwai *et al.* (2012), abundant Fe is restricted in the aleurone and subaleurone cells on the dorsal side, where it is bound primarily with phytic acid. Zn stays near the aleurone/subaleurone layer but is more widely distributed through the whole rice grain. Figure 5.1A, B and C represent a proposal model for the movement of Fe and Zn in non-transgenic rice IR64. Most Fe would immediately bind to phytic acid, resulting in its limited mobilisation into the inner endosperm, locked mainly in the first layer of the aleurone cells of the aleurone cells. Zn on the other hand could not only bind to phytic acid, but also to protein bodies containing sulphur (Iwai *et al.* 2012; Persson *et al.* 2009), leading to its wider distribution in the whole of rice grain (see Section 4.3.3 in Chapter 4). Very little Fe is mobilised from the dorsal towards the ventral side in the non-transgenic rice grain, probably due to few soluble complexes of Fe available for mobilisation in the aleurone cells.

To modify Fe and Zn mobilisation in the rice aleurone cells by increasing nicotianamine (NA) level, the transgenic rice overexpressing *OsNAS2* alone under the regulation of the *GluA2* promoter (SC2.15) is represented in Figure 5.1A, D and E. The model presented above assumes that there is no difference between SC2.15 and non-transgenic grains in nutrient flow translocating to the grain, but modification to the distribution of whatever Fe and Zn is present in the rice grain. Here, under the regulation of the *GluA2* promoter, *OsNAS2* expression is proposed in the outer layers of endosperm with stronger levels in the aleurone and subaleurone layers during grain development. NA is presumed to increase in the outer layers of the rice endosperm. Increasing NA concentration would allow NA-Fe or NA-Zn complexes to form after Fe and Zn unloading into the aleurone cells to enhance their mobility into the inner endosperm. Therefore, more Fe penetrating the second layer of the aleurone cells and subaleurone layer were detected on the dorsal side of rice grains from the SC2.15 line. Furthermore, early expression of OsNAS2 at the stage of storage (5 DAA) when the inner endosperm is still alive for nutrient uptake (Wu *et al.* 2016b) and phytic acid expression is low (Iwai *et al.* 2012), may facilitate Fe and Zn mobility into the inner endosperm. However, endosperm-specific expression of *OsNAS2* is unlikely to increase Fe and Zn uptake from the soil and translocation into the rice grain during grain filling. Ideally, it would be possible for further increase in Fe and Zn content by coupling OsNAS2 expression with an improvement in Fe and Zn loading into the rice grains (Oliva *et al.* 2014; Zheng *et al.* 2010), hence the DC1 lines generated in this study.

For the transgenic rice with *HvSUT1* expression alone, the proposed localisation of HvSUT1 in the plasma membranes of endosperm cells is shown in Figure 5.1 F, G and H. Like endogenous SUT1 (OsSUT1), HvSUT1 is likely to be localised on the aleurone cells to uptake sucrose from the apoplasmic space into the aleurone cells (Aoki *et al.* 2003; Furbank *et al.* 2001;

Scofield *et al.* 2002) after the translocated sucrose is released from the nucellar epidermis via OsSWEET11 or/and OsSWEET15 (Ma *et al.* 2017; Yang *et al.* 2018). Furthermore, *HvSUT1* under the control of the *Glb-1* promoter, also would be localised to the inner endosperm cells with a possible role of sucrose retrieval to the symplasm. Endosperm-specific overexpressing *HvSUT1* is proposed to modify the sucrose uptake capacity and partitioning into the rice endosperm of the transgenic grains. Once entering the rice endosperm cells, sucrose undergoes a wide range of metabolic, signalling and storage processes. Sucrose is a global signal molecule in the plant's response to nutrient demand for growing and storage compartments (Doll *et al.* 2017; Paul *et al.* 2017; Weber *et al.* 2005). Therefore, elevated sucrose uptake into the endosperm cells via overexpressed *HvSUT1* activity, is likely to stimulate multiple metabolic, signalling and storage activities to respond to the increased sucrose uptake.

It is likely that the flow rate of sucrose translocating into the developing grain may rapidly occur in order to respond to the increased sucrose demand of grain growth and storage (Huynh 2015; Saalbach *et al.* 2014; Weichert *et al.* 2017; Weichert *et al.* 2010). Because sucrose is one of the major components in the rice phloem sap, a further effect on the translocation rate of other minor components in the phloem sap could be happening (Patrick & Offler 2001; Patrick *et al.* 2015). Under these transgenic conditions, micronutrients (especially Fe and Zn) that are minor components of the solutes are potentially enhanced in translocation from leaves into the rice endosperm, along with the flow of sucrose translocated into the endosperm. Furthermore, increased sucrose levels might upregulate the activity or expression of micronutrient transporters. As Lin *et al.* (2016) reported, Fe deficiency-induced ferric chelate-reductase (FCR) activity, and expression of Fe acquisition-related genes *FRO2*, and a high-affinity ferrous Fe transporter (*IRT1*), were stimulated by increasing sucrose accumulation in *Arabidopsis* roots. However, as the model

represented here is in the grain, the role of two possible Fe and Zn transporters, *OsYSL2* and *OsZIPs*, can be invoked (Bashir *et al.* 2012; Ishimaru *et al.* 2010; Ishimaru *et al.* 2007; Koike *et al.* 2004). These would act in the aleurone cells to translocate Fe and Zn into the endosperm cells. More Fe and Zn are proposed to translocate into the transgenic rice grains. However, the majority of Fe is presumed to bind to phytic acid and thus be restricted to the aleurone/subaleurone cells on the dorsal side with little mobilisation into the endosperm cells on the ventral side. Zn, however, is more mobile and probably associates with other sulphur-containing peptides, hence its greater distribution in the starchy endosperm.

The model proposed here for the combined overexpression of *HvSUT1* and *OsNAS2* in Figure 5.1F, I and J invokes a synergistic action of the two transgenes shown in Figures 5.1 D, E, G, and H. Increasing sucrose uptake into the rice endosperm by *HvSUT1* expression would drive the flow of other nutrients into the rice endosperm during grain development. Similar to the model in Figure 5.1C, more Fe and Zn would be translocated to reach the aleurone cells requiring the proposed membrane transporters in the grain tissues, like *OsYSL2* (Ishimaru *et al.* 2010; Koike *et al.* 2004) and *OsZIPs* (probably *OsZIP4* or *OsZIP18*) (Bashir *et al.* 2012; Ishimaru *et al.* 2007; Yang *et al.* 2009). In the aleurone cells, at the early stage of grain development, when phytic acid is still low, Fe and Zn could have a better opportunity to bind to any available NA (a product of *OsNAS2* overexpression) to form soluble complexes with greater intercellular mobility. Fe-NA and Zn-NA in the aleurone cells are presumed to facilitate the mobility of these complexes into the subaleurone cells and then into the starchy endosperm spanning from the dorsal side to the ventral side, the latter more distant from the vascular bundle. The model demonstrates a complementary combination of increased mineral uptake and mobility of minerals in the grain sink to facilitate their intercellular mobilisation.

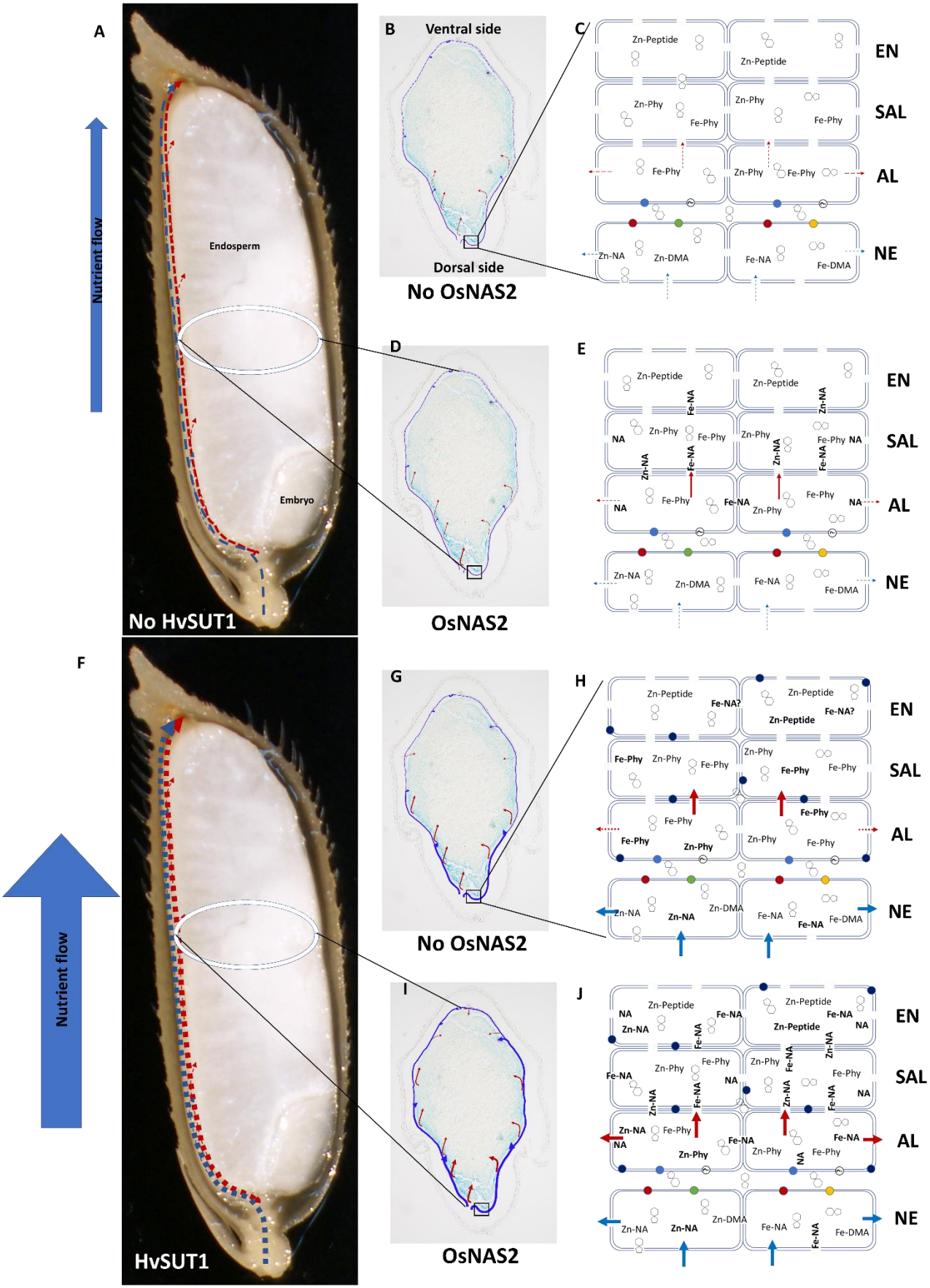
A
Nutrient flow
Endosperm
Embryo
No HvSUT1
B
Ventral side
Dorsal side
No OsNAS2
C
Zn-Peptide
Zn-Phy
Fe-Phy
Zn-NA
Zn-DMA
Fe-NA
Fe-DMA
EN
SAL
AL
NE
D
OsNAS2
E
NA
F
Nutrient flow
HvSUT1
G
No OsNAS2
H
Fe-NA?
I
OsNAS2
J

Figure 5.1. Schematic representation of the accumulation and distribution of Fe and Zn in the endosperm of rice seeds in non-transgenic grain and in the three transgenic rice grains overexpressed *HvSUT1* or/and *OsNAS2*. Blue arrows represent the pathway of nutrient flow moving from the vascular bundle into the nucellar layer and red arrows represents the pathway of nutrient flow moving in the aleurone and endosperm cells of the rice grain. The thickness of arrows represents more or less mobility of nutrients in the endosperm cells (aleurone, subaleurone, and starchy endosperm). The nutrient and water flow mainly move along the dorsal vascular bundle from the source to reach the grain. No difference in nutrient flow loading into the grain was proposed in the non-transgenic IR64 grain, and the transgenic grain overexpressing *OsNAS2* (proposed model for SC2.15) (A). With *HvSUT1* overexpression (F), the mass flow of nutrients into the rice grain is proposed to be stronger. This model represents transgenic grains overexpressing *HvSUT1* alone (SC1.16) or with *OsNAS2* (DC1.16). The nutrients and water move from the vascular bundle to the nucellar layer via a symplasmic pathway. At the nucellar cells, the nutrients move circumferentially along the pericarp from the dorsal to ventral side in a symplasmic manner. The nucellar cells completely encircle the endosperm and are isolated by an apoplasmic space, therefore, specific membrane protein transporters at the nucellar and aleurone layers are required to deliver nutrients and water to the endosperm. For sucrose, OsSWEET11/15 (●) in the nucellar cells and OsSUT1 (●) in the aleurone cells are involved in sucrose translocation, respectively. For Fe and Zn transport, OsYSL2 (●) and OsZIP4/8 (●) protein family are proposed to transport Fe and Zn respectively. In normal conditions, Fe and Zn accumulation preferentially occurs on the dorsal side. Then Fe immediately binds to phytate restricting its mobility to the starchy endosperm, while there is more mobility of Zn, probably bound to S-contained peptides (B and C). In the scenario of *OsNAS2* overexpression alone, Fe and Zn are assumed to complex

with phytate and NA in the aleurone. By enhancing NA levels Fe and Zn (especially Fe) maybe more mobile, thus more Fe will be distributed into the inner endosperm, but no increase in Fe and Zn will be translocated from the source. In scenario of *HvSUT1* (●) overexpression (G and H), along with increasing sucrose uptake, other nutrients, including Fe and Zn are assumed to translocate into the rice endosperm. More Fe and Zn will be distributed into the aleurone, subaleurone and the outer starch endosperm. However, without other soluble chelators, like NA, the majority of Fe will still be locked in the aleurone and the mobility will be restricted from the dorsal to the ventral side of the grain. In the scenario of combined of *HvSUT1* and *OsNAS2* overexpression (I and J), NA serves as an alternative chelator of Fe and Zn in the aleurone cells, leading to enhanced Fe and Zn mobility into the starchy endosperm and from the dorsal to ventral side the latter of which is most distant from the vascular bundle. EN: Endosperm, SAL: subaleurone, AL: aleurone, and NE: nucellus epidermis.

5.2.2. Unexpected ectopic expression of transgenes as a possible explanation for effects on growth with *HvSUT1* and *OsNAS2* expression in IR64 rice.

One of the most interesting observations from this study was a vigorous growth phenotype associated with the endosperm-specific overexpression of *HvSUT1* with or without *OsNAS2*. In contrast, the *GluA2:OsNAS2* transgenic lines showed a growth penalty. Although the *HvSUT1* and *OsNAS2* transgenes were under the regulation of endosperm-specific *Glb-1* and *GluA2* promoters, respectively, miss-regulation of the promoter elements and leading to ectopic expression in other tissue during the vegetative growth stage could explain this phenotype. Data presented in Chapter 3 of this thesis was collected under the assumption that little to no expression in root and leaf tissue was occurring, and thus no analysis was performed on these tissues at earlier growth stages. Most previous studies report that the regulation of the *Glb-1* promoter was specific to the rice endosperm

when the cloned Japonica *Glb-1* promoter was introduced into Japonica rice (cultivar Nipponbare or related varieties) with the same or different cultivars (Furtado *et al.* 2008; Qu & Takaiwa 2004; Takaiwa *et al.* 1996; Wu *et al.* 1998). No expression was detected or reported in any other tissue in these studies. In this study, the *Glb-1* and *GluA2* promoters cloned from the Japonica cultivar Nipponbare were used in an Indica rice background, cultivar IR64. Oliva *et al.* (2014) used the Japonica *GluB1* promoter in IR64, to express ferritin gene but no phenotype consistent with ectopic expression was mentioned.

Transcriptional control is complex and requires the interaction of *cis* elements in promoters and transcription factors. In an IR64 background, some transcription factors may not be recognised leading to miss-regulation of the transgene. As can be seen in Chapter 2, no change was detected in the *cis* elements responsible for endosperm-specific expression. Ectopic expression of a transgene was observed by Furtado *et al.* (2008) when the control of endosperm-specific promoters from foreign species like wheat or barley were used in transgenic rice. It is also entirely plausible that the globulin and glutelin protein are naturally expressed at very low levels in other specific tissues or stages but are beyond the sensitivity of detection techniques.

Ectopic expression of *HvSUT1* would expand the size of the sucrose sink (roots and shoots) and could explain an increase in vegetative growth. Based on the analysis of the growth phenotype of the transgenic rice in Chapter 3, a significant difference was seen at two-month-old seedlings. Thus, the possibility of ectopic expression is being further explored in root, shoot and collar tissue during the first 8-10 weeks of growth via transcript detection by real-time PCR analysis. This, in combination with a *Glb-1::gfp* transgenic line, may provide greater sensitivity to a reporter gene assay to assesses the degree of specificity of the Japonica *Glb-1* promoter in a IR64 background.

The vigorous growth phenotype reported in this study provides a promising strategy for biofortification of rice with mineral elements that may be achieved without compromising yield. The analysis of the growth and yield parameters of the *HvSUT1* transgenic IR64 rice line requires repetition and at some points must be done under field conditions. If the yield trait can be maintained, even increased, while also achieving Fe and Zn enrichment, this will be the most striking finding of this study and overcome the trade-off between yield and mineral content reported by Davis *et al.* (2004). Based on analyses of historical data by White and Broadley (2009), a negative relationship between the concentrations of mineral elements and the yield of edible tissues are often observed in crop genotypes. A carbohydrate dilution effect is proposed to be a factor for this negative relationship (Loladze 2002). However, some previous studies showed that this negative relationship in wheat (Murphy *et al.* 2008; Ortiz-Monasterio *et al.* 2007; Saalbach *et al.* 2014), bean (Graham *et al.* 2001), and rice (Paul *et al.* 2014) are not always observed (White & Broadley 2009). Furthermore, a clearer understanding of this phenomenon would be very beneficial for crop breeders, particularly given the negative impacts of elevated CO_2 on grain nutrient content (especially Fe and Zn) (Liu *et al.* 2017; Loladze 2002; Myers *et al.* 2014; Smith & Myers 2018; Zhu *et al.* 2018). An initial report of Weichert *et al.* (2017) showed no negative impact of high CO_2 concentration on the Fe and Zn level in wheat grain expressing *HvSUT1*. It would be worth testing the transgenic lines made in this study grown in field and laboratory conditions with elevated CO_2 levels using Free-Air CO_2 Enrichment (FACE) or a high CO_2-equipped growth chamber.

In contrast to the lines overexpressing *HvSUT1*, a negative growth phenotype was associated with the endosperm-specific overexpression of *OsNAS2* under the control of the *GluA2* promoter. Interestingly, this phenotype was alleviated, if not reversed, when combined with *Glb*-

1 driven *HvSUT1* expression. Shorter plants, limited tillering, and low grain yield were some of the symptoms of rice grown under Fe toxicity recorded by Zheng *et al.* (2010) and Lee *et al.* (2012), when *OsNAS1* or *OsNAS2* were expressed under the regulation of the constitutive maize *ubiquitin* promoter. Both these genes share the same role in NA/DMA production, leading to increased Fe uptake from soil into roots during all growth stages. Excess accumulation of Fe levels is toxic for plant cells due to the production of free radicals via the Fenton reaction of Fe cations (Arosio *et al.* 2009). No negative growth phenotype was found in transgenic Japonica rice cultivar Xiushui 110 with *OsNAS1* overexpression under the control of an endosperm-specific promoter (Japonica *OsGluB-1* promoter) (Zheng *et al.* 2010). Therefore, the endosperm-specific control of the *OsNAS2* gene using the Japonica *OsGluA2* promoter in this study was designed for transformation into IR64 in order to avoid the negative impacts on transgenic plant where expression was under constitutive control. However, shorter plant height and low tiller number were still seen in the transgenic SC2 lines. Because the Nipponbare *GluA2* promoter was transformed into IR64, here again maybe miss-regulation of the promoter be leading to leaky expression. OsNAS2 expression in important cell types during early growth leading to toxic levels of Fe in vegetative tissues causing this growth impediment. However, when combined with similar ectopic expression of *HvSUT1,* this excess mobilisation of Fe maybe beneficial to the enhanced growth stimulated by a greater sucrose sink.

These speculative explanations for the growth phenotypes observed in the transgenic lines found in this study require more study, but they provide an excellent platform on which to build hypotheses to guide new experiments. Firstly, the degree of specificity of the Nipponbare *GluA2* and *Glb-1* promoters in an IR64 background might be assessed through the use of the *gfp* reporter gene in a *GluA2:gfp* construct. Also, RT-PCR could be used to measure *OsNAS2* and *HvSUT1*

transcript levels at various stages of growth and different tissues. Moreover, an analysis of Fe concentration in the rice tissues will be required for Fe toxicity diagnostic purposes.

5.2.3. Sucrose as a global signal for sink strength, modifying sink activities.

This study illustrates the potential to manipulate the sucrose transport pathway by targeted overexpression of a *SUT1* gene to enhance sucrose uptake and partitioning in the grain sink. Endosperm- or grain-specific overexpression of *HvSUT1* was shown as a good strategy to improve sink strength, resulting in an increased source-to-sink translocation of sucrose and other nutrients in pea (Rosche *et al.* 2002; Rosche *et al.* 2005), wheat (Saalbach *et al.* 2014; Weichert *et al.* 2017; Weichert *et al.* 2010) and rice (Huynh 2015).

In order to summarise and predict the consequences of increased SUT1 activity during grain filling, the proposed pathways of sucrose metabolic activities in the rice endosperm at the unloading site between the nucellus epidermis and aleurone is presented in Figure 5.2. Although further investigation of the effects of *HvSUT1* overexpression on sink strength via sucrose metabolic activities was not tested, the proposed model is based on the data of this study and that of several previous reports in rice (Huynh 2015; Wang *et al.* 2015a), barley (Weschke *et al.* 2000), wheat (Saalbach *et al.* 2014; Weichert *et al.* 2010), pea (Rosche *et al.* 2002; Rosche *et al.* 2005), and vegetable pea (Lu *et al.* 2020). The model identifies some of the major players for sink strength in sucrose metabolism which are possibly modified by increased sucrose via sucrose transporter overexpression. This may help guide future work to complete a more comprehensive picture and help understand the interaction between sucrose unloading and mineral uptake in the grain of rice and other important food crops.

After uptake into the aleurone and before its further metabolism, sucrose is either hydrolysed by invertase (INV) or degraded by sucrose synthase (SuSy) into glucose, fructose and uridine-diphosphoglucose (UDP-glucose) (called the hexose pool). At early stages of seed development and growth (around 2-5 DAA for rice), INVs are more active to hydrolyse sucrose into hexoses (Hirose *et al.* 2002; Wang *et al.* 2008; Weschke *et al.* 2000) that are essential for the cell cycle and growth. The sucrose:hexose ratio gradually increases at the phase of endospermal starch accumulation (from 7 DAA for rice) (Weber *et al.* 1997; Weichert *et al.* 2010; Weschke *et al.* 2000).

With an increase in sucrose uptake into the endosperm of the grain with *HvSUT1* overexpression, the sucrose:hexose ratio is likely to remain high. This was revealed in the *HvSUT1*-overexpressed Nipponbare rice grains where no change in hexose sugars (fructose and glucose) were found, but sucrose levels increased (Huynh 2015). An increased ratio of sucrose: hexoses may initiate the transition into the storage mode, inducing storage-associated gene expression in the cereal endosperm (Weschke *et al.* 2003; Weschke *et al.* 2000). The increased sucrose uptake is assumed to up-regulate sucrose synthase (SuSy) activity, leading to high metabolic fluxes into storages products. This is because SuSy is correlated with the sucrose concentration, and it directly converts sucrose into hexoses that are important in biosynthesis of storage products (Weschke *et al.* 2000). SuSy serves as a biochemical marker of sink strength, and thus measuring the expression of *SuSy* at the transcript level should be investigated in future work following this study, to confirm the effect of *HvSUT1* overexpression.

Hexoses can be phosphorylated into the hexose phosphate pool (glucose-6-phosphate (G6P), fructose-6-phosphate (F6P), and glucose-1-phosphate (G1P)) involved in the biosynthesis of storage products, including starch, cellulose, lipid, and protein. However, increased sucrose

uptake via *HvSUT1* expression is unlikely to be used for starch biosynthesis, because starch content did not increase in mature rice and wheat grains expressing *HvSUT1* (Huynh 2015; Saalbach *et al.* 2014; Weichert *et al.* 2010). ADP-glucose pyrophosphrylase and soluble starch synthase play important roles in starch biosynthesis in the rice grain, but these may be unchanged due to increasing sucrose uptake by *HvSUT1* overexpression. The genes related to these components can also be easily be measured in the transgenic lines generated in this study to determine whether starch biosynthesis is modified. This would be a priority for future work.

Although starch is not very sensitive to variation of sucrose uptake, protein is found to respond more actively to increased sucrose uptake via *HvSUT1* overexpression. The protein accumulation responding to increased sucrose uptake capacity was reported in pea and wheat seeds expressing *SUT1* (Saalbach *et al.* 2014; Weichert *et al.* 2017; Weichert *et al.* 2010), but Nipponbare rice grains expressing *HvSUT1* had increased levels of amino acids (Huynh 2015). Furthermore, Huynh (2015) reported noticeable changes in fatty acid composition. This suggests that sucrose in grains with *HvSUT1* overexpression builds up the hexose phosphate pool, which provides intermediates for the synthesis of storage protein, lipid and may increase phytic acid as well through the availability of carbon skeletons from 3-phosphoglycerate (3PGA), phosphoenolpyruvate (PEP), or pyruvate.

Phosphorylation of hexose requires ATP to produce hexose phosphates that would lead to increased P demand in grain expressing *HvSUT1*. There is little information about this possibility in rice and other cereals. In *Arabidopsis*, high sucrose levels in root tissue signalled an upregulation of Pi starvation-induced genes, leading to increased Pi demand (Lei *et al.* 2011) and possibly also Fe transporter genes (IRT2) (Lin *et al.* 2016), but this is unknown in the endosperm tissue of the *Arabidopsis* seed. Interestingly, P concentration was found to increase in the mature IR64

overexpressing *HvSUT1* in this study and in Nipponbare rice grain with overexpressing *HvSUT1* (Huynh 2015). A transcriptome analysis will be important for future work to determine whether these genes related to P translocation and uptake and Fe transport are also stimulated by increased sucrose in the transgenic rice grains overexpressing *HvSUT1*.

The interconnected pathways described above and outlined in Fig. 5.2B clearly indicate that increased sucrose and hexose substrates, partitioning into the various biosynthetic pathways, could account for the altered storage product composition in *HvSUT1* overexpressing rice grains. Gene expression and enzyme activity can also be regulated in a feedback loop by substrates, intermediates, and products of each biosynthetic pathway. A detailed discussion of these reactions is beyond the scope of this study, however future work could, as mentioned, incorporate a transcriptome and metabolome analysis of transgenic grains to further elucidate the details of these regulatory networks.

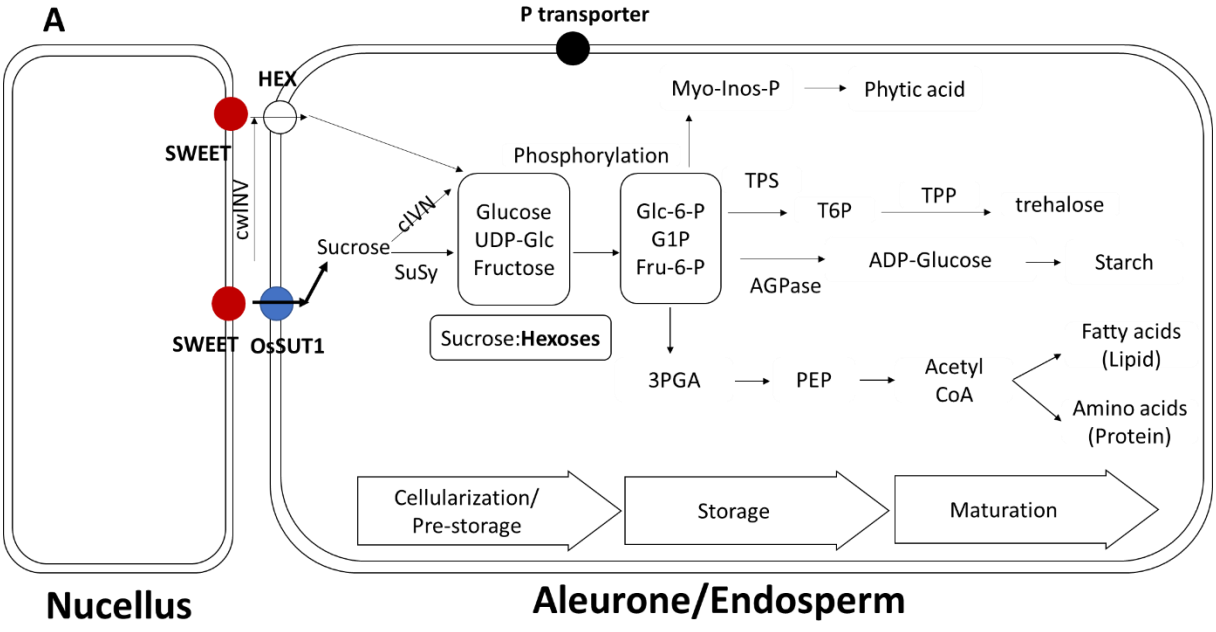

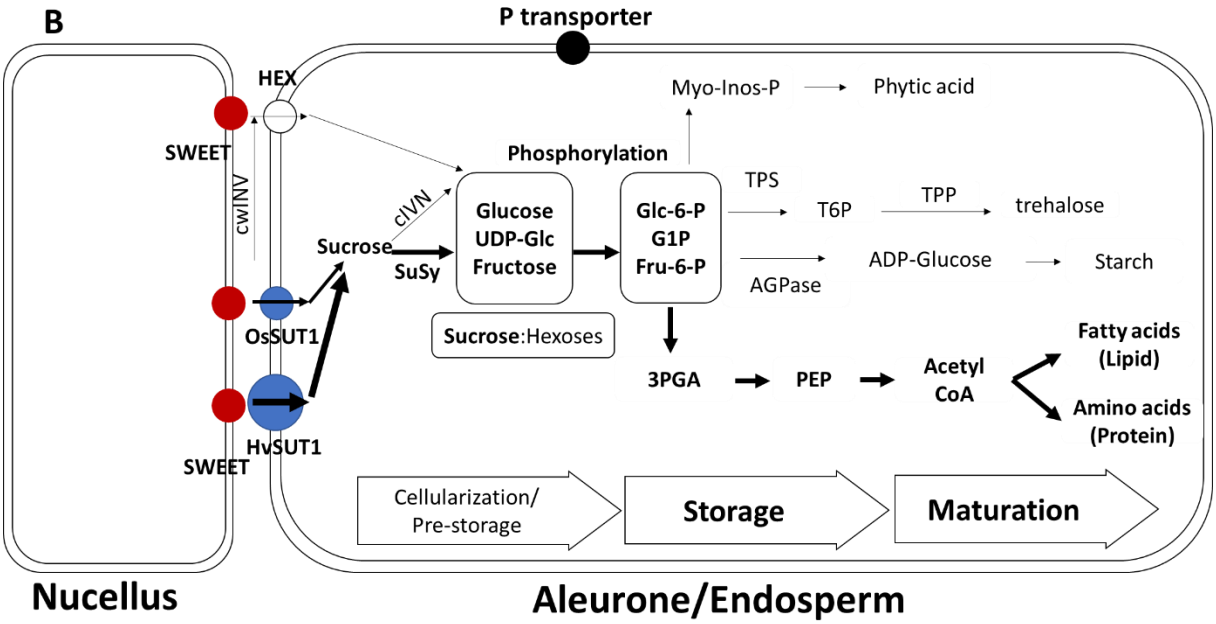

Figure 5.2. A proposed pathway of increased sucrose to alter potential players of storage product biosynthesis in rice grain sink. A. Non-transgenic grain. B. The *HvSUT1*-overexpressing grain. HEX: hexose transporter (OsSWEET4) (Sosso *et al.* 2015); SWEET: and SUT1: sucrose transporters, cwINV: cell wall invertase, cINV: cytoplasm invertase; SuSy: Sucrose synthase, UDP-Glc:: UDP-glucose; Glc-6-P: glucose-6-phosphate; G1P: glucose-1-phosphate; Fru-6-P; fructose-6-Phosphate; AGPase: ADP-glucose pyrophosphorylase. TPS: trehalose-6-phosphate synthase; T6P: trehalose-6-phosphate; TPP: trehalose-6-phosphate phosphatase; 3PGA: Glyceraldehyde 3-phosphate; PEP: Phosphoenolpyruvate.

5.2.4. NA or/and DMA, chelators synthesised by OsNAS2 modify Fe and Zn mobility and bioavailability.

NA and DMA are key compounds in the homeostasis of Fe, Zn, and other mineral elements. They contribute to all important sub-processes of Fe and Zn translocation: mobilisation, uptake, and intercellular and intracellular transport. In this project, endosperm-specific overexpression of *OsNAS2* was proposed to enhance NA production in the grain. Although the OsNAS2 protein was detected during grain development, NA/DMA concentration in the rice grain was not measured, due to time constraints and the availability of a reliable and optimised assay. The measurement of these compounds should be highly prioritised in future work. A number of studies, however, have verified that constitutive overexpression of one of the rice *NAS* genes (*OsNAS1*, *OsNAS2* or *OsNAS3*) results in elevated NA concentration in the rice grain (Johnson *et al.* 2011; Kyriacou *et al.* 2014; Lee *et al.* 2009b; Lee *et al.* 2012; Trijatmiko *et al.* 2016; Zheng *et al.* 2010). Therefore, it can be presumed that an increase in the NA concentration in the transgenic rice overexpressing *OsNAS2* will be found in the transgenic line developed in this study.

NA, a non-protein peptide, is a natural chelator of many metal cations in higher plants, including Fe, Zn, Cu, and Mn (von Wirén *et al.* 1999). NA plays a major role in long-distance transport of metals in the phloem from the vegetative source into the sinks, including during grain filling (Takahashi *et al.* 2003). Therefore, enhancement of NA levels in the whole plant would result in an increase in Fe and Zn concentration in the whole plant including the grains. However, after transport into the filial tissue of the rice grain, many questions remain unanswered; for example, are the Fe and Zn complexes modified and the various movement and distribution of Fe and Zn reflected in the difference in their complexes (Iwai *et al.* 2012), and can NA be an alternative chelator to phytate and thus alter Fe and Zn mobility in the rice endosperm. This study

aimed to understand the role of NA in the inter- and intra-cellular mobility of Fe and Zn in the rice endosperm cells. To this end *OsNAS2* was targeted to express in the rice endosperm by the promoter *GluA2*, and therefore NA or/and DMA concentration are presumed to increase preferentially in the grain sink, rather than in source (Zheng *et al.* 2010). Therefore, any change in Fe and Zn mobility in the rice endosperm could be explained by the role of NA/DMA. As the *OsNAS2* gene was overexpressed in this study, any changes in Fe and Zn mobility in the rice endosperm is likely caused by NA rather than DMA. If so, this would be consistent with what occurs during the early stage of rice grain germination, as *OsNAS1* is strongly expressed in the endosperm, but *OsNAAT1* and *OsDMAS1*, two genes involved in DMA biosynthesis, are not (Nozoye *et al.* 2007). Determining the change in NA and DMA level and expression of rice genes in NA and DMA biosynthesis in the rice endosperm during grain development will be essential to understand the role of NA or/and DMA in Fe and Zn mobility during grain filling.

In non-transgenic rice grains (Inoue *et al.* 2003), the cellular localisation of the OsNAS2 protein in the rice endosperm is unknown. In the model of vesicular localisation of OsNAS2 in root cells presented by Nozoye *et al.* (2014a) and Nozoye *et al.* (2014b), the OsNAS2 protein is localised to vesicles originating from the rough endoplasmic reticulum (rER). NA and/or DMA biosynthesis is thought to occur in the vesicles before they are released to the cytosol of the cell (Nozoye *et al.* 2014a; Nozoye *et al.* 2014b). Therefore, based on this model, a similar mechanism of NA and/or DMA production may also be occurring in the rice endosperm cells. This requires further verification in which a transgenic rice carrying *GluA2:OsNAS2/GFP* fusion could assist in answering this question (Nozoye *et al.* 2014a). Based on that prediction of NA production by *OsNAS2* overexpression in the cytosol of the rice endosperm cells will produce far more NA than in the non-transgenic endosperm cells. This will compete with phytic acid for binding Fe and Zn

to form soluble metal complexes. The soluble forms of Fe-NA and Zn-NA would facilitate Fe and Zn mobility in the aleurone cells from the dorsal to ventral side and from the aleurone cell to the inner endosperm. This could explain the striking difference in Fe and Zn (especially Fe) distribution in transgenic rice with *OsNAS2* and *HvSUT1*.

In this study, enhancing NA concentration in the rice grain is proposed to improve the Fe and Zn mobility in the inner endosperm where a trace amount of phytate is detected (Iwai *et al.* 2012). This could be beneficial for Fe and Zn bioavailability in the human gut (Glahn *et al.* 2002) and this can be assumed, as the molar ratios of phytate to Fe and Zn in the transgenic rice grain expressing *OsNAS2* with and without *HvSUT1* was lower than in the non-transgenic control tissue. Several reports suggest that NA and DMA serve as novel enhancers of Fe bioavailability (Beasley *et al.* 2019b; Eagling *et al.* 2014; Lee *et al.* 2012; Zheng *et al.* 2010), thus NA enhancement in the transgenic rice grain expressing *OsNAS2* with and without *HvSUT1* may be beneficial for Fe and Zn bioavailability. However, improvement in Fe and Zn bioavailability can only be confirmed using more accurate tools, such as the Caco-2 cell system or animal feeding experiments. This is planned for future work.

In summary, the results of this study demonstrate that increasing sucrose uptake via endosperm-specific overexpression of *HvSUT1* is a promising strategy for changing micronutrient levels (especially Fe and Zn) in the endosperm of Indica rice. In a novel combination of *HvSUT1* and *OsNAS2* overexpression under the control of endosperm-specific promoters *Glb-1* and *GluA2*, respectively, the distribution of Fe and Zn (particularly Fe) on both dorsal and ventral sides of the rice grain was strikingly higher, not visible in single *HvSUT1* or *OsNAS2* overexpression, or non-transgenic rice. NA/DMA was proposed as an alternative chelator for Fe and Zn, leading to remarkable changes in the Fe distribution and accumulation, and to exist in a form more available

for uptake in the human gut. A vigorous growth phenotype of the transgenic rice overexpressing *HvSUT1* was an unexpected outcome of this study and is worthy of further investigation to unlock opportunities for breeding higher yielding rice with increased Fe and Zn levels. These findings reported in the study contribute to a better understanding of the complicated interaction between photo-assimilate partitioning and other nutrient deposition in cereal grains and raise some speculative hypotheses to stimulate and foster further experimentation. The Fe and Zn concentrations in polished transgenic grains reported in this study account for more than 40% of the recommended Fe (13 mg/kg Fe biofortification target) and roughly 200% of recommended Zn (28 mg/kg Zn biofortification target). An important caveat to this conclusion is that many differences in micronutrient levels reported in the literature can be accounted for by the differences in rice cultivars, growth conditions, analysis conditions, and analysis facilities. In conclusion, a potential combination of high yield and nutrient-enriched traits in the transgenic lines overexpressing *HvSUT1* and *OsNAS2* is expected to aid in efforts to breed more nutritious staple crops to address micronutrient deficiencies in developing nations, and respond to the negative impacts of future elevated CO_2 levels on grain nutrient content.

APPENDICES

Appendix A. PCR primers, components, and conditions

Table 6.1. Primers for PCR

Name	Sequence (5'→3')	Tm
HvSUT1 3F	GGTTCTGGGGTTTAGCTCGT	64.2
NosTR	AAGACCGGCAACAGGATTC	64
OsNAS2-F1	CTCTTCACCGACCTCGTCAC	65
OsNAS2-F2	CAAGTGCTGCAAGATGGAGG	65.9
HvSUT1R1	TGTCACTGTAGAGCCCAACG	64
pGluA2F	GAACAACACAATGCTGCGTC	64.4
SpeI-GluA2F	GCactagtGTTAATCATGGTGTAGGCAACC	70.9
HindIII-GluA2R	GCaagcttGTTGTTGTAGGACTAATGAACTGAATG	73.1
SpeI-NosTR	GCactagtGCGATCTAGTAACATAGATGACACC	
attB1-OsNAS2	GGGGACAAGTTTGTACAAAAAAGCAGGCTTCATGGAG GCTCAGAACCAAGA	
attB2-OsNAS2	GGGGACCACTTTGTACAAGAAAGCTGGGTCTCAGACG GATAGCCTCTTGG	

Table 6.2. PCR 1 for detecting transgene

Component	**A 25-µl reaction**	**Final concentration**	
MiliQ water	13.375		
5X Green buffer (Promega)	5	1X	
25mM $MgCl_2$	2	2mM	
10mM dNTPs	0.5	0.2mM	
5 µM Primer Forward (*)	1	200nM	
5 µM Primer Reverse	1	200nM	
GoTaq DNA polymerase	0.125		
Genomic DNA (10^5 copies/ µl)	2		
(*): HvSUT1 3F and NosTR for detecting the single construct of HvSUT1 (SC1); OsNAS2-F1 and NosTR for detecting the single construct of OsNAS2 (SC2); OsNAS2-F2 and HvSUT1R1 for detecting the double construct of OsNAS2 and HvSUT1.			
Thermocycling			
Step	**Temperature**	**Time**	**Cycle**
Initial denaturation	95^0C	2 minutes	1
Denaturation	95^0C	30 seconds	30
Annealing	64^0C	30 seconds	
Extension	72^0C	90 seconds	
Final extension	72^0C	10 minutes	1
Hold	4^0C	∞	

Table 6.3. PCR for cloning promoter *GluA2*

Component	A 25-µl reaction	Final concentration	
MiliQ water	14.5 µl		
5X GC buffer (NEB)	5 µl	1X	
10mM dNTPs	0.5 µl	0.2mM	
5 µM Primer Forward	1 µl of SpeI-GluA2F	200nM	
5 µM Primer Reverse	1 µl of HindIII-GluA2R	200nM	
DMSO (100%)	0.75 µl	3%	
Phusion HF DNA polymerase	0.25 µl		
Nipponbare gDNA (10^4 copies/ µl)	2 µl		
Thermocycling			
Step	**Temperature**	**Time**	**Cycle**
Initial denaturation	98^0C	2 minutes	1
Denaturation	98^0C	10 seconds	35
Annealing	65^0C	30 seconds	
Extension	72^0C	30 seconds	
Final extension	72^0C	10 minutes	1
Hold	4^0C	∞	

Table 6.4. PCR for amplifying *OsNAS2*

Component	**A 25-µl reaction**	**Final concentration**	
MiliQ water	14.5 µl		
5X GC buffer (NEB)	5 µl	1X	
10mM dNTPs	0.5 µl	0.2mM	
5 µM Primer Forward	1 µl of attB1-OsNAS2	200nM	
5 µM Primer Reverse	1 µl of attB2-OsNAS2	200nM	
DMSO (100%)	0.75 µl	3%	
Phusion HF DNA polymerase	0.25 µl		
DNA plasmid	2 µl		
Thermocycling			
Step	Temperature	Time	Cycle
Initial denaturation	98^0C	2 minutes	1
Denaturation	98^0C	10 seconds	35
Annealing	70^0C	30 seconds	
Extension	72^0C	30 seconds	
Final extension	72^0C	10 minutes	1
Hold	4^0C	∞	

Table 6.5. PCR for amplifying *GluA2:OsNAS2* cassette

Component	**A 25-µl reaction**	**Final concentration**	
MiliQ water	14.5 µl		
5X GC buffer (NEB)	5 µl	1X	

10mM dNTPs	0.5 µl	0.2mM	
5 µM Primer Forward	1 µl of SpeI-GluA2F	200nM	
5 µM Primer Reverse	1 µl of SpeI-NosTR	200nM	
DMSO (100%)	0.75 µl	3%	
Phusion HF DNA polymerase	0.25 µl		
DNA plasmid	2 µl		
Thermocycling			
Step	Temperature	Time	Cycle
Initial denaturation	98^{0}C	2 minutes	1
Denaturation	98^{0}C	10 seconds	35
Annealing	70^{0}C	30 seconds	
Extension	72^{0}C	30 seconds	
Final extension	72^{0}C	10 minutes	1
Hold	4^{0}C	∞	

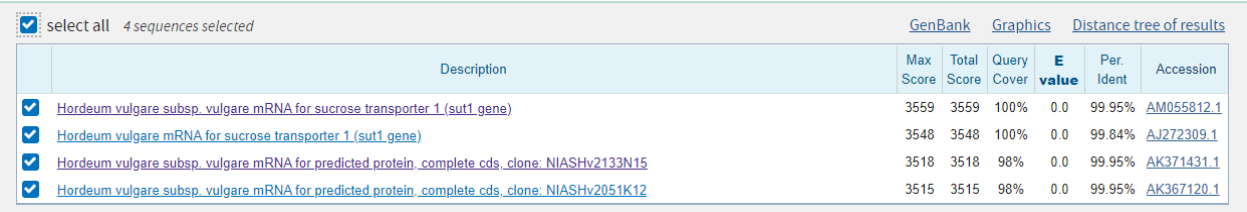

A

B.

Figure 6.1. Sequence of *Glb-1* promoter from rice. A. A blast analysis of *HvSUT1* sequence aligned against the barley's data collection (taxid:4512) in the NCBI database; B. Nucleic acid alignment of *Glb-1* promoter with AY427575.1

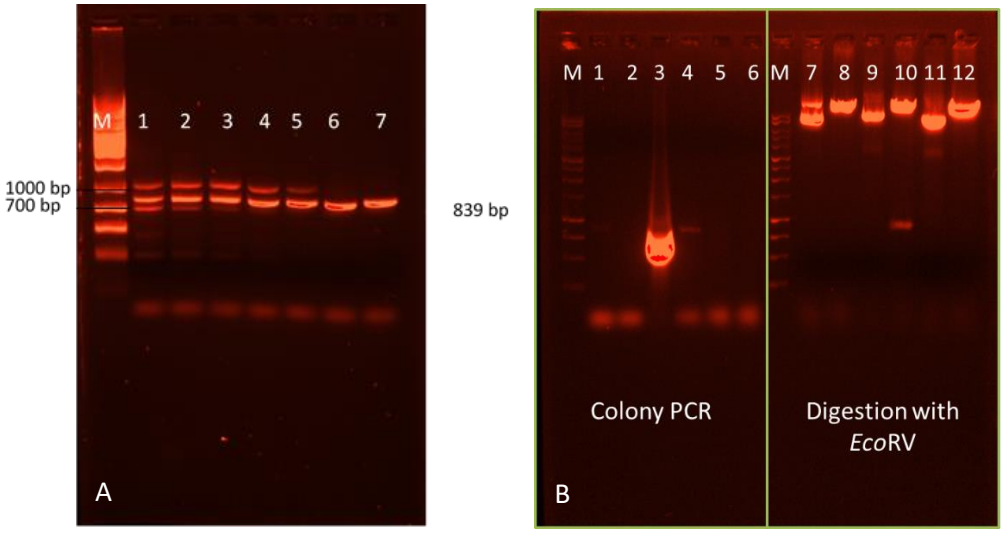

Figure 6.2. PCR product of *GluA2* promoter, colony PCR and digests to confirm identity of cloned destination plasmids.

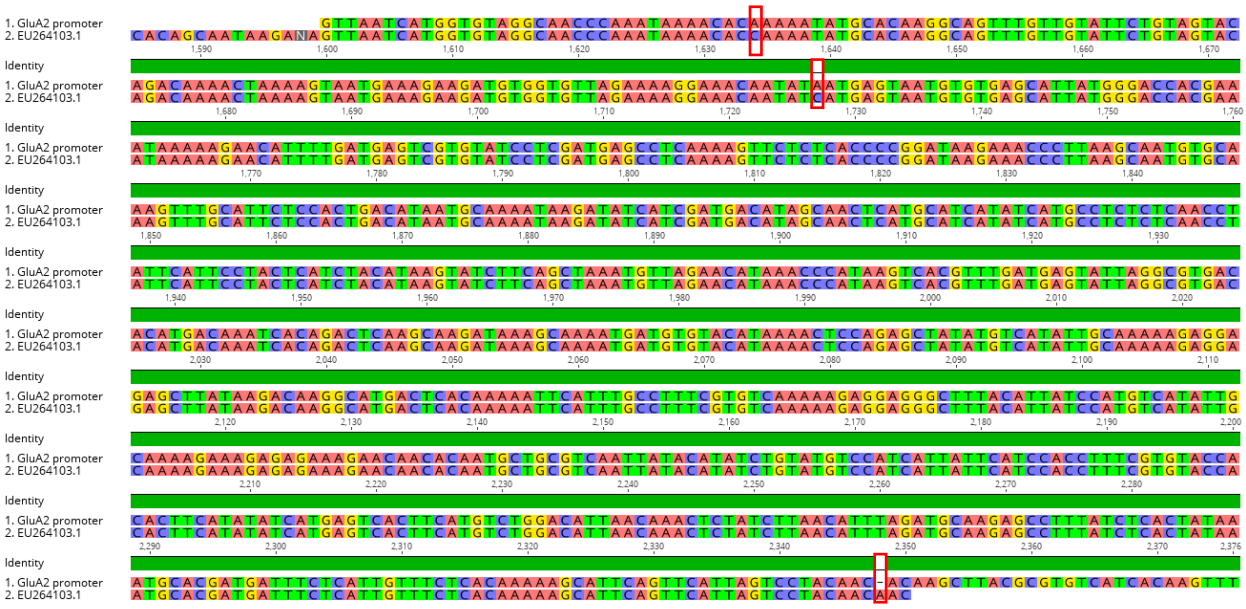

Figure 6.3. Alignment of *GluA2* promoter' sequence against the reference EU264103.1, three different sites in red boxes.

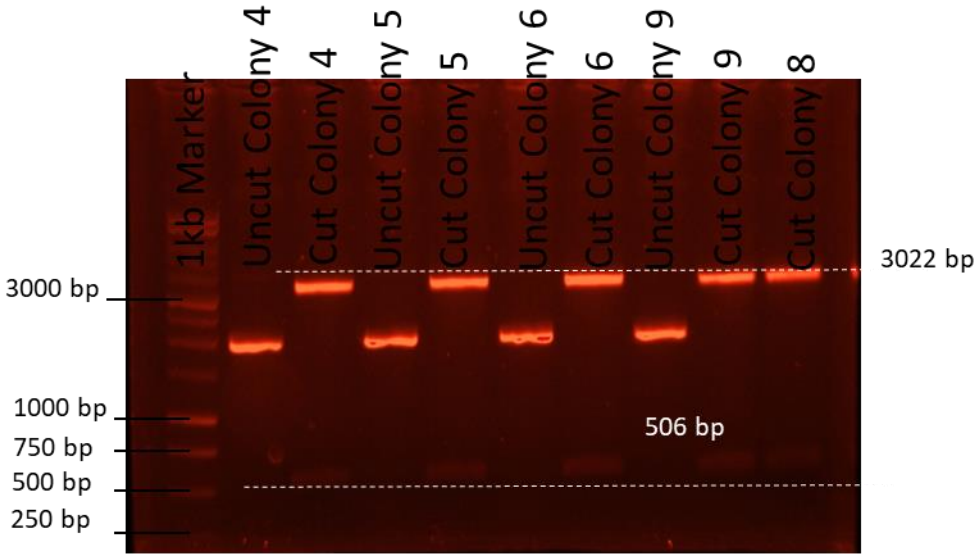

Figure 6.4. Analysis of restriction digestion for pENTRY221:*OsNAS2* vector with *Apa*I. There were two bands (506 bp and 3022 bp) for plasmids DNA extraction from nine colonies containing the recombined pENTRY221:*OsNAS2* vector and single band for empty pDORN221. For intact plasmids, bands of empty pDORN221 vector were larger size than those of the recombined pENTRY221:*OsNAS2* vector.

Appendix B. Medium components for IR64 transformation using immature embryos

Table 6.7. Stock solutions of antibiotics and growth regulators

Stock solution	Concentration	Preparation	Storage temperature
Growth regulators			
2,4 D	2 mg/ml	Dissolve in few drops of 1N KOH, then complete to volume with MiliQ water, then filter-sterilise.	-20^{0}C
BAP	1 mg/ml		-20^{0}C
Kinetin	2 mg/ml		-20^{0}C
NAA	1 mg/ml		-20^{0}C
Antibiotics			
Rifampicin	10 mg/ml	Dissolve in absolute methanol, then filter-sterilise.	-20^{0}C
Kanamycin	50 mg/ml	Dissolve in MiliQ water, then filter-sterilise	-20^{0}C
Spectinomycin	50 mg/ml		-20^{0}C
Timentin	100 mg/ml		-20^{0}C
Hygromycin	50 mg/ml	Commercial stock	4^{0}C
Others			
Acetosyringone	20 mg/ml	Dissolve in DMSO, then filter-sterilise	-20^{0}C
Glycine	100 mM	Dissolve in MiliQ water, then filter-sterilise	-20^{0}C

Table 6.8. Media for culture of bacteria.

Components	LB plate (100ml)	LB broth (100ml)	SOC (100ml)
Tryptone	1 g	1 g	2 g
Yeast extract	0.5 g	0.5 g	0.5 g
NaCl	1 g	1 g	-
Agar	1.5 g	-	-
1M NaCl	-	-	1 ml
1M KCl	-	-	0.25 ml
2M Mg^{2+} stock (filter-sterilised)	-	-	1 ml (after autoclaving)
2M Glucose (filter-sterilised)	-	-	1 ml (after autoclaving)
pH	7.0	7.0	7.0

Table 6.9. Stock solutions prepared for immature embryo transformation

Name of stock solution (volume)	Component	Weight (g)	Concentration (M)
N6 major 1 (1L)	KNO_3	141.5 g	1.40
N6 major 2 (1L)	$MgSO_4.7H_2O$ $(NH_4)_2SO_4$	18.5 g 46.3 g	0.075 0.35
N6 major 3 (1L)	KH_2PO_4	40 g	0.294
N6 major 4 (1L)	$CaCl_2.\ 2H_2O$	16.6 g	0.11
B5 minor 1 (100ml)	20 mM $FeSO_4.\ 7H_2O$ 20 mM Na_4EDTA (Mixing 1:1 ratio before adding into medium)	0.278 g in 50 ml 0.380 g in 50 ml (prepared separately)	0.02 0.02
B5 minor 2 (1L)	$MnSO_4.\ 4H_2O$ $ZnSO_4.\ 7H_2O$ H_3BO_3	1 g 0.2 g 0.3 g	4.4×10^{-3} 7.0×10^{-4} 4.85×10^{-3}
B5 minor 3 (1L)	KI	0.075 g	4.5×10^{-4}
B5 minor 4 (1L)	$CuSO_4.\ 5H_2O$ $Na_2MoO_4.\ 2H_2O$ $CoCl_2.\ 6H_2O$	0.0025 g 0.025 g 0.0025 g	1.0×10^{-5} 1.0×10^{-4} 1.0×10^{-5}
B5 vitamins (100ml)	Thiamine HCl Pyridoxine HCl Nicotinic acid Myo-inositol	0.2 g 0.02 g 0.02 g 2 g	6.0×10^{-4} 1.0×10^{-4} 1.6×10^{-5} 0.011
AA macro salts (1L)	$MgSO_4.7H_2O$ $CaCl_2.\ 2H_2O$ $NaH_2PO_4.\ 2H_2O$ KCl	2.49 g 1.5 g 1.7 g 29.5 g	0.01 0.01 0.01 0.4
AA micro salts (1L)	H_3BO_3 KI $CuSO_4.\ 5H_2O$ $CoCl_2.\ 6H_2O$ $MnSO_4.\ H_2O$	3 g 0.75 g 0.025 g 0.025 g 9.971 g	0.0485 4.5×10^{-3} 1.0×10^{-4} 1.0×10^{-4} 0.059

	$ZnSO_4$. $7H_2O$ Na_2MoO_4. $2H_2O$	2 g 0.25 g	7.0×10^{-3} 1.0×10^{-3}
MS 1 (1L)	KNO_3 NH_4NO_3	95 g 82.5 g	0.94 1.03
MS 2 (1L)	$MgSO_4.H_2O$ $MnSO_4$. $4H_2O$ $ZnSO_4$. $7H_2O$ $CuSO_4$. $5H_2O$	37 g 2.23 g 0.86 g 0.0025 g	0.267 0.01 0.003 1.0×10^{-5}
MS 3 (1L)	$CaCl_2$. $2H_2O$ KI $CoCl_2$. $6H_2O$	44 g 0.083 g 0.0025 g	0.3 5.0×10^{-4} 1.0×10^{-5}
MS 4 (1L)	KH_2PO_4 H_3BO_3 Na_2MoO_4. $2H_2O$	17 g 0.62 g 0.025 g	0.125 0.01 1.0×10^{-4}
MS vitamins (100mL)	Nicotinic acid Pyridoxine HCl Thiamine HCl Glycine Myo-inositol	0.01 g 0.01 g 0.002 g 0.04 g 2 g	8.1×10^{-5} 4.9×10^{-5} 6.0×10^{-6} 5.33×10^{-4} 0.011

All components were dissolved in MiliQ water and all stock solutions were stored at 4^0C.

Table 6.10. Preparation of competent cell for heat-shock transformation

Component	**TSS buffer (50 ml)**
PEG 3350	5 g
$MgCl_2$. $6H_2O$	0.3 g
DMSO	2.5 ml
LB broth	Add LB broth to 50 ml, followed by filter-sterilisation with 0.2 µm filter.

Table 6.11. Media prepared for immature embryo transformation

Stock solution	A200 (1L) (Suspension medium)	A201 (1L) (Co-cultivation medium)	A202 (1L) (Resting medium)	A203 (1L) (Selection medium)	A204 (1L) (Pre-regeneration medium)	A205 (1L) (Regeneration medium)	MS30 (1L) (Rooting medium)
N6 major 1		20 ml	20 ml	20 ml			
N6 major 2		10 ml	10 ml	10 ml			
N6 major 3		10 ml	10 ml	10 ml			
N6 major 4		10 ml	10 ml	10 ml			
B5 minor 1		10 ml	10 ml	10 ml	10 ml	10 ml	10 ml
	(Mixing 5 ml of 20 mM $FeSO_4$. $7H_2O$ and 5 ml of 20 mM Na_4EDTA before adding to medium)						
B5 minor 2		10 ml	10 ml	10 ml			
B5 minor 3		10 ml	10 ml	10 ml			
B5 minor 4		10 ml	10 ml	10 ml			
B5 vitamins	1 ml	5 ml	5 ml	5 ml			
AA macro salts	100 ml						
AA micro salts	1 ml						
Glycine stock	1 ml						
MS 1					20 ml	20 ml	20 ml
MS 2					10 ml	10 ml	10 ml
MS 3					10 ml	10 ml	10 ml
MS 4					10 ml	10 ml	10 ml
MS vitamins					5 ml	5 ml	5 ml
Chemicals							
L-Glutamine	0.876 g	0.876 g	0.3 g	0.3 g			
Aspartic acid	0.26 g	0.26 g					
Arginine	0.174 g	0.174 g					
Casamino acid	0.5 g	0.5 g	0.5 g	0.5 g			
L-Proline		0.5 g	0.5 g	0.5 g			
Sucrose	20 g	20 g				30 g	30 g
D-Glucose	10 g	10 g					
D-Mannitol			36 g	36 g			

Maltose. H_2O			20.9 g	20.9 g	31.71 g		
Sorbitol					20 g		
Volume to	999 ml	990 ml	992 ml	991 ml	986 ml	993 ml	996 ml
pH	5.2	5.2	5.8	5.8	5.8	5.8	5.8
	Adjust to appropriate pH by 1N KOH						
Gelzan		5.5 g	5 g	5 g	6 g	3 g	2 g
Added after autoclaving at 121^{0}C for 15 minutes							
Acetosyringone	1ml (***added before use***)	1ml					
2,4-D		1 ml	0.5 ml	0.5 ml			
NAA		1 ml	1 ml	1 ml	5 ml	1 ml	
BAP		1 ml	0.2 ml	0.2 ml			
Kinetin					1 ml	1 ml	
Antibiotic							
Timentin			1 ml	1 ml	1 ml	1 ml	1 ml
Hygromycin B				0.6 ml	1 ml	1 ml	0.6 ml
Light condition/ Temperature	Dark condition/ 23^{0}C -25^{0}C	Continuous light 30^{0}C					

Appendix C. Quantitative real-time PCR

Table 6.12. Primers for the qPCR assay to determine insert number of the transgenes

Name	Sequence (5'→3')
SBE4	GTTTTAGTTGGGTGAAAGCGGTT
	CCTGTTAGTTCTTCCAATGCCCTTA
NosTYA	ATCATCGCAAGACCGGCAA
	ATGACTCGAATTTCCCCGAT
NosT16	GTATAATTGCGGGACTCTAA
	CGGTCTTGCGATGATTA
pUbi1	AACCCTAAACCCTAAATGGATG
	TGTGCATGTGTTCTCCTTTTT

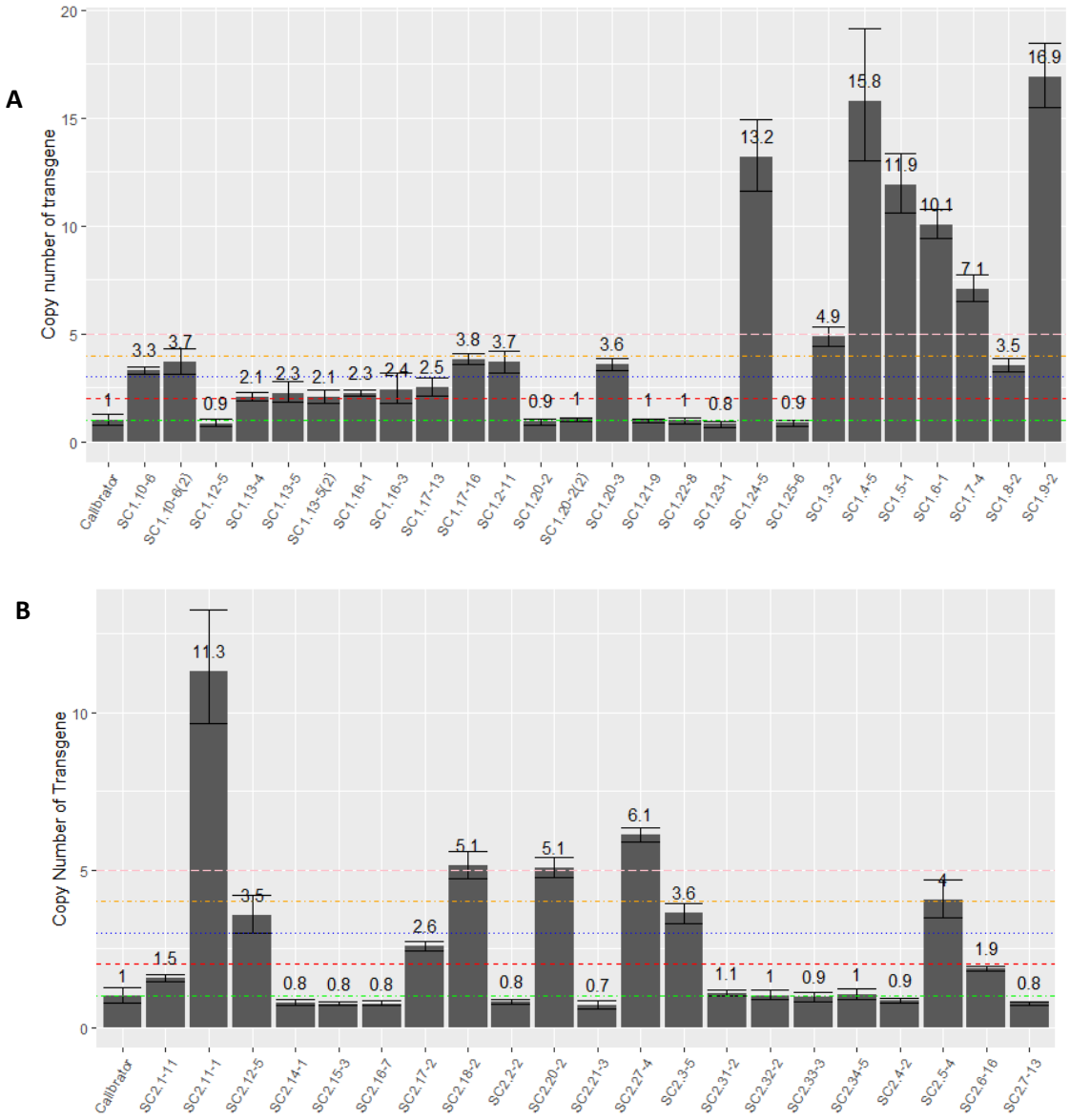

Figure 6.5. Copy number of transgene gene in three population of T0 putatively transgenic plants analysed by qPCR using the set of NostYA/NosT16 and SBE4 primers. A. Copy number of *transgenes*

in 26 independent lines transformed *Glb1*:*HvSUT1:NosT*; B. Copy number of *transgenes* in 21 independent T0 transgenic plants carrying *GluA2:OsNAS2:NosT*. The values present the means ± SD of $2^{-\Delta\Delta Ct}$ in three replicates (calculated in the section 2.2.7). Green, red, blue, orange, and pink dash lines represent for 1, 2, 3, 4, and 5 copies.

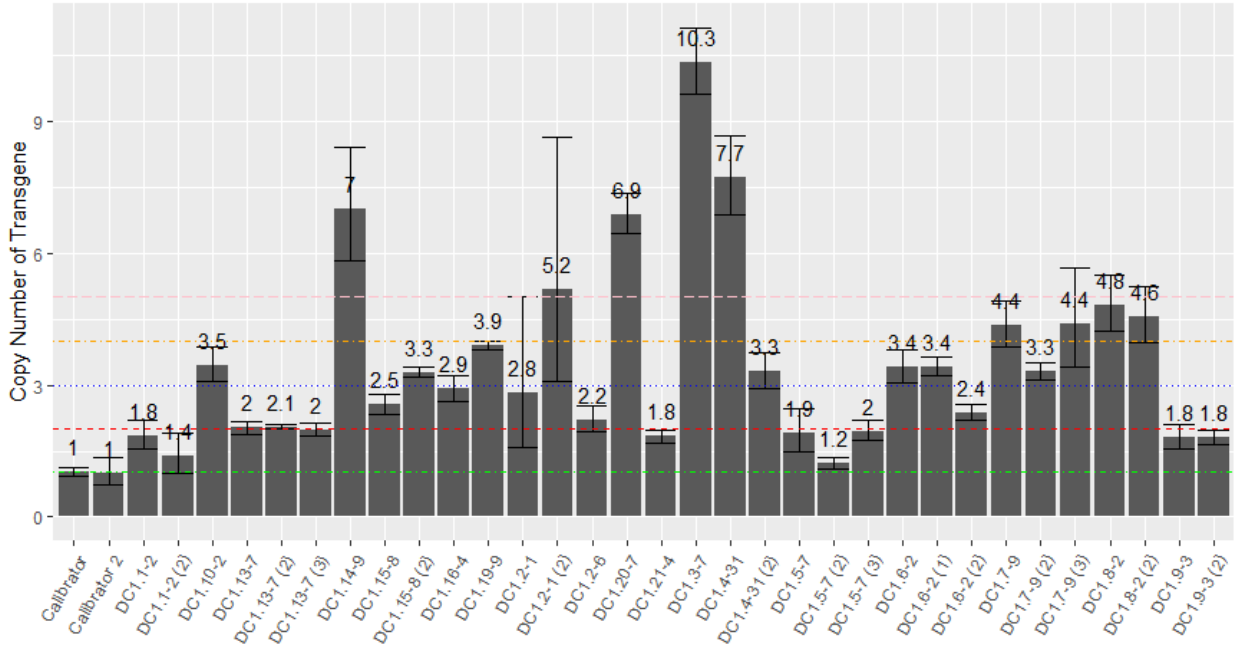

Figure 6.5. Copy number of transgenes in 21 independent lines T0 transformed *GluA2:OsNAS2:NosT-Glb1*:*HvSUT1:NosT* analysed by qPCR using the set of NostYA/NosT16 and SBE4 primers. The values present the means ± SD of $2^{-\Delta\Delta Ct}$ in three replicates (calculated in the section 2.2.7). Green, red, blue, orange, and pink dash lines represent for 1, 2, 3, 4, and 5 copies.

Appendix D. Western blot analysis and nutrient analysis

Table 6.13. All components were used to make buffers for protein analyses

Chemicals	Amount for 1X buffer	Final concentration
Gel Electrode Buffer		
Tris-Base	15g	25mM
Glycine	72g	192mM
SDS	5g	0.1%
H_2O	Add to 1L and adjust pH 8.3	
1X transfer buffer		
Tris-Base	3.03	25mM
Glycine	14.42	192mM
H_2O	Add to 1L and adjust pH 8.3	
1X TBST		
Tris-base	2.42g	20mM
NaCl	8.77g	150mM

Tween20	1 ml	0.1%
H_2O	Add to 1L and adjust pH 7.4	
1X Blotto buffer		
Tris-base	2.42g	20mM
NaCl	8.77g	150mM
Skim Milk	12.5	5%
Tween20	1 ml	0.1%
H_2O	Add to 1L and adjust pH 7.4	
Coomassie stain		
Glacial acetic Acid	50 ml	10%
Methanol	250 ml	50%
Coomassie Brilliant Blue	0.5 g	0.1%
H_2O	Add to 500 ml	
De-staining		
Methanol	50 ml	10%
Acetid acid	50 ml	10%
H_2O	400 ml	80%
Laemmli buffer (3X)		
Tris-HCl, pH 6.8	1.44 ml 1 M Tris-HCl stock, pH 6.8	0.34 M
SDS	1.8 ml 20% SDS stock	7 %
Glycerol	1.8 ml 100% Glycerol	34 %
Bromophenol blue	36 µl 1% Bromophenol blue	0.007 %
DTT		200mM
- Grind together a 1:3 ratio of tissue (that's been crushed in liquid nitrogen) with Lammeli buffer. Add 300 µl of Laemmli buffer in 100 mg of tissue grind and immediately add 80 µl of 1M DTT. Vigorously vortex. - Heat at 100 °C for 10 minutes (heat block). - Centrifuge at max speed for 15-20 min. - Load 15 µl of supernatant into each well		
SDS-PAGE gel preparation		
10% Acrylamide resolving gel for 1 glass plate		
40% Acrylamide (37.5:1 acrylamide:BIS	1.25 ml	10%
Autoclaved MiliQ H_2O	2.4225 ml	
1.5M Tris HCL pH8.8	1.25 ml	0.375M
10% SDS	50 µl	0.1%
20% APS	25 µl	0.1%
TEMED	2.5 µl	0.05%
4% Acrylamide resolving gel for 1 glass plate		
40% Acrylamide (37.5:1 acrylamide:BIS	0.25 ml	4%
Autoclaved MiliQ H_2O	1.585 ml	
0.5M Tris HCL pH6.8	625 µl	0.125M
10% SDS	25 µl	0.1%
20% APS	12.5 µl	0.1%
TEMED	2.5 µl	0.1%

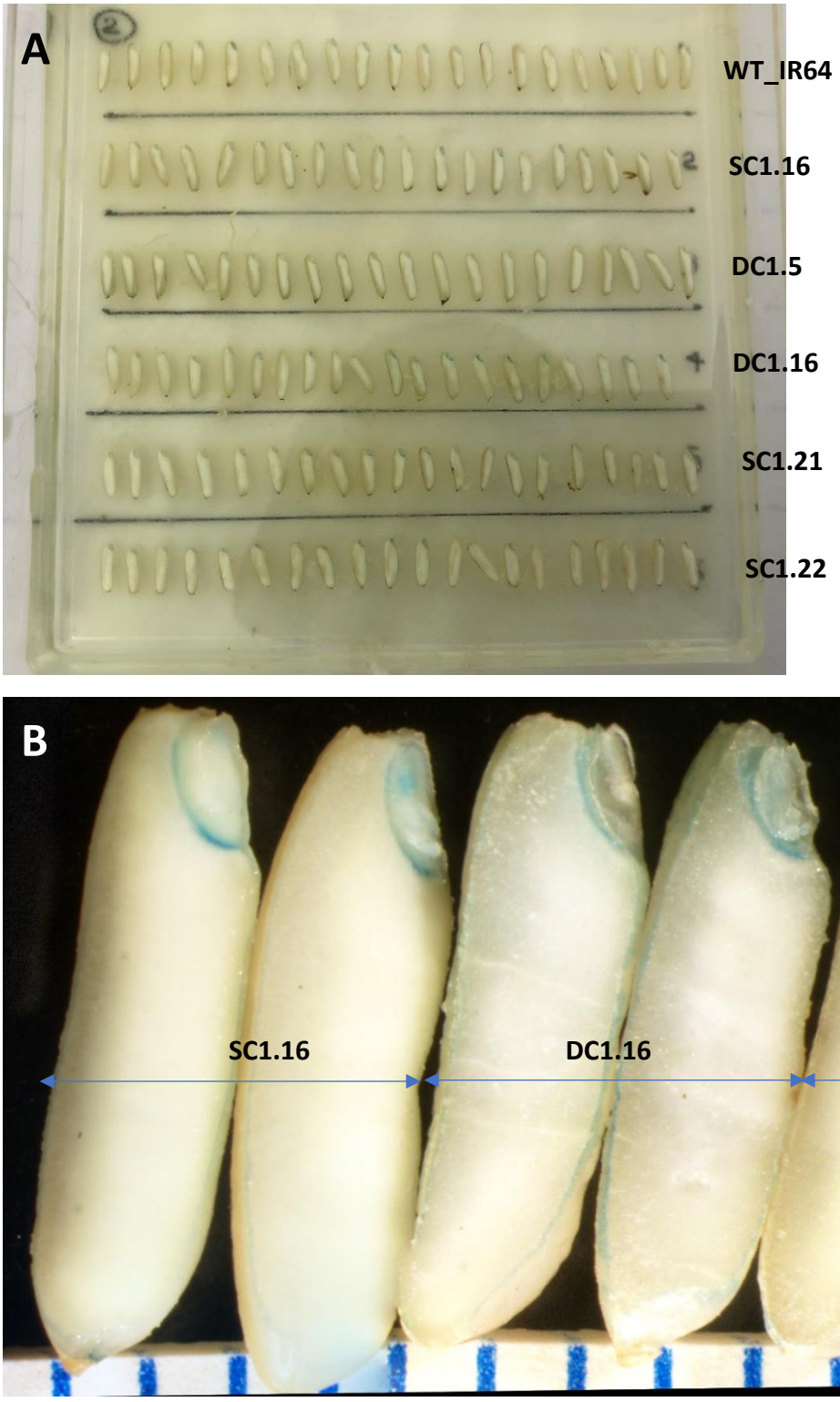

Figure 6.7. Histochemical analysis of Fe distribution using Perls staining to visualise Fe distribution in mature rice grains. A: Twenty mature grains from non-transgenic IR64, *HvSUT1*-expressed grains (SC1.16, SC1.21, and SC1.22), and *OsNAS2+HvSUT1* expressed grains (DC1.5 and DC1.16). B. Haft -longitual sections stained with Perls and captured under stereoscope.

Table 6.14. Molar ratios of phytate to iron (Phytate:Fe), zinc (Phytate:Zn), calcium (Phytate:Ca)
Molar ratios of phytate to minerals were calculated to estimate their relative bioavailabilty. First, the levels of phytate, Fe, Zn and Ca in mg/g to millimole/g were converted using molecular weight of 660.8 g/mol for phytate and atomic mass units of 55.845 g/mol, 65.38 g/mol and 40.078 g/mol for iron, zinc and calcium, respectively. Values present means±SD (n=3). Critical values are <1 for Phytate:Fe, <15 for Phytate:Zn and <0.24 for Phytate:Ca.

Sample	Line	Gene	Phytate:Iron	Phytate:Zinc	Phytate:Calcium	Phytate x Calcium:Zinc
Polished grain	**DC1.1**	***GluA2:OsNAS2 - Glb1:HvSUT1***	64.96 ± 15.18	4.56 ± 1.38	1.23 ± 0.30	1.41 ± 0.26
	DC1.13		66.06 ± 5.39	5.61 ± 0.56	1.73 ± 0.07	1.40 ± 0.22
	DC1.16		56.09 ± 5.58	7.00 ± 0.76	2.15 ± 0.25	1.63 ± 0.30
	DC1.19		119.55 ± 37.05	9.97 ± 3.05	2.32 ± 0.67	2.88 ± 1.07
	DC1.5		71.42 ± 15.93	5.45 ± 0.53	1.58 ± 0.34	1.58 ± 0.33
	DC1.9		65.97 ± 13.48	5.82 ± 0.76	1.30 ± 0.01	2.02 ± 0.54
	SC1.12	***Glb1:HvSUT1***	72.66 ± 14.23	9.07 ± 2.88	2.36 ± 0.29	2.26 ± 1.03
	SC1.13		76.85 ± 33.33	6.41 ± 1.52	1.70 ± 0.57	2.27 ± 0.04
	SC1.16		62.27 ± 11.49	7.62 ± 0.84	2.16 ± 0.21	1.87 ± 0.28
	SC1.17		65.29 ± 9.05	8.21 ± 1.80	2.29 ± 0.67	2.12 ± 0.02
	SC1.21		47.37 ± 19.70	4.75 ± 2.06	1.40 ± 0.74	1.46 ± 0.48
	SC1.22		90.74 ± 26.19	7.76 ± 1.59	1.95 ± 0.51	1.86 ± 0.35
	SC1.25		66.43 ± 4.91	5.30 ± 0.26	1.57 ± 0.11	1.15 ± 0.25
	SC2.14	***GluA2:OsNAS2***	81.53 ± 9.88	8.85 ± 0.78	2.69 ± 0.17	1.76 ± 0.17
	SC2.15		85.91 ± 7.97	7.82 ± 0.73	1.79 ± 0.10	2.37 ± 0.34
	SC2.31		90.98 ± 11.72	9.20 ± 1.56	2.68 ± 0.35	2.23 ± 0.30
	WT-IR64		151.58 ± 15.66	10.83 ± 4.10	2.85 ± 0.52	2.25 ± 0.71
Unpolished grain	**DC1.1**	***GluA2:OsNAS2 - Glb1:HvSUT1***	45.82 ± 7.63	13.28 ± 2.45	1.91 ± 0.57	8.67 ± 0.72
	DC1.13		38.72 ± 3.57	13.49 ± 1.19	1.78 ± 0.76	9.88 ± 1.86
	DC1.16		47.38 ± 1.31	18.91 ± 1.66	2.57 ± 0.45	12.42 ± 2.13
	DC1.19		49.24 ± 4.68	12.08 ± 3.87	1.09 ± 0.35	11.38 ± 3.24
	DC1.5		51.58 ± 9.82	17.54 ± 4.01	2.49 ± 1.57	13.43 ± 2.36
	DC1.9		31.98 ± 2.94	11.61 ± 2.38	1.37 ± 0.16	9.06 ± 2.66
	SC1.12	***Glb1:HvSUT1***	47.47 ± 26.17	23.24 ± 17.23	2.82 ± 0.68	15.65 ± 16.3
	SC1.13		24.25 ± 0.98	6.66 ± 1.36	0.69 ± 0.08	7.90 ± 2.53
	SC1.16		46.87 ± 7.63	20.01 ± 3.89	2.84 ± 0.78	10.88 ± 1.13
	SC1.17		46.98 ± 14.33	20.20 ± 7.08	3.09 ± 1.28	10.69 ± 2.82
	SC1.21		56.74 ± 10.16	18.44 ± 3.88	2.42 ± 1.04	14.23 ± 3.78
	SC1.22		74.87 ± 14.76	28.25 ± 4.54	3.69 ± 1.22	15.33 ± 1.16
	SC1.25		37.15 ± 3.32	12.23 ± 1.58	2.33 ± 0.35	5.24 ± 0.35
	SC2.14	***GluA2:OsNAS2***	30.00 ± 1.72	12.14 ± 1.61	1.73 ± 0.32	6.83 ± 1.12
	SC2.15		48.90 ± 9.44	15.15 ± 3.77	1.42 ± 0.51	12.65 ± 0.75
	SC2.31		37.52 ± 6.19	13.30 ± 0.83	2.29 ± 0.05	6.56 ± 0.53
	WT-IR64		76.68 ± 11.60	27.41 ± 6.09	2.52 ± 0.79	18.60 ± 7.05

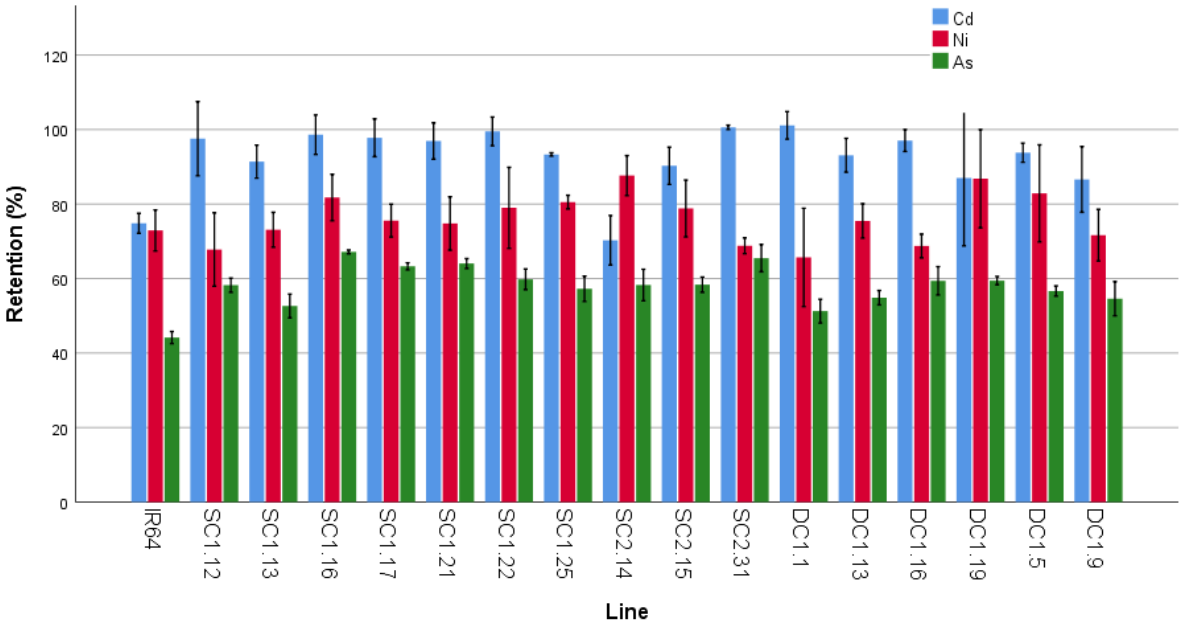

Figure 6.8. Analysis of toxic metal retention (%) in polished grains, namely Cd (blue), Ni (red), and As (green). Bars represent mean ± SE of at least 3 biological replicates of the DC1 (DC1.1, DC1.13, DC1.16, DC1.19, DC1.5, and DC1.9), SC1 (SC1.12, SC1.13, SC1.16, SC1.17, SC1.21, SC1.22, and SC1.25), and SC2 (SC2.14, SC2.15, SC2.31) lines, compared to the non-transgenic control (IR64). DC1 lines were overexpressed the *OsNAS2* and *HvSUT1*, SC1 lines were overexpressed the *HvSUT1* and SC2 lines were overexpressed the *OsNAS2*.

BIBLIOGRAPHY

Abadía, J, López-Millán, A-F, Rombolà, A & Abadía, A 2002, 'Organic acids and Fe deficiency: A review', *Plant and Soil*, vol. 241, no. 1, pp. 75-86.

Aoki, N, Hirose, T & Furbank, RT 2012, 'Sucrose transport in higher plants: From source to sink', in JJ Eaton-Rye, BC Tripathy & TD Sharkey (eds), *Photosynthesis*, Springer Netherlands, vol. 34, pp. 703-729.

Aoki, N, Hirose, T, Scofield, GN, Whitfeld, PR & Furbank, RT 2003, 'The sucrose transporter gene family in rice', *Plant and Cell Physiology*, vol. 44, no. 3, pp. 223-232.

Aoki, N, Hirose, T, Takahashi, S, Ono, K, Ishimaru, K & Ohsugi, R 1999, 'Molecular cloning and expression analysis of a gene for a sucrose transporter in maize *(Zea mays* L.)', *Plant and Cell Physiology*, vol. 40, no. 10, pp. 1072-1078.

Aoki, N, Scofield, GN, Wang, XD, Patrick, JW, Offler, CE & Furbank, RT 2004, 'Expression and localisation analysis of the wheat sucrose transporter *TaSUT1* in vegetative tissues', *Planta*, vol. 219, no. 1, pp. 176-184.

Aoyama, T, Kobayashi, T, Takahashi, M, Nagasaka, S, Usuda, K, Kakei, Y, Ishimaru, Y, Nakanishi, H, Mori, S & Nishizawa, N 2009, 'OsYSL18 is a rice iron(III)–deoxymugineic acid transporter specifically expressed in reproductive organs and phloem of lamina joints', *Plant Molecular Biology*, vol. 70, no. 6, pp. 681-692.

Arosio, P, Ingrassia, R & Cavadini, P 2009, 'Ferritins: A family of molecules for iron storage, antioxidation and more', *Biochimica et Biophysica Acta (BBA) - General Subjects*, vol. 1790, no. 7, pp. 589-599.

Aung, MS, Masuda, H, Kobayashi, T, Nakanishi, H, Yamakawa, T & Nishizawa, NK 2013, 'Iron biofortification of Myanmar rice', *Frontiers in Plant Science*, vol. 4, no. 158.

Aung, MS, Masuda, H, Nozoye, T, Kobayashi, T, Jeon, J-S, An, G & Nishizawa, NK 2019, 'Nicotianamine synthesis by *OsNAS3* is important for mitigating iron excess stress in rice', *Frontiers in Plant Science*, vol. 10, no. 660.

Baker, RF, Leach, KA, Boyer, NR, Swyers, MJ, Benitez-Alfonso, Y, Skopelitis, T, Luo, A, Sylvester, A, Jackson, D & Braun, DM 2016, 'Sucrose transporter *ZmSut1* expression and localization uncover new insights into sucrose phloem loading', *Plant Physiology*, vol. 172, no. 3, pp. 1876-1898.

Banakar, R, Alvarez Fernández, Á, Abadía, J, Capell, T & Christou, P 2017, 'The expression of heterologous Fe (III) phytosiderophore transporter HvYS1 in rice increases Fe uptake, translocation and seed loading and excludes heavy metals by selective Fe transport', *Plant Biotechnology Journal*, vol. 15, no. 4, pp. 423-432.

Bashir, K, Inoue, H, Nagasaka, S, Takahashi, M, Nakanishi, H, Mori, S & Nishizawa, NK 2006, 'Cloning and characterization of deoxymugineic acid synthase genes from graminaceous plants', *Journal of Biological Chemistry*, vol. 281, no. 43, pp. 32395-32402.

Bashir, K, Ishimaru, Y & Nishizawa, NK 2010, 'Iron uptake and loading into rice grains', *Rice*, vol. 3, no. 2-3, pp. 122-130.

Bashir, K, Ishimaru, Y & Nishizawa, NK 2012, 'Molecular mechanisms of zinc uptake and translocation in rice', *Plant and Soil*, vol. 361, no. 1-2, pp. 189-201.

Bashir, K, Nozoye, T, Ishimaru, Y, Nakanishi, H & Nishizawa, NK 2013a, 'Exploiting new tools for iron bio-fortification of rice', *Biotechnology Advances*, vol. 31, no. 8, pp. 1624-1633.

Bashir, K, Nozoye, T, Nagasaka, S, Rasheed, S, Miyauchi, N, Seki, M, Nakanishi, H & Nishizawa, NK 2017, 'Paralogs and mutants show that one DMA synthase functions in iron homeostasis in rice', *Journal of experimental botany*, vol. 68, no. 7, pp. 1785-1795.

Bashir, K, Takahashi, R, Nakanishi, H & Nishizawa, NK 2013b, 'The road to micronutrient biofortification of rice: Progress and prospects', *Frontiers in Plant Science*, vol. 4, no. 15.

Beach, RH, Sulser, TB, Crimmins, A, Cenacchi, N, Cole, J, Fukagawa, NK, Mason-D'Croz, D, Myers, S, Sarofim, MC, Smith, M & Ziska, LH 2019, 'Combining the effects of increased atmospheric carbon dioxide on protein, iron, and zinc availability and projected climate change on global diets: a modelling study', *The Lancet Planetary Health*, vol. 3, no. 7, pp. e307-e317.

Beasley, JT, Bonneau, JP, Sánchez-Palacios, JT, Moreno-Moyano, LT, Callahan, DL, Tako, E, Glahn, RP, Lombi, E & Johnson, AAT 2019a, 'Metabolic engineering of bread wheat improves grain iron concentration and bioavailability', *Plant Biotechnology Journal*, vol. 17, no. 8, pp. 1514-1526.

Beasley, JT, Hart, JJ, Tako, E, Glahn, RP & Johnson, AAT 2019b, 'Investigation of nicotianamine and 2′ deoxymugineic acid as enhancers of iron bioavailability in Caco-2 cells', *Nutrients*, vol. 11, no. 7.

Belide, S, Vanhercke, T, Petrie, JR & Singh, SP 2017, 'Robust genetic transformation of sorghum (*Sorghum bicolor* L.) using differentiating embryogenic callus induced from immature embryos', *Plant Methods*, vol. 13.

Berthier, A, Desclos, M, Amiard, V, Morvan-Bertrand, A, Demmig-Adams, B, Adams, WW, 3rd, Turgeon, R, Prud'homme, MP & Noiraud-Romy, N 2009, 'Activation of sucrose transport in defoliated *Lolium perenne* L.: An example of apoplastic phloem loading plasticity', *Plant and Cell Physiology*, vol. 50, no. 7, pp. 1329-1344.

Bihmidine, S, Hunter, C, Johns, C, Koch, K & Braun, D 2013, 'Regulation of assimilate import into sink organs: Update on molecular drivers of sink strength', *Frontiers in Plant Science*, vol. 4, no. 177.

Bohn, L, Josefsen, L, Meyer, AS & Rasmussen, SK 2007, 'Quantitative analysis of phytate globoids isolated from wheat bran and characterization of their sequential dephosphorylation by wheat phytase', *Journal of Agricultural and Food Chemistry*, vol. 55, no. 18, pp. 7547-7552.

Bohn, L, Meyer, AS & Rasmussen, SK 2008, 'Phytate: impact on environment and human nutrition. A challenge for molecular breeding', *Journal of Zhejiang University. Science. B*, vol. 9, no. 3, pp. 165-191.

Boonyaves, K, Wu, T-Y, Gruissem, W & Bhullar, NK 2017, 'Enhanced grain iron levels in rice expressing an IRON-REGULATED METAL TRANSPORTER, NICOTIANAMINE SYNTHASE, and FERRITIN gene cassette', *Frontiers in Plant Science*, vol. 8, no. 130.

Bouis, HE, Hotz, C, McClafferty, B, Meenakshi, JV & Pfeiffer, WH 2011a, 'Biofortification: A new tool to reduce micronutrient malnutrition', *Food and Nutrition Bulletin*, vol. 32, no. 1_suppl1, pp. S31-S40.

Bouis, HE, Hotz, C, McClafferty, B, Meenakshi, JV & Pfeiffer, WH 2011b, 'Biofortification: A new tool to reduce micronutrient malnutrition', *Food and Nutrition Bulletin*, vol. 32, no. 1 Suppl, pp. S31-40.

Bouis, HE & Saltzman, A 2017, 'Improving nutrition through biofortification: A review of evidence from HarvestPlus, 2003 through 2016', *Global Food Security*, vol. 12, pp. 49-58.

Braun, DM 2012, 'SWEET! The pathway is complete', *Science*, vol. 335, no. 6065, pp. 173-174.

Braun, DM, Wang, L & Ruan, YL 2014, 'Understanding and manipulating sucrose phloem loading, unloading, metabolism, and signalling to enhance crop yield and food security', *Journal of Experimental Botany*, vol. 65, no. 7, pp. 1713-1735.

Brune, M, Rossander-Hultén, L, Hallberg, L, Gleerup, A & Sandberg, A-S 1992, 'Iron absorption from bread in humans: Inhibiting effects of cereal fiber, phytate and inositol phosphates with different numbers of phosphate groups', *The Journal of Nutrition*, vol. 122, no. 3, pp. 442-449.

Bubner, B & Baldwin, IT 2004, 'Use of real-time PCR for determining copy number and zygosity in transgenic plants', *Plant Cell Reports*, vol. 23, no. 5, pp. 263-271.

Bubner, B, Gase, K & Baldwin, I 2004, 'Two-fold differences are the detection limit for determining transgene copy numbers in plants by real-time PCR', *BMC Biotechnology*, vol. 4, no. 14.

Cakmak, I, Pfeiffer, WH & McClafferty, B 2010, 'Biofortification of durum wheat with zinc and iron', *Cereal Chemistry*, vol. 87, no. 1, pp. 10-20.

Callahan, DL, Kolev, SD, O'Hair, RAJ, Salt, DE & Baker, AJM 2007, 'Relationships of nicotianamine and other amino acids with nickel, zinc and iron in *Thlaspi* hyperaccumulators', *New Phytologist*, vol. 176, no. 4, pp. 836-848.

Cao, Z, Mou, R, Cao, Z, Lin, X, Xu, P, Chen, Z, Zhu, Z & Chen, M 2017, 'Nickel in milled rice (*Oryza sativa* L.) from the three main rice-producing regions in China', *Food Additives & Contaminants: Part B*, vol. 10, no. 1, pp. 69-77.

Carsono, N & Yoshida, T 2007, 'Variation in spikelet-related traits of rice plants regenerated from mature seed-derived callus culture', *Plant Production Science*, vol. 10, no. 1, pp. 86-90.

Cegłowski, M, Balcerzak, P, Frański, R & Schroeder, G 2016, 'Determination of conditional stability constants for phytic acid complexes with Mg^{2+}, Ca^{2+} and Zn^{2+} ions using electrospray ionization mass spectrometry', *European Journal of Mass Spectrometry*, vol. 22, no. 5, pp. 245-252.

Charrier, B, Scollan, C, Ross, S, Zubko, E & Meyer, P 2000, 'Co-silencing of homologous transgenes in tobacco', *Molecular Breeding*, vol. 6, no. 4, pp. 407-419.

Chen, L-Q 2014, 'SWEET sugar transporters for phloem transport and pathogen nutrition', *New Phytologist*, vol. 201, no. 4, pp. 1150-1155.

Chen, L-Q, Qu, X-Q, Hou, B-H, Sosso, D, Osorio, S, Fernie, AR & Frommer, WB 2012, 'Sucrose efflux mediated by sweet proteins as a key step for phloem transport', *Science*, vol. 335, no. 6065, pp. 207-211.

Chen, P, Shen, Z, Ming, L, Li, Y, Dan, W, Lou, G, Peng, B, Wu, B, Li, Y, Zhao, D, Gao, G, Zhang, Q, Xiao, J, Li, X, Wang, G & He, Y 2018, 'Genetic basis of variation in rice seed storage protein (albumin, globulin, prolamin, and glutelin) content revealed by genome-wide association analysis', *Frontiers in Plant Science*, vol. 9, no. 612.

Choi, EY, Graham, R & Stangoulis, J 2007, 'Semi-quantitative analysis for selecting Fe- and Zn-dense genotypes of staple food crops', *Journal of Food Composition and Analysis*, vol. 20, no. 6, pp. 496-505.

Ciccolini, V, Pellegrino, E, Coccina, A, Fiaschi, AI, Cerretani, D, Sgherri, C, Quartacci, MF & Ercoli, L 2017, 'Biofortification with iron and zinc improves nutritional and nutraceutical properties of common wheat flour and bread', *Journal of Agricultural and Food Chemistry*, vol. 65, no. 27, pp. 5443-5452.

Clemens, S, Aarts, MG, Thomine, S & Verbruggen, N 2013, 'Plant science: The key to preventing slow cadmium poisoning', *Trends in Plant Science*, vol. 18, no. 2, pp. 92-99.

Crowe, AR & Yue, W 2019, 'Semi-quantitative determination of protein expression using immunohistochemistry staining and analysis: An integrated protocol', *Bio-protocol*, vol. 9, no. 24.

Datta, K & Datta, SK 2006, 'Indica rice (*Oryza sativa*, BR29 and IR64)', in K Wang (ed.), *Agrobacterium Protocols*, Humana Press Inc., Totowa, New Jersey, vol. 1, pp. 201-212.

Davis, DR, Epp, MD & Riordan, HD 2004, 'Changes in USDA food composition data for 43 garden crops, 1950 to 1999', *Journal of the American College of Nutrition*, vol. 23, no. 6, pp. 669-682.

De Schepper, V, De Swaef, T, Bauweraerts, I & Steppe, K 2013, 'Phloem transport: A review of mechanisms and controls', *Journal of Experimental Botany*, vol. 64, no. 16, pp. 4839-4850.

Decourteix, M, Alves, G, Brunel, N, AmÉGlio, T, Guilliot, A, Lemoine, R, PÉTel, G & Sakr, S 2006, 'JrSUT1, a putative xylem sucrose transporter, could mediate sucrose influx into xylem parenchyma cells and be up-regulated by freeze–thaw cycles over the autumn–winter period in walnut tree *(Juglans regia* L.)', *Plant, Cell & Environment*, vol. 29, no. 1, pp. 36-47.

Díaz-Benito, P, Banakar, R, Rodríguez-Menéndez, S, Capell, T, Pereiro, R, Christou, P, Abadía, J, Fernández, B & Álvarez-Fernández, A 2018, 'Iron and zinc in the embryo and endosperm of rice (*Oryza sativa* L.) seeds in contrasting 2′-deoxymugineic acid/nicotianamine scenarios', *Frontiers in Plant Science*, vol. 9, no. 1190.

Doll, NM, Depège-Fargeix, N, Rogowsky, PM & Widiez, T 2017, 'Signaling in early maize kernel development', *Molecular Plant*, vol. 10, no. 3, pp. 375-388.

Douchkov, D, Gryczka, C, Stephan, UW, Hell, R & Bäumlein, H 2005, 'Ectopic expression of nicotianamine synthase genes results in improved iron accumulation and increased nickel tolerance in transgenic tobacco', *Plant, Cell and Environment*, vol. 28, no. 3, pp. 365-374.

Drakakaki, G, Christou, P & Stöger, E 2000, 'Constitutive expression of soybean ferritin cDNA intransgenic wheat and rice results in increased iron levels in vegetative tissues but not in seeds', *Transgenic Research*, vol. 9, no. 6, pp. 445-452.

Duarte, RF, Prom-u-thai, C, Amaral, DC, Faquin, V, Guilherme, LRG, Reis, AR & Alves, E 2016, 'Determination of zinc in rice grains using DTZ staining and ImageJ software', *Journal of Cereal Science*, vol. 68, pp. 53-58.

Durrett, TP, Gassmann, W & Rogers, EE 2007, 'The FRD3-mediated efflux of citrate into the root vasculature is necessary for efficient iron translocation', *Plant Physiology*, vol. 144, no. 1, pp. 197-205.

Eagling, T, Wawer, AA, Shewry, PR, Zhao, F-J & Fairweather-Tait, SJ 2014, 'Iron bioavailability in two commercial cultivars of wheat: Comparison between whole grain and white flour and the effects of nicotianamine and 2′-deoxymugineic acid on iron uptake into Caco-2 cells', *Journal of Agricultural and Food Chemistry*, vol. 62, no. 42, pp. 10320-10325.

EFSA, EFSA 2004, 'Opinion of the scientific panel on genetically modified organisms on the use of antibiotic resistance genes as marker genes in genetically modified plants', *EFSA Journal*, vol. 48, pp. 1-18.

Eide, D, Broderius, M, Fett, J & Guerinot, ML 1996, 'A novel iron-regulated metal transporter from plants identified by functional expression in yeast', *Proceedings of the National Academy of Sciences of the United States of America*, vol. 93, no. 11, pp. 5624-5628.

Endler, A, Meyer, S, Schelbert, S, Schneider, T, Weschke, W, Peters, SW, Keller, F, Baginsky, S, Martinoia, E & Schmidt, UG 2006, 'Identification of a vacuolar sucrose transporter in barley and Arabidopsis mesophyll cells by a tonoplast proteomic approach', *Plant Physiology*, vol. 141, no. 1, pp. 196-207.

Eom, JS, Cho, JI, Reinders, A, Lee, SW, Yoo, Y, Tuan, PQ, Choi, SB, Bang, G, Park, YI, Cho, MH, Bhoo, SH, An, G, Hahn, TR, Ward, JM & Jeon, JS 2011, 'Impaired function of the

tonoplast-localized sucrose transporter in rice, *OsSUT2*, limits the transport of vacuolar reserve sucrose and affects plant growth', *Plant Physiology*, vol. 157, no. 1, pp. 109-119.

Eom, JS, Choi, SB, Ward, JM & Jeon, JS 2012, 'The mechanism of phloem loading in rice (*Oryza sativa*)', *Molecules and Cells*, vol. 33, no. 5, pp. 431-438.

FAO/WHO 2017, *Code of practice for the prevention and reduction of arsenic contamination in rice (CXC 77-2017)*, Food Agriculture Organization/World Health Organization.

Fredlund, K, Isaksson, M, Rossander-Hulthén, L, Almgren, A & Sandberg, A-S 2006, 'Absorption of zinc and retention of calcium: Dose-dependent inhibition by phytate', *Journal of Trace Elements in Medicine and Biology*, vol. 20, no. 1, pp. 49-57.

Fukumorita, T & Chino, M 1982, 'Sugar, amino acid and inorganic contents in rice phloem sap', *Plant and Cell Physiology*, vol. 23, no. 2, pp. 273-283.

Furbank, RT, Scofield, GN, Hirose, T, Wang, X-D, Patrick, JW & Offler, CE 2001, 'Cellular localisation and function of a sucrose transporter *OsSUT1* in developing rice grains', *Functional Plant Biology*, vol. 28, no. 12, pp. 1187-1196.

Furtado, A, Henry, RJ & Takaiwa, F 2008, 'Comparison of promoters in transgenic rice', *Plant Biotechnology Journal*, vol. 6, no. 7, pp. 679-693.

Gadaleta, A, Giancaspro, A, Cardone, MF & Blanco, A 2011, 'Real-time PCR for the detection of precise transgene copy number in durum wheat', *Cellular & Molecular Biology Letters*, vol. 16, no. 4, pp. 652-668.

Garnett, TP & Graham, RD 2005, 'Distribution and remobilization of iron and copper in wheat', *Annals of Botany*, vol. 95, no. 5, pp. 817-826.

Gelvin, SB 2003, '*Agrobacterium*-mediated plant transformation: The biology behind the "Gene-Jockeying" tool', *Microbiology and Molecular Biology Reviews*, vol. 67, no. 1, pp. 16-37.

German, MA, Kandel-Kfir, M, Swarzberg, D, Matsevitz, T & Granot, D 2003, 'A rapid method for the analysis of zygosity in transgenic plants', *Plant Science*, vol. 164, no. 2, pp. 183-187.

Gibson, RS, Bailey, KB, Gibbs, M & Ferguson, EL 2010, 'A review of phytate, iron, zinc, and calcium concentrations in plant-based complementary foods used in low-income countries and implications for bioavailability', *Food and Nutrition Bulletin*, vol. 31, no. 2_Suppl2, pp. S134-146.

Glahn, RP, Cheng, Z, Welch, RM & Gregorio, GB 2002, 'Comparison of iron bioavailability from 15 rice genotypes: Studies using an in vitro digestion/Caco-2 cell culture model', *Journal of Agricultural and Food Chemistry*, vol. 50, no. 12, pp. 3586-3591.

Goto, F, Yoshihara, T, Shigemoto, N, Toki, S & Takaiwa, F 1999, 'Iron fortification of rice seed by the soybean ferritin gene', *Nature Biotechnology*, vol. 17, no. 3, pp. 282-286.

Graf, E & Eaton, JW 1993, 'Suppression of colonic cancer by dietary phytic acid', *Nutrition and Cancer*, vol. 19, no. 1, pp. 11-19.

Graf, E, Empson, KL & Eaton, JW 1987, 'Phytic acid. A natural antioxidant', *Journal of Biological Chemistry*, vol. 262, no. 24, pp. 11647-11650.

Graham, RD, Welch, RM & Bouis, HE 2001, 'Addressing micronutrient malnutrition through enhancing the nutritional quality of staple foods: Principles, perspectives and knowledge gaps', in *Advances in Agronomy*, Academic Press, vol. 70, pp. 77-142.

GRiSP, GRSP 2013, *Rice almanac*, 4th edn, International Rice Research Institute, Los Baños (Philippines).

Grusak, MA 1994, 'Iron transport to developing ovules of *Pisum sativum* (I. seed import characteristics and phloem iron-loading capacity of source regions)', *Plant Physiology*, vol. 104, no. 2, pp. 649-655.

Guerinot, ML 2010, 'Iron', in R Hell & R-R Mendel (eds), *Cell Biology of Metals and Nutrients*, Springer Berlin Heidelberg, Berlin, Heidelberg, pp. 75-94.

Gupta, RK, Gangoliya, SS & Singh, NK 2015, 'Reduction of phytic acid and enhancement of bioavailable micronutrients in food grains', *Journal of Food Science and Technology*, vol. 52, no. 2, pp. 676-684.

Hallberg, L, Brune, M & Rossander, L 1989, 'Iron absorption in man: Ascorbic acid and dose-dependent inhibition by phytate', *The American Journal of Clinical Nutrition*, vol. 49, no. 1, pp. 140-144.

Hansen, TH, Lombi, E, Fitzgerald, M, Laursen, KH, Frydenvang, J, Husted, S, Boualaphanh, C, Resurreccion, A, Howard, DL, de Jonge, MD, Paterson, D & Schjoerring, JK 2012, 'Losses of essential mineral nutrients by polishing of rice differ among genotypes due to contrasting grain hardness and mineral distribution', *Journal of Cereal Science*, vol. 56, no. 2, pp. 307-315.

HarvestPlus 2012, 'Biofortification: Improving nutrition through agriculture', *AIARD Annual Conference, Washington, DC*.

Hayashi, H & Chino, M 1990, 'Chemical composition of phloem sap from the uppermost internode of the rice plant', *Plant and Cell Physiology*, vol. 31, no. 2, pp. 247-251.

Hellens, R, Mullineaux, P & Klee, H 2000, 'Technical focus: A guide to *Agrobacterium* binary Ti vectors', *Trends in Plant Science*, vol. 5, no. 10, pp. 446-451.

Hennion, N, Durand, M, Vriet, C, Doidy, J, Maurousset, L, Lemoine, R & Pourtau, N 2018, 'Sugars en route to the roots. Transport, metabolism and storage within plant roots and towards microorganisms of the rhizosphere', *Physiologia Plantarum*, vol. 165, no. 1, pp. 44-57.

Hervé, P & Kayano, T 2006, 'Japonica Rice Varieties (*Oryza sativa*, Nipponbare, and Others)', in K Wang (ed.), *Vol. 343: Agrobacterium protocols*, 2nd edn, Humana Press Inc., Totowa, NJ, vol. 1, pp. 213 - 222.

Hiei, Y, Ishida, Y, Kasaoka, K & Komari, T 2006, 'Improved frequency of transformation in rice and maize by treatment of immature embryos with centrifugation and heat prior to infection with *Agrobacterium tumefaciens*', *Plant Cell, Tissue and Organ Culture*, vol. 87, no. 3, pp. 233-243.

Hiei, Y, Ishida, Y & Komari, T 2014, 'Progress of cereal transformation technology mediated by *Agrobacterium tumefaciens*', *Frontiers in Plant Science*, vol. 5, no. 628.

Hiei, Y & Komari, T 2008, '*Agrobacterium*-mediated transformation of rice using immature embryos or calli induced from mature seed', *Nature Protocols*, vol. 3, no. 5, pp. 824-834.

Hiei, Y, Ohta, S, Komari, T & Kumashiro, T 1994, 'Efficient transformation of rice (*Oryza sativa* L.) mediated by *Agrobacterium* and sequence analysis of the boundaries of the T-DNA', *The Plant Journal*, vol. 6, no. 2, pp. 271-282.

Hirose, T, Endler, A & Ohsugi, R 1999, 'Gene expression of enzymes for starch and sucrose metabolism and transport in leaf sheaths of rice (*Oryza sativa* L.) during the heading period in relation to the sink to source transition', *Plant production science*, vol. 2, no. 3, pp. 178-183.

Hirose, T, Imaizumi, N, Scofield, GN, Furbank, RT & Ohsugi, R 1997, 'cDNA cloning and tissue specific expression of a gene for sucrose transporter from rice (*Oryza sativa* L.)', *Plant and Cell Physiology*, vol. 38, no. 12, pp. 1389-1396.

Hirose, T, Takano, M & Terao, T 2002, 'Cell wall invertase in developing rice caryopsis: Molecular cloning of *OsCIN1* and analysis of its expression in relation to its role in grain filling', *Plant and Cell Physiology*, vol. 43, no. 4, pp. 452-459.

Hoekema, A, Hirsch, PR, Hooykaas, PJJ & Schilperoort, RA 1983, 'A binary plant vector strategy based on separation of vir- and T-region of the *Agrobacterium tumefaciens* Ti-plasmid', *Nature*, vol. 303, no. 5913, pp. 179-180.

Huang, S, Sasaki, A, Yamaji, N, Okada, H, Mitani-Ueno, N & Ma, JF 2020, 'The ZIP transporter family member OsZIP9 contributes to root Zn uptake in rice under Zn-limited conditions', *Plant Physiology*, vol. 183, no. 3, pp. 1224-1234.

Huang, Z, Pan, X-D, Wu, P-G, Han, J-L & Chen, Q 2013, 'Health risk assessment of heavy metals in rice to the population in Zhejiang, China', *PLoS ONE*, vol. 8, no. 9: e75007.

Hussain, D, Haydon, MJ, Wang, Y, Wong, E, Sherson, SM, Young, J, Camakaris, J, Harper, JF & Cobbett, CS 2004, 'P-type ATPase heavy metal transporters with roles in essential zinc homeostasis in Arabidopsis', *The Plant Cell*, vol. 16, no. 5, pp. 1327-1339.

Huynh, M-m 2015, 'Examining the role of the barley sucrose transporter *HvSUT1* in increasing grain nutrients in rice (*Oryza sativa* L.).', Doctor of Philosophy thesis, Flinders University.

Hwang, YS, Yang, D, McCullar, C, Wu, L, Chen, L, Pham, P, Nandi, S & Huang, N 2002, 'Analysis of the rice endosperm-specific globulin promoter in transformed rice cells', *Plant Cell Reports*, vol. 20, no. 9, pp. 842-847.

Ingham, DJ, Beer, S, Money, S & Hansen, G 2001, 'Quantitative real-time PCR assay for determining transgene copy number in transformed plants', *Biotechniques*, vol. 31, no. 1, pp. 132-134, 136-140.

Inoue, H, Higuchi, K, Takahashi, M, Nakanishi, H, Mori, S & Nishizawa, NK 2003, 'Three rice nicotianamine synthase genes, *OsNAS1*, *OsNAS2*, and *OsNAS3* are expressed in cells involved in long-distance transport of iron and differentially regulated by iron', *The Plant Journal*, vol. 36, no. 3, pp. 366-381.

Inoue, H, Kobayashi, T, Nozoye, T, Takahashi, M, Kakei, Y, Suzuki, K, Nakazono, M, Nakanishi, H, Mori, S & Nishizawa, NK 2009, 'Rice OsYSL15 is an iron-regulated iron(III)-deoxymugineic acid transporter expressed in the roots and is essential for iron uptake in early growth of the seedlings', *Journal of Biological Chemistry*, vol. 284, no. 6, pp. 3470-3479.

Inoue, H, Mizuno, D, Takahashi, M, Nakanishi, H, Mori, S & Nishizawa, NK 2004, 'A rice FRD3-like (*OsFRDL1*) gene is expressed in the cells involved in long-distance transport', *Soil Science and Plant Nutrition*, vol. 50, no. 7, pp. 1133-1140.

Inoue, H, Takahashi, M, Kobayashi, T, Suzuki, M, Nakanishi, H, Mori, S & Nishizawa, NK 2008, 'Identification and localisation of the rice nicotianamine aminotransferase gene *OsNAAT1* expression suggests the site of phytosiderophore synthesis in rice', *Plant Molecular Biology*, vol. 66, no. 1-2, pp. 193-203.

International Rice Genome Sequencing Project 2005, 'The map-based sequence of the rice genome', *Nature*, vol. 436, no. 7052, pp. 793-800.

ISAAA 2020, *GM approval database*, viewed 05/04/2020, <https://www.isaaa.org/gmapprovaldatabase/gene/default.asp?GeneID=25>.

Ishimaru, K, Hirose, T, Aoki, N, Takahashi, S, Ono, K, Yamamoto, S, Wu, J, Saji, S, Baba, T, Ugaki, M, Matsumoto, T & Ohsugi, R 2001, 'Antisense expression of a rice sucrose transporter OsSUT1 in rice (*Oryza sativa* L.)', *Plant and Cell Physiology*, vol. 42, no. 10, pp. 1181-1185.

Ishimaru, K, Kosone, M, Sasaki, H & Kashiwagi, T 2004, 'Leaf contents differ depending on the position in a rice leaf sheath during sink–source transition', *Plant Physiology and Biochemistry*, vol. 42, no. 11, pp. 855-860.

Ishimaru, Y, Bashir, K & Nishizawa, NK 2011, 'Zn uptake and translocation in rice plants', *Rice*, vol. 4, no. 1, pp. 21-27.

Ishimaru, Y, Masuda, H, Bashir, K, Inoue, H, Tsukamoto, T, Takahashi, M, Nakanishi, H, Aoki, N, Hirose, T, Ohsugi, R & Nishizawa, NK 2010, 'Rice metal-nicotianamine transporter, OsYSL2, is required for the long-distance transport of iron and manganese', *The Plant Journal*, vol. 62, no. 3, pp. 379-390.

Ishimaru, Y, Masuda, H, Suzuki, M, Bashir, K, Takahashi, M, Nakanishi, H, Mori, S & Nishizawa, NK 2007, 'Overexpression of the OsZIP4 zinc transporter confers disarrangement of zinc distribution in rice plants', *Journal of Experimental Botany*, vol. 58, no. 11, pp. 2909-2915.

Ishimaru, Y, Suzuki, M, Tsukamoto, T, Suzuki, K, Nakazono, M, Kobayashi, T, Wada, Y, Watanabe, S, Matsuhashi, S, Takahashi, M, Nakanishi, H, Mori, S & Nishizawa, NK 2006, 'Rice plants take up iron as an Fe^{3+}-phytosiderophore and as Fe^{2+}', *The Plant Journal*, vol. 45, no. 3, pp. 335-346.

Iwai, T, Takahashi, M, Oda, K, Terada, Y & Yoshida, KT 2012, 'Dynamic changes in the distribution of minerals in relation to phytic acid accumulation during rice seed development', *Plant Physiology*, vol. 160, no. 4, pp. 2007-2014.

Jaksomsak, P, Sangruan, P, Thomson, G, Rerkasem, B, Dell, B & Prom-u-thai, C 2014, 'Uneven distribution of zinc in the dorsal and ventral sections of rice grain', *Cereal Chemistry*, vol. 91, no. 2, pp. 124-129.

Johnson, AAT, Kyriacou, B, Callahan, DL, Carruthers, L, Stangoulis, J, Lombi, E & Tester, M 2011, 'Constitutive overexpression of the *OsNAS* gene family reveals single-gene strategies for effective iron- and zinc-biofortification of rice endosperm', *PLoS ONE*, vol. 6, no. 9: e24476.

Julius, BT, Leach, KA, Tran, TM, Mertz, RA & Braun, DM 2017, 'Sugar transporters in plants: New insights and discoveries', *Plant and Cell Physiology*, vol. 58, no. 9, pp. 1442-1460.

Kakei, Y, Ishimaru, Y, Kobayashi, T, Yamakawa, T, Nakanishi, H & Nishizawa, N 2012, 'OsYSL16 plays a role in the allocation of iron', *Plant Molecular Biology*, vol. 79, no. 6, pp. 583-594.

Kato, M, Ishikawa, S, Inagaki, K, Chiba, K, Hayashi, H, Yanagisawa, S & Yoneyama, T 2010, 'Possible chemical forms of cadmium and varietal differences in cadmium concentrations in the phloem sap of rice plants *(Oryza sativa* L.)', *Soil Science and Plant Nutrition*, vol. 56, no. 6, pp. 839-847.

Kawakatsu, T & Takaiwa, F 2010, 'Cereal seed storage protein synthesis: Fundamental processes for recombinant protein production in cereal grains', *Plant Biotechnology Journal*, vol. 8, no. 9, pp. 939-953.

Kawakatsu, T, Yamamoto, MP, Hirose, S, Yano, M & Takaiwa, F 2008, 'Characterization of a new rice glutelin gene *GluD-1* expressed in the starchy endosperm', *Journal of experimental botany*, vol. 59, no. 15, pp. 4233-4245.

Kehr, J 2013, 'Systemic regulation of mineral homeostasis by micro RNAs', *Frontiers in plant science*, vol. 4, pp. 145-145.

Kim, S, Takahashi, M, Higuchi, K, Tsunoda, K, Nakanishi, H, Yoshimura, E, Mori, S & Nishizawa, NK 2005, 'Increased nicotianamine biosynthesis confers enhanced tolerance of high levels of metals, in particular nickel, to plants', *Plant and Cell Physiology*, vol. 46, no. 11, pp. 1809-1818.

Kobayashi, T, Suzuki, M, Inoue, H, Itai, RN, Takahashi, M, Nakanishi, H, Mori, S & Nishizawa, NK 2005, 'Expression of iron-acquisition-related genes in iron-deficient rice is co-ordinately induced by partially conserved iron-deficiency-responsive elements', *Journal of Experimental Botany*, vol. 56, no. 415, pp. 1305-1316.

Koike, S, Inoue, H, Mizuno, D, Takahashi, M, Nakanishi, H, Mori, S & Nishizawa, NK 2004, 'OsYSL2 is a rice metal-nicotianamine transporter that is regulated by iron and expressed in the phloem', *The Plant Journal*, vol. 39, no. 3, pp. 415-424.

Koller, A, Washburn, MP, Lange, BM, Andon, NL, Deciu, C, Haynes, PA, Hays, L, Schieltz, D, Ulaszek, R, Wei, J, Wolters, D & Yates, JR 2002, 'Proteomic survey of metabolic pathways in rice', *Proceedings of the National Academy of Sciences of the United States of America*, vol. 99, no. 18, pp. 11969-11974.

Komari, T, Takakura, Y, Ueki, J, Kato, N, Ishida, Y & Hiei, Y 2006, 'Binary vectors and super-binary vectors', *Methods in Molecular Biology*, vol. 343, pp. 15-41.

Kooter, JM, Matzke, MA & Meyer, P 1999, 'Listening to the silent genes: Transgene silencing, gene regulation and pathogen control', *Trends in Plant Science*, vol. 4, no. 9, pp. 340-347.

Krishnan, S & Dayanandan, P 2003, 'Structural and histochemical studies on grain-filling in the caryopsis of rice (*Oryza sativa* L.)', *Journal of Biosciences*, vol. 28, no. 4, pp. 455-469.

Kühn, C & Grof, CPL 2010, 'Sucrose transporters of higher plants', *Current Opinion in Plant Biology*, vol. 13, no. 3, pp. 287-297.

Kyriacou, B, Moore, KL, Paterson, D, de Jonge, MD, Howard, DL, Stangoulis, J, Tester, M, Lombi, E & Johnson, AAT 2014, 'Localization of iron in rice grain using synchrotron X-ray fluorescence microscopy and high resolution secondary ion mass spectrometry', *Journal of Cereal Science*, vol. 59, no. 2, pp. 173-180.

Kyriacou, BA 2013, 'Iron loading in rice endosperm controlled by cell-type specific over-expression of *OsNAS*', Flinders University of South Australia.

Lalonde, S, Wipf, D & Frommer, WB 2004, 'Transport mechanisms for organic forms of carbon and nitrogen between source and sink', *Annual Review of Plant Biology*, vol. 55, pp. 341-372.

Larson, SR, Rutger, JN, Young, KA & Raboy, V 2000, 'Isolation and genetic mapping of a non-lethal rice (*Oryza sativa* L.) low *phytic acid 1* mutation', *Crop Science*, vol. 40, no. 5, pp. 1397-1405.

Lee, S & An, G 2009, 'Over-expression of *OsIRT1* leads to increased iron and zinc accumulations in rice', *Plant, Cell & Environment*, vol. 32, no. 4, pp. 408-416.

Lee, S, Chiecko, JC, Kim, SA, Walker, EL, Lee, Y, Guerinot, ML & An, G 2009a, 'Disruption of *OsYSL15* leads to iron inefficiency in rice plants', *Plant Physiology*, vol. 150, no. 2, pp. 786-800.

Lee, S, Jeon, US, Lee, SJ, Kim, YK, Persson, DP, Husted, S, Schjørring, JK, Kakei, Y, Masuda, H, Nishizawa, NK & An, G 2009b, 'Iron fortification of rice seeds through activation of the *nicotianamine synthase* gene', *Proceedings of the National Academy of Sciences of the United States of America*, vol. 106, no. 51, pp. 22014-22019.

Lee, S, Kim, Y-S, Jeon, U, Kim, Y-K, Schjoerring, J & An, G 2012, 'Activation of Rice *nicotianamine synthase 2* (*OsNAS2*) enhances iron availability for biofortification', *Molecules and Cells*, vol. 33, no. 3, pp. 269-275.

Lei, M, Liu, Y, Zhang, B, Zhao, Y, Wang, X, Zhou, Y, Raghothama, KG & Liu, D 2011, 'Genetic and genomic evidence that sucrose is a global regulator of plant responses to phosphate starvation in *Arabidopsis*', *Plant physiology*, vol. 156, no. 3, pp. 1116-1130.

Lemoine, R 2000, 'Sucrose transporters in plants: Update on function and structure', *Biochimica et Biophysica Acta (BBA) - Biomembranes*, vol. 1465, no. 1, pp. 246-262.

Lemoine, R, Bürkle, L, Barker, L, Sakr, S, Kühn, C, Regnacq, M, Gaillard, C, Delrot, S & Frommer, WB 1999, 'Identification of a pollen-specific sucrose transporter-like protein NtSUT3 from tobacco', *FEBS Letters*, vol. 454, no. 3, pp. 325-330.

Lemoine, R, Kühn, C, Thiele, N, Delrot, S & Frommer, WB 1996, 'Antisense inhibition of the sucrose transporter in potato: Effects on amount and activity', *Plant, Cell & Environment*, vol. 19, no. 10, pp. 1124-1131.

Li, Z, Hansen, J, Liu, Y, Zemetra, R & Berger, P 2004, 'Using real-time PCR to determine transgene copy number in wheat', *Plant Molecular Biology Reporter*, vol. 22, no. 2, pp. 179-188.

Liang, C, Wang, Y, Zhu, Y, Tang, J, Hu, B, Liu, L, Ou, S, Wu, H, Sun, X, Chu, J & Chu, C 2014, 'OsNAP connects abscisic acid and leaf senescence by fine-tuning abscisic acid biosynthesis and directly targeting senescence-associated genes in rice', *Proceedings of the National Academy of Sciences of the United States of America*, vol. 111, no. 27, pp. 10013-10018.

Liang, J, Han, B-Z, Nout, MJR & Hamer, RJ 2009, 'Effect of soaking and phytase treatment on phytic acid, calcium, iron and zinc in rice fractions', *Food Chemistry*, vol. 115, no. 3, pp. 789-794.

Lin, XY, Ye, YQ, Fan, SK, Jin, CW & Zheng, SJ 2016, 'Increased sucrose accumulation regulates iron-deficiency responses by promoting auxin signaling in *Arabidopsis* plants', *Plant Physiology*, vol. 170, no. 2, pp. 907-920.

Liu, J, Samac, DA, Bucciarelli, B, Allan, DL & Vance, CP 2005, 'Signaling of phosphorus deficiency-induced gene expression in white lupin requires sugar and phloem transport', *The Plant Journal*, vol. 41, no. 2, pp. 257-268.

Liu, S, Waqas, MA, Wang, S-h, Xiong, X-y & Wan, Y-f 2017, 'Effects of increased levels of atmospheric CO_2 and high temperatures on rice growth and quality', *PLoS ONE*, vol. 12, no. 11: e0187724.

Loladze, I 2002, 'Rising atmospheric CO_2 and human nutrition: Toward globally imbalanced plant stoichiometry?', *Trends in Ecology & Evolution*, vol. 17, no. 10, pp. 457-461.

Lu, M-Z, Snyder, R, Grant, J & Tegeder, M 2020, 'Manipulation of sucrose phloem and embryo loading affects pea leaf metabolism, carbon and nitrogen partitioning to sinks as well as seed storage pools', *The Plant Journal*, vol. 101, no. 1, pp. 217-236.

Lu, Y, Xu, W, Kang, A, Luo, Y, Guo, F, Yang, R, Zhang, J & Huang, K 2007, 'Prokaryotic expression and allergenicity assessment of hygromycin B phosphotransferase protein derived from genetically modified plants', *Journal of Food Science*, vol. 72, no. 7, pp. M228-232.

Lucca, P, Hurrell, R & Potrykus, I 2002, 'Fighting iron deficiency anemia with iron-rich rice', *Journal of the American College of Nutrition*, vol. 21, no. 3 Suppl, pp. 184s-190s.

Ma, G, Jin, Y, Piao, J, Kok, F, Guusje, B & Jacobsen, E 2005, 'Phytate, calcium, iron, and zinc contents and their molar ratios in foods commonly consumed in China', *Journal of Agricultural and Food Chemistry*, vol. 53, no. 26, pp. 10285-10290.

Ma, L, Zhang, D, Miao, Q, Yang, J, Xuan, Y & Hu, Y 2017, 'Essential role of sugar transporter OsSWEET11 during the early stage of rice grain filling', *Plant and Cell Physiology*, vol. 58, no. 5, pp. 863-873.

Mackill, DJ & Khush, GS 2018, 'IR64: A high-quality and high-yielding mega variety', *Rice*, vol. 11, no. 18.

Mahesh, HB, Shirke, MD, Singh, S, Rajamani, A, Hittalmani, S, Wang, G-L & Gowda, M 2016, 'Indica rice genome assembly, annotation and mining of blast disease resistance genes', *BMC Genomics*, vol. 17, no. 242.

Marr, KM, Batten, GD & Blakeney, AB 1995, 'Relationships between minerals in Australian brown rice', vol. 68, no. 3, pp. 285-291.

Mason, G, Provero, P, Vaira, AM & Accotto, GP 2002, 'Estimating the number of integrations in transformed plants by quantitative real-time PCR', *BMC Biotechnology*, vol. 2, no. 20.

Masuda, H, Aung, MS & Nishizawa, NK 2013a, 'Iron biofortification of rice using different transgenic approaches', *Rice*, vol. 6, no. 1, p. 40.

Masuda, H, Ishimaru, Y, Aung, MS, Kobayashi, T, Kakei, Y, Takahashi, M, Higuchi, K, Nakanishi, H & Nishizawa, NK 2012, 'Iron biofortification in rice by the introduction of multiple genes involved in iron nutrition', *Scientific Reports*, vol. 2, no. 543.

Masuda, H, Kobayashi, T, Ishimaru, Y, Takahashi, M, Aung, MS, Nakanishi, H, Mori, S & Nishizawa, NK 2013b, 'Iron-biofortification in rice by the introduction of three barley genes participated in mugineic acid biosynthesis with soybean ferritin gene', *Frontiers in Plant Science*, vol. 4, no. 132.

Masuda, H, Suzuki, M, Morikawa, KC, Kobayashi, T, Nakanishi, H, Takahashi, M, Saigusa, M, Mori, S & Nishizawa, NK 2008, 'Increase in iron and zinc concentrations in rice grains via the introduction of barley genes involved in phytosiderophore synthesis', *Rice*, vol. 1, no. 1, pp. 100-108.

Masuda, H, Usuda, K, Kobayashi, T, Ishimaru, Y, Kakei, Y, Takahashi, M, Higuchi, K, Nakanishi, H, Mori, S & Nishizawa, N 2009, 'Overexpression of the barley nicotianamine synthase gene *HvNAS1* increases iron and zinc concentrations in rice grains', *Rice*, vol. 2, no. 4, pp. 155-166.

Matsukura, C, Saitoh, T, Hirose, T, Ohsugi, R, Perata, P & Yamaguchi, J 2000, 'Sugar uptake and transport in rice embryo. Expression of companion cell-specific sucrose transporter (*OsSUT1*) induced by sugar and light', *Plant Physiology*, vol. 124, no. 1, pp. 85-93.

Matsumoto, T, Tanaka, T, Sakai, H, Amano, N, Kanamori, H, Kurita, K, Kikuta, A, Kamiya, K, Yamamoto, M, Ikawa, H, Fujii, N, Hori, K, Itoh, T & Sato, K 2011, 'Comprehensive sequence analysis of 24,783 barley full-length cDNAs derived from 12 clone libraries', *Plant Physiology*, vol. 156, no. 1, pp. 20-28.

Matzke, AJM, Neuhuber, F, Park, YD, Ambros, PF & Matzke, MA 1994, 'Homology-dependent gene silencing in transgenic plants: Epistatic silencing loci contain multiple copies of methylated transgenes', *Molecular and General Genetics MGG*, vol. 244, no. 3, pp. 219-229.

Matzke, MA & Matzke, AJM 1995, 'How and why do plants inactivate homologous (trans)genes?', *Plant physiology*, vol. 107, no. 3, pp. 679-685.

Mayer, JE, Pfeiffer, WH & Beyer, P 2008, 'Biofortified crops to alleviate micronutrient malnutrition', *Current Opinion in Plant Biology*, vol. 11, no. 2, pp. 166-170.

Meguro, R, Asano, Y, Odagiri, S, Li, C, Iwatsuki, H & Shoumura, K 2007, 'Nonheme-iron histochemistry for light and electron microscopy: A historical, theoretical and technical review', *Archives of Histology and Cytology*, vol. 70, no. 1, pp. 1-19.

Meharg, AA, Norton, G, Deacon, C, Williams, P, Adomako, EE, Price, A, Zhu, Y, Li, G, Zhao, F-J, McGrath, S, Villada, A, Sommella, A, De Silva, PMCS, Brammer, H, Dasgupta, T & Islam, MR 2013, 'Variation in rice cadmium related to human exposure', *Environmental Science & Technology*, vol. 47, no. 11, pp. 5613-5618.

Meharg, AA, Williams, PN, Adomako, E, Lawgali, YY, Deacon, C, Villada, A, Cambell, RCJ, Sun, G, Zhu, Y-G, Feldmann, J, Raab, A, Zhao, F-J, Islam, R, Hossain, S & Yanai, J 2009, 'Geographical variation in total and inorganic arsenic content of polished (white) rice', *Environmental Science & Technology*, vol. 43, no. 5, pp. 1612-1617.

Mieog, J, Howitt, C & Ral, J-P 2013, 'Fast-tracking development of homozygous transgenic cereal lines using a simple and highly flexible real-time PCR assay', *BMC Plant Biology*, vol. 13, no. 71.

Mizuno, D, Higuchi, K, Sakamoto, T, Nakanishi, H, Mori, S & Nishizawa, NK 2003, 'Three nicotianamine synthase genes isolated from maize are differentially regulated by iron nutritional status', *Plant Physiology*, vol. 132, no. 4, pp. 1989-1997.

Mizuno, K, Kobayashi, E, Tachibana, M, Kawasaki, T, Fujimura, T, Funane, K, Kobayashi, M & Baba, T 2001, 'Characterization of an isoform of rice starch branching enzyme, RBE4, in developing seeds', *Plant and Cell Physiology*, vol. 42, no. 4, pp. 349-357.

Mori, S, Nishizawa, N, Hayashi, H, Chino, M, Yoshimura, E & Ishihara, J 1991, 'Why are young rice plants highly susceptible to iron deficiency?', *Plant and Soil*, vol. 130, no. 1-2, pp. 143-156.

Morris, ER & Ellis, REX 1985, 'Bioavailability of dietary calcium', in *Nutritional Bioavailability of Calcium*, American Chemical Society, vol. 275, pp. 63-72.

Murphy, KM, Reeves, PG & Jones, SS 2008, 'Relationship between yield and mineral nutrient concentrations in historical and modern spring wheat cultivars', *Euphytica*, vol. 163, no. 3, pp. 381-390.

Myers, SS, Zanobetti, A, Kloog, I, Huybers, P, Leakey, ADB, Bloom, AJ, Carlisle, E, Dietterich, LH, Fitzgerald, G, Hasegawa, T, Holbrook, NM, Nelson, RL, Ottman, MJ, Raboy, V, Sakai, H, Sartor, KA, Schwartz, J, Seneweera, S, Tausz, M & Usui, Y 2014, 'Increasing CO_2 threatens human nutrition', *Nature*, vol. 510, no. 7503, pp. 139-142.

Nakandalage, N, Nicolas, M, Norton, RM, Hirotsu, N, Milham, PJ & Seneweera, S 2016, 'Improving rice zinc biofortification success rates through genetic and crop management approaches in a changing environment', *Frontiers in Plant Science*, vol. 7, no. 764.

Nakase, M, Hotta, H, Adachi, T, Aoki, N, Nakamura, R, Masumura, T, Tanaka, K & Matsuda, T 1996, 'Cloning of the rice seed α-globulin-encoding gene: Sequence similarity of the 5'-flanking region to those of the genes encoding wheat high-molecular-weight glutenin and barley D hordein', *Gene*, vol. 170, no. 2, pp. 223-226.

Nguyen-legros, J, Bizot, J, Bolesse, M & Pulicani, J 1980, '["Diaminobenzidine black" as a new histochemical demonstration of exogenous iron (author's transl)]', *Histochemistry*, vol. 66 3, pp. 239-244.

Nishiyama, R, Kato, M, Nagata, S, Yanagisawa, S & Yoneyama, T 2012, 'Identification of Zn–nicotianamine and Fe–2′-deoxymugineic acid in the phloem sap from rice plants (*Oryza sativa* L.)', *Plant and Cell Physiology*, vol. 53, no. 2, pp. 381-390.

Norton, GJ 2019, '6 - Rice minerals and heavy metal(oid)s', in J Bao (ed.), *Rice Chemistry and Technology*, 4th edn, AACC International Press, pp. 169-194.

Norton, GJ, Williams, PN, Adomako, EE, Price, AH, Zhu, Y, Zhao, F-J, McGrath, S, Deacon, CM, Villada, A, Sommella, A, Lu, Y, Ming, L, De Silva, PMCS, Brammer, H, Dasgupta, T, Islam, MR & Meharg, AA 2014, 'Lead in rice: Analysis of baseline lead levels in market and field collected rice grains', *Science of The Total Environment*, vol. 485-486, pp. 428-434.

Nozoye, T 2018, 'The nicotianamine synthase gene is a useful candidate for improving the nutritional qualities and Fe-deficiency tolerance of various crops', *Frontiers in Plant Science*, vol. 9, no. 340.

Nozoye, T, Inoue, H, Takahashi, M, Ishimaru, Y, Nakanishi, H, Mori, S & Nishizawa, N 2007, 'The expression of iron homeostasis-related genes during rice germination', *Plant Molecular Biology*, vol. 64, no. 1-2, pp. 35-47.

Nozoye, T, Nagasaka, S, Bashir, K, Takahashi, M, Kobayashi, T, Nakanishi, H & Nishizawa, NK 2014a, 'Nicotianamine synthase 2 localizes to the vesicles of iron-deficient rice roots, and its mutation in the YXXφ or LL motif causes the disruption of vesicle formation or movement in rice', *The Plant Journal*, vol. 77, no. 2, pp. 246-260.

Nozoye, T, Nagasaka, S, Kobayashi, T, Takahashi, M, Sato, Y, Sato, Y, Uozumi, N, Nakanishi, H & Nishizawa, NK 2011, 'Phytosiderophore efflux transporters are crucial for iron acquisition in graminaceous plants', *Journal of Biological Chemistry*, vol. 286, no. 7, pp. 5446-5454.

Nozoye, T, Tsunoda, K, Nagasaka, S, Bashir, K, Takahashi, M, Kobayashi, T, Nakanishi, H & Nishizawa, NK 2014b, 'Rice nicotianamine synthase localizes to particular vesicles for proper function', *Plant signaling & behavior*, vol. 9, no. 5: e28660.

Nühse, TS, Stensballe, A, Jensen, ON & Peck, SC 2004, 'Phosphoproteomics of the *Arabidopsis* plasma membrane and a new phosphorylation site database', *The Plant Cell*, vol. 16, no. 9, pp. 2394-2405.

Ogiyama, S, Tagami, K & Uchida, S 2008, 'The concentration and distribution of essential elements in brown rice associated with the polishing rate: Use of ICP-AES and Micro-PIXE', *Nuclear Instruments and Methods in Physics Research Section B: Beam Interactions with Materials and Atoms*, vol. 266, no. 16, pp. 3625-3632.

Ogo, Y, Itai, RN, Kobayashi, T, Aung, MS, Nakanishi, H & Nishizawa, NK 2011, 'OsIRO2 is responsible for iron utilization in rice and improves growth and yield in calcareous soil', *Plant Molecular Biology*, vol. 75, no. 6, pp. 593-605.

Do Health 2017, *Risk assessment reference: Marker genes in GM plants*, by OGTR, OotGTR.

Oliva, N, Chadha-Mohanty, P, Poletti, S, Abrigo, E, Atienza, G, Torrizo, L, Garcia, R, Dueñas, C, Poncio, MA, Balindong, J, Manzanilla, M, Montecillo, F, Zaidem, M, Barry, G, Hervé, P, Shou, H & Slamet-Loedin, IH 2014, 'Large-scale production and evaluation of marker-free *indica* rice IR64 expressing phytoferritin genes', *Molecular Breeding*, vol. 33, no. 1, pp. 23-37.

Olsen, L & Palmgren, M 2014, 'Many rivers to cross: The journey of zinc from soil to seed', *Frontiers in Plant Science*, vol. 5, no. 30.

Oparka, KJ & Gates, P 1981a, 'Transport of assimilates in the developing caryopsis of rice (*Oryza sativa* L.): The pathways of water and assimilated carbon', *Planta*, vol. 152, no. 5, pp. 388-396.

Oparka, KJ & Gates, P 1981b, 'Transport of assimilates in the developing caryopsis of rice (*Oryza sativa* L.): Ultrastructure of the pericarp vascular bundle and its connections with the aleurone layer', *Planta*, vol. 151, no. 6, pp. 561-573.

Ortiz-Monasterio, JI, Palacios-Rojas, N, Meng, E, Pixley, K, Trethowan, R & Peña, RJ 2007, 'Enhancing the mineral and vitamin content of wheat and maize through plant breeding', *Journal of Cereal Science*, vol. 46, no. 3, pp. 293-307.

Ozturk, L, Yazici, MA, Yucel, C, Torun, A, Cekic, C, Bagci, A, Ozkan, H, Braun, H-J, Sayers, Z & Cakmak, I 2006, 'Concentration and localization of zinc during seed development and germination in wheat', *Physiologia Plantarum*, vol. 128, no. 1, pp. 144-152.

Paine, JA, Shipton, CA, Chaggar, S, Howells, RM, Kennedy, MJ, Vernon, G, Wright, SY, Hinchliffe, E, Adams, JL, Silverstone, AL & Drake, R 2005, 'Improving the nutritional value of Golden Rice through increased pro-vitamin A content', *Nature Biotechnology*, vol. 23, no. 4, pp. 482-487.

Palmer, C & Guerinot, ML 2009, 'A question of balance: Facing the challenges of Cu, Fe and Zn homeostasis', *Nature chemical biology*, vol. 5, no. 5, pp. 333-340.

Palmgren, MG, Clemens, S, Williams, LE, Krämer, U, Borg, S, Schjørring, JK & Sanders, D 2008, 'Zinc biofortification of cereals: Problems and solutions', *Trends in Plant Science*, vol. 13, no. 9, pp. 464-473.

Patrick, J & Offler, C 1995, 'Post-sieve element transport of sucrose in developing seeds', *Functional Plant Biology*, vol. 22, no. 4, pp. 681-702.

Patrick, JW & Offler, CE 2001, 'Compartmentation of transport and transfer events in developing seeds', *J Exp Bot*, vol. 52, no. 356, pp. 551-564.

Patrick, JW, Tyerman, SD & Bel, AJEv 2015, 'Long-distance transport', in BB Buchanan, W Gruissem & RL Jones (eds), *Biochemistry & Molecular Biology of Plants*, Second edition edn, John Wiley & Sons, Ltd, USA.

Paul, MJ, Oszvald, M, Jesus, C, Rajulu, C & Griffiths, CA 2017, 'Increasing crop yield and resilience with trehalose 6-phosphate: Targeting a feast–famine mechanism in cereals for better source–sink optimization', *Journal of Experimental Botany*, vol. 68, no. 16, pp. 4455-4462.

Paul, S, Ali, N, Datta, SK & Datta, K 2014, 'Development of an iron-enriched high-yieldings indica rice cultivar by introgression of a high-iron trait from transgenic iron-biofortified rice', *Plant Foods for Human Nutrition*, vol. 69, no. 3, pp. 203-208.

Paul, S, Ali, N, Gayen, D, Datta, SK & Datta, K 2012, 'Molecular breeding of *Osfer2* gene to increase iron nutrition in rice grain', *GM Crops & Food*, vol. 3, no. 4, pp. 310-316.

Perera, I, Seneweera, S & Hirotsu, N 2018, 'Manipulating the phytic acid content of rice grain toward improving micronutrient bioavailability', *Rice*, vol. 11, no. 4.

Persson, DP, Hansen, TH, Laursen, KH, Schjoerring, JK & Husted, S 2009, 'Simultaneous iron, zinc, sulfur and phosphorus speciation analysis of barley grain tissues using SEC-ICP-MS and IP-ICP-MS', *Metallomics*, vol. 1, no. 5, pp. 418-426.

Prom-u-thai, C, Dell, B, Thomson, G & Rerkasem, B 2003, 'Easy and rapid detection of iron in rice grain', *ScienceAsia*, vol. 29, pp. 203-207.

Prom-u-thai, C, Rerkasem, B, Cakmak, I & Huang, L 2010, 'Zinc fortification of whole rice grain through parboiling process', *Food Chemistry*, vol. 120, no. 3, pp. 858-863.

Qu, LQ & Takaiwa, F 2004, 'Evaluation of tissue specificity and expression strength of rice seed component gene promoters in transgenic rice', *Plant Biotechnology Journal*, vol. 2, no. 2, pp. 113-125.

Qu, LQ, Xing, YP, Liu, WX, Xu, XP & Song, YR 2008, 'Expression pattern and activity of six glutelin gene promoters in transgenic rice', *Journal of Experimental Botany*, vol. 59, no. 9, pp. 2417-2424.

Qu, LQ, Yoshihara, T, Ooyama, A, Goto, F & Takaiwa, F 2005, 'Iron accumulation does not parallel the high expression level of ferritin in transgenic rice seeds', *Planta*, vol. 222, no. 2, pp. 225-233.

Raboy, V 2003, '*myo*-Inositol-1,2,3,4,5,6-hexa*kis*phosphate', *Phytochemistry*, vol. 64, no. 6, pp. 1033-1043.

Raboy, V 2007, 'The ABCs of low-phytate crops', *Nature Biotechnology*, vol. 25, no. 8, pp. 874-875.

Ramesh, S, Shin, R, Eide, D & Schachtman, D 2003, 'Differential metal selectivity and gene expression of two zinc transporters from rice', *Plant physiology*, vol. 133, pp. 126-134.

Rao, RN, Allen, NE, Hobbs, JN, Jr., Alborn, WE, Jr., Kirst, HA & Paschal, JW 1983, 'Genetic and enzymatic basis of hygromycin B resistance in *Escherichia coli*', *Antimicrobial agents and chemotherapy*, vol. 24, no. 5, pp. 689-695.

Reichman, S & Parker, D 2002, 'Revisiting the metal-binding chemistry of nicotianamine and 2'-deoxymugineic acid. Implications for iron nutrition in Strategy II plants', *Plant physiology*, vol. 129, pp. 1435-1438.

Reinders, A, Sivitz, AB, Hsi, A, Grof, CPL, Perroux, JM & Ward, JM 2006, 'Sugarcane ShSUT1: Analysis of sucrose transport activity and inhibition by sucralose', *Plant, Cell & Environment*, vol. 29, no. 10, pp. 1871-1880.

Rengel, Z, Batten, GD & Crowley, DE 1999, 'Agronomic approaches for improving the micronutrient density in edible portions of field crops', *Field Crops Research*, vol. 60, no. 1–2, pp. 27-40.

Ricachenevsky, F, Sperotto, R, Menguer, P, Sperb, E, Lopes, K & Fett, J 2011, 'Zinc-induced facilitator-like family in plants: Lineage-specific expansion in monocotyledons and conserved genomic and expression features among rice (*Oryza sativa*) paralogs', *BMC Plant Biology*, vol. 11, no. 20.

Riesmeier, JW, Willmitzer, L & Frommer, WB 1992, 'Isolation and characterization of a sucrose carrier cDNA from spinach by functional expression in yeast', *The EMBO Journal*, vol. 11, no. 13, pp. 4705-4713.

Ritchie, H & Roser, M 2020, 'Agricultural production', *Our World in Data*.

Robinson, NJ, Procter, CM, Connolly, EL & Guerinot, ML 1999, 'A ferric-chelate reductase for iron uptake from soils', *Nature*, vol. 397, no. 6721, pp. 694-697.

Roitsch, T 1999, 'Source-sink regulation by sugar and stress', *Current Opinion in Plant Biology*, vol. 2, no. 3, pp. 198-206.

Römheld, V & Marschner, H 1990, 'Genotypical differences among graminaceous species in release of phytosiderophores and uptake of iron phytosiderophores', *Plant and Soil*, vol. 123, no. 2, pp. 147-153.

Rosche, E, Blackmore, D, Tegeder, M, Richardson, T, Schroeder, H, Higgins, TJV, Frommer, WB, Offler, CE & Patrick, JW 2002, 'Seed-specific overexpression of a potato sucrose transporter increases sucrose uptake and growth rates of developing pea cotyledons', *The Plant Journal*, vol. 30, no. 2, pp. 165-175.

Rosche, EG, Blackmore, D, Offler, CE & Patrick, JW 2005, 'Increased capacity for sucrose uptake leads to earlier onset of protein accumulation in developing pea seeds', *Functional Plant Biology*, vol. 32, no. 11, pp. 997-1007.

Roschzttardtz, H, Conéjéro, G, Curie, C & Mari, S 2009, 'Identification of the endodermal vacuole as the iron storage compartment in the *Arabidopsis* embryo', *Plant Physiology*, vol. 151, no. 3, pp. 1329-1338.

Roschzttardtz, H, Conéjéro, G, Divol, F, Alcon, C, Verdeil, J-L, Curie, C & Mari, S 2013, 'New insights into Fe localization in plant tissues', *Frontiers in Plant Science*, vol. 4, no. 350.

Rose, TJ, Welling, MT, Julia, CC, Jeong, K, Tong, C, Waters, DLE & Liu, L 2020, 'Accumulation of phytate and starch lysophospholipids in rice grains and responses to alterations in P supply or source-sink relations', *Journal of Cereal Science*, vol. 91.

Ruan, Y-L 2014, 'Sucrose metabolism: Gateway to diverse carbon use and sugar signaling', *Annual Review of Plant Biology*, vol. 65, no. 1, pp. 33-67.

Saalbach, I, Mora-Ramírez, I, Weichert, N, Andersch, F, Guild, G, Wieser, H, Koehler, P, Stangoulis, J, Kumlehn, J, Weschke, W & Weber, H 2014, 'Increased grain yield and micronutrient concentration in transgenic winter wheat by ectopic expression of a barley sucrose transporter', *Journal of Cereal Science*, vol. 60, no. 1, pp. 75-81.

Sahoo, KK, Tripathi, AK, Pareek, A, Sopory, SK & Singla-Pareek, SL 2011, 'An improved protocol for efficient transformation and regeneration of diverse indica rice cultivars', *Plant Methods*, vol. 7, pp. 49-49.

Sahoo, RK & Tuteja, N 2012, 'Development of *Agrobacterium*-mediated transformation technology for mature seed-derived callus tissues of indica rice cultivar IR64', *GM Crops & Food*, vol. 3, no. 2, pp. 123-128.

Sakai, H, Iwai, T, Matsubara, C, Usui, Y, Okamura, M, Yatou, O, Terada, Y, Aoki, N, Nishida, S & Yoshida, KT 2015, 'A decrease in phytic acid content substantially affects the distribution of mineral elements within rice seeds', *Plant Science*, vol. 238, pp. 170-177.

Santi, S & Schmidt, W 2009, 'Dissecting iron deficiency-induced proton extrusion in *Arabidopsis* roots', *New Phytologist*, vol. 183, no. 4, pp. 1072-1084.

Sato, Y, Antonio, BA, Namiki, N, Takehisa, H, Minami, H, Kamatsuki, K, Sugimoto, K, Shimizu, Y, Hirochika, H & Nagamura, Y 2010, 'RiceXPro: A platform for monitoring gene expression in japonica rice grown under natural field conditions', *Nucleic Acids Research*, vol. 39, no. suppl_1, pp. D1141-D1148.

Sato, Y, Antonio, BA, Namiki, N, Takehisa, H, Minami, H, Kamatsuki, K, Sugimoto, K, Shimizu, Y, Hirochika, H & Nagamura, Y 2011, 'RiceXPro: A platform for monitoring gene expression in japonica rice grown under natural field conditions', *Nucleic Acids Res*, vol. 39, no. Database issue, pp. D1141-1148.

Sato, Y, Takehisa, H, Kamatsuki, K, Minami, H, Namiki, N, Ikawa, H, Ohyanagi, H, Sugimoto, K, Antonio, BA & Nagamura, Y 2012, 'RiceXPro Version 3.0: Expanding the informatics resource for rice transcriptome', *Nucleic Acids Research*, vol. 41, no. D1, pp. D1206-D1213.

Sauer, N 2007, 'Molecular physiology of higher plant sucrose transporters', *FEBS Letters*, vol. 581, no. 12, pp. 2309-2317.

Sauer, N & Stolz, J 1994, 'SUC1 and SUC2: Two sucrose transporters from *Arabidopsis thaliana*; expression and characterization in baker's yeast and identification of the histidine-tagged protein', *The Plant Journal*, vol. 6, no. 1, pp. 67-77.

Schaaf, G, Ludewig, U, Erenoglu, BE, Mori, S, Kitahara, T & von Wirén, N 2004, 'ZmYS1 functions as a proton-coupled symporter for phytosiderophore- and nicotianamine-chelated metals', *Journal of Biological Chemistry*, vol. 279, no. 10, pp. 9091-9096.

Schmidt, M & Parrott, W 2001, 'Quantitative detection of transgenes in soybean [*Glycine max* (L.) Merrill] and peanut (*Arachis hypogaea* L.) by real-time polymerase chain reaction', *Plant Cell Reports*, vol. 20, no. 5, pp. 422-428.

Schramm, C 2015, 'Characterisation of *HvSUT1* transgenic rice engineered for iron and zinc biofortification', Master thesis, Flinders University.

Scofield, GN, Hirose, T, Aoki, N & Furbank, RT 2007, 'Involvement of the sucrose transporter, OsSUT1, in the long-distance pathway for assimilate transport in rice', *Journal of Experimental Botany*, vol. 58, no. 12, pp. 3155-3169.

Scofield, GN, Hirose, T, Gaudron, JA, Furbank, RT, Upadhyaya, NM & Ohsugi, R 2002, 'Antisense suppression of the rice transporter gene, *OsSUT1*, leads to impaired grain filling and

germination but does not affect photosynthesis', *Functional Plant Biology*, vol. 29, no. 7, pp. 815-826.

Scofield, GN, Ruuska, SA, Aoki, N, Lewis, DC, Tabe, LM & Jenkins, CLD 2009, 'Starch storage in the stems of wheat plants: Localization and temporal changes', *Annals of Botany*, vol. 103, no. 6, pp. 859-868.

Sharma, SS & Dietz, K-J 2006, 'The significance of amino acids and amino acid-derived molecules in plant responses and adaptation to heavy metal stress', *Journal of Experimental Botany*, vol. 57, no. 4, pp. 711-726.

Shou, H, Frame, B, Whitham, S & Wang, K 2004, 'Assessment of transgenic maize events produced by particle bombardment or *Agrobacterium*-mediated transformation', *Molecular Breeding*, vol. 13, no. 2, pp. 201-208.

Singh, C, K V, S, S P, JK, K, BN, Pal, G, K, UB, K V, R & G, S 2017a, 'Delineation of inheritance pattern of aleurone layer colour through chemical tests in rice', *Rice*, vol. 10, no. 48.

Singh, SP, Gruissem, W & Bhullar, NK 2017b, 'Single genetic locus improvement of iron, zinc and *β*-carotene content in rice grains', *Scientific Reports*, vol. 7, no. 6883.

Singh, SP, Keller, B, Gruissem, W & Bhullar, NK 2017c, 'Rice *NICOTIANAMINE SYNTHASE 2* expression improves dietary iron and zinc levels in wheat', *Theoretical and Applied Genetics*, vol. 130, no. 2, pp. 283-292.

Sivitz, AB, Reinders, A & Ward, JM 2005, 'Analysis of the transport activity of barley sucrose transporter HvSUT1', *Plant and Cell Physiology*, vol. 46, no. 10, pp. 1666-1673.

Slamet-Loedin, IH, Chadha-Mohanty, P & Torrizo, L 2014, '*Agrobacterium*-mediated transformation: Rice transformation', *Methods in Molecular Biology*, vol. 1099, pp. 261-271.

Slamet-Loedin, IH, Johnson-Beebout, SE, Impa, S & Tsakirpaloglou, N 2015, 'Enriching rice with Zn and Fe while minimizing Cd risk', *Frontiers in Plant Science*, vol. 6, no. 121.

Slewinski, TL, Meeley, R & Braun, DM 2009, 'Sucrose transporter1 functions in phloem loading in maize leaves', *Journal of Experimental Botany*, vol. 60, no. 3.

Smith, MR & Myers, SS 2018, 'Impact of anthropogenic CO_2 emissions on global human nutrition', *Nature Climate Change*, vol. 8, no. 9, pp. 834-839.

Smith, MR, Rao, IM & Merchant, A 2018, 'Source-sink relationships in crop plants and their influence on yield development and nutritional quality', *Frontiers in plant science*, vol. 9, pp. 1889-1889.

Song, P, Cai, C, Skokut, M, Kosegi, B & Petolino, J 2002, 'Quantitative real-time PCR as a screening tool for estimating transgene copy number in WHISKERS™-derived transgenic maize', *Plant Cell Reports*, vol. 20, no. 10, pp. 948-954.

Sosso, D, Luo, D, Li, QB, Sasse, J, Yang, J, Gendrot, G, Suzuki, M, Koch, KE, McCarty, DR, Chourey, PS, Rogowsky, PM, Ross-Ibarra, J, Yang, B & Frommer, WB 2015, 'Seed filling in domesticated maize and rice depends on SWEET-mediated hexose transport', *Nature Genetics*, vol. 47, no. 12, pp. 1489-1493.

Southern, EM 1975, 'Detection of specific sequences among DNA fragments separated by gel electrophoresis', *Journal of Molecular Biology*, vol. 98, no. 3, pp. 503-517.

Sparvoli, F & Cominelli, E 2015, 'Seed biofortification and phytic acid reduction: A conflict of interest for the plant?', *Plants*, vol. 4, no. 4, pp. 728-755.

Sperotto, RA 2013, 'Zn/Fe remobilization from vegetative tissues to rice seeds: Should I stay or should I go?Ask Zn/Fe supply!', *Frontiers in Plant Science*, vol. 4, pp. 14-17.

Sperotto, RA, Boff, T, Duarte, GL, Santos, LS, Grusak, MA & Fett, JP 2010, 'Identification of putative target genes to manipulate Fe and Zn concentrations in rice grains', *Journal of Plant Physiology*, vol. 167, no. 17, pp. 1500-1506.

Sperotto, RA, Ricachenevsky, FK, Waldow Vde, A & Fett, JP 2012, 'Iron biofortification in rice: It's a long way to the top', *Plant Science*, vol. 190, pp. 24-39.

Stangoulis, J, Huynh, BL, Welch, R, Choi, EY & Graham, R 2007, 'Quantitative trait loci for phytate in rice grain and their relationship with grain micronutrient content', *Euphytica*, vol. 154, pp. 289-294.

Stolz, J, Ludwig, A, Stadler, R, Biesgen, C, Hagemann, K & Sauer, N 1999, 'Structural analysis of a plant sucrose carrier using monoclonal antibodies and bacteriophage lambda surface display', *FEBS Letters*, vol. 453, no. 3, pp. 375-379.

Stomph, TJ, Choi, EY & Stangoulis, JCR 2011, 'Temporal dynamics in wheat grain zinc distribution: is sink limitation the key?', *Annals of Botany*, vol. 107, no. 6, pp. 927-937.

Stomph, Tj, Jiang, W & Struik, PC 2009, 'Zinc biofortification of cereals: Rice differs from wheat and barley', *Trends in Plant Science*, vol. 14, no. 3, pp. 123-124.

Stroud, H, Ding, B, Simon, SA, Feng, S, Bellizzi, M, Pellegrini, M, Wang, G-L, Meyers, BC & Jacobsen, SE 2013, 'Plants regenerated from tissue culture contain stable epigenome changes in rice', *eLife*, vol. 2, no. e00354.

Suzuki, M, Morikawa, KC, Nakanishi, H, Takahashi, M, Saigusa, M, Mori, S & Nishizawa, NK 2008a, 'Transgenic rice lines that include barley genes have increased tolerance to low iron availability in a calcareous paddy soil', *Soil Science & Plant Nutrition*, vol. 54, no. 1, pp. 77-85.

Suzuki, M, Tsukamoto, T, Inoue, H, Watanabe, S, Matsuhashi, S, Takahashi, M, Nakanishi, H, Mori, S & Nishizawa, NK 2008b, 'Deoxymugineic acid increases Zn translocation in Zn-deficient rice plants', *Plant Molecular Biology*, vol. 66, no. 6, pp. 609-617.

Taiz, L & Zeiger, E 2010, *Plant physiology*, 5th ed.. edn, Sunderland, MA : Sinauer Associates, Sunderland, MA.

Takahashi, K, Kohno, H, Kanabayashi, T & Okuda, M 2019, 'Glutelin subtype-dependent protein localization in rice grain evidenced by immunodetection analyses', *Plant Molecular Biology*, vol. 100, no. 3, pp. 231-246.

Takahashi, M, Terada, Y, Nakai, I, Nakanishi, H, Yoshimura, E, Mori, S & Nishizawa, NK 2003, 'Role of nicotianamine in the intracellular delivery of metals and plant reproductive development', *The Plant cell*, vol. 15, no. 6, pp. 1263-1280.

Takahashi, R, Bashir, K, Ishimaru, Y, Nishizawa, NK & Nakanishi, H 2012a, 'The role of heavy-metal ATPases, HMAs, in zinc and cadmium transport in rice', *Plant signaling & behavior*, vol. 7, no. 12, pp. 1605-1607.

Takahashi, R, Ishimaru, Y, Shimo, H, Ogo, Y, Senoura, T, Nishizawa, NK & Nakanishi, H 2012b, 'The OsHMA2 transporter is involved in root-to-shoot translocation of Zn and Cd in rice', *Plant, Cell and Environment*, vol. 35, no. 11, pp. 1948-1957.

Takaiwa, F, Yamanouchi, U, Yoshihara, T, Washida, H, Tanabe, F, Kato, A & Yamada, K 1996, 'Characterization of common cis-regulatory elements responsible for the endosperm-specific expression of members of the rice glutelin multigene family', *Plant Molecular Biology*, vol. 30, no. 6, pp. 1207-1221.

Tan, S, Han, R, Li, P, Yang, G, Li, S, Zhang, P, Wang, W-B, Zhao, W-Z & Yin, L-P 2015, 'Over-expression of the *MxIRT1* gene increases iron and zinc content in rice seeds', *Transgenic Research*, vol. 24, no. 1, pp. 109-122.

Thorpe, M, Minchin, P, Gould, N & McQuen, J 2005, *The stem apoplast: A potential communication channel in plant growth regulation*, eds NM Holbrook & MA Zwieniecki, Academic Press, Burlington, MA, USA, <http://site.ebrary.com/lib/flinders1/docDetail.action?docID=10138240>.

Tie, W, Zhou, F, Wang, L, Xie, W, Chen, H, Li, X & Lin, Y 2012, 'Reasons for lower transformation efficiency in indica rice using *Agrobacterium tumefaciens*-mediated transformation: lessons from transformation assays and genome-wide expression profiling', *Plant Molecular Biology*, vol. 78, no. 1, pp. 1-18.

Toki, S, Hara, N, Ono, K, Onodera, H, Tagiri, A, Oka, S & Tanaka, H 2006, 'Early infection of scutellum tissue with *Agrobacterium* allows high-speed transformation of rice', *The Plant Journal*, vol. 47, no. 6, pp. 969-976.

Tran, TH 2015, 'Molecular characterisation of transgenic rice (*Oryza sativa* L.) over-expressing barley sucrose transporter (*HvSUT1*) gene', Master thesis, Flinders University.

Trijatmiko, KR, Dueñas, C, Tsakirpaloglou, N, Torrizo, L, Arines, FM, Adeva, C, Balindong, J, Oliva, N, Sapasap, MV, Borrero, J, Rey, J, Francisco, P, Nelson, A, Nakanishi, H, Lombi, E, Tako, E, Glahn, RP, Stangoulis, J, Chadha-Mohanty, P, Johnson, AAT, Tohme, J, Barry, G & Slamet-Loedin, IH 2016, 'Biofortified indica rice attains iron and zinc nutrition dietary targets in the field', *Nature Scientific Reports*, vol. 6, no. 19792.

Tsukamoto, T, Nakanishi, H, Uchida, H, Watanabe, S, Matsuhashi, S, Mori, S & Nishizawa, NK 2009, '^{52}Fe translocation in barley as monitored by a positron-emitting tracer imaging system (PETIS): evidence for the direct translocation of Fe from roots to young leaves via phloem', *Plant and Cell Physiology*, vol. 50, no. 1, pp. 48-57.

Uauy, C, Distelfeld, A, Fahima, T, Blechl, A & Dubcovsky, J 2006, 'A NAC gene regulating senescence improves grain protein, zinc, and iron content in wheat', *Science*, vol. 314, no. 5803, pp. 1298-1301.

Uraguchi, S, Kamiya, T, Sakamoto, T, Kasai, K, Sato, Y, Nagamura, Y, Yoshida, A, Kyozuka, J, Ishikawa, S & Fujiwara, T 2011, 'Low-affinity cation transporter (OsLCT1) regulates cadmium transport into rice grains', *Proceedings of the National Academy of Sciences of the United States of America*, vol. 108, no. 52, pp. 20959-20964.

Uraguchi, S, Mori, S, Kuramata, M, Kawasaki, A, Arao, T & Ishikawa, S 2009, 'Root-to-shoot Cd translocation via the xylem is the major process determining shoot and grain cadmium accumulation in rice', *Journal of Experimental Botany*, vol. 60, no. 9, pp. 2677-2688.

USAID 2019, *Interventions for addressing vitamin and mineral inadequacies*, viewed 9/06/2020 2020, <https://www.usaid.gov/global-health/health-areas/nutrition/technical-areas/micronutrients-brief#references>.

Van Bel, AJE 2003, 'Transport phloem: Low profile, high impact', *Plant Physiology*, vol. 131, no. 4, pp. 1509-1510.

Van Bel, AJE & Hafke, JB 2005, *Physiochemical determinants of phloem transport*, 2, Academic Press, Stanford University, Stanford, California.

Vanangamudi, K, Palanismy, V & Natesan, P 1988, 'Variety determination in rice — phenol and potassium hydroxide tests', *Seed science and technology*, vol. 16, no. 2, pp. 465-470.

Varghese, F, Bukhari, AB, Malhotra, R & De, A 2014, 'IHC profiler: An open source plugin for the quantitative evaluation and automated scoring of immunohistochemistry images of human tissue samples', *PLoS ONE*, vol. 9, no. 5: e96801.

Vasconcelos, M, Datta, K, Oliva, N, Khalekuzzaman, M, Torrizo, L, Krishnan, S, Oliveira, M, Goto, F & Datta, SK 2003, 'Enhanced iron and zinc accumulation in transgenic rice with the *ferritin* gene', *Plant Science*, vol. 164, no. 3, pp. 371-378.

Vaucheret, H, Béclin, C, Elmayan, T, Feuerbach, F, Godon, C, Morel, J-B, Mourrain, P, Palauqui, J-C & Vernhettes, S 1998, 'Transgene-induced gene silencing in plants', *The Plant Journal*, vol. 16, no. 6, pp. 651-659.

Vaucheret, H, Béclin, C & Fagard, M 2001, 'Post-transcriptional gene silencing in plants', *Journal of Cell Science*, vol. 114, no. 17, pp. 3083-3091.

von Wirén, N, Klair, S, Bansal, S, Briat, J-F, Khodr, H, Shioiri, T, Leigh, RA & Hider, RC 1999, 'Nicotianamine chelates both Fe(III) and Fe(II). Implications for metal transport in plants', *Plant Physiology*, vol. 119, no. 3, pp. 1107-1114.

Vucenik, I & Shamsuddin, AM 2006, 'Protection against cancer by dietary IP6 and inositol', *Nutrition and Cancer*, vol. 55, no. 2, pp. 109-125.

Walker, EL & Connolly, EL 2008, 'Time to pump iron: Iron-deficiency-signaling mechanisms of higher plants', *Current Opinion in Plant Biology*, vol. 11, no. 5, pp. 530-535.

Wang, F, King, JDM, Rose, T, Kretzschmar, T & Wissuwa, M 2017, 'Can natural variation in grain P concentrations be exploited in rice breeding to lower fertilizer requirements?', *PLoS ONE*, vol. 12, no. 6, p. e0179484.

Wang, G, Wu, Y, Ma, L, Lin, Y, Hu, Y, Li, M, Li, W, Ding, Y & Chen, L 2021, 'Phloem loading in rice leaves depends strongly on the apoplastic pathway', *Journal of Experimental Botany*, vol. 72, no. 10, pp. 3723-3738.

Wang, H, Li, X, Chen, Y, Li, Z, Hedding, DW, Nel, W, Ji, J & Chen, J 2020, 'Geochemical behavior and potential health risk of heavy metals in basalt-derived agricultural soil and crops: A case study from Xuyi County, eastern China', *Science of The Total Environment*, vol. 729, p. 139058.

Wang, HL, Offler, CE & Patrick, JW 1995, 'The cellular pathway of photosynthate transfer in the developing wheat grain. II. A structural analysis and histochemical studies of the pathway from the crease phloem to the endosperm cavity', *Plant, Cell & Environment*, vol. 18, no. 4, pp. 373-388.

Wang, L, Lu, Q, Wen, X & Lu, C 2015a, 'Enhanced sucrose loading improves rice yield by increasing grain size', *Plant Physiology*, vol. 169, no. 4, pp. 2848-2862.

Wang, L, Xie, W, Chen, Y, Tang, W, Yang, J, Ye, R, Liu, L, Lin, Y, Xu, C, Xiao, J & Zhang, Q 2010, 'A dynamic gene expression atlas covering the entire life cycle of rice', *The Plant Journal*, vol. 61, no. 5, pp. 752-766.

Wang, X, Jiang, D & Yang, D 2015b, 'Fast-tracking determination of homozygous transgenic lines and transgene stacking using a reliable quantitative real-time PCR assay', *Applied Biochemistry and Biotechnology*, vol. 175, no. 2, pp. 996-1006.

Wang, Y-Q, Wei, X-L, Xu, H-L, Chai, C-L, Meng, K, Zhai, H-L, Sun, A-J, Peng, Y-G, Wu, B, Xiao, G-F & Zhu, Z 2008, 'Cell-wall invertases from rice are differentially expressed in caryopsis during the grain filling stage', *Journal of Integrative Plant Biology*, vol. 50, no. 4, pp. 466-474.

Watson, MR, Lin, Y-f, Hollwey, E, Dodds, RE, Meyer, P & McDowall, KJ 2016, 'An improved binary vector and *Escherichia coli* strain for *Agrobacterium tumefaciens*-mediated plant transformation', *G3: Genes|Genomes|Genetics*, vol. 6, no. 7, pp. 2195-2201.

Weber, H, Borisjuk, L, Heim, U, Sauer, N & Wobus, U 1997, 'A role for sugar transporters during seed development: molecular characterization of a hexose and a sucrose carrier in fava bean seeds', *The Plant Cell*, vol. 9, no. 6, pp. 895-908.

Weber, H, Borisjuk, L & Wobus, U 2005, 'Molecular physiology of legume seed development', *Annual Review of Plant Biology*, vol. 56, pp. 253-279.

Weber, M, Harada, E, Vess, C, Roepenack-Lahaye, E & Clemens, S 2004, 'Comparative microarray analysis of *Arabidopsis thaliana* and *Arabidopsis halleri* roots identifies nicotianamine synthase, a ZIP transporter and other genes as potential metal hyperaccumulation factors', *The Plant Journal*, vol. 37, no. 2, pp. 269-281.

Weichert, H, Högy, P, Mora-Ramirez, I, Fuchs, J, Eggert, K, Koehler, P, Weschke, W, Fangmeier, A & Weber, H 2017, 'Grain yield and quality responses of wheat expressing a barley sucrose transporter to combined climate change factors', *Journal of Experimental Botany*, vol. 68, no. 20, pp. 5511-5525.

Weichert, N, Saalbach, I, Weichert, H, Kohl, S, Erban, A, Kopka, J, Hause, B, Varshney, A, Sreenivasulu, N, Strickert, M, Kumlehn, J, Weschke, W & Weber, H 2010, 'Increasing sucrose uptake capacity of wheat grains stimulates storage protein synthesis', *Plant physiology*, vol. 152, no. 2, pp. 698-710.

Welch, RM & Graham, RD 2004, 'Breeding for micronutrients in staple food crops from a human nutrition perspective', *Journal of Experimental Botany*, vol. 55, no. 396, pp. 353-364.

Welch, RM, House, WA, Beebe, S, Senadhira, D, Gregorio, GB & Cheng, Z 2000, 'Testing iron and zinc bioavailability in genetically enriched beans (*Phaseolus Vulgaris* L.) and rice (*Oryza Sativa* L.) in a rat model', *Food and Nutrition Bulletin*, vol. 21, no. 4, pp. 428-433.

Welch, RM & Shuman, L 1995, 'Micronutrient nutrition of plants', *Critical Reviews in Plant Sciences*, vol. 14, no. 1, pp. 49-82.

Weschke, W, Panitz, R, Gubatz, S, Wang, Q, Radchuk, R, Weber, H & Wobus, U 2003, 'The role of invertases and hexose transporters in controlling sugar ratios in maternal and filial tissues of barley caryopses during early development', *The Plant Journal*, vol. 33, no. 2, pp. 395-411.

Weschke, W, Panitz, R, Sauer, N, Wang, Q, Neubohn, B, Weber, H & Wobus, U 2000, 'Sucrose transport into barley seeds: Molecular characterization of two transporters and implications for seed development and starch accumulation', *The Plant Journal*, vol. 21, no. 5, pp. 455-467.

Wessells, KR & Brown, KH 2012, 'Estimating the global prevalence of zinc deficiency: Results based on zinc availability in national food supplies and the prevalence of stunting', *PLoS ONE*, vol. 7, no. 11, p. e50568.

Wheal, MS, Fowles, TO & Palmer, LT 2011, 'A cost-effective acid digestion method using closed polypropylene tubes for inductively coupled plasma optical emission spectrometry (ICP-OES) analysis of plant essential elements', *Analytical Methods*, vol. 3, no. 12, pp. 2854-2863.

White, PJ & Broadley, MR 2009, 'Biofortification of crops with seven mineral elements often lacking in human diets – iron, zinc, copper, calcium, magnesium, selenium and iodine', *New Phytologist*, vol. 182, no. 1, pp. 49-84.

WHO & FAO 2006, 'PART I: The role of food fortification in the control of micronutrient malnutrition', in L. Allen, B. de Benoist, O. Dary & R. Hurrell (eds), *Guidelines on food fortification with micronutrients*, World Health Organization, Switzerland.

Wirth, J, Poletti, S, Aeschlimann, B, Yakandawala, N, Drosse, B, Osorio, S, Tohge, T, Fernie, AR, Günther, D, Gruissem, W & Sautter, C 2009, 'Rice endosperm iron biofortification by targeted and synergistic action of nicotianamine synthase and ferritin', *Plant Biotechnology Journal*, vol. 7, no. 7, pp. 631-644.

Wu, C-Y, Adach, T, Hatano, T, Washida, H, Suzuki, A & Takaiwa, F 1998, 'Promoters of Rice Seed Storage Protein Genes Direct Endosperm-Specific Gene Expression in Transgenic Rice', *Plant and Cell Physiology*, vol. 39, no. 8, pp. 885-889.

Wu, C-Y, Washida, H, Onodera, Y, Harada, K & Takaiwa, F 2000, 'Quantitative nature of the Prolamin-box, ACGT and AACA motifs in a rice glutelin gene promoter: minimal *cis*-element requirements for endosperm-specific gene expression', *The Plant Journal*, vol. 23, no. 3, pp. 415-421.

Wu, CY, Lu, LL, Yang, XE, Feng, Y, Wei, YY, Hao, HL, Stoffella, PJ & He, ZL 2010, 'Uptake, translocation, and remobilization of zinc absorbed at different growth stages by rice genotypes of different Zn densities', *Journal of Agricultural and Food Chemistry*, vol. 58, no. 11, pp. 6767-6773.

Wu, T-Y, Gruissem, W & Bhullar, NK 2018, 'Facilitated citrate-dependent iron translocation increases rice endosperm iron and zinc concentrations', *Plant Science*, vol. 270, pp. 13-22.

Wu, TY, Gruissem, W & Bhullar, NK 2019, 'Targeting intracellular transport combined with efficient uptake and storage significantly increases grain iron and zinc levels in rice', *Plant Biotechnology Journal*, vol. 17, pp. 9-20.

Wu, X, Liu, J, Li, D & Liu, C-M 2016a, 'Rice caryopsis development I: Dynamic changes in different cell layers', *Journal of Integrative Plant Biology*, vol. 58, no. 9, pp. 772-785.

Wu, X, Liu, J, Li, D & Liu, C-M 2016b, 'Rice caryopsis development II: Dynamic changes in the endosperm', *Journal of Integrative Plant Biology*, vol. 58, no. 9, pp. 786-798.

Xi, J, Patel, M, Dong, S, Que, Q & Qu, R 2018, 'Acetosyringone treatment duration affects large T-DNA molecule transfer to rice callus', *BMC biotechnology*, vol. 18, no. 1, pp. 48-48.

Xuan, Y, Scheuermann, EB, Meda, AR, Hayen, H, von Wirén, N & Weber, G 2006, 'Separation and identification of phytosiderophores and their metal complexes in plants by zwitterionic hydrophilic interaction liquid chromatography coupled to electrospray ionization mass spectrometry', *Journal of Chromatography A*, vol. 1136, no. 1, pp. 73-81.

Yamaji, N, Xia, J, Mitani-Ueno, N, Yokosho, K & Feng Ma, J 2013, 'Preferential delivery of zinc to developing tissues in rice is mediated by P-type heavy metal ATPase OsHMA2', *Plant Physiology*, vol. 162, no. 2, pp. 927-939.

Yang, J, Luo, D, Yang, B, Frommer, WB & Eom, J-S 2018, 'SWEET11 and 15 as key players in seed filling in rice', *New Phytologist*, vol. 218, no. 2, pp. 604-615.

Yang, L, Ding, J, Zhang, C, Jia, J, Weng, H, Liu, W & Zhang, D 2005, 'Estimating the copy number of transgenes in transformed rice by real-time quantitative PCR', *Plant Cell Reports*, vol. 23, no. 10-11, pp. 759-763.

Yang, X, Huang, J, Jiang, Y & Zhang, HS 2009, 'Cloning and functional identification of two members of the *ZIP* (Zrt, Irt-like protein) gene family in rice (*Oryza sativa* L.)', *Molecular Biology Reports*, vol. 36, no. 2, pp. 281-287.

Yang, Y, Guo, M, Sun, S, Zou, Y, Yin, S, Liu, Y, Tang, S, Gu, M, Yang, Z & Yan, C 2019, 'Natural variation of *OsGluA2* is involved in grain protein content regulation in rice', *Nature Communications*, vol. 10, no. 1, p. 1949.

Yokosho, K, Yamaji, N, Ueno, D, Mitani, N & Ma, JF 2009, 'OsFRDL1 is a citrate transporter required for efficient translocation of iron in rice', *Plant Physiology*, vol. 149, no. 1, pp. 297-305.

Yordem, BK, Conte, SS, Ma, JF, Yokosho, K, Vasques, KA, Gopalsamy, SN & Walker, EL 2011, 'Brachypodium distachyon as a new model system for understanding iron homeostasis in grasses: phylogenetic and expression analysis of Yellow Stripe-Like (YSL) transporters', *Annals of Botany*, vol. 108, no. 5, pp. 821-833.

Yoshida, KT, Wada, T, Koyama, H, Mizobuchi-Fukuoka, R & Naito, S 1999, 'Temporal and spatial patterns of accumulation of the transcript of *Myo*-inositol-1-phosphate synthase and phytin-containing particles during seed development in rice', *Plant Physiology*, vol. 119, no. 1, pp. 65-72.

Yu, S-M, Lo, S-F & Ho, T-HD 2015, 'Source-sink communication: Regulated by hormone, nutrient, and stress cross-signaling', *Trends in Plant Science*, vol. 20, no. 12, pp. 844-857.

Yuan, M, Chu, Z, Li, X, Xu, C & Wang, S 2009, 'Pathogen-induced expressional loss of function is the key factor in race-specific bacterial resistance conferred by a recessive R gene *xa13* in rice', *Plant and Cell Physiology*, vol. 50, no. 5, pp. 947-955.

Zamski, E & Schaffer, AA 1996, *Photoassimilate distribution in plants and crops: source-sink relationships*, Marcel Dekker Inc.

Zhang, C & Turgeon, R 2018, 'Mechanisms of phloem loading', *Current Opinion in Plant Biology*, vol. 43, pp. 71-75.

Zhang, J, Chen, L-L, Xing, F, Kudrna, DA, Yao, W, Copetti, D, Mu, T, Li, W, Song, J-M, Xie, W, Lee, S, Talag, J, Shao, L, An, Y, Zhang, C-L, Ouyang, Y, Sun, S, Jiao, W-B, Lv, F, Du, B, Luo, M, Maldonado, CE, Goicoechea, JL, Xiong, L, Wu, C, Xing, Y, Zhou, D-X, Yu, S, Zhao, Y, Wang, G, Yu, Y, Luo, Y, Zhou, Z-W, Hurtado, BEP, Danowitz, A, Wing, RA & Zhang, Q 2016, 'Extensive sequence divergence between the reference genomes of two elite indica rice varieties Zhenshan 97 and Minghui 63', *Proceedings of the National Academy of Sciences of the United States of America*, vol. 113, no. 35, pp. E5163-E5171.

Zhang, W-H, Zhou, Y, Dibley, KE, Tyerman, SD, Furbank, RT & Patrick, JW 2007, 'Nutrient loading of developing seeds', *Functional Plant Biology*, vol. 34, no. 4, pp. 314-331.

Zheng, L, Cheng, Z, Ai, C, Jiang, X, Bei, X, Zheng, Y, Glahn, RP, Welch, RM, Miller, DD, Lei, XG & Shou, H 2010, 'Nicotianamine, a novel enhancer of rice iron bioavailability to humans', *PLoS ONE*, vol. 5, no. 4, p. e10190.

Zhu, C, Kobayashi, K, Loladze, I, Zhu, J, Jiang, Q, Xu, X, Liu, G, Seneweera, S, Ebi, KL, Drewnowski, A, Fukagawa, NK & Ziska, LH 2018, 'Carbon dioxide (CO_2) levels this century will alter the protein, micronutrients, and vitamin content of rice grains with potential health consequences for the poorest rice-dependent countries', *Science Advances*, vol. 4, no. 5.